Universidad de Valladolid

Escuela de Doctorado Universidad de Valladolid

PROGRAMA DE DOCTORADO EN INGENIERÍA QUÍMICA Y AMBIENTAL

TESIS DOCTORAL:

WHEAT BRAN BIOREFINERY: VALORIZATION OF HEMICELLULOSES TO SUGAR ALCOHOLS

FRACTIONATION – HYDROLYSIS – PURIFICATION - HYDROGENATION

Presentada por Nuria Sánchez Bastardo para optar al grado de

Doctor por la Universidad de Valladolid

Dirigida por:

Dra. Gloria Esther Alonso Sánchez

Memoria para optar al grado de Doctor,

con **Mención Doctor Internacional,** presentada por la

Graduada en Ingeniería Química:

Nuria Sánchez Bastardo

Siendo el tutor en la **Universidad de Valladolid:**

Dra. Gloria Esther Alonso Sánchez

Y en el **Institut für Technische und**

Makromolekulare Chemie,

RWTH Aachen (Alemania):

Prof. Dra. Regina Palkovits y

Dra. Irina Delidovich

Valladolid, Julio de 2018

Gloria Esther Alonso Sánchez

Profesora Titular de Universidad

Departamento de Ingeniería Química y Tecnología del Medio Ambiente

Universidad de Valladolid (UVa)

CERTIFICA QUE:

NURIA SÁNCHEZ BASTARDO ha realizado bajo su dirección el trabajo ***"WHEAT BRAN BIOREFINERY: VALORIZATION OF HEMICELLULOSES TO SUGAR ALCOHOLS. FRACTIONATION – HYDROLYSIS – PURIFICATION – HYDROGENATION"***, en el Departamento de Ingeniería Química y Tecnología del Medio Ambiente de la Escuela de Ingenierías Industriales de la Universidad de Valladolid. Considerando que dicho trabajo reúne los requisitos para ser presentado como Tesis Doctoral expresa su conformidad con dicha presentación.

Valladolid a_____de_____de 2018

Fdo. Gloria Esther Alonso Sánchez

Reunido el tribunal que ha juzgado la Tesis Doctoral "***WHEAT BRAN BIOREFINERY: VALORIZATION OF HEMICELLULOSES TO SUGAR ALCOHOLS. FRACTIONATION – HYDROLYSIS – PURIFICATION – HYDROGENATION***" presentada por Nuria Sánchez Bastardo y en cumplimiento con lo establecido por el Real Decreto 861/2010 (BOE 28.01.2011) ha acordado conceder por__ _____la calificación de_____.

Valladolid a_____de_____de 2018

PRESIDENTE SECRETARIO

1er Vocal 2do Vocal 3er Vocal

ABSTRACT

WHEAT BRAN BIOREFINERY: VALORIZATION OF HEMICELLULOSES TO SUGAR ALCOHOLS

FRACTIONATION – HYDROLYSIS – PURIFICATION – HYDROGENATION

In recent years, the conversion of lignocellulosic biomass towards platform chemicals or fuels has received special attention. This fact is a consequence of the exhaustion of fossil resources, the greater concerning about global warming and the more severe environmental laws enacted by the government. Unlike fossil resources, biomass is a sustainable, renewable and abundant feedstock. A biorefinery is "a facility that integrates biomass conversion processes and equipment to produce fuels, power, heat and value-added chemicals from biomass". The processes of a biorefinery are designed to maximize value products and minimize waste streams. Different processes have been described in literature for the conversion of biomass into high added-value products. In this sense, the transformation of biomass by means of heterogeneous catalysts appears to be a suitable process which allows the development of environmentally-friendly processes working under mild conditions.

This PhD Thesis is focused on upgrading the hemicellulosic fraction of wheat bran by its transformation into sugar alcohols. To accomplish this goal, the global process has been divided in several sequential steps, which are described along the five chapters of the Thesis.

In **Chapter 1**, the isolation of the arabinoxylan fraction from wheat bran was studied under hot compressed water conditions combined with heterogeneous catalysts. The aims of this chapter were to obtain high extraction yields of arabinoxylans with low molecular weight to facilitate their subsequent hydrolysis into monosaccharides as well as minimize the co-extraction of the cellulosic fraction. Different mesoporous silica materials (MCM-48 and Al-MCM-48) as well as the corresponding $RuCl_3$-based catalysts were investigated. The effects of temperature (140 – 180 ºC) and time (10 – 30 minutes) were also examined. The arabinoxylans extraction yield was directly related to the catalyst acidity: MCM-48 < Al-MCM-48 < $RuCl_3$/MCM-48 < $RuCl_3$/Al-MCM-48. A high total

acidity and the combination of Brönsted and moderate Lewis acid sites of $RuCl_3$/Al-MCM-48 demonstrated to be suitable for arabinoxylan extraction. High yields of arabinoxylans with low molecular weight were achieved combining high temperatures, short times and using solid acid catalysts. Optimum conditions were obtained over $RuCl_3$/Al-MCM-48 at 180 ºC after 10 minutes. Under such conditions, around 78% of total arabinoxylans was extracted with an average molecular weight of ca. 9 kDa. A relation between the experimental conditions (time, temperature, catalyst), the arabinoxylans yield and their molecular weight was also established. Soft operating conditions resulted in a low amount of arabinoxylans extracted with a low molecular weight, which means that only side chains of the polysaccharides were solubilized. Moderate operating conditions led to higher yields and molecular weights. In this case, the backbone of the arabinoxylans was solubilized but not hydrolyzed into short oligomers. Under more severe experimental conditions, the yield increased and the molecular weight decreased drastically. These results exhibited the solubilization of the arabinoxylans backbone as well as its hydrolysis into short chain oligomers.

In **Chapter 2**, the arabinoxylans previously extracted were subjected to a further catalytic hydrolysis process to complete their rupture into monomers. This process was optimized to maximize the production of pentoses (*i.e.* arabinose and xylose) avoiding their further degradation to furfural. The hydrolysis of poly/oligosaccharides is usually carried out by means of acids or enzymes. In this chapter, different solid acid catalysts were successfully employed for arabinoxylan hydrolysis. Mesoporous silicas (MCM-48 and Al-MCM-48) and $RuCl_3$ catalysts supported on them were tested. As happened in the previous extraction process, $RuCl_3$/Al-MCM-48 resulted to be the most active catalyst due to its high acidity and the combination of Lewis and Brönsted acid sites. Arabinoxylan hydrolysis was then optimized by investigating the influence of catalyst loading and

reaction time. Under optimum experimental conditions (180 ºC, 15 min, 4.8 g $RuCl_3$/Al-MCM-48·g C^{-1}), the yields corresponding to arabinose and xylose were 96% and 94%, respectively, without major degradation to furfural. The effect of different Lewis cations (Ru^{+3}, Fe^{+3}) was also discussed. $RuCl_3$ supported on Al-MCM-48 proved to be more efficient in arabinoxylan hydrolysis than $FeCl_3$/Al-MCM-48, which was attributed to the moderate Lewis acidity of Ru^{+3} cations compared to the strong Lewis acid sites of Fe^{+3}.

In **Chapter 3**, the behavior of different mesoporous silicas (MCM-48 and Al-MCM-48) and microporous aluminosilicates (commercial zeolites; H-Y (12), H-ZSM-5 (23) and H-ZSM-5 (80) from Zeolyst International Inc.) was compared in the hydrolysis of wheat bran arabinoxylans. Not only the number of acid sites, but also their strength and nature played an important role. Al-MCM-48 was more active than MCM-48. MCM-48 has a low acidity which corresponds mainly to weak Lewis acid sites. However, Al-MCM-48 has a higher acidity and a combination of Lewis and Brönsted acid sites, which improved the arabinoxylan hydrolysis compared to MCM-48. H-ZSM-5 (23) showed the highest catalytic activity, which was attributed to its high acidity and strong Brönsted acid sites. The process was then optimized over H-ZSM-5 (23) at 180 ºC. Optimum reaction time and catalyst loading were 15 minutes and 9.2 g catalyst·g C^{-1}, respectively. The yields corresponding to arabinose and xylose were 96% and 76%, respectively. Arabino-oligosaccharides were therefore more readily hydrolyzed than xylo-oligosaccharides. This is related to the type of bond existing between arabinose (linked by α-glycosidic bonds, weak) and xylose (linked by β-glycosidic bonds, strong) molecules. The easier access to the side chains (composed of arabinose) than to the backbone (composed of xylose) also explains the faster release of arabinose than xylose.

Prior to the hydrogenation of sugars from wheat bran, a kinetic study with sugar model mixtures was carried out in **Chapter 4** using ruthenium catalysts supported on H-ZSM-5

zeolites with different SiO_2/Al_2O_3 ratio (23 and 80). Reaction temperature was varied from 80 to 120 ºC and time between 5 and 30 minutes. Likewise, the influence of catalyst loading was analyzed in the range 0 – 0.060 g Ru·g C^{-1}. The acidity of the support (SiO_2/Al_2O_3 ratio) played a crucial role in the reaction mechanism. Ru/H-ZSM-5 (80) resulted in higher conversion and selectivity than Ru/H-ZSM-5 (23), since low acidic supports promoted hydrogenation over secondary reaction pathways, such as isomerization. Experimental results showed that C_5 sugars were faster hydrogenated than C_6 sugars. Indeed, the optimum temperature for arabinose and xylose hydrogenation was 100 ºC, whereas 120 ºC was the most suitable temperature for glucose hydrogenation. In this sense, operating conditions could be tuned to maximize the yield of pentitols and/or hexitols. Additionally, experimental data was successfully reproduced by a pseudo-first order kinetic model with relatively low absolute deviations (< 11%) and high regression coefficients (> 0.950). The activation energy values were 47.9 kJ·mol^{-1}, 43.7 kJ·mol^{-1} and 92.0 kJ·mol^{-1} for the hydrogenation of arabinose, xylose and glucose, respectively, using Ru/H-ZSM-5 (80) as catalyst.

In **Chapter 5**, the purification of wheat bran hydrolysates and the subsequent catalytic production of sugar alcohols was investigated. This hydrolysate was composed of xylose (5.6 g·L^{-1}), arabinose (2.8 g·L^{-1}), glucose (0.8 g·L^{-1}), furfural (0.3 g·L^{-1}), proteins (0.9 g·L^{-1}), different inorganic elements (Mg, Ca, K, S) and some lignin derivatives. A purification strategy was defined to maximize the sugar content in this hydrolysate. The process was based on the selective recovery of sugars by anionic extraction with a boronic acid (hydroxymethyl phenylboronic acid) which was dissolved in an organic phase composed by a quaternary ammonium salt (Aliquat® 336) and 1-octanol. The sugars were then back-extracted in an acidic solution which was further purified by means of ion exchange resins (Amberlyst® 15 and Amberlite® IRA-96). After this process, an aqueous

phase with a purity in sugars of 90% (based on carbon balance) was obtained. It was free of inorganic salts and proteins and it had a lower content of sugar degradation products and lignin derivatives than the initial hydrolysate. Importantly, the organic phase was successfully recycled. Purified sugars were then hydrogenated over Ru/H-ZSM-5 (80). A high pentitols yield of ~70% with 100% selectivity was achieved at 100 ºC after 10 minutes with a catalyst loading of 0.060 g Ru·g C^{-1}. An attempt to hydrogenate the sugars in the hydrolysate prior to purification was performed. However, neither sugar conversion nor sugar alcohol production were observed. It was determined that proteins deactivated the ruthenium catalyst and consequently the production of sugar alcohols was inhibited. Therefore, a purification step to remove proteins from wheat bran hydrolysates was crucial for the successful catalytic hydrogenation of sugars.

INTRODUCTION

WHEAT BRAN BIOREFINERY: VALORIZATION OF HEMICELLULOSES TO SUGAR ALCOHOLS

FRACTIONATION – HYDROLYSIS – PURIFICATION – HYDROGENATION

1. Lignocellulosic biomass: a good candidate for fuels and chemicals production

The transformation of biomass into fuels and chemicals is becoming increasingly attractive in recent years (Briens et al., 2008). The depletion of fossil resources and the need to decrease greenhouse gas emissions are forcing society to create an economy based on renewable carbon from biomass (Gallezot, 2012). Biomass is a sustainable, renewable and abundant raw material which is considered as a real alternative to fossil resources (Irmak, 2017). Lignocellulosic biomass, such as woody and agricultural waste, has received special attention because it is one of the most plentiful available resources on the earth (Oh et al., 2015). It belongs to second generation feedstocks since it is nonedible and therefore do not compete with food crops intended for human consumption (Naik et al., 2010). Lignocellulose is a polymeric material composed of three main fractions: cellulose, hemicelluloses and lignin (Figure 1) (De Jong, 2014; Oh et al., 2015; Serrano-Ruiz et al., 2011). Cellulose is the most common organic biopolymer worldwide and accounts for about 40 – 50 wt.% of most biomass materials (Kamm et al., 2008). It is a linear homopolysaccharide $(C_6H_{10}O_5)_n$ composed of between 2,000 and 14,000 glucose units (C_6 sugar) linked by β-glycosidic bonds (Mohan et al., 2006). The –OH groups of glucose molecules interact with each other and form inter- and intramolecular hydrogen bonds, resulting in a crystalline structure which confers cellulose a high chemical stability (Bochek and Kalyuzhnaya, 2002; Dhyani and Bhaskar, 2017). Hemicelluloses are the second most abundant biopolymer in biomass (ca. 30 %) (Tathod and Dhepe, 2015). They are heteropolysaccharides consisting of C_5 (xylose, arabinose) and C_6 sugars (mannose, galactose, glucose) which are linked by covalent and hydrogen bonds to lignin and cellulose, respectively (Zhang et al., 2011). Hemicelluloses consist of relatively short chains containing 50 – 200 sugar units interconnected by different structural bonds α- or β-(1→2, 1→3, 1→4, 1→6) (Pettersen, 1984). and are classified according to the kind of

monosaccharides in their structure: D-xylans, L-arabino-D-xylans, D-mannans, D-galacto-D-mannans, D-gluco-D-mannans and L-arabino-D-galactans (De Jong, 2014). Hemicelluloses are easier to hydrolyze into monosaccharides than cellulose due to their less stable intramolecular linkages (Mäki-Arvela et al., 2011). Lignin is a three-dimensional amorphous polymer composed of aromatic compounds and represent around 20 – 30 wt.% of most biomass (De Jong, 2014). It fills the space between cellulose and hemicelluloses and keeps the lignocellulose matrix together. In addition to this, lignin is cross-linked with carbohydrates, providing strength and rigidity to the system (Zakzeski et al., 2010). Besides cellulose, hemicelluloses and lignin, other minor compounds such as extractives, proteins, starch or ash are also part of biomass composition (Sluiter J., and Sluiter, A., 2011). Extractives correspond to non-structural components (non-chemically bound) soluble in either water or ethanol during exhaustive extraction. Water soluble materials include inorganic compounds, non-structural sugars and nitrogenous products, whereas chlorophyll and waxes belong to ethanol soluble material (Sluiter et al., 2008c). Proteins are biopolymers present in biomass composed of α-amino acids joined by peptide linkages and whose nature depends on the biomass source (De Jong, 2014). Starch is a polymer formed by glucose units. Unlike cellulose, starch is a non-structure component of biomass. The difference between cellulose and starch lies in the type of linkage: glucose is joined by β-glycosidic bonds in cellulose whereas α-glycosidic bonds are present in starch. The α-glycosidic bonds in starch are weaker than the β-glycosidic linkages in cellulose, which makes starch more readily accessible (De Jong, 2014; Sluiter, A., and Sluiter, J., 2008a). A minor biomass component is ash, which refers to the inorganic material. It can be classified as structural or extractable ash. Structural ash is bound in the physical structure of biomass, whilst extractable ash corresponds to the inorganic material which can be removed by washing or extraction (Sluiter et al., 2008b).

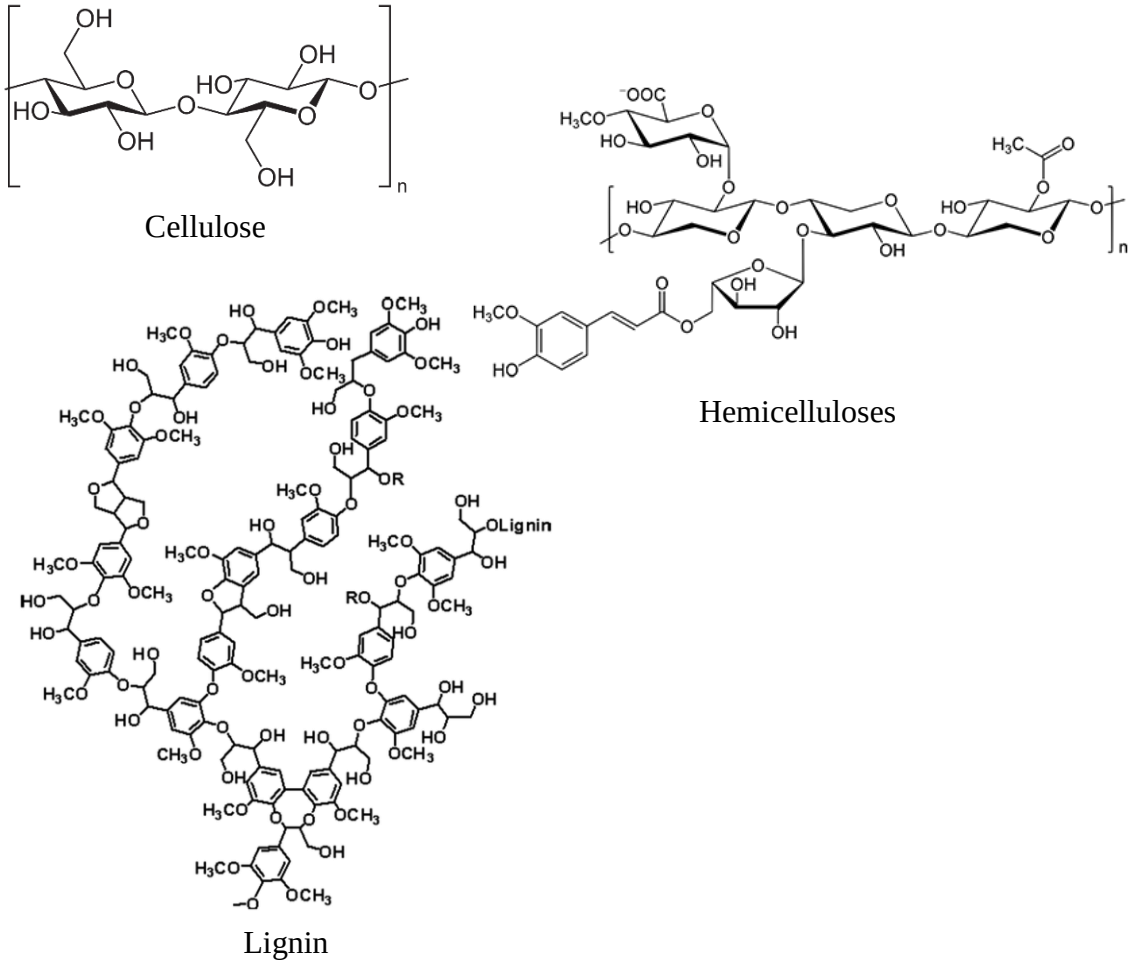

Figure 1. Main components of lignocellulosic biomass (adapted from De Jong, 2014).

2. Biorefinery concept

Currently, fossil resources, such as petroleum, coal and gas natural, provide about three quarters of the primary energy worldwide. The focus has recently turned towards improved utilization of renewable energy resources due to the limited deposits of fossil resources, the greater concern about climate change, the growing demand for fuels and the political commitment. Unlike the energy from fossil resources, the energy production from biomass has the advantage of carbon footprint reduction, since the carbon dioxide generated is consumed during biomass regrowth (Figure 2) (Stöcker, 2008). In addition to this, the residue from one biorefinery (*e.g.* lignin from a lignocellulosic ethanol

production plant) becomes an input for other industries, giving rise to an integrated system (Cherubini, 2010).

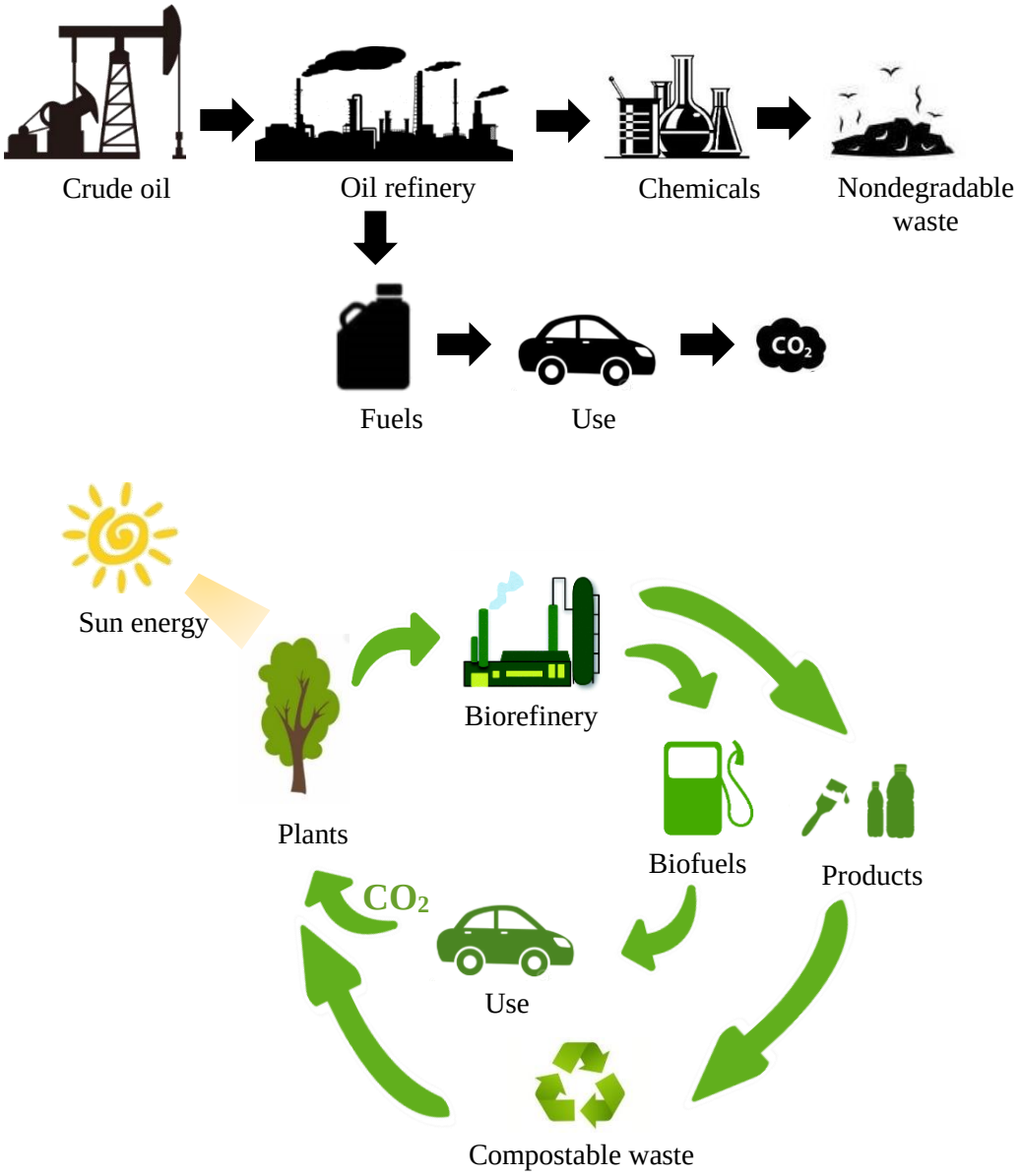

Figure 2. Lifecycle of oil refinery (up) and biorefinery (down). Adapted from Soudham, 2015.

Biorefinery is defined as "a facility that integrates biomass conversion processes and equipment to produce fuels, power, heat and value-added chemicals from biomass" (Bajpai, 2014). The biorefinery concept includes a wide range of technologies able to convert biomass resources into building blocks and platforms which can be further

transformed into chemicals and biofuels. A wider concept of biorefinery includes the synthesis of materials from the solid moieties derived from biorefineries and the recovery of energy from side streams. This concept is analogous to petroleum refinery, which produces fuels and products from petroleum (Cherubini, 2010). The processes of a biorefinery are designed to maximize value products and minimize waste streams by converting the low value intermediates into energy (Fernando et al., 2006). The renewable carbon-based materials used as feedstocks in a biorefinery can be classified in four sectors: i) agriculture (dedicated crops and residues), ii) forestry, iii) industries (process residues and leftovers) and households (municipal solid waste and wastewaters) and iv) aquaculture (algae and seaweeds) (Cherubini, 2010).

3. Wheat bran biorefinery

This PhD Thesis focuses on the valorization of wheat bran, which is a high ton by-product of the milling industry. Wheat, together with maize and rice, accounts for about 90% of the world's cereal production. Over 650 million tons of wheat are produced worldwide per year, of which around 70% is intended for human food consumption. Wheat for human consumption is usually processed into flour by a milling process. However, some by-products, such as wheat germ and wheat bran, derive from this process. Wheat bran is the major by-product, accounting for about 25% of the total grain weight. Indeed, about 150 million tons of wheat bran per year result as by-product of the milling industry. Wheat bran is mainly used as a low value ingredient in animal food and only minor amounts are intended as commercial bran for food purposes. This fact is making the milling industry look for new valuable applications for wheat bran. An integrated biorefinery concept must combine flour milling with the production of novel functional food, nutrient enriched animal feed and value-added chemicals (Prückler et al., 2014). These valuable derivatives can be produced from the carbohydrate (starch, lactic acid and polylactic acid, succinic

acid, acetone/butanol/ethanol, furfural and 5-hydroxymethylfurfural, arabinoxylans, β-glucan) and non-carbohydrate (phenolic compounds, vanillin, protein, wheat bran oil) fractions of wheat bran (Apprich et al., 2014).

3.1 Wheat bran composition

A general composition of wheat bran was given by Apprich et al. (2014) in a previous work and can be summarized as follows: water (12.1%), protein (13.2 – 18.4%), fat (3.5 – 3.9%), total carbohydrates (56.8), phenolic acids (1.1%) and ash (3.4 – 8.1%). Starch is also a main component of wheat bran, which accounts for about 15 – 25% of total weight (dry matter) (Beaugrand et al., 2004b). Wheat bran is a source of carbohydrates, which can be extracted and further converted into platform chemicals or fuels. Carbohydrates account for about 50 – 60% of the total weight of wheat bran. These values increase up to 62 – 70% in destarched wheat bran. Once destarched, the sugars from cellulose and hemicelluloses represent around 18 – 23% and 38 – 47% of the dry weight, respectively. Table 1 shows the carbohydrates composition of wheat bran and destarched wheat bran (Beaugrand et al., 2004b).

Table 1. Carbohydrates composition of wheat bran and destarched wheat bran Adapted from (Beaugrand et al., 2004b).

Raw material	Carbohydrates (wt.% dry basis)			
	Glucose	Arabinose	Xylose	Galactose
Wheat bran	24 – 36	7 – 10	11 – 17	1 – 2
Destarched wheat bran	18 – 23	13 – 18	23 – 29	1 – 2

3.2 Production of C_5 sugar alcohols from wheat bran

The aim of this PhD Thesis is to study the production of sugar alcohols from the hemicellulosic fraction (arabinoxylans) of wheat bran. Wheat bran was chosen as raw material due to its high arabinoxylan content (19 – 25%) (Zhang et al., 2014). In addition to this, our region Castilla y León is the main producer of wheat in Spain

(https://es.statista.com/estadisticas/501733/produccion-de-trigo-en-espana/) and thus, the supply of wheat bran is guaranteed. The production of sugar alcohols from wheat bran arabinoxylans involves several stages (Figure 3), which will be reviewed in the following sections:

1. Extraction of arabinoxylans from wheat bran.
2. Hydrolysis of arabinoxylans into arabinose and xylose.
3. Purification of hemicellulosic wheat bran hydrolysates.
4. Hydrogenation of sugars into sugar alcohols.

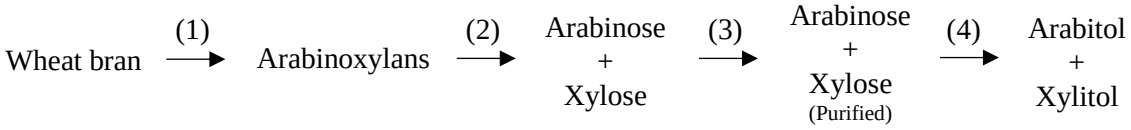

Figure 3. Production of sugar alcohols from wheat bran.

3.2.1 Extraction of arabinoxylans from wheat bran

Arabinoxylans, which belong to the hemicellulosic part of biomass, are a major structural component of cell walls in wheat bran (Beaugrand et al., 2004b). They consist of a backbone formed by xylose molecules connected by β-(1→4) bonds. Xylose units are highly substituted with primarily single α-(1→3) and/or α-(1→2)-linked L-arabinose residues as well as short arabinooligosaccharides, D-galactose, D-4-*O*-methylglucuronic acid, ferulic units and *p*-coumaric acid which form the side chains (Koutinas et al., 2008; Peng et al., 2012; Zhang et al., 2014). Arabinoxylans have potential applications in many industrial sectors, such as cosmetics, pharmaceutics or materials (films). Due to their prebiotic character, the use of arabinoxylans has also been extended to the field of nutrition, in scientific research and food applications (Peng et al., 2012). They are also suitable as additives to improve bread quality and can be used as soluble dietary fiber or stabilizers for food and non-food products (Cui et al., 2000). In addition to this,

arabinoxylans are susceptible to be hydrolyzed into xylose and arabinose, which are platform chemicals to produce building blocks such as sugar alcohols (xylitol and arabitol) or furans derivatives (furfural and 2,5-furan dicarboxylic acid) (Werpy and Petersen, 2004).

Different methods for the extraction of arabinoxylans from lignocellulosic biomass have been investigated: water and hydrothermal treatments, chemical solvent extractions (alkali or acid), enzymatic processes, mechanical-chemical methods (ultrasound, microwave, steam explosion and extrusion) (Zhang et al., 2014) and in minor extent extractions assisted by heterogeneous catalysts (Vilcocq et al., 2014). Experimental conditions and main results on arabinoxylans extraction obtained by different processes are shown in Table 2.

Table 2. Main results on arabinoxylans extraction by different processes reported in literature.

Raw material	Extraction conditions	AX yield (%)	Reference
Hydrothermal treatments			
Destarched corn fiber	H_2O, 180 ºC, 20 min	72[c]	(Dien et al., 2006)
Corncob	H_2O, 190 ºC, 15 min	58[c]	(Nabarlatz et al., 2004)
Corncob	H_2O, 175 ºC, 30 min	69[c]	(Garrote et al., 2001b)
Corncob	H_2O, 190 ºC, 12 min	70[c]	(Garrote et al., 2001b)
Chemical solvent extractions			
Destarched wheat bran	0.44 M NaOH, 80 ºC, 15 h	21[b]	(Aguedo et al., 2004)
Destarched wheat bran	1 M H_2SO_4, 180 ºC, 3 min	19[b]	(Aguedo et al., 2004)
Destarched bran	40% NaOH, 40 ºC, 6 h	28[b]	(Bataillon et al., 1998)
Destarched wheat bran	0.16 M NaOH + H_2O_2	21[b]	(Zhang et al., 2008)
Wheat bran	2% H_2O_2, 40 ºC, 6 h	12[a]	(Hollmann and Lindhauer, 2005)
Destarched corn bran	NaOH, R.T., 2 h	40[b]	(Doner et al., 1998)

Continued			
Barley husks	HCl 0.05 M (pretreatment) + NaOH 1 M (extraction), R.T., 16 h	26[a]	(Höije et al., 2005)
Destarched flax sives	30% EtOH, 180 ºC, 10 min	81[c]	(Buranov and Mazza, 2010)
Destarched wheat straw	Formic acid, acetic acid, H_2O, 85 ºC, 4 h	77[c]	(Xu et al., 2006)
Wheat bran	Alkaline hydrogen peroxide solution, 60 ºC, 4 h	69[c]	(Maes and Delcour, 2001)
Enzymatic processes			
Destarched wheat bran	Endoxylanase, 24 h	23[b]	(Beaugrand et al., 2004b)
Destarched wheat bran	Xylanase, 60 ºC, 2 h	12[d]	(Zhou et al., 2010)
Destarched wheat bran	Pentopan mono BG (0.75%), 60 ºC, 3 h	15[d]	(Zhang et al., 2008b)
Barley husks	α-amyloglucosidase, 80 ºC, 1 h	25[a]	(Höije et al., 2005)
Destarched wheat bran	Endoxylanase, 55 ºC, 24 h	17[a]	(Aguedo et al., 2004)
Soissons (wheat flour)	Alcalase, Termamyl, Amyloglucosidase, up to 100 ºC, long times	71[a] (soluble AX) 73[a] (insoluble AX)	(Faurot et al., 1995)
Thesée (wheat flour)	Alcalase, Termamyl, Amyloglucosidase, up to 100 ºC, long times	78[a] (soluble AX) 47[a] (insoluble AX)	(Faurot et al., 1995)
Apollo (wheat flour)	Alcalase, Termamyl, Amyloglucosidase, up to 100 ºC, long times	91[a] (soluble AX) 49[a] (insoluble AX)	(Faurot et al., 1995)
Mechanical-chemical methods			
Destarched flax sives	H_2O + microwave, 180 ºC, 10 min	18[c]	(Buranov and Mazza, 2010)
Destarched flax sives	EtOH + microwave, 180 ºC, 10 min	40[c]	(Buranov and Mazza, 2010)
Maize	H_2O + microwave, 200 ºC, 2 min or 180 ºC, 10 min	50[c]	(Rose and Inglett, 2010)
Brewers' spent grain	Removal of starch (140 ºC) + microwave H_2O (180 ºC) + microwave KOH (180 ºC)	62[c]	(Coelho et al., 2014)
Wheat straw	0.5 M KOH + ultrasounds, 35 ºC, 30 min	25[d]	(Sun and Tomkinson, 2002)

Continued			
Destarched wheat bran	Endoxylanase + ultrasound (180 W), 50 ºC, 70 min	34[c]	(Wang et al., 2014)
Destarched wheat bran	Twin-screw extrusion (Clextral BC45) combined with alkaline	24[c]	(Zeitoun et al., 2010)
Wheat straw	Steam explosion pre-treatment (200 ºC/10 – 33 min or 220 ºC/3 – 8 min) + H_2O_2 (50 ºC, 5 h)	77 – 88[c]	(Sun et al., 2005)
Extraction with heterogeneous catalysts			
Bagasse	H-Beta (Si/Al = 19), H_2O, 170 ºC, 1 h, 50 bar N_2	62[c]	(Sahu and Dhepe, 2012)
Bagasse	H-USY (Si/Al = 15), H_2O, 170 ºC, 2.5 h, 50 bar N_2	45[c]	(Dhepe and Sahu, 2010)
Wheat straw	H-USY (Si/Al = 17), H_2O, 140 ºC, 6 h, 10 bar N_2	72[c]	(Zhou et al., 2013)

[a] Yield as total sugars extracted by original sugar content in raw material.
[b] Yield as total sugars extracted by initial raw material.
[c] Yield as total hemicelluloses extracted by original hemicelluloses content in raw material.
[d] Yield as total hemicelluloses extracted by initial raw material.

3.2.1.1 Water and hydrothermal treatments

Water extractions at temperatures between 25 and 100 ºC allow the recovery of arabinoxylans with a good preservation of their initial structure. However, the extraction yields at these temperatures are relatively low (Bastos et al., 2018). Under these conditions, the cross-links between the arabinoxylans and the cell wall matrix are not broken, so only the water-extractable arabinoxylans (WEAXs) are solubilized in water, whereas the water-unextractable arabinoxylans (WUAXs) remain in the cereal matrix. The fraction of WEAXs (0.88 – 1%) is much lower than that of WUAXs (19 – 24%), so many efforts have been done to improve the extractability of WUAXs (Izydorczyk and Biliaderis, 2007). Hydrothermal treatments (hot compressed water), which are usually carried out between 150 and 230 ºC, have been proposed to increase the efficiency of water-based extractions. This temperature range is chosen due to two reasons: i) as

mentioned before, a low extraction yield is obtained below 100 ºC and ii) cellulose degradation becomes significant above 210 – 220 ºC (Garrote et al., 1999). The extraction mechanism of hydrothermal treatments is based on a process called autohydrolysis. During autohydrolysis, the water undergoes autoionization, which generates hydronium ions (H_3O^+) responsible for the first stages of hemicelluloses depolymerization (arabinoxylans in this case) (Carvalheiro et al., 2016; Garrote et al., 2001b). Hydrothermal treatments are environmentally-friendly since they only use water as a solvent. Moreover, the WUAXs fraction is solubilized under these conditions and relatively high arabinoxylans yields can be achieved (58 – 72%) (Table 2). Hydrothermal treatments are suitable as biomass pretreatments for obtaining arabinoxylans with high molecular weight. Nevertheless, the production of arabinoxylans with low molecular weight, which are more easily convertible into arabinose and xylose by a subsequent hydrolysis process, is not possible by using only water in subcritical conditions. Solid/soluble acids or enzymes are required to favor the hydrolysis of arabinoxylans into short chain oligosaccharides. Dien et al. (2006) pretreated corn fiber under hot compressed water conditions. Around 72% of arabinoxylans (mainly as oligosaccharides) were dissolved at 180 ºC after 20 minutes. β-glucosidase containing β-xylosidase side-activity was then used to convert arabinoxylans into simple sugars.

3.2.1.2 Chemical solvent extraction

Chemical treatments are another alternative for the extraction of arabinoxylans from cereals. These processes can be carried out by means of acids or bases. Both are highly efficient treatments which lead to relatively high yields of arabinoxylans (26 – 81%) (Table 2). The most common type of dilute acid is sulfuric acid (H_2SO_4). Aguedo et al. (2014) extracted arabinoxylans from destarched wheat bran by different methods. One of them consisted of subjecting wheat bran to a treatment with H_2SO_4 at 180 ºC and 3

minutes. The extracted arabinoxylans were then precipitated by adding ethanol and recovered by filtration. The final sugar fraction represented 19% of the initial weight of destarched wheat bran. Organic acids such as formic and acetic acids also demonstrated to be effective in arabinoxylans extraction (Xu et al., 2006). Xu et al. (2006) examined the isolation of hemicelluloses from wheat straw by means of different acid mixtures. They reported a high hemicelluloses yield of ~77% at 85 ºC (4 hours) using a mixture composed of formic acid, acetic acid and water (30/60/10). Regarding the extraction with alkalis, it includes a wide variety of solvents such as NaOH (Aguedo et al., 2004; Bataillon et al., 1998; Doner et al., 1998; Zhang et al., 2008a; Zhou et al., 2010), $Ca(OH)_2$ (Ogawa et al., 2005), $Ba(OH)_2$ (Gruppen et al., 1992) and KOH (DuPont and Selvendran, 1987). Aguedo et al. (2014) studied the fractionation of arabinoxylans from destarched wheat bran by alkaline extraction with NaOH. The sugars extracted with NaOH (0.44 M) at 80 ºC after 15 hours corresponded to the 21% of the initial wheat bran weight. Alkaline solutions of ethanol (Buranov and Mazza, 2010) and hydrogen peroxide (Hollmann and Lindhauer, 2005; Maes and Delcour, 2001) have also been tested for arabinoxylans extraction. Buranov et al. (2010) investigated the removal of hemicelluloses from biomass by different methods. A high hemicelluloses yield (~80%) was obtained at 180 ºC and 10 minutes using an aqueous solution of ethanol (30%). However, a higher amount of lignin was extracted by using ethanol instead of pure water, which is a drawback in terms of hemicelluloses purity. The main difference between the arabinoxylans extracted by alkaline and acid treatments remains in their molecular weight. The extraction with bases results in arabinoxylans with a high molecular weight (Doner et al., 1998), whilst a low branched degree arabinoxylans are obtained by using acids (Zhang et al., 2014). Despite the high arabinoxylans extraction yields obtained by chemical treatments, these processes have also important drawbacks. For instance, alkaline treatments cause the

breakdown of functional groups, *e.g.* ferulic acid, and releases lignin from the cereal cell walls, thus decreasing the arabinoxylans purity (Buranov and Mazza, 2010; Doner et al., 1997). Furthermore, the use of acids is not selective for arabinoxylans extraction, since saccharification of cellulose also occurs under acidic conditions. From an experimental point of view, chemical treatments are not environmentally-friendly. The removal of the acid/base at the end of the extraction increases the operating costs and leads to the formation of lime deposits. Moreover, the corrosion problems associated to acid treatments raise the equipment costs (Negahdar et al., 2016).

3.2.1.3 Enzymatic processes

The enzymatic fractionation of arabinoxylans from wheat bran has been used in previous works by several authors (Aguedo et al., 2004; Beaugrand et al., 2004b; Zhang et al., 2008b; Zhou et al., 2010). The most common enzymes used in arabinoxylans extraction are the endo-β-1,4-xylanases. Endoxylanases attack the xylan backbone and cleave the internal β-1,4-linkages, originating a mixture of substituted and non-substituted xylooligosaccharides. Endoxylanases cause the partial solubilization and extraction of WUAXs and the depolymerization of WEAXs into arabinoxylans with a lower molecular weight (Courtin and Delcour, 2001). The most effective xylanases reported are GH10 and GH11 from the glycoside hydrolase (GH) family. GH10 xylanases are more active in the hydrolysis of arabinoxylans previously extracted, whereas GH11 xylanases have higher selectivity for insoluble substrates since they can penetrate better the cell wall network (Beaugrand et al., 2004a). Other enzymes, such as exo-β-1,4-xylanases, are able to hydrolyze the xylan chain from the nonreducing end, but they are less effective and increase the xylooligosaccharides chain length. Besides these types, there are some kinds of enzymes which can selectively cleave the arabinose side residues or the side chains, such as the linkages between uronic acids and acetyl groups with xylose units, and the

existing between ferulic and coumaric acids with arabinose molecules (Bastos et al., 2018). Extraction of arabinoxylans by means of enzymes is a very selective green process. However, enzymatic treatments usually exhibit lower arabinoxylans extraction yields comparing to chemical extractions with alkalis or bases. This fact has been ascribed to the physical barrier of lignin, which makes polysaccharides inaccessible to endoxylanases (Escarnot et al., 2012). In addition to this, enzymatic methods are not currently commercial due to the high price of enzymes. The long time required and the nonexistence of recovery methods of enzymes are additional problems attributed to enzymatic treatments (Aden et al., 2002; Cará et al., 2013; Hendriks and Zeeman, 2009; Ormsby et al., 2012). Zhou et al. (2010) studied the extraction of arabinoxylans from wheat bran by means of enzymes. Using a type of xylanase, a yield of 12% of arabinoxylans (based on destarched wheat bran weight in dry basis) was achieved at 60 ºC after 2 hours. Importantly, the arabinoxylans content of the extract was very high, around 86%, demonstrating the high selectivity of enzymes. Zhang et al. (2008b) optimized the enzymatic extraction to isolate arabinoxylans from wheat bran. The optimum experimental conditions were 60 ºC and 3 hours using an enzyme concentration of 0.75% at a pH 5, obtaining an arabinoxylans yield of 15% (based on the initial raw material weight). It should be noted that enzymes are usually employed to hydrolyze arabinoxylans previously extracted into arabinose and xylose (Dien et al., 2006; Reisinger et al., 2013). This will be discussed in a later section.

3.2.1.4 Mechanical-chemical methods

Hydrothermal and chemical extractions as well as enzymatic methods can be assisted by mechanical processes to improve the efficiency of the extraction and the sustainability of the process. Mechanical processes comprise ultrasound, microwave, steam explosion and extrusion treatments (Zhang et al., 2014).

The use of ultrasound combined with other processes (alkaline, acid, enzymatic) allows to achieve higher hemicelluloses yields at shorter times and lower temperatures (Sun and Tomkinson, 2002). The ultrasound treatment improves the biological activity of the xylans extracted (Hromadkova et al., 1999) and modifies their molecular weight (Ebringerova and Hromadkova, 1997). Sun et al. (2002) examined the extraction of hemicelluloses from wheat straw using alkaline extraction assisted by ultrasound. Ultrasonically assisted extraction resulted in a higher yield of hemicelluloses with a higher thermal stability than those obtained by classical alkali procedure. Wang et al. (2014) compared the extraction of arabinoxylans from wheat bran by enzymatic and ultrasound-assisted enzymatic treatments. They concluded that ultrasound increased the efficiency of enzymatic extraction resulting in a higher extraction yield. In this work, a surface response methodology was used to optimize the arabinoxylans extraction, achieving a yield of 34% at 50 ºC, 70 minutes, using endo-β-1,4-xylanases and an ultrasonic power of 180 W.

Microwave-assisted processes can shorten the operation times at the expense of increasing rapidly temperature. Nevertheless, the uncontrolled degradation of the arabinoxylans molecules may occur if the temperature is high enough (Rose and Inglett, 2010). Rose and Inglett (2010) investigated the obtaining of arabinoxylo-oligosaccharides from maize using microwave-assisted autohydrolysis. A maximum yield of ~50% was achieved at 180 ºC/10 minutes or 200 ºC/2 minutes. The authors claimed that higher temperatures and longer treatment times resulted in low yields as a result of the degradation of sugars into furfural. Coelho et al. (2014) evaluated the feasibility of microwave superheated water extractions for the recovery of arabinoxylans from brewers' spent grain. An increase in the arabinoxylans yield was observed by increasing the temperature from 140 ºC to 210 ºC for 2 minutes. Higher temperatures promoted the

depolymerization, debranching and deesterification of polysaccharides as well as the formation of brown products. The experimental conditions were optimized by achieving a compromise between the yield and the thermal degradation of the arabinoxylans using a sequential procedure: 1) removal of starch and β-glucans at 140 ºC, 2) treatment of the residue suspended in water at 180 ºC and 3) treatment of the residue suspended in 0.1 M KOH at 180 ºC. Microwave was applied in all the steps for 2 minutes. After this treatment, a 62% of arabinoxylans was recovered without further degradation.

Steam explosion has demonstrated to be successful in the extraction of arabinoxylans from cereal by-products. This method consists of treating the raw material with high-pressure steam followed by a rapid release of the pressure, leading to explosive depolymerization which breaks down the lignocellulosic structure and facilitates the hemicelluloses extraction (Cara et al., 2006). Sun et al. (2005) achieved a very high extraction yield of hemicelluloses (77 – 88%) by means of a two-step process consisting of a steam explosion pretreatment (200 ºC/10 – 33 min or 220 ºC/3 – 8 min) and a subsequent posttreatment with hydrogen peroxide (50 ºC, 5 h) and precipitation with ethanol.

Twin-extrusion shows relatively lower extraction yields of arabinoxylans compared to other mechanically assisted treatments (Zhang et al., 2014). However, extrusion has the advantages of requiring shorter residence times and lower chemical and water consumption (Zeitoun et al., 2010). Zeitoun et al. (2010) compared the twin-extrusion process with a stirred reactor on the extraction of wheat bran hemicelluloses. The twin-screw extruder resulted in a lower extraction rate (24% of hemicelluloses in wheat bran) than the stirred reactor extraction. Nevertheless, they pointed out the environmental advantages of the extrusion procedure.

3.2.1.5 Water-based extractions assisted with heterogeneous catalysts

Heterogeneous catalysts appear to be a good alternative to these treatments. The operating time and thus the degradation of molecules and the energy consumption can be reduced by using solid acid catalysts. In addition to this, heterogeneous catalysts can be easily separated, and they are safe and non-corrosive (Vilcocq et al., 2014). They have also lower operating costs than homogeneous acids and avoid the corrosion of the reactors (Bhaumik and Dhepe, 2016). These reasons have made solid catalysts be increasingly used in numerous biorefinery processes (Guo et al., 2012). Nonetheless, works related to hemicelluloses extraction from real biomass by means of solid acids are scarce (Dhepe and Sahu, 2010; Li et al., 2012; Sahu and Dhepe, 2012; Zhou et al., 2013). Zeolites are the preferred option chosen by different authors. Dhepe and Sahu (2010) described for the first time a one-pot method for the extraction of hemicelluloses from bagasse, achieving a yield of 45% at 170 ºC after 2.5 h using a H-USY zeolite (Si/Al = 15). Zhou et al. (2013) also studied the conversion of hemicelluloses from different lignocellulosic materials (wheat straw, rice hull, corn stalk and poplar). For instance, a total reducing sugars yield of 72% from wheat straw was obtained at 140 ºC (6 hours) using H-USY (Si /Al = 17) under an inert atmosphere.

In this PhD Thesis, the extraction of hemicelluloses (specifically arabinoxylans) from wheat bran has been investigated over moderate Lewis metal cations (Ru^{+3}) supported on different mesoporous materials (MCM-48 type). Results on this research are discussed in Chapter 1. Solid acid catalysts were chosen because of their advantages respect to the traditional hydrothermal treatments and processes carried out with homogeneous catalysts or enzymes. Comparing to hydrothermal treatments, solid acid catalysts reduce the operating time and give rise to arabinoxylans with a lower molecular weight, which facilitates and shortens the next hydrolysis step into monomers. Unlike chemical

processes, water-based extractions assisted with heterogeneous catalysts allow to recover the hemicellulosic fraction and simultaneously to minimize the solubilization of other biomass components, such as cellulose and lignin, which mainly remain in the residual solid. This gives the possibility to revalorize the residual solid in a subsequent treatment. The easier separation of solid catalysts is also an important advantage respect to chemical and enzymatic processes. The latter also take long times, not only hours but also days, which are reduced in the processes with solid acid catalysts.

3.2.2 Hydrolysis of arabinoxylans into arabinose and xylose

Although arabinoxylans have important applications in pharmaceutical and food industries, the market volume is larger for the C_5 monosaccharides-derived products (Vilcocq et al., 2014). For example, conversion of C_5 sugars to biohydrogen is a very promising process (Kaparaju et al., 2009; Lin et al., 2008; Wu et al., 2008). In addition to this, platform molecules, such as xylitol/arabitol or furfural, can be also obtained from C_5 carbohydrates (Mäki-Arvela et al., 2007). A one-pot conversion of hemicelluloses (arabinoxylans) from biomass (without any pretreatment) into monosaccharides is a complex process, since at severe operating conditions not only hemicelluloses are extracted and hydrolyzed into monomers but also cellulose starts to be degraded (Garrote et al., 1999). For this reason, it is more suitable to carry out the process in two steps: i) extraction of arabinoxylans as poly and oligosaccharides from raw material and ii) hydrolysis of solubilized arabinoxylans into simple carbohydrates. The hydrolysis of arabinoxylans into monomers is thus a crucial step for an integrated biorefinery concept. Table 3 displays some results on hemicelluloses hydrolysis. This process has been historically restricted to the use of dilute acids or enzymes (Duarte et al., 2009; Sahu and Dhepe, 2012). Li et al. (2016) compared the enzymatic and acid hydrolysis of beech xylan. Acid hydrolysis was faster but needed to be operated at a higher temperature than

enzymatic hydrolysis. Moreover, acid hydrolysis was suitable to produce monomeric xylose, whereas enzymatic treatment was more appropriate to obtain xylooligosaccharides with a low molecular weight. Enzymatic hydrolysis yielded fewer undesirable by-products, such as furfural. This also represents an advantage over acid hydrolysis.

Table 3. Hydrolysis of hemicelluloses by different processes.

Raw material	Hydrolysis conditions	Xyl. Yield (%)	Ara. Yield (%)	Xyl. + Ara. Yield (%)	Reference
Acid hydrolysis					
Oat spelt	1 wt.% H_2SO_4, 170 ºC, 1 h	-	-	50	(Dhepe and Sahu, 2010)
Arabinogalactan	0.1 M HCl, 90 ºC, 4 h	-	96	-	(Kusema et al., 2011)
O-acetyl-(4-O-methylglucurono) xylan	Oxalic acid (pH = 1), 90 ºC, 20 h	89	-	-	(Hilpmann et al., 2016)
O-acetyl-(4-O-methylglucurono) xylan	H_2SO_4 (pH = 1), 90 ºC, 24 h	62	-	-	(Hilpmann et al., 2016)
O-acetyl-(4-O-methylglucurono) xylan	HCl (pH = 1), 90 ºC, 20 h	89	-	-	(Hilpmann et al., 2016)
Beech xylan	Trifluoroacetic acid (0.5 M), 140 ºC, 1 h	75	-	-	(Li et al., 2016)
Xylan from wood pulp	30 wt.% acetic acid, 160 ºC, 30 min	60	-	-	(Zhang et al., 2016)
Xylooligosaccharides from sugarcane bagasse	H_2SO_4, 120 ºC, 20 min	97	-	-	(Nakasu et al., 2016)
Enzymatic hydrolysis					
Beech xylan	Xylanase (5 U/mL), 37 ºC, 8 h	6	-	-	(Li et al., 2016)
Xylan	Xylanase + sodium lignosulfate + *n*-decanol, 50 ºC, 72 h	70	-	-	(Lou et al., 2016)
Oat spelt xylan	Xylanase, 30 ºC, 48 h	8	-	-	(Lee et al., 2013)

Continued					
Hydrolysate from empty fruit bunches	NS 22146 (Novozymes), 50 ºC, 120 h	55	-	-	(Bouza et al., 2016)
Hydrolysis over solid acid catalysts					
Beechwood xylan	Amberlyst 35, 120 ºC, 4 h	-	-	80	(Cará et al., 2013)
Beechwood xylan	Amberlyst 70, 120 ºC, 4 h	-	-	76	(Cará et al., 2013)
Beechwood xylan	Sulfonated resin (D5081), 120 ºC, 4 h	-	-	55	(Cará et al., 2013)
Beechwood xylan	Sulfonated resin (D5082), 120 ºC, 4 h	-	-	68	(Cará et al., 2013)
Beechwood xylan	Sulfonated silica, 140 ºC, 3 h	-	-	50	(Cará et al., 2013)
Beechwood xylan	H-Y (Si/Al = 5.1), 120 ºC, 20 h	-	-	20	(Cará et al., 2013)
Beechwood xylan	H-ZSM-5 (Si/Al = 50), 120 ºC, 20 h	-	-	33	(Cará et al., 2013)
Beechwood xylan	H-ZSM-5 (Si/Al = 80), 120 ºC, 20 h	-	-	29	(Cará et al., 2013)
Beechwood xylan	H-Ferrierite, 120 ºC, 20 h	-	-	43	(Cará et al., 2013)
Oat Spelt	H-USY (Si/Al = 15), 170 ºC, 3 h	-	-	41	(Dhepe and Sahu, 2010)
Oat Spelt	H-Beta (Si/Al = 19), 170 ºC, 3 h	-	-	37	(Dhepe and Sahu, 2010)
Oat Spelt	H-MOR (Si/Al = 10), 170 ºC, 3 h	-	-	36	(Dhepe and Sahu, 2010)
Oat Spelt	Al-MCM-41 (Si/Al = 50), 170 ºC, 3 h	-	-	15	(Dhepe and Sahu, 2010)
Oat Spelt	Al-SBA-15 (Si/Al = 100), 170 ºC, 3 h	-	-	5	(Dhepe and Sahu, 2010)
Oat Spelt	γ-Al_2O_3, 170 ºC, 3 h	-	-	20	(Dhepe and Sahu, 2010)
Oat Spelt	Nb_2O_5, 170 ºC, 3 h	-	-	20	(Dhepe and Sahu, 2010)
Oat Spelt	$Cs_{2.5}H_{0.5}PW_{12}O_{40}$, 170 ºC, 3 h	-	-	35	(Dhepe and Sahu, 2010)
Arabinogalactan	Smopex-101 (pH = 2), 90 ºC, 24 h	-	85	-	(Kusema et al., 2011)

Continued					
Arabinogalactan	Amberlyst 15 (pH = 2), 90 ºC, 24 h	-	50	-	(Kusema et al., 2011)
O-acetyl-(4-O-methylglucurono) xylan	Smopex-101 (pH = 2), 90 ºC, 22 h	34	-	-	(Hilpmann et al., 2016)
Beechwood xylan	H-USY, 140 ºC, 6 h	68	-	-	(Zhou et al., 2013)

3.2.2.1 Acid hydrolysis

Acid hydrolysis leads to high yields and productivity, although monosaccharide degradation reactions may take place. Examples of such reactions are the degradation of pentoses to furfural and the subsequent production of formic and levulinic acids (Duarte et al., 2009). Common acids for hemicelluloses hydrolysis are mineral acids, such as sulfuric acid (H_2SO_4), phosphoric acid (H_3PO_4), nitric acid (HNO_3) and hydrochloric acid (HCl) as well as organic acids such as trifluoroacetic acid (CF_3COOH), oxalic acid (HOOC COOH) and acetic acid (CH_3COOH) (Mäki-Arvela et al., 2011; Marzialetti et al., 2008). Hilpmann et al. (2016) analyzed the effect of different homogeneous acids (oxalic acid, H_2SO_4, HCl) as well as the influence of temperature, pH and substrate concentration on the hydrolysis of a commercial xylan. A high xylose yield (89%) was achieved at 90 ºC using oxalic acid and HCl (pH 1), whilst only a yield of 62% was obtained with H_2SO_4. Nakasu et al. (2016) considered a two-step process for the production of xylose from sugarcane bagasse: i) solubilization of hemicelluloses by a hydrothermal pretreatment and ii) acid post-hydrolysis of xylooligosaccharides. After the first step, 65% of the hemicelluloses in sugarcane bagasse was solubilized, but nearly 80% of the recovered xylose was present as xylooligosaccharides. In the second stage, a kinetic study of xylooligosaccharides hydrolysis was performed. A hydrolysis yield of 97% was obtained with sulfuric acid (1.25%) at 120 ºC after 20 minutes. Li et al. (2016) studied the hydrolysis of beech xylan by trifluoroacetic acid at different acid

concentrations (0.2 – 1.5 M), temperatures (80 – 140 ºC) and times (0.5 – 2 hour). The maximum yield of monomeric xylose (75%) was obtained at 140 ºC after 1 hour using an acid concentration of 0.5 M. Zhang et al. (2016) investigated the influences of acetic acid concentration, reaction temperature and reaction time on the yield and component profiles of xylooligosaccharides and xylose from xylan (from wood pulp). Xylose achieved its maximum yield (60%) at 160 ºC, 30 min with an acetic acid concentration of 30%. Nevertheless, the formation of furfural under these conditions was high (10%) due to the dehydration reaction of xylose. A reaction temperature around 130 ºC was found to be preferable to prevent the formation of furfural. At 130 ºC, most of xylan hydrolyzed into xylooligosaccharides (X2 – X5) and only around 20% was converted into monomeric xylose.

3.2.2.2 Enzymatic hydrolysis

The enzymatic hydrolysis is a selective process which avoids the degradation of monosaccharides. However, the action of several enzymes (endoxylanase, exoxylanase, β-xylosidase, etc.) is usually required for the complete hydrolysis of hemicelluloses due to their complex structure (Duarte et al., 2009). Lou et al. (2016) studied the hydrolysis of a commercial xylan by means of xylanases. They reported a xylose yield of 48% at 50 ºC after 72 hours, which could be improved up to 58% by using sodium lignosulfate and *n*-dodecanol. Bouza et al. (2016) examined the enzymatic hydrolysis of a mixture derived from the fractionation of empty fruit bunches. The best xylan to xylose conversion was observed at 50 ºC after 120 hours and corresponded to a xylose yield of 55%. Reisinger et al. (2013) pretreated wheat bran under hot compressed water conditions to extract arabinoxylans, which were further subjected to an enzymatic hydrolysis to obtain monosaccharides. During the enzymatic hydrolysis (40 ºC, 42 hours), approximately 50% of the arabinoxylans was disintegrated to monomers. Dien et al. (2006) obtained

arabinose and xylose yields of 80% from corn fiber by a hydrothermal pretreatment (180 ºC, 30 minutes) followed by the subsequent enzymatic hydrolysis of arabinoxylans at 50 ºC. As mentioned before, enzymatic hydrolysis leads to lower monosaccharides yields and requires longer times comparing to acid hydrolysis. However, lower operating temperatures are needed.

3.2.2.3 Hydrolysis over solid acid catalysts

Despite the different advantages offered by the processes described above, the use of acids or enzymes, as discussed in the previous section, has still significant drawbacks which can be overcome by using solid acids. Solid acid catalysts are defined as "solid materials having acidic properties because of the presence of either Brönsted acid sites or Lewis acid sites or both". Heterogeneous acid catalysts keep the advantages of soluble acids, but improve the selectivity towards sugars, avoiding degradation reactions into by-products. An easy separation and recovery of solid catalysts are also important advantages (Vilcocq et al., 2014). They include zeolites, ion-exchanged resins, functionalized mesoporous silica, functionalized carbons, functionalized and supported metal oxides, heteropolyacids, etc. (Bhaumik and Dhepe, 2016; Vilcocq et al., 2014). The advantages and disadvantages of these materials have been well described by Vilcocq et al. (2014). Zeolites have become popular in recent years for the hydrolysis of complex oligosaccharides (Cará et al., 2013; Dhepe and Sahu, 2010; Sahu and Dhepe, 2012; Zhou et al., 2013). Zeolites are crystalline aluminosilicates with tridimensional structures which create different types of porosity: mesopores (2 – 50 nm) and micropores (< 2 nm). They have a medium number of acid sites (0.5 – 1.2 $mmol_{H^+} \cdot g^{-1}$) but some of them are strong enough to hydrolyze oligosaccharides. In addition to this, they have also shown a good recyclability. The Si/Al ratio is an important parameter of zeolites: a lower Si/Al ratio implies a higher number of acid sites, which leads to higher hydrolysis yields. Ion-

exchange resins are the most used catalysts in hydrolysis processes. They are highly active due to the high number of acid sites (4 – 5 $mmol_{H+} \cdot g^{-1}$) derives from their sulfonic groups. However, the main drawback is the leaching of sulfonic groups during the reaction which causes a fast deactivation of these materials. Mesoporous silicas can be functionalized by sulfonic groups. Sulfonated silica gels present a high acidity and result in a high conversion rate. Their stability is higher than that of resins but still the sulfonic groups can be easily leached. Functionalized carbons can be easily prepared from raw or treated biomass by a treatment with sulfuric acid to generate sulfonic groups. The leaching of sulfonated surface groups during hydrolysis reactions is also a drawback of functionalized carbons. Another group of solid acid catalysts is the corresponding to oxides. Oxides, such as titania, zirconia, alumina and niobia, show medium activity. The activity may be increased by adding sulfonic groups, although their stability is lower. Heteropolyacids are protonic acids with polyoxometalate anions having metal-oxygen octahedral as the basic structure units into the complex cluster. They have a stronger acidity than soluble acids, such as H_2SO_4 (Vilcocq et al., 2014). Carà et al. (2013) compared the activity of sulfonated resins (Amberlyst 35, Amberlyst 70, D5081 and D5082), sulfonated silica gels and zeolites (H-Y, H-ZSM-5 and H-ferrierite) in hemicelluloses hydrolysis (beechwood wood). They stated that sulfonated resins were highly active, but they leached out their sulfonic groups, resulting in a rapid loss of their activity. Sulfonated silica gels, which have weak and strong acid sites, were less active, but more stable over time. The weak acid sites leached, whereas the strong ones remained in the silicas. This led to a loss of activity after the first run which was maintained in further tests. Finally, zeolites demonstrated to be moderately active and stable. Among the tested zeolites, H-ferrierite gave the best results in terms of activity and stability. Dhepe and Sahu (2010) investigated the hydrolysis of oat spelt hemicelluloses over

different solid catalysts: zeolites (H-USY, H-Beta and H-MOR), Al-incorporated mesoporous silicas (Al-MCM-41 and Al-SBA-15), metal oxides (γ-Al_2O_3 and Nb_2O_5) and heteropolyacids ($Cs_{2.5}H_{0.5}PW_{12}O_{40}$). H-USY (Si/Al = 15) showed the highest activity, with a 41% yield of xylose + arabinose. Other zeolites, such as H-Beta (Si/Al = 19) and H-MOR (Si/Al = 10), were also active, with yields of 37% and 36%, respectively. Although the other catalysts improved the hydrolysis yield respect the blank experiment, they showed lower xylose + arabinose yields than zeolites. For instance, γ-Al_2O_3 and Nb_2O_5 gave both 20% yield, while Al-MCM-41 (Si/Al = 50) and Al-SBA-15 (Si/Al = 100) showed 15% and 5% yield, respectively. The Cs-exchanged heteropolyacid ($Cs_{2.5}H_{0.5}PW_{12}O_{40}$) resulted in 35% xylose + arabinose yield, but its activity dropped to 5% after the first run. Besides these materials, salts of metal cations (*e.g.* Ru^{+3}, La^{+3}, Ag^{+}, Ca^{+2}, Co^{+2}, Y^{+3}, Sn^{+4}, Sc^{+3}, Fe^{+3}, Hf^{+4}, Ga^{+3} and Al^{+3}), which possess Lewis acidity, have been successfully used for the selective hydrolysis of polysaccharides to sugars (Seri et al., 2002; Shimizu et al., 2009). For example, Shimizu et al. (2009) studied the conversion of cellulose to monosaccharides over different metal cations. They observed the highest cellulose hydrolysis rates and sugar selectivity over metal cations with moderate Lewis acidity such as Sn^{+4} and Ru^{+3}. Lewis metal cations seem therefore a good alternative for poly/oligosaccharides hydrolysis.

The conversion of cellulose into glucose over solid acid catalysts has been extensively studied during the last years (Das et al., 2016; De Almedia et al., 2016; Hara, 2010; Hu et al., 2016; Huang and Fu, 2013; Negahdar et al., 2016). Hydrolysis of commercial hemicelluloses over heterogeneous catalysts has also received special attention in the last decade (Cará et al., 2013; Chareonlimkun et al., 2010; Dhepe and Sahu, 2010; Hilpmann et al., 2016; Kusema et al., 2011; Zhou et al., 2013) but works on hydrolysis of real hemicelluloses previously extracted from biomass over solid catalysts are scarce (Vilcocq

et al., 2014). Most research related to real biomass focuses on a first solubilization of hemicelluloses followed by a subsequent post hydrolysis with soluble acids or enzymes (Akoinar et al., 2009; Dien et al., 2006; Garrote et al., 2001a; Nakasu et al., 2016; Reisinger et al., 2013; Shevchenko et al., 2000).

Since solid acid catalysts have mainly been used for the hydrolysis of biomass model polysaccharides, there is a need to study the hydrolysis of real polysaccharides over heterogeneous catalysts. The behavior of solid catalysts may be affected by other biomass components which are not present when commercial substrates are used as raw materials. Solid acid catalysts were chosen to overcome the drawbacks of acids or enzymes, which are commonly used for this kind of processes. Acids do not only hydrolyze the bonds existing between arabinoxylan molecules, but they also cause the degradation of sugars into by-products. Soluble acids can also cause the corrosion of the reactors, resulting in high operating costs. In the case of enzymes, they give rise to low monosaccharides yields. The difficult recovery and the high price of enzymes as well as the long time required for these treatments are also important drawbacks. Solid acid catalysts convert selectively arabinoxylans into arabinose and xylose with a minor formation of degradation products. Moreover, they reduce the operating time and can be easily recovered by a filtration process. In this PhD Thesis, the hydrolysis of arabinoxylans (previously extracted from wheat bran) over solid acid catalysts is discussed in Chapter 2 (over $RuCl_3$ supported on MCM-48 type materials) and Chapter 3 (over mesoporous silica and microporous aluminosilicates).

3.2.3 Purification of hemicellulosic hydrolysates from wheat bran

During the fractionation and hydrolysis processes of wheat bran, other components, such as proteins and inorganic cations, may be solubilized in water. Furthermore, some degradation products derived from sugars (furfural, 5-HMF, acetic acid, formic acid) may

also be formed. Therefore, a purification process to obtain sugar-rich hydrolysates is necessary. It is well known that organic acids, furans and phenolic compounds are potential inhibitors of fermentation processes (Chandel et al., 2011a). Some of these compounds may also poison the heterogenous catalysts required for a further processing of the hydrolysates, *e.g.* the hydrogenation of sugars to produce sugar alcohols. Several works have been published related to the deactivation of heterogeneous catalysts by different biomass components. Arena (1992) reported a negative effect of sulfur and organic acids on the hydrogenation of glucose due to the deactivation of ruthenium catalysts. Borg et al. (2011) studied the effect of different cations (K, Ca, Mg) on the deactivation of metal catalysts. They observed a decreased of their activity as a consequence of the blocking of the active metal sites, the reduction of the particles and the electronic effects. Elliot et al. (2004) came to the same conclusions about the deactivation of metal catalysts by cations and reported also the inhibitory effect of proteins on the catalytic hydrogenation of sugars. The composition of the hydrolysates varies depending on the biomass source and the operating conditions. Thus, the deactivation mechanism of metal catalysts must be studied for each specific hydrolysate. A purification process is therefore required not only for obtaining sugar-rich hydrolysates, but also to make subsequent treatments (fermentation, catalytic processes) feasible to produce high added-value products.

Table 4 shows different purification strategies of hydrolysates and the removal of the corresponding chemicals. These purification methods can be classified in four groups: a) physical methods (evaporation, membrane separation), b) chemical methods (neutralization, calcium hydroxide over-liming, activated charcoal, ion exchange resins, extraction with ethyl acetate), c) biotechnological methods (enzymes) and d) solvent extraction methods (by using boronic acids dissolved in an organic solvent).

Table 4. Purification methods applied to lignocellulosic hydrolysates.

Purification method	Hydrolysate	Changes in hydrolysate composition	Reference
Physical methods			
Evaporation	Aspen wood	Removal of furfural and most acetic acid but not lignin derivatives	(Wilson et al., 1989)
Evaporation	Spruce wood	Removal of furfural (90%) and 5-HMF (4%)	(Larsson et al., 1999;)
Evaporation	*Eucalyptus globulus* wood	Removal of acetic acid (90%)	(Converti et al., 2000)
Anion exchange membrane	Corn stover	Removal of acetic acid	(Wickramasinghe and Grzenia, 2008)
Membrane extraction	Corn stover	Removal of acetic, formic, levulinic and sulfuric acid, 5-HMF and furfural	(Grzenia et al., 2010)
Chemical methods			
Neutralization	Sugarcane bagasse	Removal of minor amounts of furfural and phenolics	(Chandel et al., 2007)
Neutralization	Spruce wood	Removal of part of furfural, 5-HMF and phenolic compounds, but not acetic acid, formic acid or levulinic acid	(Larsson et al., 1999;)
Calcium hydroxide over-liming	*Eucalyptus globulus* wood	Removal of lignin-derived compounds (60%)	(Converti et al., 2000)
Calcium hydroxide over-liming	Sugarcane bagasse	Removal of furans (46%) and phenolics (36%) but not acetic acid	(Chandel et al., 2007)
Calcium hydroxide over-liming	Sugarcane bagasse	Removal of furfural and 5-HMF but not organic acids	(Martínez et al., 2000)
Calcium hydroxide over-liming	*Saccharum spontaneum*	Removal of furans (42%) and phenolics (33%) but no effect on acetic acid content	(Chandel et al., 2011b)
Calcium hydroxide over-liming	Sugarcane bagasse	Removal of acetic acid (18%), furans (25%) and phenols (17%)	(Martín et al., 2002)
Activated charcoal	*Eucalyptus globulus* wood	Removal of lignin-derived compounds (95%)	(Converti et al., 2000)

Continued			
Activated charcoal	Sugarcane bagasse	Removal of furans (39%), phenolics (57%) and acetic acid (47%)	(Chandel et al., 2007)
Activated charcoal + evaporation	Sugarcane bagasse	Removal of furfural, 5-HMF and partial elimination of acetic acid and phenolic compounds	(Rodrigues et al., 2001)
Ion exchange resin	Spruce wood	Removal of most acetic acid, formic acid, levulinic acid and phenolic compounds and an important part of furfural and 5-HMF	(Larsson et al., 1999;)
Ion exchange resin	Sugarcane bagasse	Removal of furans (63%), phenolics (76%) and acetic acid (85%)	(Chandel et al., 2007)
Extraction with ethyl acetate	Aspen wood	Removal of furfural and lignin derivatives, and part of acetic acid	(Wilson et al., 1989)
Extraction with ethyl acetate	*Eucalyptus* wood	Removal of lignin-derived compounds (84%)	(Cruz et al., 1999)
Biotechnological methods			
Laccase	Spruce wood	Removal of phenolic compounds but not furfural, 5-HMF, acetic acid, formic acid or levulinic acid	(Larsson et al., 1999;)
Laccase	Sugarcane bagasse	Removal phenolics (78%) but not furans or acetic acid	(Chandel et al., 2007)
Laccase	Sugarcane bagasse	Removal of phenolic compounds (80%)	(Martín et al., 2002)
Peroxidase from *Coprinus cinereus* IFO 8371	Lignocellulosic hydrolysates	Removal of phenolic compounds	(Cho et al., 2009)
Lignin residue	Spruce	Removal of phenolic compounds (53%) and furan aldehydes (68%)	(Björklund et al., 2002)
Coniochaeta ligniaria	Corn stover	Removal of furfural (80%) and 5-HMF (80%)	(López et al., 2004)
Issatchenkia Occidentalis CCTCC M 206097 yeast	Hemicellulosic hydrolysates from different biomass plants	Removal of ferulic acid (73%), furfural (62%) and 5-HMF (85%)	(Fonseca et al., 2011)

Continued			
Solvent extraction of sugars			
3,5-Dimethylphenylboronic acid/Aliquat 336	Sugarcane bagasse	Recovery of xylose (65%) + glucose (75%) and removal of acid soluble lignin (90%)	(Griffin, 2005)
Naphthalene-2-boronic acid/Aliquat 336	Sugarcane bagasse	Recovery of xylose (50%) + glucose (80%) and removal of acid soluble lignin (90%)	(Griffin and Shu, 2004)
Phenylboronic acid/Aliquat 336	Corn stover hydrolysates in ionic liquids	Recovery of xylose (77%) + glucose (63%)	(Brennan et al., 2010)

3.2.3.1 Physical methods

Purification of hydrolysates by physical methods includes evaporation and membrane separation.

Compounds such as acetic acid and furfural can be removed by evaporation. Nevertheless, lignin derivatives remain in the hydrolysates. Wilson et al. (1989) found that rotoevaporation removed furfural and most acetic acid from aspen wood hydrolysates but did not reduce the lignin-derivatives levels. Larsson et al. (1999) claimed the removal of most furfural (90%) from a dilute-acid hydrolysate of spruce under vacuum evaporation. The content of 5-HMF however did not vary significantly, only around 4% compared to the initial concentration in the hydrolysate. Converti et al. (2000) reported a high decrease in the acetic acid content (90%) in a *Eucalyptus globulus* wood hydrolysate by subjecting the hydrolysate to boiling for 3 h.

Adsorptive membranes have surface functional groups attached to their internal pores, which can remove some inhibitors from the lignocellulosic hydrolysates (Wickramasinghe and Grzenia, 2008). Wickramasinghe et al. (2008) compared the efficiency of an anion exchange membrane to that of an anion exchange resin for acetic acid removal and observed a better performance of the membranes in terms of acetic acid capacity adsorption. They also pointed out the reduction of the operating time and the

lower pressure drop through adsorption membranes than in packed beds composed of ion exchange resins. Grzenia et al. (2010) investigated the reactive membrane extraction to purify corn stover hydrolysates after a pretreatment with sulfuric acid. They achieved a successful extraction of acetic, formic, levulinic and sulfuric acid as well as furfural and 5-HMF using octanol and oleyl alcohol as organic solvents and Alamine 336 as reactive amine extractant.

3.2.3.2 Chemical methods

Chemical methods for hydrolysates purification are classified as follows: neutralization, calcium hydroxide over-liming, activated charcoal, ion exchange resins and extraction with ethyl acetate.

Hemicellulosic hydrolysates possess some acidic compounds which can be partially removed by neutralization with sodium or calcium hydroxide. For example, Chandel et al. (2007) treated sugarcane bagasse hydrolysates with different methods (neutralization, anion exchange resins, activated charcoal, laccase). Although neutralization could reduce the levels of furfural and phenolics, it was the least effective method of all the tested and had to be combined with other processes. Larsson et al. (1999) neutralized spruce wood hydrolysates with calcium and sodium hydroxide. The amount of furfural, 5-HMF and phenolic compounds was reduced in a similar extent (~20%).

Calcium hydroxide over-liming has been demonstrated to be effective in the reduction of furfural, 5-HMF and phenolic compounds, but it did not affect the amount of organic acids (acetic acid, formic acid, levulinic acid) (Chandel et al., 2007, 2011b; Martínez et al., 2000). Chandel et al. (2007) described several treatments for the purification of sugarcane bagasse hydrolysates, over-liming among them. This process led to removal of furans (46%) and phenolics (36%) but did not cause any effect on acetic acid levels. The same trend was observed by Martínez et al. (2000) in the treatment of sugarcane bagasse

hydrolysates: over-liming revealed a substantial reduction in furfural and 5-HMF, but organic acids (acetic, formic, levulinic) were not affected. In a later work, Chandel et al. (2011b) claimed a significant decrease in furans (42%) and phenolics (33%) in *Saccharum spontaneum* acidic hydrolysates. The acetic acid content however did not vary.

The purification of hemicellulosic hydrolysates by activated charcoal is a cost-effective process. Activated charcoal has a high capacity of adsorption of several compounds and does not affect the levels of sugars (Chandel et al., 2011a). Converti et al. (2000) treated *Eucalyptus globulus* wood hydrolysates with activated charcoal and 95% of the lignin-derived compounds were removed. Chandel et al. (2007) described a treatment of sugarcane bagasse hydrolysates with activated charcoal, which caused a reduction of 39%, 57% and 47% in the content of furans, phenolics and acetic acid, respectively. Activated charcoal is also known for its good properties to remove sulfur (Hariz et al., 2014; Kumar and Srivastava, 2012). As mentioned before, this may be crucial for a successful performance of heterogeneous catalysts in a further processing.

Ion exchange resins can remove lignin derivatives, acetic acid and furans (Chandel et al., 2007; Larsson et al., 1999). Larsson et al. (1999) used an anion exchange resin (polystyrenedivinylbenzene, AG 1-X8, Bio-Rad) to treat spruce wood hydrolysates at different pH. Higher pH favored the removal of toxic compounds. For example, at pH 10, levulinic, acetic and formic acids as well as phenolics were almost completely removed, and the levels of furfural and 5-HMF decreased in ~70%. Chandel et al. (2007) examined the treatment of sugarcane bagasse hydrolysates with an anion exchange resin and a high reduction of furans (63%), phenolics (76%) and acetic acid (85%) was achieved. In addition to this, ion exchange resins can also be used to eliminate inorganic elements (*e.g.*

cations) which may poison heterogeneous catalysts used in subsequent processes (Raij et al., 1986).

Extraction with ethyl acetate is another method to reduce the amount of furfural, phenolic compounds and acetic acid (Cruz et al., 1999; Wilson et al., 1989) Wilson et al. (1989) compared the purification of aspen wood hydrolysates by rotoevaporation and ethyl acetate extraction. They demonstrated that the latter was more efficient for the removal of acetic acid and sugar- and lignin-degradation products. Cruz et al. (1999) explored the purification of *Eucalyptus globulus* wood hydrolysates with ethyl acetate and 84% of the initial lignin-derived compounds was extracted under optimal experimental conditions.

3.2.3.3 Biotechnological methods

Biological methods use microorganisms and/or enzymes to eliminate impurities from biomass hydrolysates. These methods are more feasible and environmentally-friendly than physico-chemical treatments. The inhibition of side reactions and the lower energy consumption are additional advantages of biological processes. Nevertheless, the slow reaction rate makes them unattractive (Chandel et al., 2011a).

Laccase is one of the most commonly used enzymes. Laccase has been proved to remove successfully phenolic compounds from biomass hydrolysates (Chandel et al., 2007; Larsson et al., 1999; Martín et al., 2002). Larsson et al. (1999) reported the efficiency of laccase to eliminate phenolic compounds (~80%) from spruce hydrolysates. However, organic acids and furans remained basically constant. Chandel et al. (2007) also stated a similar trend: phenolics compounds were eliminated from sugarcane bagasse hydrolysates by means of laccase, but the acetic acid content was not affected. In another work, Martín et al. (2002) claimed the good performance of this enzyme to remove a high percentage of phenolic compounds (~80%) from a sugarcane bagasse hydrolysate.

Microorganisms have also demonstrated to be active in the removal of phenolic compounds. Cho et al. (2009) investigated the removal of model phenolic compounds by peroxidase from *Coprinus cinereus*. The removal efficiency was almost 100% in the case of *p*-coumaric acid, ferulic acid, vanillic acid and vanillin. Fonseca et al. (2011) used *Issatchenkia occidentalis* CCTCC M 206097 yeast to reduce the levels of contaminants. They achieved a successful removal of several compounds, such as ferulic acid (73%), furfural (62%) and 5-HMF (85%).

3.2.3.4 Solvent extraction methods

One potential method to improve the quality of biomass hydrolysates is the use of reactive solvent extraction of sugars: sugars are first extracted from the hydrolysate into an immiscible phase and then recovered in an acidic solution (Griffin, 2005). This method consists of isolating sugars from biomass hydrolysates, as opposed to removing inhibitory compounds as happened in the processes described previously (Relue and Varanasi, 2012). The solvent extraction method is based on the chemical affinity of boronates (*e.g.* phenylboronic acid) to form reversibly stable complexes with sugars (Brennan et al., 2010; Gori et al., 2015; Griffin and Shu, 2004; Griffin, 2005; Matsumoto et al., 2005; Relue and Varanasi, 2012). The mechanism of this process can be summarized as follows (Brennan et al., 2010; Griffin, 2005). A boronic acid and a quaternary ammonium salt are dissolved in an organic phase, which is contacted with the sugar aqueous hydrolysate. At the interface between the organic and aqueous phases the boronic acid ionizes to form a tetrahedral anion. This tetrahedral anion forms an anion complex with the cis-diol groups of the sugar molecules, resulting in the extraction of the sugars into the organic phase. The sugars can be finally recovered in an acidic solution since the complexes decomposes under acidic conditions thus releasing the bond sugars. This method has also the advantage of enabling the concentration of sugar solutions. First, the organic phase must

be saturated in sugars by performing several extractions and then all the sugars can be recovered in a smaller volume of the acidic solution, which results in a highly concentrated sugar solution (Griffin and Shu, 2004; Griffin, 2005). Several works are based on this purification method. Griffin et al. (2004) tested different boronic acids (phenylboronic acid, 3,5-dimethylphenylboronic acid, 4-tert-butylphenylboronic acid, trans-β-styreneboronic acid and naphthalene-2-boronic acid) to purify and concentrate the sugars in hemicellulosic hydrolysates from sugarcane bagasse. In the purified hydrolysate, the concentrations of xylose and glucose increased over 7 and 17 times respect to those of the original hydrolysate, respectively. The authors also highlighted the high selectivity of the process since the concentration of the undesirable acid-soluble lignin was reduced by over 90%. In a later work, Griffin (2005) studied the extraction of xylose, glucose and fructose from sugarcane bagasse hydrolysates using 3,5-dimethylphenylboronic acid and modified Aliquat® 336 as extractants dissolved in Exxal® 10 diluent. They reported a concentration of sugars by 4 times and a reduction of 90% in the acid soluble lignin content. Brennan et al. (2010) investigated the recovery of sugars from ionic liquid biomass hydrolysates by using an organic phase (*n*-hexane/1-octanol) containing napthelene-2-boronic and Aliquat® 336. Up to 90% of mono- and disaccharides could be extracted from ionic liquids and corn stover hydrolysates containing ionic liquids.

Most research focuses on the removal of toxic compounds for fermentation processes, such as organic acids, furans and phenolic compounds (Chandel et al., 2011a). Nevertheless, hydrolysates are not only used for fermentation processes but also for other purposes, such as catalytic processes. One example is the production of sugar alcohols by catalytic hydrogenation of sugars. The performance of the required heterogeneous catalysts may be affected by some other compounds, *i.e.* sulfur, inorganic elements and

proteins, which are present in biomass hydrolysates and can deactivate the catalysts (Arena, 1992; Borg et al., 2011; Elliot et al., 2004). Therefore, a more exhaustive study of the purification process is required to determine the removal of compounds which are potential poisons of solid catalysts.

Current approaches to remove contaminating compounds from biomass hydrolysates include chemical/physical conditioning steps followed by evaporation-based concentration methods. The conditioning steps originate solid residues, whose disposal can be expensive and harmful to the environment. Similarly, evaporation concentration methods are energy-intensive and not economically viable on an industrial scale.

In this PhD Thesis, the purification of wheat bran hydrolysates followed by the subsequent hydrogenation of sugars are examined in Chapter 5. The strategy followed to purify wheat bran hydrolysates is based on the selective recovery of sugars by anionic extraction with a boronic acid dissolved in an organic phase. Sugars are then back-extracted in an acidic solution and further purified with ion exchange resins. Such an approach provides a clean sugar solution, which can be successfully hydrogenated into the corresponding sugar alcohols without the catalysts being deactivated. Unlike chemical and physical purification methods, the purification process proposed in this PhD Thesis results to be cost-effective and minimizes the waste disposal due to the recyclability of the organic phase.

3.2.4 Hydrogenation of sugars into sugar alcohols

Sugars from biomass hydrolysates are susceptible to be converted into high added-value chemicals, such as sugar alcohols. Sugar alcohols, *i.e.* sorbitol, xylitol and arabitol, are among the top 12 value added chemicals which can be produced from biomass sugars (Werpy and Petersen, 2004). They have important applications in food, beverage, confectionary and pharmaceutical industries. Sugar alcohols are widely used as reduced-

calorie sweeteners for sugar substitution and as excipients in medicines (Grembecka, 2015). In addition to this, they are building blocks of important chemicals, such as isosorbide, lactic acid, glycerol, ethylene glycol or propylene glycol (Werpy and Petersen, 2004).

Sugar alcohols can be produced biologically or chemically. Table 5 shows some results on sugar alcohols production via biotechnological and chemical processes.

Table 5. Results on production of sugar alcohols via biotechnological and chemical processes.

Raw material	Catalyst/ Enzyme	Operating conditions	Sorbitol yield (%)	Xylitol yield (%)	Arabitol yield (%)	Reference
Biotechnological processes						
Fructose (+ Glucose)	*Zymomonas mobilis* ATCC 29191	39 ºC, 8 h	92	-	-	(Silveira et al., 1999)
Fructose (+ Glucose)	*Zymomonas mobilis* ATCC 29191	39 ºC, 8 h	95	-	-	(Erzinger and Vitolo, 2006)
Inulin + Starch	*Zymomonas mobilis* (pHW20a-gfo)	39 ºC, several hours	97	-	-	(An et al., 2013)
Xylose	*Candida tropicalis* DSM 7524	37 ºC, several hours	-	84	-	(Tamburini et al., 2015)
Xylose	*Candida mogii* ATCC 18364	30 ºC, 20 h	-	62	-	(Sirisansaneeyakul et al., 1995)
Beech wood hydrolysate	*Candida tropicalis* IFO0618	30 ºC, 24 h	-	50	-	(Tran et al., 2004)
Sugarcane bagasse	*Candida guilliermondii*	30 ºC, 24 h	-	59	-	(Da Silva et al., 2007)
Arabinose	*Candida parapsilosis* strain 27RL-4	28 ºC, 48 h	-	-	55	(Kordowska-Wiater et al., 2017)

Continued						
Arabinose	*Candida parapsilosis* DSM 70125	28 ºC, several hours	-	-	78	(Kordowska-Wiater et al., 2008)
Soybean flour and hulls hydrolysates	*Debaryomyces hansenii*	30 ºC, 48 h	-	-	54	(Loman et al., 2018)
Chemical processes						
Glucose	Ni(20)/SiO_2	120 ºC, 5 h, 120 bar H_2	42	-	-	(Schimpf et al., 2007)
Glucose	Pt(2)Sn(0.25)/Al	130 ºC, 2 h, 16 bar H_2 at R.T.	78	-	-	(Tathod and Dhepe, 2015)
Glucose	Ru(1)/HY (80)	120 ºC, 20 min, 55 bar H_2	98	-	-	(Mishra et al., 2014)
Glucose	Ru(1)/NiO-TiO_2	120 ºC, 20 min, 55 bar H_2	96	-	-	(Mishra et al., 2014)
Glucose	Ru(1)/TiO_2	120 ºC, 20 min, 55 bar H_2	93	-	-	(Mishra et al., 2014)
Glucose	Ru(5)/C	120 ºC, 20 min, 55 bar H_2	93	-	-	(Mishra et al., 2014)
Glucose	Ru(4)/MCM-48	120 ºC, 25 min, 25 bar H_2	90	-	-	(Romero et al., 2016)
Glucose	Ru(4)/TiO_2	120 ºC, 20 min, 25 bar H_2	91	-	-	(Romero et al., 2016)
Glucose	Ru(5)/C	120 ºC, 10 min, 25 bar H_2	95	-	-	(Romero et al., 2016)
Glucose	Ru/ZSM-5	120 ºC, 2 h, 40 bar H_2	96	-	-	(Guo et al., 2014)
Xylose	Pt(2)Sn(0.25)/Al	130 ºC, 2 h, 16 bar H_2 at R.T.	-	85	-	(Tathod and Dhepe, 2015)
Xylose	Raney Nickel	120 ºC, 2 h, 55 bar H_2	-	94	-	(Yadav et al., 2012)
Xylose	Ru(1)/TiO_2	120 ºC, 3 h, 20 bar H_2	-	93	-	(Hernández-Mejia et al., 2016)
Xylose	Ru(1)/C	120 ºC, 2 h, 55 bar H_2	-	98	-	(Yadav et al., 2012)
Xylose	Ru(1)/TiO_2	120 ºC, 2 h, 55 bar H_2	-	99	-	(Yadav et al., 2012)
Xylose	Ru(1)/NiO(5)-TiO_2	120 ºC, 2 h, 55 bar H_2	-	100	-	(Yadav et al., 2012)

Continued

Xylose	Ru(1)/HY (5.1)	120 ºC, 1 h, 55 bar H_2	-	68	-	(Mishra et al., 2013)
Xylose	Ru(1)/HY (5.2)	120 ºC, 1 h, 55 bar H_2	-	70	-	(Mishra et al., 2013)
Xylose	Ru(1)/HY (30)	120 ºC, 1 h, 55 bar H_2	-	86	-	(Mishra et al., 2013)
Xylose	Ru(1)/HY (60)	120 ºC, 1 h, 55 bar H_2	-	94	-	(Mishra et al., 2013)
Xylose	Ru(1)/HY (80)	120 ºC, 1 h, 55 bar H_2	-	98	-	(Mishra et al., 2013)
Arabinose	Pt(2)Sn(0.25)/Al	130 ºC, 2 h, 16 bar H_2 at R.T.	-	-	92	(Tathod and Dhepe, 2015)
Cellulose	Pt(2.5)/γ-Al_2O_3	190 ºC, 24 h, 50 bar H_2	32	-	-	(Fukuoka and Dhepe, 2006)
Cellulose	Pt(2.5)/H-USY (40)	190 ºC, 24 h, 50 bar H_2	26	-	-	(Fukuoka and Dhepe, 2006)
Cellulose	Pt(2.5)/SiO_2-Al_2O_3	190 ºC, 24 h, 50 bar H_2	23	-	-	(Fukuoka and Dhepe, 2006)
Cellulose	Pt(2.5)/H-USY(20)	190 ºC, 24 h, 50 bar H_2	24	-	-	(Fukuoka and Dhepe, 2006)
Cellulose	Ru(2.5)/H-USY(20)	190 ºC, 24 h, 50 bar H_2	25	-	-	(Fukuoka and Dhepe, 2006)
Xylan	Rh(0.4)/CNT	205 ºC, 2 h, 50 bar H_2	-	5	-	(Ribeiro et al., 2017)
Xylan	Ru(0.4)/CNT	205 ºC, 2 h, 50 bar H_2	-	38	-	(Ribeiro et al., 2017)
Xylan	Pt(0.4)/CNT	205 ºC, 2 h, 50 bar H_2	-	10	-	(Ribeiro et al., 2017)
Xylan	Pd(0.4)/CNT	205 ºC, 2 h, 50 bar H_2	-	4	-	(Ribeiro et al., 2017)
Xylan	Ni(0.4)/CNT	205 ºC, 2 h, 50 bar H_2	-	6	-	(Ribeiro et al., 2017)
Arabinoxylan	Ru(0.6)/USY(6)	160 ºC, 5 h, 50 bar H_2	-	90[a]		(Ennaert et al., 2016)
Arabinogalactan	Ru(5)/MCM-48	185 ºC, 24 h, 20 bar H_2	-	25[b]		(Kusema et al., 2012)

Continued					
Arabinogalactan	Ru(2.5)/H-USY	185 ºC, 24 h, 31 bar H_2	-	25[b]	(Murzin et al., 2015a)
Arabinogalactan	Ru/Beta	185 ºC, 4 h, 21 bar H_2		10[b]	(Faba et al., 2014)

[a] Arabitol + xylitol yield.
[b] Arabitol + galactitol yield.

3.2.4.1 Biotechnological processes

Biotechnologically, sorbitol is usually produced by *Zymomonas mobilis* strains from fructose present in sucrose or glucose/fructose mixtures. The presence of glucose is crucial for the formation of sorbitol from fructose. The production of sorbitol from fructose is a result of a glucose-fructose transhydrogenase which is involved in the oxidation of glucose to gluconic acid and the subsequent reduction of fructose to sorbitol (Duvnjak et al., 1991). Therefore, the bioproduction of sorbitol from fructose is always accompanied by the co-production of gluconic acid from glucose, which is a drawback since an additional purification step is required. Silveira et al. (1999) studied the bioconversion of glucose and fructose to gluconic acid and sorbitol, respectively, by untreated cells of *Zymomonas mobilis*. A high sorbitol yield was obtained (92%) using a mixture of glucose/fructose (750 $g \cdot L^{-1}$) at 39 ºC for 8 hours. Gluconic acid was produced from glucose also with a high yield (90%). In a later work, Erzinger et al. (2006) also reported the production of sorbitol from glucose/fructose mixtures with cells of *Zymomonas mobilis*. They achieved a yield of sorbitol of 95% at 39 ºC and 8 hours. An et al. (2013) investigated the conversion of inulin and starch into sorbitol after an enzymatic hydrolysis of the substrates. Cells of *Zymomonas mobilis* were successfully used to convert fructose into sorbitol and glucose into gluconic acid.

The bioproduction of xylitol and arabitol from xylose and arabinose, respectively, is usually carried out by different types of *Candida* yeasts (Da Silva et al., 2007; Dien et al., 1996; Kordowska-Wiater et al., 2008, 2017; Saha and R.J. Bothast, 1996;

Sirisansaneeyakul et al., 1995; Tamburini et al., 2015; Tran et al., 2004). The yeast *Candida tropicalis* DSM 7524 was used to produce xylitol from xylose by Tamburini et al. (2015), who reported a maximum xylitol yield of 84% at 37 ºC after several hours. Da Silva et al. (2007) examined the effect of glucose on the bioconversion of xylose from sugarcane bagasse hydrolysate to xylitol by *Candida guilliermondii*. Glucose demonstrated to have a positive effect on the production of xylitol. The optimum xylitol yield (59%) was achieved at a ratio glucose : xylose = 1:5 at 30 ºC after 24 hours. Kordowska-Wiater et al. (2017) used *Candida parapsilosis* 27RL-4 to convert arabinose into arabitol. The optimal conditions for this strain were as follows: concentration of arabinose in the medium 20 $g \cdot L^{-1}$, initial pH 5.5, incubation temperature 28 ºC, time 48 hours, and rotational speed 150 rpm. Under these conditions, the final product concentration was closed to 11 $g \cdot L^{-1}$, *i.e.* an arabitol yield of 55%. Loman et al. (2018) studied for the first time the effects of medium composition, operating conditions and culture stage on the production of arabitol from mixed hydrolysates of soy flour and hulls. An arabitol yield of 54% was obtained at 30 ºC after 48 hours.

3.2.4.2 Chemical processes

The biotechnological production of sugar alcohols based on microbial fermentation is safe and environmentally friendly and occurs under milder operating conditions than chemical processes (Park et al., 2016). However, most sugar alcohols are industrially produced by catalytic hydrogenation of sugars since it offers higher yields and conversion efficiencies as well as an economical large-scale production (Dasgupta et al., 2017). Catalytic hydrogenation of sugars is carried out under relatively high temperatures (80 – 160 ºC) and hydrogen pressures (40 – 70 bar) (Guo et al., 2014; Hernández-Mejia et al., 2016; Mikkola et al., 1999, 2000; Mishra et al., 2013, 2014; Müller et al., 2017; Romero et al., 2016; Yadav et al., 2012). Table 5 shows some results on hydrogenation of sugars

and polysaccharides over different metals and catalyst supports. Nickel has historically been used as active metal in the catalytic hydrogenation of sugars (Brahme and Doraiswamy, 1976; Gallezot et al., 1994; Kusserow et al., 2003; Wisniak and Simon, 1979; Wisniak et al. 1974; Yadav et al., 2012). Specifically, Raney nickel started to be used in the early research due to its economic price and later supported nickel catalysts became more common because of their higher activity (Kusserow et al., 2003). The main advantages of nickel catalysts are their low price, their easy use as suspended slurry in typical batch reactor and their good activity and selectivity (Mikkola and Salmi, 2001; Yadav et al., 2012). However, the fast deactivation of nickel catalysts due to metal leaching and poisoning of the active sites by organic impurities are the major drawbacks. Consequently, conversion and selectivity decrease. In addition to this, nickel must be removed from the hydrogenated solution which adds further expensive costs (Kusserow et al., 2003; Mäki-Arvela et al., 2007; Schimpf et al., 2007; Yadav et al., 2012). In recent years, catalysts based on other active metals, including platinum (Fukuoka and Dhepe, 2006; Guha et al., 2011; Käldström et al., 2011; Kobayashi et al., 2014; Perrard et al., 2007; Ribeiro et al., 2017; Tathod and Dhepe, 2015; Tathod et al., 2014), palladium (Ribeiro et al., 2017; Sanz-Moral et al., 2016; Wisniak et al. 1974), rhodium (Ribeiro et al., 2017; Wisniak and Simon, 1979; Wisniak et al. 1974) and ruthenium (Aho et al., 2015; Baudel et al., 2005; Dietrich et al., 2017; Ennaert et al., 2016; Faba et al., 2014; Fukuoka and Dhepe, 2006; Geboers et al., 2011; Guha et al., 2011; Guo et al., 2014; Hernández-Mejia et al., 2016; Herrera et al., 2012; Käldström et al., 2011; Kusema et al., 2012; Kusserow et al., 2003; Mishra et al., 2013, 2014; Murzin et al., 2015a, 2015b; Ribeiro et al., 2016; Ribeiro et al., 2017; Romero et al., 2016; Wisniak et al. 1974; Yadav et al., 2012; Yi and Zhang, 2012) have been evaluated. Among them, ruthenium-based catalysts have been the most used since they are more effective than other metal catalysts

in terms of activity and selectivity under similar conditions (Baudel et al., 2005; Kusserow et al., 2003). Ribeiro et al. (2017) has recently studied the conversion of xylan to xylitol over different metal catalysts (Rh, Ru, Pt, Pd, Ni) supported on carbon nanotubes (CNT). Ruthenium supported on CNT exhibited the highest yield of xylitol (~38%) among all the catalysts tested, followed by Pt/CNT (~10%), Ni/CNT (~6%), Rh/CNT (~5%) and Pd/CNT (~4%). The maximum xylitol yield (~80%) was achieved over Ru(0.4%)/CNT at 170 ºC, 50 bar H_2 after 2 hours of reaction. Yadav et al. (2012) evaluated the hydrogenation of xylose over Raney nickel and ruthenium catalysts supported on NiO modified TiO_2 materials. The results indicated higher selectivity of all Ru catalysts compared to conventional Raney nickel catalyst due to the higher reactivity of Ru than Ni. The catalyst Ru/NiO-TiO_2 showed optimum conversion of xylose (99.9%) with a xylitol yield of 99.7% and a selectivity of 99.8%. Besides higher activity, ruthenium supported catalysts show much less or no deactivation compared to other metal catalysts (Yadav et al., 2012). Kusserow et al. (2003) compared the activity and deactivation of supported nickel and ruthenium catalysts in the hydrogenation of glucose. Nickel catalysts were deactivated by leaching of the metal, changes in the crystallite size distribution and degradation of the support. Nevertheless, ruthenium catalysts demonstrated to be superior to nickel catalysts in terms of specific activity and lifetime. Moreover, no ruthenium leaching was detected after long times. Although ruthenium is more expensive than nickel, the global costs involved with ruthenium catalysts are reduced because a much lower metal content is required, and the lifetime of the catalyst is longer.

Not only the active metal but also the structure and properties of the support may play an important role in the hydrogenation of sugars (Romero et al., 2016). Different materials have been employed as catalyst supports: carbon (Aho et al., 2015; Dietrich et al., 2017;

Guha et al., 2011; Herrera et al., 2012; Kobayashi et al., 2014; Murzin et al., 2015b; Ribeiro et al., 2016, 2017; Yi and Zhang, 2012), Al_2O_3 (Guha et al., 2011; Tathod and Dhepe, 2015; Tathod et al., 2014), TiO_2 (Hernández-Mejia et al., 2016; Yadav et al., 2012), MCM-48 (Käldström et al., 2011; Kusema et al., 2012; Romero et al., 2016) and zeolites, such as beta (Faba et al., 2014), H-Y (Ennaert et al., 2016; Fukuoka and Dhepe, 2006; Geboers et al., 2011; Mishra et al., 2013, 2014; Murzin et al., 2015a) and H-ZSM-5 (Guo et al., 2014). Yadav et al. (2012) compared the catalytic activity of ruthenium catalysts over different supports (C, TiO_2, NiO-TiO_2) on the conversion of xylose to xylitol. The order of catalytic activity in terms of selectivity was as follows: Ru(1.0%)/NiO(5.0%)-TiO_2 > Ru(1.0%)/TiO_2 > Ru(1.0%)/C. They determined that the NiO incorporated in modified support (NiO-TiO_2) played an important role to minimize the amount of arabitol and other by-products. Guha et al. (2011) compared ruthenium and platinum catalysts, and different supports on the catalytic hydrogenolysis of sugar beet fiber. A higher arabitol yield was reported over Ru/C (33%) than Ru/γ-Al_2O_3 (2%). Mishra et al. (2013) examined the conversion of xylose to xylitol over ruthenium catalysts and studied the effect of the catalyst support (H-Y zeolites, carbon). On the one hand, a positive impact on xylitol production was reported by increasing the Si/Al ratio of H-Y zeolites. Zeolites with high Si/Al ratios promotes hydrogenation over secondary reaction pathways, resulting in a higher xylitol selectivity. On the other hand, the activity of Ru(3%)/H-Y was compared to that of Ru(5%)/C commercial. Ru(3%)/H-Y (80) catalyst even at lower Ru loading demonstrated a higher activity than Ru(5%)/C due to the lower activation energy and higher selectivity to xylitol. In another work, Mishra et al. (2014) evaluated the activity of ruthenium catalysts impregnated on different supports (H-Y, NiO-TiO_2, TiO_2, C) on glucose hydrogenation. Ru/H-Y gave the maximum value of turn over frequency (TOF) and a sorbitol yield of 98% was reached at 120 ºC after 20 minutes.

This catalyst increased the selectivity to sorbitol by suppressing the formation of other by-products. Only one work on hydrogenation of glucose over ruthenium catalysts supported on ZSM-5 zeolites was found (Guo et al., 2014). In this work, Guo et. al compared the activity of Ru/ZSM-5 catalysts synthesized by different methods. A high conversion of glucose (99.6%) with high selectivity to sorbitol (99.2%) was obtained over the Ru/ZSM-5 catalyst prepared by a one-step template-free process. Ru/ZSM-5 showed high stability against leaching and poisoning and could be reused several times. This fact was attributed to the high dispersion of Ru particles onto the support, the strong interaction between Ru species and ZSM-5 and the suitable surface acidity-basicity balance.

Ruthenium supported on ZSM-5 zeolites demonstrated to be a promising catalyst for sugars hydrogenation. However, as mentioned before, only one work related to hydrogenation of sugars over this catalyst was found. This motivated a further study of the sugar hydrogenation process over Ru/ZSM-5 in the present PhD Thesis. In Chapter 4, the hydrogenation of sugar model mixtures (glucose, xylose, arabinose) over ruthenium supported on different ZSM-5 zeolites was discussed. Likewise, a kinetic study was performed to reproduce the experimental data. The conversion of model hemicellulosic compounds, *i.e.* C_5 sugars and commercial oligosaccharides into sugar alcohols has been widely studied for many years. However, works related to the catalytic hydrogenation of real biomass or pentosane-rich hydrolysates are scarce. Therefore, a study on hydrogenation of sugars from real hydrolysates is required since the activity of the metal catalyst may be affected by different biomass compounds. In Chapter 5, the hydrogenation of sugars from wheat bran hydrolysates was investigated before and after a purification process.

References

Aden, A., Ruth, M., Ibsen, K., Jechura, J., Neeves, K., Sheehan, J., Wallace, B., Montague, L., Slayton, A., and Lukas, J. Lignocellulosic biomass to ethanol process design and economics utilizing co-current dilute acid prehydrolysis and enzymatic hydrolysis for corn stover, NREL/TP-510-32438, 2002.

Aguedo, M., Fougnies, C., Dermience, M., and Richel, A. Extraction by three processes of arabinoxylans from wheat bran and characterization of the fractions obtained. *Carbohydrate Polymers*, 105 (2004) 317–324.

Aho, A., Roggan, S., Simakova, O.A., Salmi, T., and Murzin, D.Y. Structure sensitivity in catalytic hydrogenation of glucose over ruthenium. *Catalysis Today*, 241 (2015) 195–199.

Akoinar, O., Erdogan, K., and Bostanci, S. Production of xylooligosaccharides by controlled acid hydrolysis of lignocellulosic materials. *Carbohydrate Research,* 344 (2009) 660–666.

An, K., Hu, G., and Bao, J. Simultaneous saccharification of inulin and starch using commercial glucoamylase and the subsequent bioconversion to high titer sorbitol and gluconic acid. *Applied Biochemistry and Biotechnology,* 171 (2013) 2093–2104.

Apprich, S., Tirpanalan, Ö., Hell, J., Reisinger, M., Böhmdorfer, S., Siebenhandl-Ehn, S., Novalin, S., and Kneifel, W. Wheat bran-based biorefinery 2: Valorization of products. *LWT – Food Science and Technology,* 56 (2014) 222–231.

Arena, B.J. Deactivation of ruthenium catalysts in continuous glucose hydrogenation. *Applied Catalysis A: General,* 87 (1992) 219–229.

Bajpai, P. Uses of recovered paper other than papermaking. *Recycling and Deinking of Recovered Paper,* (2014) 283–295.

Bastos, R., Coelho, E., and Coimbra, M.A. Arabinoxylans from cereal by-products: Insights into structural features, recovery and applications. In *Sustainable Recovery and Reutilization of Cereal Processing By-Products*, Galanakis, C.M., (Ed.), Woodhead Publishing, 2018.

Bataillon, M., Mathaly, P., Cardinali, A-P.N., and Duchiron, F. Extraction and purification of arabinoxylan from destarched wheat bran in a pilot scale. *Industrial Crops and Products,* 8 (1998) 37–43.

Baudel, H.M., De Abreu, C.A.M., and Zaror, C.Z. Xylitol production via catalytic hydrogenation of sugarcane bagasse dissolving pulp liquid effluents over Ru/C catalyst. *Journal of Chemical Technology and Biotechnology,* 80 (2005) 230–233.

Beaugrand, J., Chambat, G., Wong, V.W.K., Goubet, F., Rémond, C., Päes, G., Benamrouche, S., Debeire, P., O´Donohue, M., and Chabbert, B. Impact and efficiency of GH10 and GH11 thermostable endoxylanases on wheat bran and alkali-extractable arabinoxylans. *Carbohydrate Research,* 339 (2004a) 2529–2540.

Beaugrand, J., Crônier, D., Debeire, P., and Chabbert, B. Arabinoxylan and hydroxycinnamate content of wheat bran in relation to endoxylanase susceptibility. *Journal of Cereal Science,* 40 (2004b) 223–230.

Bhaumik, P., and Dhepe, P.L. Conversion of biomass into sugars. In *Biomass sugars for non-fuel applications*, Murzin, D., and Simakova, O., (Eds.), RSC Green Chemistry, 2016.

Björklund, L., Larsson, S., Jönsson, L.J., Reimann, E., and Nilvebrant, N.O. Treatment with lignin residue: a novel method for detoxification of lignocellulose hydrolysates. *Applied Biochemistry and Biotechnology,* 98–100 (2002) 563–575.

Bochek, A.M., and Kalyuzhnaya, L.M. Interaction of water with cellulose and cellulose acetates as influenced by the hydrogen bond system and hydrophilic-hydrophobic balance of the macromolecules. *Russian Journal of Applied Chemistry,* 75 (2002) 989–993.

Borg, Ø., Hammer, N., Enger, B.C., Myrstad, R., Lindvåg, O.A., Eri, S., Skagseth, T.H., and Rytter, E. Effect of biomass-derived synthesis gas impurity elements on cobalt Fischer-Tropsch catalyst performance including in situ sulphur and nitrogen addition. *Journal of Catalysis*, 279 (2011) 163–173.

Bouza, R.J., Gu, Z., and Evans, J.H. Screening conditions for acid pretreatment and enzymatic hydrolysis of empty fruit bunches. *Industrial Crops and Products,* 84 (2016) 67–71.

Brahme, P.H., and Doraiswamy, L.K. Modelling of a slurry reaction. Hydrogenation of glucose on Raney nickel. *Industrial & Engineering Chemistry Process Design and Development,* 15 (1976) 130–137.

Brennan, T.C.R., Datta, S., Blanch, H.W., Simmons, B.A., and Holmes, B.M. Recovery of sugars from ionic liquid biomass liquor by solvent extraction. *Bioenergy Research*, 3 (2010) 123–133.

Briens, C., Piskorz, J., and Berruti, F. Biomass valorization for fuel and chemicals production – A review. *International Journal of Chemical Reactor Engineering,* 6 (2008) 1542–6580.

Buranov, A.U., and Mazza, G. Extraction and characterization of hemicelluloses from flax shives by different methods. *Carbohydrate Polymers*, 79 (2010) 17–25.

Cara, C., Ruiz, E., Ballesteros, I., Negro, M.J., and Castro, E. Enhanced enzymatic hydrolysis of olive tree wood by steam explosion and alkaline peroxide delignification. *Process Biochemistry,* 41 (2006) 423–429.

Cará, P.D., Pagliaro, M., Elmekawy, A., Brown, D.R., Verschuren, P., Shiju, N.R., and Rothenberg, G. Hemicellulose hydrolysis catalysed by solid acids. *Catalysis Science & Technology*, 3 (2013) 2057–2061.

Carvalheiro, R., Duarte, L.C., Gírio, F., and Moniz, P. Hydrothermal/liquid hot water pretreatment (autohydrolysis): a multipurpose process for biomass upgrading. In *Biomass Fractionation Technologies for a Lignocellulosic Feedstock Based Biorefinery*, Mussatto, S.I., (Ed.), Elsevier: Amsterdam, 2016.

Chandel, A.K., Da Silva, S.S., and Singh, O.V. Detoxification of lignocellulosic hydrolysates for improved bioethanol production. In *Biofuel Production - Recent Developments and Prospects*, Dr. Bernardes, M.A.D.S., (Ed.), InTech, 2011a.

Chandel, A.K., Kapoor, R.K., Singh, A., and Kuhad, R.C. Detoxification of sugarcane bagasse hydrolysate improves ethanol production by *Candida shehatae* NCIM 350. *Bioresource Technology*, 98 (2007) 1947–1950.

Chandel, A.K., Singh, O.V., Chandrasekhar, G., Rao, L.V., and Narasu, M.L. Bioconversion of novel substrate, *Saccharum spontaneum*, a weedy material into ethanol by *Pichia stipites* NCIM3498. *Bioresource Technology*, 102 (2011b) 1709–1714.

Chareonlimkun, A., Champreda, V., Shotipruk, A., and Laosiripojana, N. Reactions of C_5 and C_6-sugars, cellulose, and lignocellulose under hot compressed water (HCW) in the presence of heterogeneous acid catalysts. *Fuel*, 89 (2010) 2873–2880.

Cherubini, F. The biorefinery concept: Using biomass instead of oil for producing energy and chemicals. *Energy Conversion and Management*, 51 (2010) 1412–1421.

Cho, D.H., Lee, Y.J., Um, Y., Sang, B-I., and Kim, Y.H. Detoxification of model phenolic compounds in lignocellulosic hydrolysates with peroxidase for butanol production from

Clostridium beijerinckii. *Applied Microbiology and Biotechnology,* 83 (2009) 1035–1043.

Coelho, E., Rocha, M.A.M., Saraiva, J.A., and Coimbra, M.A. Microwave superheated water and dilute alkali extraction of brewers' spent grain arabinoxylans and arabinoxylo-oligosaccharides. *Carbohydrate polymers,* 99 (2014) 415–422.

Converti, A., Domínguez, J.M., Perego, P., Da Silva, S.S., and Zilli, M. Wood hydrolysis and hydrolysate detoxification for subsequent xylitol production. *Chemical Engineering and Technology*, 23 (2000) 1013–1020.

Courtin, C.M., and Delcour, J.A. Relative activity of endoxylanases towards water-extractable and water-unextractable arabinoxylan. *Journal of Cereal Science,* 33 (2001) 301–312.

Cruz, J.M., Domínguez, J.M., Domínguez, H., and Parajó, J.C. Solvent extraction of hemicellulosic wood hydrolysates: a procedure useful for obtaining both detoxified fermentation media and polyphenols with antioxidant activity. *Food Chemistry,* 67 (1999) 147–153.

Cui, W.S., Wood, P.J., Weisz, J., and Beer, M.U. Non-starch polysaccharides from pre-processed wheat bran: Chemical composition and novel rheological properties. *Cereal Chemistry,* 76 (2000) 129–133.

Da Silva, D.D.V., De Mancilha, I.M., Da Silva, S.S., and Felipe, M.D.G.D.A. Improvement of biotechnological xylitol production by glucose during cultive of *Candida guilliermondii* in sugarcane bagasse hydrolysate. *Brazilian Archives of Biology and Technology,* 50 (2007) 207–215.

Das, A.M., Hazarika, M.P., Goswami, M., Yadav, A., and Khound, P. Extraction of cellulose from agricultural waste using Montmorillonite K-10/LiOH and its conversion

to renewable energy: Biofuel by using Myrothecium gramineum. *Carbohydrate Polymers*, 141 (2016) 20–27.

Dasgupta, D., Bandhu, S., Adhikari, D.K., and Ghosh, S. Challenges and prospects of xylitol production with whole cell bio-catalysis: A review. *Microbiological Research*, 197 (2017) 9–21.

De Almedia, R.M., De Albuquerque, N.J.A., Souza, F.T.C., and Meneghetti, S.M.P. Catalysts based on TiO_2 anchored with MoO_3 or SO_4^{2-} for conversion of cellulose into chemicals. *Catalysis Science & Technology*, 6 (2016) 3137–3142.

De Jong, W. Biomass composition, properties, and characterization. In *Biomass as a Sustainable Energy Source for the Future*, De Jong, W., and Van Ommen, J.R., (Eds.), American Institute of Chemical Engineers, Inc., 2014.

Dhepe, P.L., and Sahu, R. A solid-acid-based process for the conversion of hemicellulose. *Green Chemistry*, 12 (2010) 2153–2156.

Dhyani, V., and Bhaskar, T. A comprehensive review on the pyrolysis of lignocellulosic biomass. *Renewable Energy*, (2017). DOI: 10.1016/j.renene.2017.04.035.

Dien, B.S., Kurtzman, C.P., Saha, B.C., and Bothast, R.J. Screening for L-arabinose fermenting yeasts. *Applied Biochemistry and Biotechnology*, 57–58 (1996) 233–242.

Dien, B.S., Li, X-L., Iten, L.B., Jordan, D.B., Nichols, N.N., O´Bryan, P.J., and Cotta, M.A. Enzymatic saccharification of hot-water pretreated corn fiber for production of monosaccharides. *Enzyme and Microbial Technology*, 39 (2006) 1137–1144.

Dietrich, K., Hernández-Mejia, C., Verschuren, P., Rothenberg, G., and Shiju, N.R. One-pot selective conversion of hemicellulose to xylitol. *Organic Process Research & Development*, 21 (2017) 165–170.

Doner, L.W., and Hicks, K.B. Isolation of hemicellulose from corn fiber by alkaline hydrogen peroxide extraction. *Cereal Chemistry,* 74 (1997) 176–181.

Doner, L.W., Chau, H.K., Fishman, M.L., and Hicks, K.B. An improved process for isolation of corn fiber gum. *Cereal Chemistry,* 75 (1998) 408–411.

Duarte, L.C., Silva-Fernandes, T., Carvalheiro, F., and Gírio, F.M. Dilute acid hydrolysis of wheat straw oligosaccharides. *Applied Biochemistry and Biotechnology,* 153 (2009) 116–126.

DuPont, M.S., and Selvendran, R.R. Hemicellulose polymers from the cell walls of beeswing wheat bran: Part I, polymers solubilized by alkali. *Carbohydrate Research,* 163 (1987) 99–113.

Duvnjak, Z., Turcotte, G., and Duan, Z.D. Production and consumption of sorbitol and fructose by *Saccharomyces cerevisiae* ATCC 36859. *Journal of Chemical Technology & Biotechnology,* 52 (1991) 527–237.

Ebringerova, A., and Hromadkova, Z. The effect of ultrasound on the structure and properties of the water-soluble corn hull heteroxylan. *Ultrasonics Sonochemistry,* 4 (1997) 304–309.

Elliot, D.C., Peterson, K.L., Muzatko, D.S., Alderson, E.V., Hart, T.R., and Neuenschwander, G.G. Effects of trace contaminants on catalytic processing of biomass-derived feedstocks. *Applied Biochemistry and Biotechnology,* 113–116 (2004) 807–825.

Ennaert, T., Feys, S., Hemdrikx, D., Jacobs, P.A., and Sels, B.F. Reductive splitting of hemicellulose with stable ruthenium-loaded USY zeolites. *Green Chemistry,* 18 (2016) 5295–5304.

Erzinger, G.S., and Vitolo, M. *Zymomonas mobilis* as catalyst for the biotechnological production of sorbitol and gluconic acid. *Applied Biochemistry and Biotechnology,* 131 (2006) 787–794.

Escarnot, E., Aguedo, M., and Paquot, M. Enzymatic hydrolysis of arabinoxylans from spelt bran and hull. *Journal of Cereal Science,* 55 (2012) 243–253.

Faba, L., Kusema, B.T., Murzina, E.V., Tokarev, A., Kumar, N., Smeds, A., Díaz, E., Ordóñez, S., Mäki-Arvela, P., Willför, S., Salmi, T., and Murzin, D.Y. Hemicellulose hydrolysis and hydrolytic hydrogenation over proton- and metal modified zeolites. *Microporous and Mesoporous Materials,* 189 (2014) 189–199.

Faurot, A-L., Saulnier, L., Bérot, S., Popineau, Y., Petit, M-D., Rouau, X., and Thibault, J-F. Large scale isolation of water-soluble and water-insoluble pentosans from wheat flour. *LWT – Food Science and Technology,* 28 (1995) 436–441.

Fernando, S., Adhikari, S., Chandrapal, C., and Murali, N. Biorefineries: Current status, challenges and future direction. *Energy & Fuels,* 20 (2006) 1727–1737.

Fonseca, B.G., Moutta, R.O., Ferraz, F.O., Vieira, E.R., Nogueira, A.S., Baratella, B.F., Rodrigues, L.C., Hou-Rui, Z., and Da Silva, S.S. Biological detoxification of different hemicellulosic hydrolysates using *Issatchenkia occidentalis* CCTCC M 206097 yeast. *Journal of Industrial Microbiology and Biotechnology,* 38 (2011) 199–207.

Fukuoka, A., and Dhepe, P.L. Catalytic conversion of cellulose into sugar alcohols. *Angewandte Chemie International Edition,* 45 (2006) 5161–5163.

Gallezot, P. Conversion of biomass to selected chemicals products. *Chemical Society Reviews,* 41 (2012) 1538–1558.

Gallezot, P., Cerino, P.J., Blanc, B., Flèche, G., and Fuertes, P. Glucose hydrogenation on promoted raney-nickel catalysts. *Journal of Catalysis,* 146 (1994) 93–102.

Garrote, G., Domínguez, H., and Parajó, J.C. Generation of xylose solutions from Eucalyptus globulus wood by autohydrolysis-posthydrolysis processes: posthydrolysis kinetics. *Bioresource Technology,* 79 (2001a) 155–164.

Garrote, G., Dominguez, H., and Parajó, J.C. Hydrothermal processing of lignocellulosic materials. *Holz als Roh- und Werkstoff,* 57 (1999) 191–202.

Garrote, G., Dominguez, H., and Parajo, J.C. Kinetic modelling of corncob autohydrolysis. *Process Biochemistry,* 36 (2001b) 571–578.

Geboers, J., Van de Vyver, S., Carpentier, K., Jacobs, P., and Sels, B. Efficient hydrolytic hydrogenation of cellulose in the presence of Ru-loaded zeolites and trace amounts of mineral acid. *Chemical Communications,* 47 (2011) 5590–5592.

Gori, S.S., Raju, M.R., Fonseca, D.A., Satyavolu, J., Burns, C.T., and Nantz, M.H. Isolation of C-5 sugars from the hemicellulose-rich hydrolysate of distillers dried grains. *ACS Sustainable Chemistry and Engineering,* 3 (2015) 2452–2457.

Grembecka, M. Sugar alcohols – their role in the modern world of sweetener: A review. *European Food Research and Technology,* 241 (2015) 1–14.

Griffin, G.J. Purification and concentration of xylose and glucose from neutralized bagasse hydrolysates using 3,5-Dimethylphenylboronic acid and modified Aliquat 336 as coextractants. *Separation Science and Technology,* 40 (2005) 2337–2351.

Griffin, G.J., and Shu, L. Solvent extraction and purification of sugars from hemicellulose hydrolysates using boronic acid carriers. *Journal of Chemical Technology and Biotechnology,* 79 (2004) 505–511.

Gruppen, H., Hamer, R.J., and Voragen, A.G.J. Water-unextractable cell wall material from wheat flour. 1. Extraction of polymers with alkali. *Journal of Cereal Science,* 16 (1992) 41–51.

Grzenia, D.L., Schell, D.J., and Wickramsinghe, S.R. Detoxification of biomass hydrolysates by reactive membrane extraction. *Journal of Membrane Science,* 348 (2010) 6–12.

Guha, S.K., Kobayashi, H., Hara, K., Kikuchi, H., Aritsuka, T., and Fukuoka, A. Hydrogenolysis of sugar beet fiber by supported metal catalyst. *Catalysis Communications,* 12 (2011) 980–983.

Guo, F., Fang, Z., Xu, C.C., and Smith Jr, R.L. Solid acid mediated hydrolysis of biomass for producing biofuels. *Progress in Energy and Combustion Science,* 38 (2012) 672–690.

Guo, X., Wang, X., Guan, J., Chen, X., Qin, Z., Mu, X., and Xian, M. Selective hydrogenation of D-glucose to D-sorbitol over Ru/ZSM-5 catalysts. *Chinese Journal of Catalysis,* 35 (2014) 733–740.

Hara, M. Biomass conversion by a solid acid catalyst. *Energy & Environmental Science,* 3 (2010) 601–607.

Hariz, I.B., Ayni, F.A., and Monser, L. Removal of sulfur compounds from petroleum refinery wastewater through adsorption on modified activated carbon. *Water Science & Technology,* 70 (2014) 1376–1382.

Hendriks, A.T.W.M., and Zeeman, G. Pretreatments to enhance the digestibility of lignocellulosic biomass. *Bioresource Technology,* 100 (2009) 10–18.

Hernández-Mejia, C., Gnanakumar, E.S., Olivos-Suarez, A., Gascon, J., Greer, H., Zhour, W., Rothenberg, G., and Shiju, N.R. Ru/TiO_2-catalysed hydrogenation of xylose: the role of crystal structure of the support. *Catalysis Science and Technology,* 6 (2016) 577–582.

Herrera, V.A.S., Saleem, F., Kusema, B., Eränen, K., and Salmi. T. Hydrogenation of L-arabinose and D-galactose mixtures over a heterogeneous Ru/C catalyst. *Topics in Catalysis,* 55 (2012) 550–555.

Hilpmann, G., Becher, N., Pahner, F-A., Kusema, B., Mäki-Arvela, P., Lange, R., Murzin, D.Y., and Salmi, T. Acid hydrolysis of xylan. *Catalysis Today,* 259 (2016) 376–380.

Höije, A., Gröndahl, M., Tommeraas, K., and Gatenholm, P. Isolation and characterization of physicochemical and material properties of arabinoxylans from barley husks. *Carbohydrate Polymers,* 61 (2005) 266–275.

Hollmann, J., and Lindhauer, M.G. Pilot-scale isolation of glucuronoarabinoxylans from wheat bran. *Carbohydrate Polymers,* 59 (2005) 225–230.

Hromadkova, Z., Kovacikova, J., and Ebringerova, A. Study of the classical and ultrasound-assisted extraction of the corn xylan. *Industrial Crops and Products,* 9 (1999) 101–109.

Hu, H., Li, Z., Wu, Z., Lin, L., and Zhou, S. Catalytic hydrolysis of microcrystalline and rice straw-derived cellulose over a chlorine-doped magnetic carbonaceous solid acid. *Industrial Crops and Products,* 84 (2016) 408–417.

Huang, Y-B., and Fu, Y. Hydrolysis of cellulose to glucose by solid acid catalysts. *Green Chemistry,* 15 (2013) 1095–1111.

Irmak, S. Biomass as raw material for production of high-value products. In *Biomass Volume Estimation and Valorization for Energy*, Dr. Tumuluru, J.S., (Ed.), InTech, 2017.

Izydorczyk, M.S., and Biliaderis, C.G. Arabinoxylans: Technologically and nutritionally functional plant polysaccharides. In *Functional food carbohydrates*, Izydorczyk, M.S., and Biliaderis, C.G., (Eds.), CRC Press: Boca Raton, 2007.

Käldström, M., Kumar, N., and Murzin, D.Y. Valorization of cellulose over metal supported on mesoporous materials. *Catalysis Today,* 167 (2011) 91–95.

Kamm, B., Gruber, P.R., and Kamm, M. Biorefineries - Industrial Processes and Products. Wiley-VCH Verlag GmbH: Weinheim, 2008.

Kaparaju, P., Serrano, M., Thomsen, A.B., Kongjan, P., and Angelidaki, I. Bioethanol, biohydrogen and biogas production from wheat bran straw in a biorefinery concept. *Bioresource Technology*, 100 (2009) 2562–2568.

Kobayashi, H., Yamakoshi, Y., Hosaka, Y., Yabushita, M., and Fukuoka, A. Production of sugar alcohols from real biomass by supported platinum catalyst. *Catalysis Today*, 226 (2014) 204–209.

Kordowska-Wiater, M., Kuzdralinski, A., Czernecki, T., Targonski, Z., Frac, M., and Oszust, K. The production of arabitol by a novel plant yeast isolate *Candida parapsilosis* 27RL-4. *Open Life Sciences*, 12 (2017) 326–336.

Kordowska-Wiater, M., Targonski, Z., and Jarosz, A. Biotransformation of L-arabinose to arabitol by yeasts from genera *Pichia* and *Candida*. *Biotechnologia*, 1 (2008) 177–188.

Koutinas, A.A., Wang, R., Campbell, G.M., and Webb, C. A whole crop biorefinery system: A closed system for the manufacture of non-food products from cereals. In *Biorefineries – Industrial Processes and Products*, Kamm, B., Gruber, P.R., and Kamm, M., (Eds.), Wiley-VCH Verlag GmbH: Weinheim, 2008.

Kumar, D.R., and Srivastava, V.C. Studies on adsorptive desulfurization by activated carbon. *Soil Air Water*, 40 (2012) 545–550.

Kusema, B.T., Faba, L., Kumar, N., Mäki-Arvela, P., Díaz, E., Ordóñez, S., Salmi, T., and Murzin, D.Y. Hydrolytic hydrogenation of hemicellulose over metal modified mesoporous catalyst. *Catalysis Today*, 196 (2012) 26–33.

Kusema, B.T., Hilmann, G., Mäki-Arvela, P., Willför, S., Holmbom, B., Salmi, T., and Murzin, D.Y. Selective hydrolysis of arabinogalactan into arabinose and galactose over heterogeneous catalysts. *Catalysis Letters*, 141 (2011) 408–412.

Kusserow, B., Schimpf, S., and Claus, P. Hydrogenation of glucose to sorbitol over nickel and ruthenium catalysts. *Advanced Synthesis & Catalysis*, 345 (2003) 289–299.

Larsson, S., Reimann, A., Nilvebrant, N-O., and Jönsson, L.J. Comparison of different methods for the detoxification of lignocellulose hydrolyzates of spruce. *Applied Biochemistry and Biotechnology*, 77 (1999) 91–103.

Lee, H.J., Kim, I.J., Kim, J.F., Choi, I-G., and Kim, K.H. An expansin from the marine bacterium *Hahella chejuensis* acts synergistically with xylanase and enhances xylan hydrolysis. *Bioresource Technology*, 149 (2013) 516–519.

Li, F., Wang, H., Xin, H., Cai, J., Fu, Q., and Jin, Y. Development, validation and application of a hydrophilic interaction liquid chromatography-evaporative light scattering detection based method for process control of hydrolysis of xylans obtained from different agricultural wastes. *Food Chemistry*, 212 (2016) 155–161.

Li, S., Qian, E.W., Shibata, T., and Hosomi, M. Catalytic hydrothermal saccharification of rice straw using mesoporous silica-based solid acid catalysts. *Journal of the Japan Petroleum Institute*, 55 (2012) 250–260.

Lin, C., Wu, C., and Hung, C. Temperature effects on fermentative hydrogen production from xylose using mixed anaerobic cultures. *International Journal of Hydrogen Energy*, 33 (2008) 43–50.

Loman, A.A., Islam, S.M.M., and Ju, L-K. Production of arabitol from enzymatic hydrolysate of soybean flour by *Debaryomyces hansenii* fermentation. *Applied Biochemistry and Biotechnology*, 102 (2018) 641–653.

López, M.J., Nichols, N.N., Dien, B.S., Moreno, J., and Bothast, R.J. Isolation of microorganisms for biological detoxification of lignocellulosic hydrolysates. *Applied Microbiology and Biotechnology,* 64 (2004) 125–131.

Lou, H., Yuan, L., Qiu, X., Qiu, K., Fu, J., Pang, Y., and Huang, J. Enhancing enzymatic hydrolysis of xylan by adding sodium lignosulfonate and long-chain fatty alcohols. *Bioresource Technology,* 200 (2016) 48–54.

Mäki-Arvela, P., Holmbom, B., Salmi, T., and Murzin, D.Y. Recent progress in synthesis of fine and specialty chemicals from wood and other biomass by heterogeneous catalytic processes. *Catalysis Reviews,* 49 (2007) 197–340.

Mäki-Arvela, P., Salmi, T., Holmbom, B., Willför, S., and Murzin, D.Y. Synthesis of sugars by hydrolysis of hemicelluloses – A review. *Chemical Reviews*, 111 (2011) 5638–5666.

Martín, C., Galbe, M., Wahlbom, C.F., Hahn-Hägerdal, B., and Jönsson, L.J. Ethanol production from enzymatic hydrolysates of sugarcane bagasse using recombinant xylose-utilising *Saccharomyces cerevisiae*. *Enzyme and Microbial Technology*, 31 (2002) 274–282.

Martínez, A., Rodríguez, M.E., York, S.W., Preston, J.F., and Ingram, L.O. Effects of $Ca(OH)_2$ treatments ("overliming") on the composition and toxicity of bagasse hemicellulose hydrolysates. *Biotechnology and Bioengineering,* 69 (2000) 526–536.

Marzialetti, T., Olarte, M.B.V., Sievers, C., Hoskins, T.J.C., Agrawal, P.K., and Jones, C.W. Dilute acid hydrolysis of Loblolly Pine: A comprehensive approach. *Industrial & Engineering Chemistry Research,* 47 (2008) 7131–7140.

Matsumoto, M., Ueba, K., and Kondo, K. Separation of sugar by solvent extraction with phenylboronic acid and trioctylmethylammonium chloride. *Separation and Purification Technology*, 43 (2005) 269–274.

Mikkola, J-P., and Salmi, T. Three-phase catalytic hydrogenation of xylose to xylitol – prolonging the catalyst activity by means of on-line ultrasonic treatment. *Catalysis Today*, 64 (2001) 271–277.

Mikkola, J-P., Sjöholm, R., Salmi, T., and Mäki-Arvela, P. Xylose hydrogenation: kinetic and NMR studies of the reaction mechanisms. *Catalysis Today*, 48 (1999) 73–81.

Mikkola, J-P., Vainio, H., Salmi, T., Sjöholm, R., Ollonqvist, T., and Väyrynen, J. Deactivation kinetics of Mo-supported Raney Ni catalyst in the hydrogenation of xylose to xylitol. *Applied Catalysis A: General*, 196 (2000) 143–155.

Mishra, D.K., Dabbawala, A.A., and Hwang, J-S. Ruthenium nanoparticles supported on zeolite Y as an efficient catalyst for selective hydrogenation of xylose to xylitol. *Journal of Molecular Catalysis A: Chemical*, 376 (2013) 63–70.

Mishra, D.K., Dabbawala, A.A., Park, J.J., Jhung, S.H., and Hwang, J-S. Selective hydrogenation of D-glucose to D-sorbitol over HY zeolite supported ruthenium nanoparticles catalysts. *Catalysis Today*, 232 (2014) 99–107.

Mohan, D., Pittman, C.U., and Steele, P.H. Pyrolysis of wood/biomass for bio-oil: a critical review. *Energy Fuels*, 20 (2006) 848–889.

Müller, A., Hilpmann, G., Haase, S., and Lange, R. Continuous hydrogenation of L-arabinose and D-galactose in a mini packed bed reactor. *Chemical Engineering & Technology*, 40 (2017) 2113–2122.

Murzin, D.Y., Kusema, B., Murzina, E.V., Aho, A., Tokarev, A., Boymirzaev, A.S., Wärna, J., Dapsens, P.Y., Mondelli, C., Pérez-Ramírez, J., and Salmi, T. Hemicellulose

arabinogalactan hydrolytic hydrogenation over Ru-modified H-USY zeolites. *Journal of Catalysis*, 330 (2015a) 93–105.

Murzin, D.Y., Murzina, E.V., Tokarez, A., Shcherban, N.D., Wärna, J., and Salmi, T. Arabinogalactan hydrolysis and hydrolytic hydrogenation using functionalized carbon materials. *Catalysis Today*, 257 (2015b) 169–176.

Nabarlatz, D., Farriol, X., and Montane, D. Kinetic modeling of the autohydrolysis of lignocellulosic biomass for the production of hemicellulose-derived oligosaccharides. *Industrial and Engineering Chemistry Research*, 43 (2004) 4124–4131.

Naik, S.N., Goud, V.V., Rout, P.K., and Dalai, A.K. Production of first and second generation biofuels: A comprehensive review. *Renewable and Sustainable Energy Reviews*, 14 (2010) 578–597.

Nakasu, P.Y.S., Ienczak, L.J., Costa, A.C., and Rabelo, S.C. Acid post-hydrolysis of xylooligosaccharides from hydrothermal pretreatment for pentose ethanol production. *Fuel*, 185 (2016) 73–84.

Negahdar, L., Delidovich, I., and Palkovits, R. Aqueous-phase hydrolysis of cellulose and hemicelluloses over molecular acidic catalysts: insights into the kinetics and reaction mechanism. *Applied Catalysis B: Environmental*, 184 (2016) 285–298.

Ogawa, K., Takeuchi, M., and Nakamura, N. Immunological effects of partially hydrolyzed arabinoxylan from corn husk in mice. *Bioscience, Biotechnology, and Biochemistry*, 69 (2005) 19–25.

Oh, Y.H., Eom, I.Y., Joo, J.C., Yu, J.H., Song, B.K., Lee, S.H., Hong, S.H., and Park, S.J. Recent advances in development of biomass pretreatment technologies used in biorefinery for the production of bio-based fuels, chemicals and polymers. *Korean Journal of Chemical Engineering*, 32 (2015) 1945–1959.

Ormsby, R., Kastner, J.R., and Miller, J. Hemicellulose hydrolysis using solid acid catalysts generated from biochar. *Catalysis Today*, 190 (2012) 89–97.

Park, Y-C., Oh, E.J., Jo, J-H., Jin, Y-S., and Seo, J-H. Recent advances in biological production of sugar alcohols. *Current Opinion in Biotechnology*, 37 (2016) 105–113.

Peng, F., Peng, P., Xu, F., and Sun, R-C. Fractional purification and bioconversion of hemicelluloses. *Biotechnology Advances*, 30 (2012) 879–903.

Perrard, A., Gallezot, P., Joly, J-P., Durand, R., Baljou, C., Coq, B., and Trens, P. Highly efficient metal catalysts supported on activated carbon cloths: A catalytic application for the hydrogenation of D-glucose to D-sorbitol. Applied Catalysis A: General, 331 (2007) 100–104.

Pettersen, R.C. The chemical composition of wood. *Advances in Chemistry*, 207 (1984) 57–126.

Prückler, M., Siebenhandl-Ehn, S., Apprich, S., Höltinger, S., Haas, C., Schmid, E., and Kneifel, W. Wheat bran-based biorefinery 1: Composition of wheat bran and strategies of functionalization. *LWT – Food Science and Technology*, 56 (2014) 211–221.

Raij, B.V., Quaggio, J.A., and Da Silva, N.M. Extraction of phosphorous, potassium, calcium and magnesium from soils by an ion-exchange resin procedure. *Communications in Soil Science and Plant Analysis*, 17 (1986) 547–566.

Reisinger, M., Tirpanalan, Ö., Prückler, M., Huber, F., Kneifel, W., and Novalin, S. Wheat bran biorefinery – A detailed investigation on hydrothermal and enzymatic treatment. *Bioresource Technology*, 144 (2013) 179–185.

Relue, B.L.P., and Varanasi, S. Simultaneous isomerization and reactive extraction of biomass sugars for high yield production of ketose sugars. *Green Chemistry*, 14 (2012) 2436–2444.

Ribeiro, L.S., Delgado, J.J., Órfão, J.J.M., and Pereira, M.F.R. A one-pot method for the enhanced production of xylitol directly from hemicellulose (corncob xylan). *RSC Advances,* 6 (2016) 95320–95327.

Ribeiro, L.S., Órfão, J.J.M., and Pereira, M.F.R. Screening of catalysts and reaction conditions for the direct conversion of corncob xylan to xylitol. *Green Processing and Synthesis,* 6 (2017) 265–272.

Rodrigues, R.C.L.B., Felipe, M.G.A., Almeida e Silva, J.B., Vitolo, M., and Gómez, P.V. The influence of pH, temperature and hydrolyzate concentration on the removal of volatile and nonvolatile compounds from sugarcane bagasse hemicellulosic hydrolyzate treated with activated charcoal before or after vacuum evaporation. *Brazilian Journal of Chemical Engineering,* 18 (2001) 299–311.

Romero, A., Alonso, E., Sastre, Á., and Nieto-Márquez, A. Conversion of biomass into sorbitol: Cellulose hydrolysis on MCM-48 and D-glucose hydrogenation on Ru/MCM-48. *Microporous and Mesoporous Materials,* 224 (2016) 1–8.

Rose, D.J., and Inglett, G.E. Production of feruloylated arabinoxylo-oligosaccharides from maize (Zea mays) bran by microwave-assisted autohydrolysis. *Food Chemistry,* 119 (2010) 1613–1618.

Saha, B.C., and Bothast, R.J. Production of L-arabitol from L-arabinose by *Candida entomaea* and *Pichia guilliermondii*. *Applied Microbiology and Biotechnology,* 45 (1996) 299–306.

Sahu, R., and Dhepe, P.L. A one-pot method for the selective conversion of hemicellulose from crop waste into C5 sugars and furfural by using solid acid catalysts. *ChemSusChem,* 5 (2012) 751–761.

Sanz-Moral, L.M., Romero, A., Holz, F., Rueda, M., Navarrete, A., and Martín, A. Tuned Pd/SiO_2 aerogel catalyst prepared by different synthesis techniques. *Journal of the Taiwan Institute of Chemical Engineers,* 65 (2016) 515–521.

Schimpf, S., Louis, C., and Claus, P. Ni/SiO_2 catalysts prepared with ethylenediamine nickel precursors: Influence of the pretreatment on the catalytic properties in glucose hydrogenation. *Applied Catalysis A: General,* 318 (2007) 45–53.

Seri, K-I., Sakaki, T., Shibata, M., Inoue, Y., and Ishida, H. Lanthanum(III)-catalyzed degradation of cellulose at 250 °C. *Bioresource Technology*, 81 (2002) 257–260.

Serrano-Ruiz, J.C., Luque, R., and Sepúlveda-Escribano, A. Transformations of biomass-derived platform molecules: from high added-value chemicals to fuels via aqueous-phase processing. *Chemical Society Reviews,* 40 (2011) 5266–5281.

Shevchenko, S.M., Chang, K., Robinson, J., and Saddler, J.N. Optimization of monosaccharide recovery by post-hydrolysis of the water-soluble hemicellulose component after steam explosion of softwood chips. *Bioresource Technology,* 72 (2000) 207–211.

Shimizu, K-I., Furukawa, H., Kobayashi, N., Itayab, Y., and Satsum, A. Effects of Brønsted and Lewis acidities on activity and selectivity of heteropolyacid-based catalysts for hydrolysis of cellobiose and cellulose. *Green Chemistry*, 11 (2009) 1627–1632.

Sirisansaneeyakul, S., Staniszewski, M., and Rizzi, M. Screening of yeasts for production of xylitol from D-xylose. *Journal of Fermentation and Bioengineering,* 80 (1995) 565–570.

Sluiter, A., and Sluiter, J. Determination of starch in solid biomass samples by HPLC. Laboratory Analytical Procedure (LAP). Technical Report NREL/TP-510-42624, 2008a.

Sluiter, A., Hames, B., Ruiz, R., Scarlata, C., Sluiter, J., and Templeton, D. Determination of ash in biomass. Laboratory Analytical Procedure (LAP). Technical Report NREL/TP-510-42622, 2008b.

Sluiter, A., Ruiz, R., Scarlata, C., Sluiter, J., and Templeton, D. Determination of extractives in biomass. Laboratory Analytical Procedure (LAP). Technical Report NREL/TP-510-42619, 2008c.

Sluiter, J., and Sluiter, A. Summative mass closure. Laboratory Analytical Procedure (LAP). Review and Integration. Technical Report NREL/TP-510-48087, 2011.

Soudham, V.P. Biochemical conversion of biomass to biofuels. Pretreatment – Detoxification – Hydrolysis – Fermentation. Ph.D Dissertation, Umeå University, Sweden, 2015.

Stöcker, M. Biofuels and biomass-to-liquid fuels in the biorefinery: catalytic conversion of lignocellulosic biomass using porous materials. *Angewandte Chemie International Edition*, 47 (2008) 9200–9211.

Sun, R.C., and Tomkinson, J. Characterization of hemicelluloses obtained by classical and ultrasonically assisted extractions from wheat straw. *Carbohydrate Polymers,* 50 (2002) 263–271.

Sun, X.F., Xu, F., Sun, R.C., Geng, Z.C., Fowler, P., and Baird, M.S. Characteristics of degraded hemicellulosic polymers obtained from steam exploded wheat straw. *Carbohydrate Polymers,* 60 (2005) 15–26.

Tamburini, E., Costa, S., Marchetti, M.G., and Pedrini, P. Optimized production of xylitol from xylose using a hyper-acidophilic *Candida tropicalis*. *Biomolecules,* 5 (2015) 1979–1989.

Tathod, A., Kane, T., Sanil, E.S., and Dhepe, P.L. Solid base supported metal catalysts for the oxidation and hydrogenation of sugars. *Journal of Molecular Catalysis A: Chemical*, 388–389 (2014) 90–99.

Tathod, A.P., and Dhepe, P.L. Efficient method for the conversion of agricultural waste into sugar alcohols over supported bimetallic catalysts. *Bioresource Technology*, 178 (2015) 36–44.

Tran, L.H., Yogo, M., Ojima, H., Idota O., Kawai, K., Suzuki, T., and Takamizawa, K. The production of xylitol by enzymatic hydrolysis of agricultural wastes. *Biotechnology and Bioprocess Engineering*, 9 (2004) 223–228.

Vilcocq, L., Castilho, P., Carvalheiro, F., and Duarte, L.C. Hydrolysis of oligosaccharides over solid acid catalysts: A review. *ChemSusChem*, 7 (2014) 1010–1019.

Wang, J., Sun, B., Liu, Y., and Zhang, H. Optimisation of ultrasound-assisted enzymatic extraction of arabinoxylan from wheat bran. *Food Chemistry*, 150 (2014) 482–488.

Werpy, T., and Petersen, G. Top Value Added Chemicals from Biomass. In *Volume I – Results of Screening for Potential Candidates from Sugars and Synthesis Gas*. U.S.D. Energy: United States, 2004.

Wickramasinghe, S.R., and Grzenia, D.L. Adsorptive membranes and resins for acetic acid removal from biomass hydrolysates. *Desalination*, 234 (2008) 144–151.

Wilson, J.J., Deschatelets, L., and Nishikawa, N.K. Comparative fermentability of enzymatic and acid hydrolysates of steam-pretreated aspenwood hemicellulose by Pichia stipites CBS 5776. *Applied Microbiology and Biotechnology*, 31 (1989) 592–596.

Wisniak, J., and Simon, R. Hydrogenation of glucose, fructose, and their mixtures. *Industrial & Engineering Chemistry Process Design and Development*, 18 (1979) 50–57.

Wisniak, J., Hershkowitz, M., and Stein, S. Hydrogenation of xylose over platinum group catalysts. *Industrial & Engineering Chemistry Product Research and Development,* 13 (1974) 232–236.

Wu, S., Lin, C., Lee, K., Hung, C., Chang, J., Lin, P., and Chang, F. Dark fermentative hydrogen production from xylose in different bioreactors using sewage sludge microflora. *Energy and Fuels,* 22 (2008) 113–119.

Xu, F., Liu, C.F., Geng, Z.C., Sun, J.X., Sun, R.C., Hei, B.H., Lin, L., Wu, S.B., and Je, J. Characterisation of degraded organosolv hemicelluloses from wheat straw. *Polymer Degradation and Stability,* 91 (2006) 1880–1886.

Yadav, M., Mishra, D.K., and Hwang, J-S. Catalytic hydrogenation of xylose to xylitol using ruthenium catalyst on NiO modified TiO_2 support. *Applied Catalysis A: General,* 425–426 (2012) 110–116.

Yi, G., and Zhang. Y. One-pot selective conversion of hemicellulose (xylan) to xylitol under mild conditions. *ChemSusChem,* 5 (2012) 1383–1387.

Zakzeski, J., Bruijnincx, P.C.A., Jongerius, A.L., and Weckhuysen, B.M. The catalytic valorization of lignin for the production of renewable chemicals. *Chemical Reviews,* 110 (2010) 3552–3599.

Zeitoun, R., Pontalier, P.Y., Marechal, P., and Rigal, L. Twin-screw extrusion for hemicellulose recovery: Influence on extract and purification performance. *Bioresource Technology*, 101 (2010) 9348–9354.

Zhang, H., Zhou, X., Xu, Y., and Yu, S. Production of xylooligosaccharides from waste xylan, obtained from viscose fiber processing, by selective hydrolysis using concentrated acetic acid. *Journal of Wood Chemistry and Technology,* 37 (2016) 1–9.

Zhang, X., Wang, S., Zhou, S., and Fu, X. Optimization of alkaline extraction conditions for arabinoxylan from wheat bran. *Journal of Nuclear Agricultural Sciences,* 22 (2008a) 60–64.

Zhang, X., Yang, W., and Blasiak, W. Modeling study of woody biomass: Interactions of cellulose, hemicellulose and lignin. *Energy Fuels,* 25 (2011) 4786–4795.

Zhang, X., Zhou, S., and Wang, S. Optimizing enzymatic hydrolysis conditions of arabinoxylan in wheat bran through quadratic orthogonal rotation combination design. *Food Science,* 28 (2008b) 141–145.

Zhang, Z., Smith, C., and Li, W. Extraction and modification technology of arabinoxylans from cereal by-products: A critical review. *Food Research International,* 65 (2014) 423–436.

Zhou, L., Shi, M., Cai, Q., Wu, L., Hu, X., Yang, X., Chen, C., and Xu, J. Hydrolysis of hemicellulose catalyzed by hierarchical H-USY zeolites – The role of acidity and pore structure. *Microporous and Mesoporous Materials,* 169 (2013) 54–59.

Zhou, S., Liu, X., Guo, Y., Wang, Q., Peng, D., and Cao, L. Comparison of the immunological activities of arabinoxylans from wheat bran with alkali and xylanase-aided extraction. *Carbohydrate Polymers,* 81 (2010) 784–789.

https://es.statista.com/estadisticas/501733/produccion-de-trigo-en-espana/ (May 2018)

AIMS

WHEAT BRAN BIOREFINERY: VALORIZATION OF HEMICELLULOSES TO SUGAR ALCOHOLS

FRACTIONATION – HYDROLYSIS – PURIFICATION – HYDROGENATION

The general aim of this work is to study the conversion of an agricultural by-product (wheat bran) into high added-value products (sugar alcohols) by a sequential process composed of the following steps:

i) Extraction of arabinoxylans from wheat bran

ii) Hydrolysis of arabinoxylans into monosaccharides

iii) Purification of wheat bran hydrolysates

iv) Hydrogenation of purified hydrolysates to obtain sugar alcohols

The specific aims are summarized as follows:

- Development of biorefinery processes applied to real biomass:
    - Revalorization of agricultural biomass from our region *Castilla y León*, such as wheat bran.
- Fractionation of wheat bran over mesoporous and acidified silicas to obtain the arabinoxylan fraction:
    - Influence of MCM-48 and Al-MCM-48 as well as the corresponding $RuCl_3$ catalysts supported on them.
    - Optimization of temperature and time to obtain high arabinoxylans extraction yields with low molecular weight.
- Hydrolysis of arabinoxylans into arabinose and xylose over heterogeneous catalysts:
    - Effect of different mesoporous silicas (MCM-48, Al-MCM-48) and $RuCl_3$ catalysts ($RuCl_3$/MCM-48, $RuCl_3$/Al-MCM-48). Investigation of different metal cations (Ru^{+3}, Fe^{+3}). Optimization of catalyst loading and reaction time to maximize the selective conversion of arabinoxylans into arabinose and xylose avoiding further degradation.

  - Comparison of mesoporous silicas (MCM-48, Al-MCM-48) and zeolites (H-Y (12), H-ZSM-5 (23), H-ZSM-5 (80)). Maximization of sugars and minimization of degradation products by tuning reaction time and catalyst loading.

- Recovery of sugars from wheat bran hydrolysates by solvent extraction with boronic acids followed by purification with ion-exchange resins:
  - Analysis of the behavior of sugars, degradation products, inorganic salts, proteins and lignin derivatives throughout the different steps of the process.
- Hydrogenation of sugar model mixtures (xylose, arabinose, glucose) over ruthenium catalysts supported on zeolites:
  - Influence of different H-ZSM-5 zeolites (SiO_2/Al_2O_3 = 23, 80) as catalysts supports.
  - Effect of reaction temperature, time and catalyst loading.
  - Fitting of the experimental data by a pseudo-first order kinetic model.
  - Determination of kinetic parameters (pre-exponential factor of Arrhenius equation and activation energy values).
- Hydrogenation of wheat bran hydrolysates over ruthenium catalysts supported on H-ZSM-5 (80):
  - Hydrogenation of wheat bran hydrolysates before and after a purification process.
  - Influence of catalyst loading on the production of sugar alcohols.
  - Analysis of the deactivation mechanism of ruthenium catalysts.

CHAPTER I

HYDROTHERMAL EXTRACTION OF ARABINOXYLANS FROM WHEAT BRAN ASSISTED BY HETEROGENEOUS CATALYSTS

Sánchez-Bastardo, N., Romero, A., and Alonso, E. Extraction of arabinoxylans from wheat bran using hydrothermal processes assisted by heterogeneous catalysts. *Carbohydrate Polymers*, 160 (2017) 143–152.

Abstract

The extraction/hydrolysis process of arabinoxylans from destarched wheat bran was studied in this work using different mesoporous silica materials and the corresponding $RuCl_3$-supported catalysts. The effects of temperature and time as well as the influence of different $RuCl_3$ catalysts and catalyst supports were investigated and discussed in terms of the arabinoxylan extraction yield and their polymerization degree. Relatively high temperatures (180 ºC), short operating times (10 minutes) and the use of $RuCl_3$ supported on Al-MCM-48 led to a high amount of extracted arabinoxylans (78%) with a low molecular weight (9 kDa). Finally, a relation between the operating conditions, the arabinoxylan extraction yield and the molecular weight was established based on the obtained results.

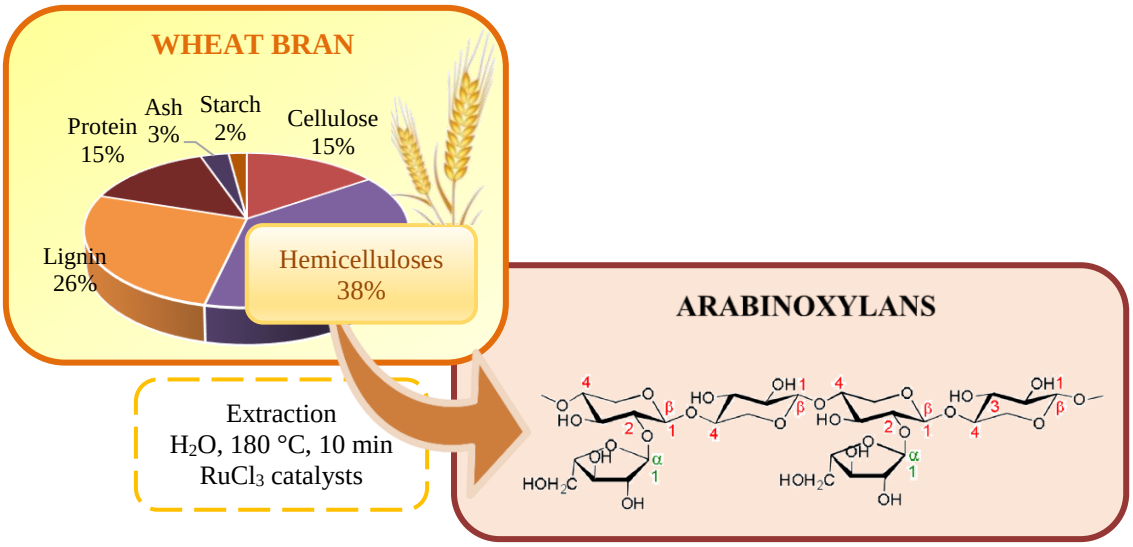

1. Introduction

The conversion of biomass within biorefineries into chemicals, materials, energy and specialty products is seen as a real possibility for the substitution of fossil resources. Fossil fuels are currently the most used energy source, but their depletion and non-renewable nature are forcing to look for other suitable feedstocks (Apprich et al., 2014; Tathod and Dhepe, 2015). Biomass is nowadays produced in huge amounts all over the world. Around 95% of this biomass is lignocellulosic material that is not edible for humans, which makes it attractive for the production of many useful platform chemicals or biofuels (Sahu and Dhepe, 2012). Lignocellulosic biomass is mainly formed by three components: cellulose (ca. 50%), hemicelluloses (ca. 30%) and lignin (ca. 20%) (Tathod and Dhepe, 2015).

Besides wood and non-food crops, agricultural residues and by-products are also of high interest as feedstocks (Apprich et al., 2014). Wheat bran (12% water, 13 – 18% protein, 3 – 8% ash and 56% carbohydrates) is a by-product of the milling process of wheat grain which accrues in enormous quantities during the production of white wheat flour. It is estimated that 150 million tons are produced per year worldwide. Currently, wheat bran is mainly used as a low value ingredient in animal feed (Nandini and Salimath, 2001; Prückler et al., 2014).

Valuable compounds can be produced from the carbohydrate fraction of wheat bran. In particular, arabinoxylans (AXs) can be hydrolyzed into xylose (Xyl) and arabinose (Ara) and then further hydrogenated to obtain xylitol and arabitol (Figure 1). These sugar alcohols are two of the top 12 value-added products derived from biomass included in the report published by the U.S. Department of Energy (DOE).

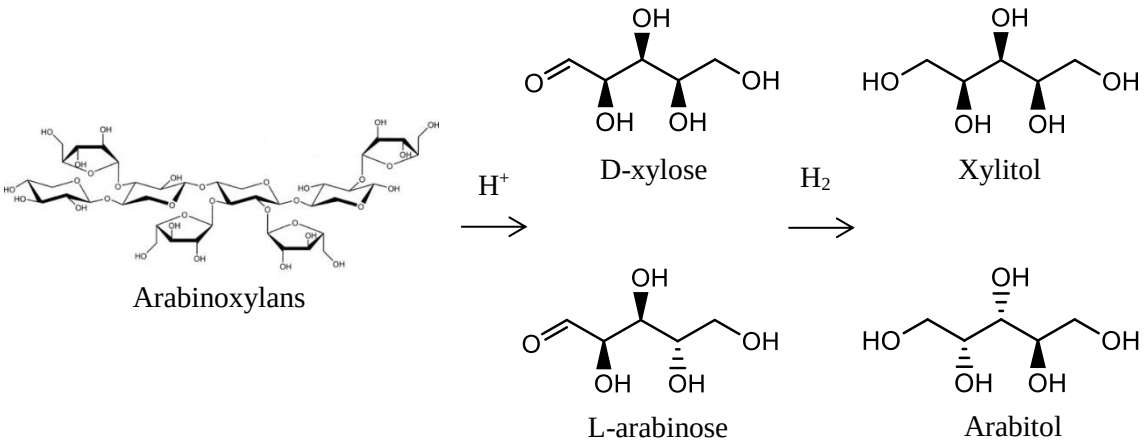

Figure 1. Conversion of arabinoxylans into sugar alcohols (Kobayashi et al., 2011; Tathod et al., 2014).

AXs belong to the hemicellulosic part of biomass and are a major structural component of cell walls of wheat bran, between 10.9 and 26.0% based on dry basis (Apprich et al., 2014). AXs of cereals can be divided into two groups: water-extractable (WEAXs) and water un-extractable (WUAXs) arabinoxylans. WEAXs are weakly connected to the cell wall surface and constitute a minor part of the total AXs. Nevertheless, WUAXs represent the most plentiful part of the AXs and are located in the cell wall of cereals linked to other AXs and other cell wall components through covalent and non-covalent bonds (Ganguli and Tumer, 2008; Gebruers et al., 2008; Izydorczyk and Biliaderis, 2007; Zhang et al. 2014).

Some authors have suggested that water at relatively mild conditions (*i.e.* below 100 ºC) is not able to break the cross-links between the WUAXs and the wall matrix (Izydorczyk and Biliaderis, 2007). In order to improve the extraction of arabinoxylans, several techniques, such as chemical-solvent extractions, enzymatic processes, mechanical-chemical methods and hydrothermal treatments have been considered. The advantages and disadvantages of all these methods have been discussed by Zhang et al. (2014). Chemical methods using bases or acids are not environmentally-friendly and the

separation process at the end of the extraction raises sharply the operating costs. Additionally, corrosion caused by severe acid treatments increases the equipment costs. AX yields obtained by chemical methods are between 26% and 81% (Aguedo et al., 2014; Buranov and Mazza, 2010; Höije et al., 2005; Hollmann and Lindhauer, 2005; Xu et al., 2006). Enzymatic extractions are green processes and lead to good extraction yields (17 – 91%) (Aguedo et al., 2014; Beaugrand et al., 2004; Höije et al., 2005; Maes and Delcour, 2002). However, the long time required and the strict control of the operating conditions as well as the difficulty of recoverying enzymes and their high price are important drawbacks of these processes. Concerning mechanical processes, they are high efficient treatments, but their main disadvantages are the uncontrolled degradation of AX molecules and the harsh pressure and temperature conditions. AX extraction yields with these methods range between 50 – 88% (Rose and Inglett, 2010; Sun et al., 2005; Coelho et al., 2014). Among them, the AX extraction assisted by microwave has been studied by several authors. Rose and Inglett (2010) reported maximum extraction yields about 50% of the original AX content at 180 ºC for 10 min or 200 ºC for 2 min by means of microwave technology. Coelho et al. (2014) achieved a high yield of arabinoxylans and arabinoxylo-oligosaccharides of 62% from brewers' spent grain using microwave superheated water extraction. They used a sequential extraction consisting of three steps: 1) removal of starch at 140 ºC, 2) suspension of the residue in water and treated at 180 ºC and 3) suspension of the residue in 0.1 M KOH and treated again at 180 ºC. Microwave was applied in these three steps for 2 minutes. Hydrothermal treatments are performed in water at relatively high temperature (150 – 230 ºC) (Garrote et al., 1999). These treatments are green processes which lead to relatively high extraction yields (58 – 71%) (Dien et al., 2006; Garrote et al., 2001; Nabarlatz et al., 2004). Nevertheless, they are not suitable for obtaining AXs with low molecular weight. A combination of hydrothermal

treatments with other agents should be applied to reduce the molecular weight of the extracted AXs. For instance, solid acid catalysts are a good alternative to intensify hydrothermal processes as well as to obtain low molecular weight arabinoxylans. Catalytic processes can reduce operating times and thus minimize the formation of degradation products and energy consumption. Moreover, solid catalysts can be easily recovered from the liquid extract by a filtration process. Several authors have reported lately the use of heterogeneous acid catalysts for the conversion of cellulose (Das et al., 2016; De Almedia et al., 2016; Hu et al., 2016; Huang and Fu, 2013; Negahdar et al., 2016). Nonetheless, not many works on fractionation and hydrolysis of hemicelluloses from real biomass over solid catalysts have been published. Sahu and Dhepe (2012) reported a one-pot process catalyzed by solid acid catalysts to convert purified hemicelluloses and bagasse into C_5 sugars. They achieved a yield of xylose and arabinose of 62% at 170 ºC after 1 hour using HBeta zeolite (Si/Al = 19).

The aim of this work is to obtain high extraction yields of low molecular weight arabinoxylans from destarched wheat bran using hydrothermal methods assisted by heterogeneous acid catalysts. Moreover, it is an objective of this research to demonstrate that solid acid catalysts can decouple the hemicelluloses from the solid matrix (destarched wheat bran, in this case) and convert them into a mixture of monosaccharides and soluble oligosaccharides/polysaccharides. Different experimental conditions (temperature and time) as well as the use of several $RuCl_3$ catalysts and catalyst supports were tested in order to discuss their influence on the arabinoxylan extraction yield and their molecular weight.

2. Experimental

2.1 Raw material

Wheat bran was supplied by Emilio Esteban S.A., a cereal milling industry located in Valladolid (Spain), and used as raw material in all experiments after a destarching pretreatment.

2.2 Wheat bran destarching pretreatment

Wheat bran contains high levels of starch (13.8 – 24.9%) (Apprich et al., 2014), which is obtained together with arabinoxylans after the extraction process. This results in viscous slurries and low purity extracts. In addition to this, the co-extraction of starch hinders the consequent separation and purification processes. Starch can be easily removed by enzymes at low temperatures before the arabinoxylan extraction. Destarching enzymes are selective for starch removal, whereas the arabinoxylan fraction remains intact.

In this work, wheat bran was destarched before the arabinoxylan extraction experiments according to an enzymatic procedure described in previous works (Benito-Román et al., 2013, 2014). 20 grams of wheat bran were suspended in 400 mL of a phosphate buffer (pH 5 – 6). This suspension was gently stirred for 1 hour at 65 ºC using 1.0 mL of α-amylase (Fungamyl® 800 L; Novozymes). Destarched wheat bran (DWB) was then rinsed thoroughly several times. Finally, the starch-free solid was frozen at -4 ºC overnight and freeze dried (LyoQuest; Telstar) for 2 days.

2.3 Destarched wheat bran characterization and product analysis

The particle size distribution (PSD) of wheat bran was determined by screening (CISA RP.20; CISA) with different mesh size sieves (50 μm – 2 mm). This sieving process was exclusively for characterization, since all the experiments were carried out with the whole fraction of wheat bran. The composition of destarched wheat bran was determined according to the Laboratory Analytical Procedure (LAP) for biomass analysis provided

by the National Renewable Energy Laboratory (Sluiter and Sluiter, 2011). The sample was subjected to two consecutive Soxhlet extractions for 24 hours each, using water and ethanol as solvents, respectively, in order to remove the extractives. For the determination of structural carbohydrates and lignin, 3 mL of sulfuric acid (72%) were added to 300 mg of DWB and incubated at 30 ºC for 1 hour. After the incubation, 84 mL of milli-Q water were added and the sample was autoclaved at 121 ºC for 1 hour. The final product was slowly cooled to room temperature and then vacuum filtered (Ref. 1244, Pore size 2 – 4 μm, FILTER-LAB). The liquid was used to determine acid soluble lignin (at 280 nm with an UV-Visible spectrophotometer) and carbohydrates (identification and quantification by HPLC). The remaining solid was collected to analyze the content of acid insoluble lignin. The solid resulting from the filtration was firstly dried at 105 ºC and then calcined at 575 ºC. The difference between the weight of the dry and calcined solid corresponded to the amount of acid insoluble lignin. For the ash content, a specific amount of the sample was calcined at 575 ºC until constant weight. The part of the sample which was not burned corresponded to the ash. The composition of DWB in terms of polymeric sugars (cellulose, hemicelluloses) was calculated from the corresponding monomeric sugars resulting from the acid hydrolysis, using an anhydro correction of 0.88 for C_5 sugars (xylose and arabinose) and a correction of 0.90 for C_6 sugars (glucose, galactose and mannose) (Sluiter et al., 2008). Glucose was considered part of cellulose, and hemicelluloses were given by the amount of xylose, arabinose, galactose and mannose. The protein content in the DWB was determined following a standardized Kjeldahl method (Hames et al., 2008) using a nitrogen to protein conversion factor of 5.7 applicable to wheat bran (Hames et al., 2008; Maes and Delcour, 2002; Seyer and Gélinas, 2009). Finally, the starch remained in wheat bran after the destarching pretreatment was

quantified using an assay kit (Total Starch Assay Procedure, Method a); Megazyme International Ltd.).

The identification and quantification of sugars (monomers and oligomers) and degradation products in the liquid after the experiments were done by High Performance Liquid Chromatography (HPLC). Monosaccharides and degradation products were directly analyzed in the liquid sample after the extraction. However, total sugars were determined after an acid hydrolysis of the samples according to the Laboratory Analytical Procedure (LAP) written by the NREL (Sluiter et al., 2008). This method consists of adding 0.8 mL of sulfuric acid (72%) to 20 mL of liquid aliquot and autoclave the sample at 121 ºC for 1 hour using the liquid setting. The pH was then adjusted to 5 – 6 with calcium carbonate. Prior to HPLC analysis, liquid samples were filtered (Pore size 0.22 μm, Diameter 25 mm, Nylon; FILTER-LAB) and treated with a mixed bed ion exchange resin (Dowex® Monosphere® MR-450 UPW; Sigma-Aldrich) to remove the ions before the HPLC analysis. The chromatography system consists of an isocratic pump (Waters 1515; Waters Corporation) and an automatic injector (Waters 717; Waters Corporation). Two different HPLC columns were used for the identification and quantification of the different products in the liquid samples: 1) Supelcogel Pb (Supelco) for sugars (milli-Q water as mobile phase, 0.5 mL min^{-1} as flow rate and 85 ºC as temperature) and 2) Sugar SH-1011 (Shodex) for degradation products (sulfuric acid 0.01 N as mobile phase, 0.8 mL min^{-1} as flow rate and 50 ºC as temperature). All the sugars and acids were identified using a RI detector (Waters 2414; Waters Corporation). 5-hydroxymethylfurfural (5-HMF) and furfural were determined with an UV-Vis detector (Waters 2487; Waters Corporation) at a wavelength of 254 and 260 nm, respectively. The standards employed for the HPLC analysis were: cellobiose (98%), glucose (99%), xylose (99%), rhamnose (99%), galactose (99%), arabinose (99%), mannose (99%), fructose

(99%), glyceraldehyde (95%), glycolaldehyde (99%), lactic acid (85%), formic acid (98%), acetic acid (99%), levulinic acid (98%), acrylic acid (99%), pyruvaldehyde (40%), 5-hydroxymethylfurfural (99%), furfural (99%) and erythrose (75%). All these chemicals were purchased from Sigma Aldrich (Spain) and used as received.

The average molecular weight of the hemicelluloses in the liquid extract was determined by Size Exclusion Chromatography (HPLC-SEC). A GPC column (SB-804 HQ; Shodex) protected by a guard column (SB-G; Shodex), and a RI detector (Waters 2414; Waters Corporation) were used to determine the molecular weight of the extracted hemicelluloses. The column was kept at 35 °C and the flow rate of the mobile phase ($NaNO_3$ 0.1M + NaN_3 0.02% in milli-Q water) was set at 0.5 mL min^{-1}. A set of eight different pullulan standards (STANDARD P-82; Shodex) ranged between 6.1 and 642 kDa of average molecular weight (Mw) were dissolved in milli-Q water and used to obtain the corresponding calibration curve. Chromatograms were processed by means of the Breeze Software (Waters Corporation). The molecular weight distribution was given in terms of the weight (Mw) and number (Mn) average molecular weight. Likewise, the polydispersity index (Mw/Mn) was calculated by the software.

The purity of the liquid extract was expressed in terms of Total Organic Carbon (TOC) analysis, using a Shimadzu TOC-VCSH equipment.

The monomeric yield of arabinose + xylose (%) and the AX total yield (%), as well as the purity of the extract, were calculated as follows:

$$\%\ \text{Ara + Xyl monomeric yield} = \frac{\text{(Ara + Xyl) as monomeric sugars (g)}}{\text{(Ara + Xyl) in raw material (g)}} \times 100 \qquad \text{(Eq. 1)}$$

$$\%\ \text{AX total yield} = \frac{\text{(Ara + Xyl) as monomeric and oligomeric sugars (g)}}{\text{(Ara + Xyl) in raw material (g)}} \times 100 \qquad \text{(Eq. 2)}$$

$$\%\ \text{Purity} = \frac{\text{Carbon in (Ara + Xyl) as monomeric and oligomeric sugars (g)}}{\text{Total carbon in liquid extract given by TOC (g)}} \times 100 \qquad \text{(Eq. 3)}$$

2.4 Support and catalyst preparation

Mesoporous silica MCM-48 and Al-MCM-48 were synthesized by a sol-gel method described by Romero et al. (2016). First, n-hexadecyltrimethylammonium bromide was dissolved in a solution composed of 42 mL of distilled water, 18 mL of absolute ethanol and 13 mL of aqueous ammonia (20%) and stirred for 15 minutes; 0.077 g of sodium aluminate were incorporated only in the case of the Al-MCM-48 preparation; and then 4 mL of tetraethyl orthosilicate were added dropwise. This solution was further stirred for 18 h. A white precipitate was then collected by filtration and washed with distilled water. This precipitate was dried at 60 ºC overnight. Dried samples were calcined from 80 to 550 ºC with a heating rate of 2 ºC·min^{-1} and maintained at 550 ºC overnight.

$RuCl_3$ supported catalysts were prepared by the wetness impregnation method using the so prepared MCM-48 or Al/MCM-48 as supports. $RuCl_3$ (ruthenium (III) chloride anhydrous; Strem Chemicals Inc.) and the corresponding mesoporous support were added to water in two different glasses and sonicated for 10 minutes. The $RuCl_3$ solution and the support suspension were then mixed and heated up with a rate of 1 ºC·min^{-1} from 30 ºC to 80 ºC. The temperature of 80 ºC was maintained until the water was visibly evaporated. The catalyst was finally dried overnight at 105 ºC.

2.5 Support and catalyst characterization

Nitrogen adsorption-desorption isotherms were performed with ASAP 2020 (Micromeritics, USA) to determine surface and pore properties of the catalysts. Prior to analysis, the samples were outgassed overnight at 350 ºC. The specific surface area was determined by the multipoint BET method at $P/P_0 \leq 0.3$, while the specific pore volume was evaluated from N_2 uptake at $P/P_0 \geq 0.99$. The pore diameter was obtained by BJH adsorption average ($4 \cdot V \cdot A^{-1}$, nm).

The metal loading of the $RuCl_3$-based catalysts was determined by atomic absorption spectroscopy (AAS) (SPECTRA 220FS analyser) after an acid digestion of the samples (Romero et al., 2016).

The acidity of the different materials was estimated by titration with NaOH. This method is based on the reported by several authors (Hu et al., 2015; Hu et al., 2016).

2.6 Arabinoxylan extraction experiments

The raw material used for this work was the whole fraction of destarched wheat bran, without making any further separation in different particle sizes. All the experiments were carried out in an AISI 304 stainless steel vessel (170 mL). The extractor was heated by an electric heater (275 W) placed around the external wall and the temperature was controlled by a PID controller (ICP, TC21). A pressure gauge from 0 to 25 bar was used to measure the autogenous pressure inside the reactor. The DWB suspension was stirred continuously during the process with a magnetic stirrer at a constant rotational speed of 300 rpm. In a typical experiment, the DWB suspension (160 mL) with a concentration of 30 $g \cdot L^{-1}$ was placed in the vessel. The catalyst was then added and the mixture was stirred at 600 rpm for 5 minutes before the vessel was closed and temperature set. The starting time (0 min) of the extraction was taken when the operating temperature was reached. At the end of the experiments, the vessel was cooled down with an ice bath. The slurries were centrifuged for 10 min at 7800 rpm (SIGMA 2-16P; SIGMA) and vacuum filtered. The liquid was recovered for further analysis.

3. Results and discussion

3.1 Raw material characterization

The chemical composition of destarched wheat bran and its particle size distribution are shown in Table 1. The hemicelluloses content was 38.0% with a ratio Ara/Xyl of 0.53. The amount of xylose and arabinose was 26.2% and 13.8% on dry basis, respectively.

Most particles (64.1 wt.%) are in the range from 2.00 to 1.00 mm. 17.1 wt.% of the particles are found between 1.00 mm and 500 μm and 14.4 wt.% have a particle size higher than 2.00 mm. The amount of particles under 500 μm is very small.

Table 1. Chemical composition and particle size distribution (PSD) of destarched wheat bran.

Chemical composition				PSD	
Component	wt.%	Sugar	wt.%	PS range	wt.%
Cellulose	15.3 ± 0.4	Glucose	19.1 ± 0.5	PS ≥ 2.00 mm	14.4
Hemicelluloses	38.0 ± 2.1	Xylose	26.2 ± 1.6	2.00 – 1.00 mm	64.1
Acid soluble lignin	21.5 ± 0.4	Galactose	2.2 ± 0.2	1.00 mm – 500 μm	17.0
Acid insoluble lignin	4.9 ± 1.3	Arabinose	13.8 ± 0.4	500 – 250 μm	3.5
Starch	2.1 ± 0.3	Mannose	0.9 ± 0.3	250 – 100 μm	1.0
Protein	14.5 ± 0.5			100 μm > PS	0.0
Ash	3.2 ± 0.1				

3.2 Catalyst characterization

The textural properties (specific surface area, total pore volume, pore diameter) and the acidity values for the different catalysts are displayed in Table 2. Specific surface areas (S_{BET}) of 1298 $m^2 \cdot g^{-1}$ and 1352 $m^2 \cdot g^{-1}$ and pore volumes (V_{pore}) of 0.87 $cm^3 \cdot g^{-1}$ and 0.81 $cm^3 \cdot g^{-1}$ were determined for MCM-48 and Al-MCM-48, respectively. According to these results, no significant changes in the specific surface area and pore volume occurred after the aluminum incorporation onto the mesoporous network of MCM-48. However, a slight increase of the pore diameter (d_{pore}) from 2.2 nm in MCM-48 to 2.5 nm in Al-MCM-48 was observed. A decrease in the specific surface area and pore volume took place after the deposition of $RuCl_3$. This fact can be attributed to the partial blocking of the porous network of the supports. After the deposition of $RuCl_3$, no changes in the pore size were detected in the case of $RuCl_3$/MCM-48. However, the pore size increased slightly from 2.5 nm in Al-MCM-48 to 2.7 nm in $RuCl_3$/Al-MCM-48. This fact is indicative of slender modifications of the pore structure, suggesting a higher pore distortion than in the case of

$RuCl_3$/MCM-48. The ruthenium content of $RuCl_3$ catalysts was around 4% in both cases, determined by atomic absorption spectroscopy (AAS).

Acidity is a key parameter of solid acid catalysts when they are used in extraction/hydrolysis processes. The acidity measurements of the catalysts are presented in Table 2. The acidity values exhibited the following trend: MCM-48 < Al-MCM-48 < $RuCl_3$/MCM-48 < $RuCl_3$/Al-MCM-48. Al-MCM-48 is more acidic than MCM-48 since the aluminum creates Brönsted acid sites (Collart et al., 2004; Kao et al., 2008). $RuCl_3$ catalysts show higher acidity than the corresponding silica supports because Ru^{+3} cations act as moderate Lewis acids (Shimizu et al., 2009).

Table 2. Characterization of supports and $RuCl_3$-based catalysts.

Catalyst	Ru (%)[a]	S_{BET} ($m^2 \cdot g^{-1}$)[b]	V_{pore} ($cm^3 \cdot g^{-1}$)[c]	d_{pore} (nm)[d]	Acidity (mEq $H^+ \cdot g\ cat^{-1}$)[e]
MCM-48	-	1298	0.87	2.2	0.293
Al-MCM-48	-	1352	0.81	2.5	0.598
$RuCl_3$/MCM-48	4	1032	0.63	2.2	0.738
$RuCl_3$/Al-MCM-48	4	1017	0.63	2.7	1.130

[a] Determined by AAS.
[b] Determined by the multipoint BET method at $P/P_0 \leq 0.3$.
[c] Determined from N_2 uptake at $P/P_0 \geq 0.99$.
[d] Determined by BJH adsorption average.
[e] Determined by titration with NaOH.

3.3 Arabinoxylan extraction experiments

The effect of several parameters ($RuCl_3$ catalysts, temperature, time and catalyst supports) was evaluated in the extraction process of AXs from destarched wheat bran in terms of monomeric and total sugars. The purity of the extracted AXs and their molecular weight were also discussed.

3.3.1 Effect of $RuCl_3$ catalysts

The influence of MCM-48 and $RuCl_3$/MCM-48 was evaluated in the hydrothermal extraction of arabinoxylans (Figure 2). Experimental conditions for this study were 160 ºC and 10 minutes.

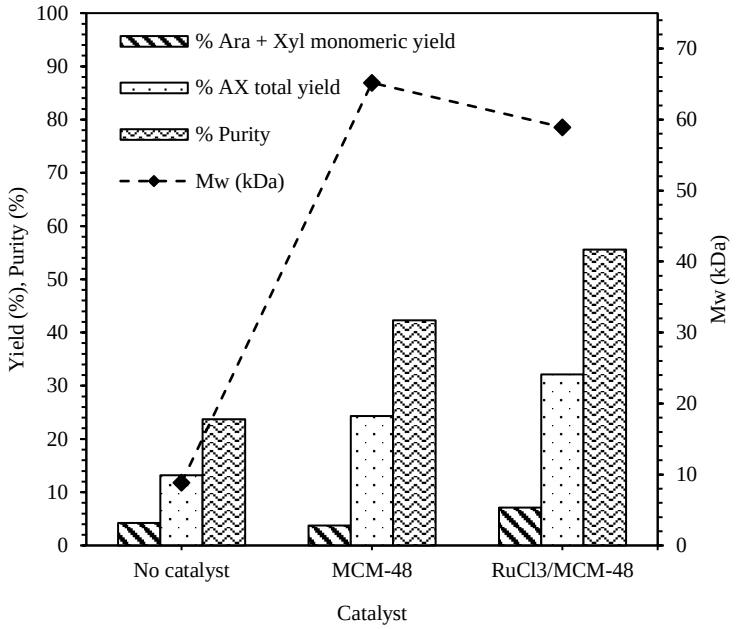

Figure 2. Effect of solid acid catalysts on AX yield, purity and molecular weight in the AX extraction process. Extraction conditions: 30 g DWB·L^{-1}, 160 ºC, 10 minutes.

In the blank experiment (no catalyst), the monomeric yield (4%) and the AX total yield (13%) were both low. The formation of this small amount of soluble oligomers may be due to the thermal hydrolysis of hemicelluloses (Sahu and Dhepe, 2012). At high temperatures, the amount of protons derived from water is higher than at room temperature. This is represented by the pK_w value of water, which is 13.99 and 11.64 at 25 ºC and 150 ºC, respectively (Bandura and Lvov, 2006). The lower the pK_w value, the higher quantity of H_3O^+ produced from water, which results in a higher thermal fractionation of arabinoxylans.

The incorporation of a solid acid catalyst improves the arabinoxylan extraction. The AX total yield was enhanced by MCM-48 (24%) and even more by means of $RuCl_3$/MCM-

48 (32%), which is accordant to the catalyst acidity. $RuCl_3$/MCM-48 has a higher number of acid sites than MCM-48 (Table 2). The acidity of MCM-48 corresponds mainly to weak Lewis acid sites due to the terminal silanol groups (Si – OH) (Xue et al., 2004). The higher acidity of $RuCl_3$/MCM-48 is related to the high acidity of the catalyst precursor ($RuCl_3$), since Ru^{+3} cations are moderate Lewis acids (Shimizu et al., 2009). The monomeric yield was similar with and without MCM-48 (4%). The incorporation of $RuCl_3$/MCM-48 improved slightly the production of monomers (7%). Therefore, both catalysts enhanced the extraction of arabinoxylans, but not affected significantly the formation of monomers under these experimental conditions (160 ºC, 10 minutes). It should be noted that the purity was also higher after the hydrothermal extraction assisted by a solid catalyst.

In the absence of a catalyst (blank experiment), the average molecular weight (9 kDa) and the amount of solubilized sugars were low, suggesting that only side chains of the arabinoxylan structure were extracted. These side chains are characterized by a low molecular weight and a larger amount of arabinose compared to xylose, which is in line with the high Ara/Xyl ratio (0.92) obtained in the blank experiment. The hydrolysis of side chains (composed by arabinose) is preferential over the hydrolysis of the backbone (composed by xylose) due to the easier access. This fact results in a greater release of arabinose than xylose under soft operating conditions, and therefore in a high Ara/Xyl ratio. The faster hydrolysis of side chains is also related to the the type of bonding. Arabinose molecules of side chains are linked by α-glycosidic bonds, whereas xylose molecules of the backbone are connected by β-glycosidic bonds. The easier hydrolysis of α-glycosidic bonds than β-glycosidic linkages also explains the faster release of arabinose than xylose (Negahdar et al., 2016). The incorporation of MCM-48 or $RuCl_3$/MCM-48 led to a higher amount of extracted oligomers with a higher molecular weight. At 160 ºC,

these solid acid catalysts promoted the solubilization of side chains as well as part of the xylan backbone, giving rise to a lower Ara/Xyl ratio (0.65 – 0.78). Nevertheless, the hydrolysis of the backbone into short oligomers did not occur, as demonstrated by the high molecular weight, since the operating conditions were not harsh enough.

In conclusion, in the absence of a catalyst under these operating conditions (160 ºC, 10 minutes) only side chains of AXs were solubilized. However, with the incorporation of a solid acid catalyst (MCM-48 or $RuCl_3$/MCM-48), part of the xylan backbone with a relatively high molecular weight was also extracted.

3.3.2 Effect of temperature

As previously discussed, $RuCl_3$/MCM-48 gave rise to a higher AX extraction yield than bare MCM-48. Therefore, this $RuCl_3$-supported catalyst was further used to study the effect of temperature. Temperature was considered between 140 and 180 ºC, whereas the same time was set in all the experiments. Figure 3 and Table S1 contain the results arising from these experiments.

The yield of monomers and oligomers increased with temperature in the range 140 – 180 ºC. The pK_w value of water does not vary significantly in this temperature range (Bandura and Lvov, 2006), so the higher yields can be explained by Arrhenius equation: the kinetic constant and therefore the reaction rate increase with increasing temperature.

The average molecular weight also changed at different temperatures. The molecular weight of the AXs extracted at 140 ºC and 180 ºC was around 8 kDa. However, the AX yield and the ratio arabinose to xylose were very different. At 140 ºC, the AX total yield was quite low (12%), whereas at 180 ºC it increased up to 71%. As explained in section 3.3.1, arabinoxylan side chains are characterized by a low molecular weight and a higher quantity of arabinose than xylose. The arabinoxylan backbone consists however of bound xylose molecules, forming long chains which can be extracted and subsequently

hydrolyzed into shorter oligosaccharides. Therefore, the results suggest that at 140 ºC only side chains of the arabinoxylans were extracted, leading to a low yield (12%) and a low molecular weight (8 kDa) but a high Ara/Xyl ratio (0.73). Nonetheless, at 180 ºC part of the arabinoxylan backbone was solubilized and further hydrolyzed into shorter oligomers, resulting in a high AX yield (71%), a low molecular weight (8 kDa) and a low Ara/Xyl ratio (0.53). This is also in agreement with the monomeric yield, since at 180 ºC (13%) was higher than at 140 ºC (2%). At 160 ºC, the AX total yield was 32% and the average molecular weight was quite high (59 kDa). In this case, the solubilized AXs came from side chains and also from the backbone, but according to the high value of the Mw, not a significant hydrolysis of the backbone into short oligomers occurred.

The highest purity was obtained at 140 ºC, although the AX yield was very low. At 160 ºC and 180 ºC, the purity decreased because more cellulose (Table S1) was co-extracted.

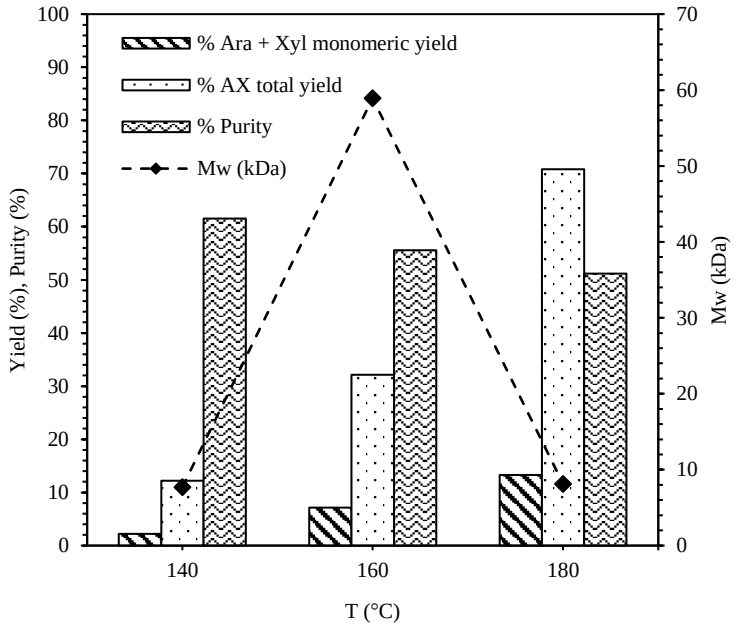

Figure 3. Effect of temperature on AX yield, purity and molecular weight in the AX extraction process. Extraction conditions: 30 g DWB·L^{-1}, 10 minutes, 500 mg $RuCl_3$/MCM-48.

3.3.3 Effect of time

The effect of time on the AX extraction process was studied at 160 ºC (Figure 4A) and 180 ºC (Figure 4B) using $RuCl_3$/MCM-48.

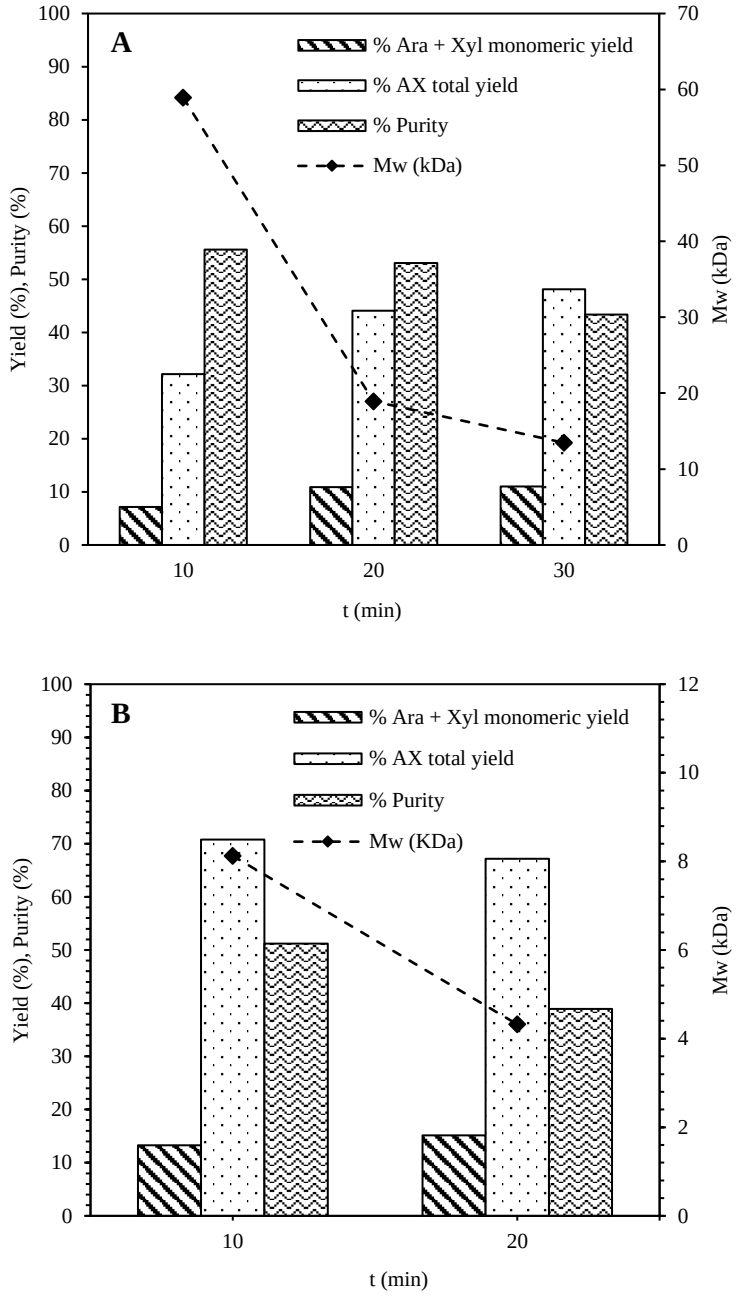

Figure 4. Effect of time on AX yield, purity and molecular weight in the AX extraction process. Extraction conditions: A) 30 g DWB·L^{-1}, 160 ºC, 500 mg $RuCl_3$/MCM-48 and B) 30 g DWB·L^{-1}, 180 ºC, 500 mg $RuCl_3$/MCM-48.

At 160 ºC, the AX total yield increased with time from 32% (10 minutes) to 48% (30 minutes). The monomeric yield (arabinose + xylose) followed a similar trend, rising from 7% to 11% in this time range. Different times had an important impact on the molecular weight. As mentioned in the previous section, the extracted AXs at 160 ºC and 10 minutes using $RuCl_3$/MCM-48 came from side chains and the arabinoxylan backbone. The average molecular weight was still quite high because the hydrolysis of oligosaccharides did not occur significantly. However, at longer times (20 and 30 minutes), the yield increased, and the molecular weight underwent a drastic drop (from 59 kDa to 19 and 13 kDa, respectively). Thus, at longer times a greater amount of arabinoxylans was extracted, and at the same time, converted into low molecular weight oligosaccharides. It should be noted that the AX total yield was very similar after 20 and 30 minutes (44 and 48%, respectively). Moreover, the purity started to decline after 30 minutes. Therefore, experiments at longer times had no sense.

The amount of AXs extracted at 180 ºC using $RuCl_3$/MCM-48 was much higher than at 160 ºC, even at short times. The AX total yields were 71% and 67% after 10 and 20 minutes, respectively, which means that arabinoxylans started to be degraded after 20 minutes. The purity also decreased after 20 minutes (from 51% at 10 minutes to 39% at 20 minutes) due to the higher cellulose co-extraction (Table S1) and the further degradation of arabinoxylans. However, not a higher quantity of degradation products (acetic acid, formic acid, glycolaldehyde, 5-HMF, furfural) was detected by HPLC after 20 minutes. This fact is in agreement with the results reported previously by Sahu and Dhepe (2012). The dark color resulting from the experiment at 20 minutes (180 ºC) is due to the insoluble and soluble degradation products. These products cannot be detected by HPLC and decrease significantly the purity of the final liquid extract. Regarding the molecular weight, shorter arabinoxylans were obtained after 20 minutes (4 kDa) than after

10 minutes (8 kDa). Nevertheless, the next study to determine the influence of the catalyst support was carried out at 180 ºC and 10 minutes in order to avoid the degradation of arabinoxylans at longer times as well as cellulose co-extraction.

3.3.4 Effect of catalyst support

The influence of the catalyst support was studied at 180 ºC and 10 minutes (Figure 5). The amount of catalyst was 500 mg for $RuCl_3$-based catalysts and 480 mg for the mesoporous materials (480 mg is the amount of support contained in 500 mg of $RuCl_3$-based catalysts). The AX total yield as well as the monomeric yield showed the following trend: MCM-48 < Al-MCM-48 < $RuCl_3$/MCM-48 < $RuCl_3$/Al-MCM-48. This is consistent with the acidity values: the higher the acidity, the higher amount of arabinoxylans solubilized. The acidity of MCM-48 is due to terminal silanol groups (Si – OH). However, this kind of acidity corresponds to weak Lewis acid sites (Xue et al., 2004), resulting in lower yields. Al-MCM-48 exhibited a better catalytic activity than MCM-48, which is attributed to its higher acidity. During the synthesis of Al-MCM-48, an atom of silicon is substituted by an atom of aluminum in a tetrahedral structure. These aluminum atoms are compensated by a proton provided by the decomposition of the surfactant during the thermal removal of the template, which results in the creation of Brönsted acid sites (Collart et al., 2004; Kao et al., 2008). As mentioned before, Ru^{+3} cations, which are moderate Lewis acids, are the responsible for the higher total acidity of the $RuCl_3$-based catalysts and therefore, for their better performance (Shimizu et al., 2009).

The molecular weight of the arabinoxylans was higher when using MCM-48 (26 kDa) or Al-MCM-48 (20 kDa) than the corresponding $RuCl_3$-based catalysts supported on them (around 8 – 9 kDa). This means that a major AX hydrolysis occurs over a more acidic catalyst. In addition to this, a decreasing trend in the Ara/Xyl ratio was observed when

the acidity of the solid increased (Table S1). This implies that the hydrolysis of the arabinoxylan backbone, composed mainly by xylose molecules, is also favored by high acidic catalysts.

$RuCl_3$ supported catalysts improved not only the arabinoxylan extraction but also their conversion into short oligomers. Comparing the two $RuCl_3$ catalysts, $RuCl_3$/Al-MCM-48 showed a better performance. At 180 ºC and after 10 minutes, the AX total yield and the monomeric yield were 78% and 15%, respectively. The purity in arabinoxylans was 54% and the average molecular weight was around 9 kDa. $RuCl_3$/Al-MCM-48 was also tested at 180 ºC and longer times (20 minutes), as in the case of $RuCl_3$/MCM-48. The same tendency was observed with both catalysts, *i.e.* the arabinoxylan yield and the purity decreased after 20 minutes. This means that, despite not having tested $RuCl_3$/Al-MCM-48 in all the experiments, optimum conditions should be the same for both catalysts (180 ºC, 10 min).

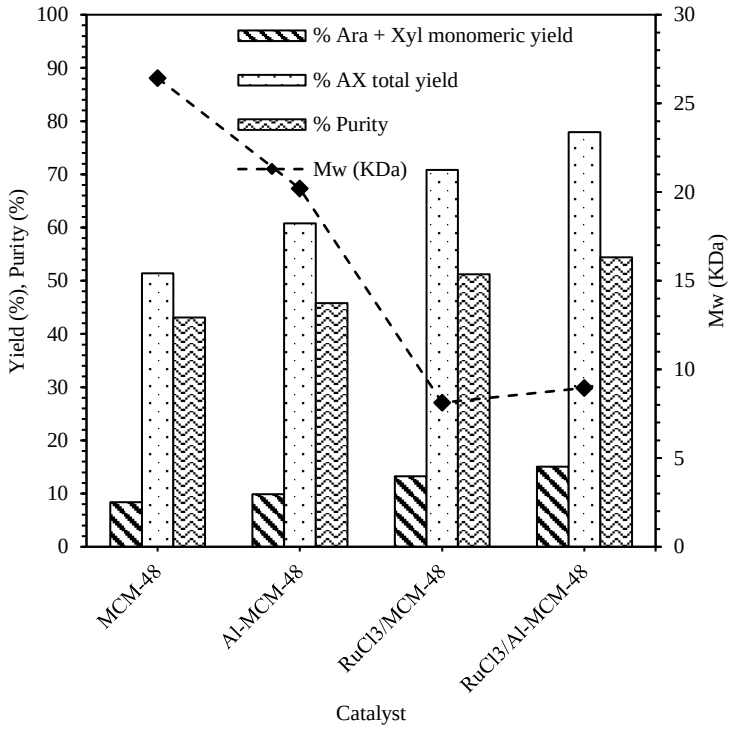

Figure 5. Effect of catalyst support on AX yield, purity and molecular weight in the AX extraction process. Extraction conditions: 30 g DWB·L^{-1}, 180 ºC, 10 minutes.

3.3.5 Relation between operating conditions, arabinoxylan yield and their molecular weight

Based on the obtained results, a relation between the different operating conditions, the arabinoxylan yield and the molecular weight was established (Table 3).

Table 3. Comparison of the experiments in terms of experimental conditions, AX total yield and Mw.

# Experiment	Experimental conditions	% AX yield	Mw (kDa)
1	140 °C, 10', 500 mg $RuCl_3$/MCM-48	12	7.7
2	160 °C, 10', no catalyst	13	8.9
3	160 °C, 10', 480 mg MCM-48	24	65.2
4	160 °C, 10', 500 mg $RuCl_3$/MCM-48	32	58.9
5	160 °C, 20', 500 mg $RuCl_3$/MCM-48	44	18.9
6	160 °C, 30', 500 mg $RuCl_3$/MCM-48	48	13.5
7	180 °C, 10', 0,4800 g MCM-48	51	26.4
8	180 °C, 10', 0,4800 g Al-MCM48	61	20.2
9	180 °C, 20', 500 mg $RuCl_3$/MCM-48	67	4.3
10	180 °C, 10', 500 mg $RuCl_3$/MCM-48	71	8.1
11	180 °C, 10', 500 mg $RuCl_3$/Al-MCM-48	78	9.0

Soft operating conditions (Exp. #1, 2) gave rise to a low AX yield (12 – 13%) and a low molecular weight (8 – 9 kDa), which means that only side chains of the arabinoxylans were solubilized. Soft operating conditions correspond to the experiments carried out at 140 ºC using $RuCl_3$/MCM-48, and at 160 ºC without any catalyst, in both cases after 10 minutes. Under moderate operating conditions (Exp. #3 – 5), the AX total yield (24 – 35%) as well as the molecular weight (59 – 65 kDa) increased. These results reflect the extraction of side chains and a part of the arabinoxylan backbone. The high molecular weight implies that the arabinoxylans from the backbone were extracted but not significantly hydrolyzed, since the experimental conditions were not harsh enough to break the bonds between the oligomers molecules. More severe operating conditions (Exp. #6 – 12) led to a high amount of AXs extracted (44 – 78%) with a low molecular

weight (4 – 26 kDa). In this case, the arabinoxylan backbone was not only solubilized but also hydrolyzed into shorter chain oligomers. Indeed, the experiment performed at 180 ºC, 10 minutes and using $RuCl_3$/Al-MCM-48 conducted to the best results in terms of yield and molecular weight. Liquid extracts enriched in arabinoxylans with a low molecular weight are excellent raw materials for further hydrogenation/oxidation reactions in which monomers or short oligomers are needed in order to obtain a high selectivity into the desired products.

4. Conclusions

In this work, a hydrothermal process assisted by heterogeneous catalysts has been successfully applied to recover the arabinoxylan fraction from destarched wheat bran. The addition of solid acid catalysts, based on mesoporous silica (MCM-48 type), enhanced the hydrolysis rate compared to the blank experiment. The tendency observed in the AX total yield and the monomeric yield was as follows: MCM-48 < Al-MCM-48 < $RuCl_3$/MCM-48 < $RuCl_3$/Al-MCM-48. The same trend exhibited the acidity of the catalyst, *i.e.* a higher acidity led to a higher extraction yield. The extraction of high amounts of arabinoxylans with a low molecular weight was favored by relatively high temperatures, short extraction times and solid catalysts with high acidity. $RuCl_3$-based catalysts demonstrated to be more active in this process than the corresponding mesoporous silica supports. Optimum conditions were achieved at 180 ºC, 10 minutes and using $RuCl_3$/Al-MCM-48 as catalyst. Under such conditions, the arabinoxylan total yield was 78% and the molecular weight was around 9 kDa. This low molecular weight facilitates the further conversion of the arabinoxylans into the corresponding monomers.

References

Aguedo, M., Fougnies, C., Dermience, M. and Richel, A. Extraction by three processes of arabinoxylans from wheat bran and characterization of the fractions obtained. *Carbohydrate Polymers,* 105 (2014) 317–324.

Apprich, S., Tirpanalan, Ö., Hell, J., Reisinger, M., Böhmdorfer, S., Siebenhandl-Ehn, S., Novalin, S. and Kneifel, W. Wheat bran-based biorefinery 2: Valorization of products. *LWT - Food Science and Technology,* 56 (2014) 222–231.

Bandura, A.V. and Lvov, S.N. The ionization constant of water over wide ranges of temperature and density. *Journal of Physical and Chemical Reference Data,* 35 (2006) 14–30.

Bataillon, M., Mathaly, P., Nunes Cardinali, A-P. and Duchiron, F. Extraction and purification of arabinoxylan from destarched wheat bran in a pilot scale. *Industrial Crops and Products,* 8 (1998) 37–43.

Beaugrand, J., Chambat, G., Wong, V.W.K., Goubet, F., Rémond, C., Paës, G., Benamrouche, S., Debeire, P., O´Donohue, M., and Chabbert, B. Impact and efficiency of GH10 and GH11 thermostable endoxylanases on wheat bran and alkali-extractable arabinoxylans. *Carbohydrate Research,* 339 (2004) 2529–2540.

Benito-Román, Ó., Alonso, E., Gairola, K., and Cocero, M.J. Fixed-bed extraction of β-glucan from cereals by means of pressurized hot water. *The Journal of Supercritical Fluids,* 82 (2013) 122–128.

Benito-Román, Ó., Alonso, E., Palacio, L., Prádanos, P., and Cocero, M.J. Purification and isolation of β-glucans from barley: Downstream process intensification. *Chemical Engineering and Processing: Process Intensification,* 84 (2014) 90–97.

Buranov, A.U., and Mazza, G. Extraction and characterization of hemicelluloses from flax shives by different methods. *Carbohydrate Polymers,* 79 (2010) 17–25.

Coelho, E., Rocha, M.A.M., Saraiva, J.A. and Coimbra., M.A. Microwave superheated wáter and dilute alkali extraction of brewers' spent grain arabinoxylans and arabinoxylo-oligosaccharides. *Carbohydrate Polymers,* 99 (2014) 415–422.

Collart, O., Cool, P., Van Der Voort, P., Meynen, V., Vansant, E.F., Houthoofd, K., Grobet, P.J., Lebedev, O.I., and Tendeloo, G.V. Aluminum Incorporation into MCM-48 toward the creation of Brønsted acidity. *The Journal of Physical Chemistry B,* 108 (2004) 13905–13912.

Das, A.M., Hazarika, M.P., Goswami, M., Yadav, A., and Khound, P. Extraction of cellulose from agricultural waste using Montmorillonite K-10/LiOH and its conversion to renewable energy: Biofuel by using Myrothecium gramineum. *Carbohydrate Polymers,* 141 (2016) 20–27.

De Almedia, R.M., De Albuquerque, N.J.A., Souza, F.T.C., and Meneghetti, S.M.P. Catalysts based on TiO_2 anchored with MoO_3 or SO_4^{2-} for conversion of cellulose into chemicals. *Catalysis Science & Technology, 6 (2016)* 3137–3142.

Dien, B.S., Li, X-L., Iten, L.B., Jordan, D.B., Nichols, N.N., O´Bryan, P.J., and Cotta, M. A. Enzymatic saccharification of hot-water pretreated corn fiber for production of monosaccharides. *Enzyme and Microbial Technology,* 39 (2006) 1137–1144.

Doner, L.W., Chau, H.K., Fishman, M.L., and Hicks, K.B. An improved process for isolation of corn fiber gum. *Cereal Chemistry,* 75 (1998) 408–411.

Ganguli, N.K., and Turner, M.A. A simplified method for extracting water-extractable arabinoxylans from wheat flour. *Journal of the Science of Food and Agriculture,* 88 (2008) 1905–1910.

Garrote, G., Domínguez, H., and Parajó, J.C. Hydrothermal processing of lignocellulosic materials. *Holz als Roh – und Werkstoff*, 57 (1999) 191–202.

Garrote, G., Domínguez, H., and Parajó, J.C. Kinetic modelling of corncob autohydrolysis. *Process Biochemistry, 36* (2001) 571–578.

Gebruers, K., Dornez, E., Boros, D., Frás, A., Dynkowska, W., Bedo, Z., Rakszegi, M., Delcour, J.A., and Courtin, C. M. Variation in the content of dietary fiber and components thereof in wheats in the HEALTHGRAIN diversity screen. *Journal of Agricultural and Food Chemistry*, 56 (2008) 9740–9749.

Hames, B., Scarlata, C., and Sluiter, A. Determination of Protein Content in Biomass. Laboratory Analytical Procedure (LAP). Technical Report NREL/TP-510-42625, 2008.

Höije, A., Gröndahl, M., TØmmeraas, K., and Gatenholm, P. Isolation and characterization of physicochemical and material properties of arabinoxylans from barley husks. *Carbohydrate Polymers,* 61 (2005) 266–275.

Hollmann, J., and Lindhauer, M.G. Pilot-scale isolation of glucuronoarabinoxylans from wheat bran. *Carbohydrate Polymers, 59* (2005) 225–230.

Hu, H., Li, Z., Wu, Z., Lin, L., and Zhou, S. Catalytic hydrolysis of microcrystalline and rice straw-derived cellulose over a chlorine-doped magnetic carbonaceous solid acid. *Industrial Crops and Products,* 84 (2016) 408–417.

Hu, L., Tang, X., Wu, Z., Lin, L., Xu, J., Xu, N., and Dai, B. Magnetic lignin-derived carbonaceous catalyst for the dehydration of fructose into 5-hydroxymethylfurfural in dimethylsulfoxide. *Chemical Engineering Journal,* 263 (2015) 299–308.

Huang, Y-B., and Fu, Y. Hydrolysis of cellulose to glucose by solid acid catalysts. *Green Chemistry,* 15 (2013) 1095–1111.

Izydorczyk, M.S., and Biliaderis, C.G. Arabinoxylans: Technologically and nutritionally functional plant polysaccharides. In *Functional food carbohydrates*, Izydorczyk, M.S., and Biliaderis, C.G., (Eds.), CRC Press: Boca Raton, 2007.

Josefsson, T., Lennholm, H., and Gellerstedt, G. Steam explosion of Aspen Wood. Characterisation of reaction products. *Holzforschung*, 56 (2002) 289–297.

Kao, H-M., Chang, P-C., Liao, Y-W., Lee, L-P., and Chien, C-H. Solid-state NMR characterization of the acid sites in cubic mesoporous Al-MCM-48 materials using trimethylphosphine oxide as a P NMR probe. *Microporous and Mesoporous Materials*, 114 (2008) 352–364.

Kobayashi, H., Komanoya, T., Guha, S.K., Hara, K., and Fukuoka, A. Conversion of cellulose into renewable chemicals by supported metal catalysis. *Applied Catalysis A: General*, 409-410 (2011) 13–20.

Maes, C. and Delcour, J.A. Structural of water-extractable and water-unextractable arabinoxylans in wheat bran. *Journal of Cereal Science*, 35 (2002) 315–326.

Morais, A.R.C, Matuchaki, M.D.D.J., Andreaus, J., and Bogel-Lukasik, R. A green and efficient approach to selective conversion of xylose and biomass hemicellulose into furfural in aqueous media using high-pressure CO_2 as a sustainable catalyst. *Green Chemistry*, 18 (2016) 2985–2994.

Nabarlatz, D., Farriol, X., and Montané, D. Kinetic modeling of the autohydrolysis of lignocellulosic biomass for the production of hemicellulose-derived oligosaccharides. *Industrial and Engineering Chemistry Research*, 43 (2004) 4124–4131.

Nandini, C.D., and Salimath, P.V. Carbohydrate composition of wheat, wheat bran, sorghum and bajra with good chapati/roti (Indian flat bread) making quality. *Food Chemistry*, 73 (2001) 197–203.

Negahdar, L., Delidovich, I., and Palkovits, R. Aqueous-phase hydrolysis of cellulose and hemicelluloses over molecular acidic catalysts: Insights into the kinetics and reaction mechanism. *Applied Catalysis B: Environmental*, 184 (2016) 285–298.

Prückler, M., Siebenhandl-Ehn, S., Apprich, S., Höltinger, S., Haas, C., Schmid, E., and Kneifel, W. Wheat bran-based biorefinery 1: Composition of wheat bran and strategies of functionalization. *LWT - Food Science and Technology*, 56 (2014) 211–221.

Romero, A., Alonso, E., Sastre, Á., and Nieto-Márquez, A. Conversion of biomass into sorbitol: cellulose hydrolysis on MCM-48 and D-glucose hydrogenation on Ru/MCM-48. *Microporous & Mesoporous Materials*, 224 (2016) 1–8.

Rose, D.J., and Inglett, G.E. Production of feruloylated arabinoxylo-oligosaccharides from maize (Zea mays) bran by microwave-assisted autohydrolysis. *Food Chemistry*, 119 (2010) 1613–1618.

Sahu, R., and Dhepe, P.L. A one-pot method for the selective conversion of hemicellulose from crop waste into C5 sugars and furfural by using solid acid catalysts. *ChemSusChem*, 5 (2012) 751–761.

Seyer, M-É., and Gélinas, P. Bran characteristics and wheat performance in whole wheat bread. *International Journal of Food Science & Technology*, 44 (2009) 688–693.

Shimizu, K-I., Furukawa, H., Kobayashi, N., Itayab, Y., and Satsum, A. Effects of Brønsted and Lewis acidities on activity and selectivity of heteropolyacid-based catalysts for hydrolysis of cellobiose and cellulose. *Green Chemistry*, 11 (2009) 1627–1632.

Sluiter, A., Hames, B., Ruiz, R., Scarlata, C., Sluiter, J., and Templeton, D. Determination of sugars, byproducts, and degradation products in liquid fraction process samples. Laboratory Analytical Procedure (LAP). Technical Report NREL/TP-510-42623, 2008.

Sluiter, J., and Sluiter, A. Summative mass closure. Laboratory Analytical Procedure (LAP). Review and Integration. Technical Report NREL/TP-510-48087, 2011.

Sun, R.C., and Tomkinson, J. Characterization of hemicelluloses obtained by classical and ultrasonically assisted extractions from wheat straw. *Carbohydrate Polymers,* 50 (2002) 263–271.

Sun, X.F., Xu, F., Sun, R.C., Geng, Z.C., Fowler, P., and Baird, M.S. Characteristics of degraded hemicellulosic polymers obtained from steam exploded wheat straw. *Carbohydrate Polymers,* 60 (2005) 15–26.

Tathod, A., Kane, T., Sanil, E.S., and Dhepe, P.L. Solid base supported metal catalysts for the oxidation and hydrogenation of sugars. *Journal of Molecular Catalysis A: Chemical,* 388-389 (2014) 90–99.

Tathod, A.P., and Dhepe, P.L. Efficient method for the conversion of agricultural waste into sugar alcohols over supported bimetallic catalysts. *Bioresource Technology,* 178 (2015) 36–44.

Xu, F., Liu, C.F., Geng, Z.C., Sun, J.X., Sun, R.C., Hei, B.H., Lin, L., Wu, S.B., and Je, J. Characterisation of degraded organosolv hemicelluloses from wheat straw. *Polymer Degradation and Stability,* 91 (2006) 1880–1886.

Xue, P., Lu, G., Guo, Y., Wang, Y., and Guo, Y. A novel support of MCM-48 molecular sieve for immobilization of penicillin G acylase. *Journal of Molecular Catalysis B: Enzymatic,* 30 (2004) 75–81.

Zhang, X., Wang, S., Zhou, S., and Fu, X. Optimization of alkaline extraction conditions for arabinoxylan from wheat bran. *Journal of Nuclear Agricultural Sciences,* 22 (2008) 60–64.

Zhang, X., Zhou, S., and Wang, S. Optimizing enzymatic hydrolysis conditions of arabinoxylan in wheat bran through quadratic orthogonal rotation combination design. *Food Science,* 28 (2008) 141–145.

Zhang, Z., Smith, C., and Li, W. Extraction and modification technology of arabinoxylans from cereal by-products: A critical review. *LWT - Food Science and Technology,* 65 (2014) 423–436.

Zhou, S., Liu, X., Guo, Y., Wang, Q., Peng, D., and Cao, L. Comparison of the immunological activities of arabinoxylans from wheat bran with alkali and xylanase-aided extraction. *Carbohydrate Polymers,* 81 (2010) 784–789.

Supplementary Information

Table S1. Set of experiments and experimental results (monomeric and total yields, Ara/Xyl ratio).

Experimental conditions			Yield as monomeric sugars (%)[a]						Yield as total sugars (%)[b]						
T (ºC)	t (min)	Catalyst	Glc	Xyl	Gal	Ara	Man	A+X yield	Glc	Xyl	Gal	Ara	Man	AX yield	Ara/Xyl[c]
140	10	500 mg $RuCl_3$/MCM-48	0.2	0.3	1.8	5.7	4.2	2.2	5.8	10.8	8.0	14.9	8.4	12.2	0.73
160	10	-	8.3	9.7	9.6	7.5	0.7	9.0	9.0	10.5	12.4	18.4	7.3	13.2	0.92
160	10	480 mg MCM-48	16.6	21.7	15.0	18.5	1.4	20.6	17.5	22.5	16.4	27.8	4.4	24.3	0.65
160	10	500 mg $RuCl_3$/MCM-48	24.6	26.4	19.2	22.4	2.1	25.0	26.8	27.6	23.7	40.8	10.9	32.1	0.78
160	20	500 mg $RuCl_3$/MCM-48	24.9	34.0	7.4	31.7	5.0	33.2	27.6	37.9	32.3	55.8	8.5	44.1	0.78
160	30	500 mg $RuCl_3$/MCM-48	25.9	39.8	28.6	31.9	1.2	37.1	28.2	42.0	38.0	59.8	14.4	48.1	0.75
180	10	480 mg MCM-48	24.5	44.5	44.2	40.4	18.8	43.1	26.4	46.3	52.1	61.2	49.3	51.4	0.70
180	10	480 mg Al-MCM-48	25.5	54.8	59.6	43.6	35.6	50.9	27.7	56.8	68.4	68.4	61.4	60.8	0.63
180	20	500 mg $RuCl_3$/MCM-48	31.5	66.0	35.8	25.5	4.8	52.1	35.1	71.7	48.3	58.6	16.4	67.2	0.43
180	10	500 mg $RuCl_3$/MCM-48	25.3	67.7	36.7	38.3	0.3	57.5	28.2	70.6	46.9	71.2	14.7	70.8	0.53
180	10	500 mg $RuCl_3$/Al-MCM-48	28.1	75.6	39.1	38.8	0.6	62.9	31.5	79.2	51.7	75.6	27.4	78.0	0.50

[a] Yield as monomeric sugars by original sugar content in raw material.
[b] Yield as total sugars (monomeric + oligomeric) by original sugar content in raw material.
[c] Arabinose/xylose ratio as total sugars.

CHAPTER II

MAXIMIZATION OF MONOMERIC C_5 SUGARS FROM WHEAT BRAN BY USING MESOPOROUS ORDERED SILICA CATALYSTS

Sánchez-Bastardo, N., and Alonso, E. Maximization of monomeric C5 sugars from wheat bran by using mesoporous ordered silica catalysts. *Bioresource Technology*, 238 (2017) 379–388.

Abstract

The hydrolysis process of a real fraction of arabinoxylans derived from wheat bran was studied. The influence of several solid acid catalysts (MCM-48 type materials and $RuCl_3$-based catalysts) and loadings, reaction time and different metal cations (Ru^{+3}, Fe^{+3}) was discussed in terms of the yields of arabinose and xylose as well as the formation of furfural as main degradation product. A high yield of arabinose and xylose (96% and 94%, respectively) was obtained at relatively high temperatures (180 ºC) and short reaction times (15 min) with a catalyst loading of 4.8 g of $RuCl_3$/Al-MCM-48 per g of carbon in initial hemicelluloses.

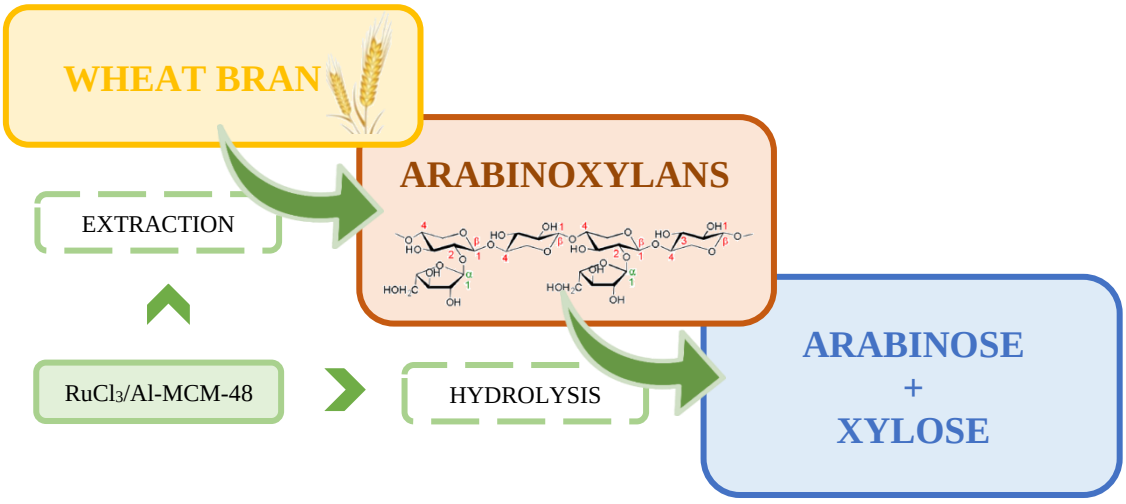

1. Introduction

The current depletion of fossil resources is forcing society to seek renewable alternatives for energy and chemicals production. Biomass is considered a sustainable and renewable feedstock to substitute fossil-based fuels (Negahdar et al., 2016; Oh et al., 2015; Putro et al., 2016; Singhvi et al., 2014). Biomass accrues in large amounts all over the world as forestry and agricultural waste. Moreover, around 95% of this biomass consists of lignocellulosic material which is not edible for humans. Thus, its application to biofuels or chemicals synthesis does not compete with food production (Negahdar et al., 2016; Sahu and Dhepe, 2012).

Agricultural residues like straw, corn stover or wheat bran appear as interesting feedstocks to obtain high added-value products (Apprich et al., 2014). Wheat bran is a by-product of the wheat grain milling. About 150 million tons are produced per year worldwide and it is basically only used as a low value ingredient in animal food (Prückler et al., 2014). The general composition of wheat bran is as follows: water (12.1%), proteins (13.2 – 18.4%), fats (3.5 – 3.9%), starch (13.8 – 24.9%), cellulose (11.0%), arabinoxylans (10.9 – 26.0%), β-glucans (2.1 – 2.5%), phenolic acids (0.02 – 1.5%) and ash (3.4 – 8.1%) (Apprich et al., 2014). Arabinoxylans (AXs) are a major component located in the cell walls of wheat bran. AXs belong to the hemicellulosic part of biomass and consist of a backbone of β-1,4 linked D-xylopyranosyl residues (Izydorczyk and Biliaderis, 2007). Xylose units are highly substituted with L-arabinose residues as well as short arabinooligosaccharides, D-galactose, D-4-*O*-methylglucuronic acid, ferulic units and *p*-coumaric acid (Koutinas et al., 2008; Peng et al., 2012; Zhang et al., 2014). Arabinoxylans can be isolated from wheat bran as poly/oligosaccharides and further converted into different intermediate or final chemicals such as furfural, succinic acid, xylitol or arabitol (Apprich et al., 2014).

In general, hemicelluloses are partly solubilized and hydrolyzed during biomass fractionation, resulting in an aqueous phase enriched in poly/oligosaccharides. Although hemicellulosic poly/oligosaccharides have important applications in pharmaceutical and food industries, the market volume is larger to the monosaccharide-derived products. For instance, xylose and arabinose as monomers are platform molecules of sugar alcohols (via hydrogenation reactions) and biofuels (via fermentation processes). In such cases, hydrolysis of oligosaccharides into pentoses without further dehydration into furfural is critical to increase the global efficiency of the process (Vilcocq et al., 2014).

Therefore, the fractionation and complete hydrolysis of hemicellulosic poly/oligosaccharides into monomers are critical steps for an integrated biorefinery. The fractionation implies the selective release of hemicelluloses from the biomass structure to an aqueous phase followed by their partial hydrolysis into poly/oligosaccharides with lower molecular weights. The subsequent conversion of these poly/oligosaccharides into monomers has historically been carried out by two different methods: using mineral acids (hydrolysis yield: 50 – 89%) (Hilpmann et al., 2016; Kim et al., 2013; Kusema et al., 2013; Li et al., 2016; Nakasu et al., 2016) or enzymes (hydrolysis yield: 6 – 84%) (Jia et al., 2016; Lee et al., 2013; Li, Wang et al., 2016; Li, Xue et al., 2016; Lou et al., 2016; Moreira and Filho, 2016). Chemical hydrolysis using mineral acids is not selective and degrades the monomeric sugars into undesired by-products. Moreover, the removal of acids requires the addition of cations, which leads to the formation of salts and corrosion problems, rising the capital costs (Negahdar et al., 2016). Enzymes are very selective, but they are currently not commercial. Enzymatic processes take long times and the operating conditions require a critical control. The extremely high price of enzymes and the non-existence of recovery methods are also important drawbacks of enzymatic treatments (Aden et al., 2002; Cará et al., 2013; Hendriks and Zeeman, 2009; Ormsby et al., 2012).

Hydrolysis of oligosaccharides using heterogeneous acid catalysts is a green alternative to these methods. Solid catalysts can be easily separated by a filtration process. Likewise, they are safe and non-corrosive. Therefore, solid acid catalysts are an opportunity to develop more efficient and greener processes for the hydrolysis of soluble poly/oligosaccharides. Vilcocq et al. (2014) described the advantages and limitations of different solid acid catalysts (zeolites, resins, carbon materials, clays, silicas and other oxides) and identified desirable characteristics in the design of future catalysts. Hydrolysis of polysaccharides over solid acid catalysts is a sequence of three first order reactions: 1) hydrolysis of polysaccharides into oligosaccharides, 2) hydrolysis of oligosaccharides into monosaccharides, 3) depending on the reaction conditions, dehydration of monosaccharides into by-products such as furfural. Acid strength, time and temperature must be carefully chosen to favor hydrolysis reactions and avoid degradation (Mäki-Arvela et al., 2011; Vilcocq et al., 2014;).

Recently, the development of solid acid catalysts for the hydrolysis of hemicelluloses has attracted the attention of several authors (Cará et al., 2013; Dhepe and Sahu, 2010; Kusema et al., 2011; Sahu and Dhepe, 2012; Salmi et al., 2014; Vilcocq et al., 2014; Zhang et al., 2017; Zhou et al., 2013; Zhong et al., 2015). Cará et al. (2013) reported a maximum hydrolysis yield of xylose + arabinose of 80% using Amberlyst 35 as solid catalyst and commercial beechwood xylan as raw material (120 ºC, 10 bar argon, 4 hours). Kusema et al. (2011) compared the activity of different sulfonated resins to study the hydrolysis of commercial arabinogalactan. The highest yield (95% monomeric arabinose) was reached with Smopex-101 (pH = 2) at 90 ºC after 3 hours. Sahu and Dhepe (2012) studied the effect of different solid acid catalysts on the hydrolysis of oat spelt. They got a hydrolysis yield (xylose + arabinose) of 41% using HUSY zeolite (Si/Al = 15) (170 ºC, 3 h, 50 bar nitrogen). These studies were performed using commercial hemicelluloses as

raw material. Nevertheless, there are only few studies on the hydrolysis of hemicelluloses derived from raw biomass (Vilcocq et al., 2014). The purity of hemicellulosic extracts is limited because some other biomass compounds, such as extractives, proteins and lignin, may have been co-extracted during the first fractionation step. All these compounds can reduce the efficiency of the hydrolysis process due to catalyst poisoning. Thus, the optimization of the hydrolysis step of a real fraction of hemicelluloses is critical for the development of a biorefinery.

In this work, we have investigated the catalytic hydrolysis of hemicellulosic poly/oligosaccharides previously extracted from wheat bran. Different solid acid catalysts based on mesoporous silica (MCM-48) as well as different catalyst loadings and reaction times have been studied to maximize the production of pentoses avoiding further degradation to furfural. The incorporation of aluminum to the support (Al-MCM-48) and the influence of different Lewis acid metals (Ru^{+3} and Fe^{+3}) have also been examined. The final aim of this work was to validate a two-step method consisting of a hydrothermal fractionation of arabinoxylans from destarched wheat bran (Sánchez-Bastardo et al., 2017) followed by a second catalytic hydrolysis step into monomers.

2. Experimental

2.1 Support and catalyst preparation

The synthesis of two different mesoporous silica materials, MCM-48 and Al-MCM-48, was carried out using the procedure described by Romero et al. (2016) in a previous work. 2.0 g of n-hexadecyltrimethylammonium bromide (for molecular biology, ≥ 99%; Sigma-Aldrich) were dissolved in 42 mL of distilled water, 18 mL of absolute ethanol (Panreac AppliChem) and 13 mL of an aqueous ammonia solution (20% $w \cdot w^{-1}$) (Panreac AppliChem). After stirring for 15 minutes, 0.077 g of sodium aluminate (technical, anhydrous; Sigma-Aldrich) were incorporated for the synthesis of Al-MCM-48. Then, 4

mL of tetraethyl orthosilicate (≥ 99.0% (GC); Sigma-Aldrich) were added dropwise and the solution was further stirred for 18 hours. The white precipitate was recovered by filtration and rinsed thoroughly with distilled water. The solid was then dried at 60 ºC overnight. After drying, the samples were calcined to remove the surfactant. The calcination was performed by increasing the temperature from 80 to 550 ºC at a heating rate of 2 ºC·min^{-1} and maintaing 550 ºC overnight.

Ruthenium and iron chloride catalysts were synthetized by wetness impregnation method using the so prepared MCM-48 and Al-MCM-48 as supports (Romero et al., 2016). Ruthenium (III) chloride (anhydrous; Strem Chemicals Inc.) or iron (III) chloride (reagent grade, 97%; Sigma-Aldrich) were dissolved in water and sonicated for 10 minutes. The corresponding support was suspended in water and sonicated also for 10 minutes. The solution of $RuCl_3$ or $FeCl_3$ and the support suspension were mixed and further sonicated for 10 minutes. This mixture was heated up from 30 to 80 ºC at a heating rate of 1 ºC·min^{-1}. Temperature was maintained at 80 ºC until the water was visibly evaporated. The catalyst was finally dried overnight at 105 ºC to eliminate the remaining water.

2.2 Support and catalyst characterization

Nitrogen adsorption-desorption isotherms were performed with ASAP 2020 (Micromeritics, USA) to determine surface and pore properties of the catalysts. Before analysis, the samples were outgassed overnight at 350 ºC. The multipoint BET method at $P/P_0 \leq 0.3$ was used to calculate the total specific surface area. The total specific pore volume was evaluated from N_2 uptake at $P/P_0 \geq 0.99$ and the pore diameter was determined by BJH adsorption average ($4 \cdot V \cdot A^{-1}$, nm).

The ruthenium and iron content of the supported catalysts was determined by atomic absorption spectroscopy (AAS) (SPECTRA 220FS analyser) after a digestion of the samples with HCl, H_2O_2 and HF using microwave at 250 ºC.

The acidity of the different catalysts was estimated by titration with NaOH. This method is based on procedures already reported in literature (Hu et al., 2015; Hu et al., 2016; Liu et al., 2013; Wang et al., 2011; Zheng et al., 2014). This acid-base titration does not distinguish between the nature of acid sites (Brönsted or Lewis) nor the strength of the acid sites. It is a measure of the total acidity.

2.3 Recovery of arabinoxylan fraction from wheat bran

A suspension composed of destarched wheat bran (30 $g \cdot L^{-1}$) and 500 mg of $RuCl_3$/Al-MCM-48 was placed in an AISI 304 stainless steel vessel of 170 mL. The isolation of the arabinoxylan fraction was performed at 180 ºC for 10 minutes under hot compressed water conditions. The optimization of the fractionation conditions is described in a previous work (Sánchez-Bastardo et al., 2017). After cooling, the final mixture was filtered to separate the remaining solid and the liquid extract. This arabinoxylan extract, composed mainly of oligomers, was further subjected to a hydrolysis process to obtain the corresponding monomers (arabinose + xylose). The composition of the arabinoxylan extract, which is the raw material in the present work, is shown in Table 1.

2.4 Hydrolysis experiments

The arabinoxylan extract obtained in the previous fractionation process was further hydrolyzed to obtain arabinose and xylose. The hydrolysis experiments of arabinoxylans were performed in a commercial stainless steel high pressure reactor (30 mL, Berghoff® BR-25) equipped with a PID controller. First, the corresponding solid catalyst was placed inside the reactor. The amount of catalyst in each experiment is given as gram of catalyst per gram of carbon content in initial hemicelluloses ($g \cdot g\ C^{-1}$). The reactor was then closed and vented with nitrogen several times to remove the oxygen. Thereafter, the reactor was pressurized with N_2 and heated up to the operating temperature (180 ºC). When the desired temperature was reached, the arabinoxylan solution preheated at 50 ºC was

pumped using a HPLC pump (PU-2080 Plus; Jasco). After pumping, temperature inside the reactor dropped to approximately 170 ºC and initial time (0 min) was considered when temperature reached again 180 ºC (this lasted approximately 3 min). At this moment, nitrogen pressure was adjusted to the operating pressure (50 bar). At the end of the experiments, the reaction was stopped by cooling the reactor in an ice-bath. The catalyst was recovered by filtration and the liquid was further used for the determination of monomeric sugars and degradation products.

2.5 Initial and final products analysis

The identification and quantification of sugars and degradation products was done by High Performance Liquid Chromatography (HPLC).

Monosaccharides and degradation products were directly analyzed in the samples after reaction. However, total sugars (monomers + oligomers) were determined after an acid hydrolysis according to the Laboratory Analytical Procedure (LAP) described by Sluiter et al. (2008). The samples were analyzed using a chromatography system consisting of an isocratic pump (Waters 1515; Waters Corporation) and an automatic injector (Waters 717; Waters Corporation). Two different HPLC columns were used for the identification and quantification of the different products: 1) Supelcogel Pb (Supelco) for sugars (milli-Q water as mobile phase, 0.5 $mL \cdot min^{-1}$ as flow rate and 85 ºC as temperature) and 2) Sugar SH-1011 (Shodex) for degradation products (sulfuric acid 0.01 N as mobile phase, 0.8 $mL \cdot min^{-1}$ as flow rate and 50 ºC as temperature). Sugars and acids were identified using a RI detector (Waters 2414; Waters Corporation). 5-hydroxymethylfurfural (5-HMF) and furfural were detected with an UV-Vis detector (Waters 2487; Waters Corporation) at a wavelength of 254 and 260 nm, respectively. The standards employed for the HPLC analysis were: cellobiose (98%), glucose (99%), xylose (99%), galactose (99%), arabinose (99%), mannose (99%), fructose (99%),

glyceraldehyde (95%), glycolaldehyde (99%), lactic acid (85%), formic acid (98%), acetic acid (99%), levulinic acid (98%), acrylic acid (99%), pyruvaldehyde (40%), 5-hydroxymethylfurfural (99%) and furfural (99%). All these chemicals were purchased from Sigma-Aldrich (Spain) and used as received.

The yield of arabinose (Ara) and xylose (Xyl) as well as the total monomeric yield and oligomers conversion were calculated according to Eq. 1 – 4:

$$\%\ \text{Ara yield} = \frac{\text{Ara as monomer (g)}}{\text{Ara as total sugars}^{a}\ \text{in initial liquid extract (g)}} \times 100 \qquad \text{(Eq. 1)}$$

$$\%\ \text{Xyl yield} = \frac{\text{Xyl as monomer (g)}}{\text{Xyl as total sugars}^{a}\ \text{in initial liquid extract (g)}} \times 100 \qquad \text{(Eq. 2)}$$

$$\%\ \text{Total yield} = \frac{\text{(Ara + Xyl) as monomers (g)}}{\text{(Ara + Xyl) as total sugars}^{a}\ \text{in initial liquid extract (g)}} \times 100 \qquad \text{(Eq. 3)}$$

$$\%\ \text{Olig. Conversion} = \frac{\text{Oligomers}_{\text{final}} - \text{Oligomers}_{\text{initial}}}{\text{Oligomers}_{\text{initial}}} \times 100 \qquad \text{(Eq. 4)}$$

[a] Total sugars refer to the sum of the corresponding sugar (arabinose and/or xylose) as monomer and oligomer

It should be noted that the yield considers total monomers after hydrolysis, *i.e.* the monomers which have been obtained during the previous fractionation step and those which have been formed and not degraded during the hydrolysis process itself. However, the oligomers conversion considers the oligomers obtained after fractionation which have been hydrolyzed during the hydrolysis step.

3. Results and discussion

3.1 Composition of initial arabinoxylan extract

The composition of the arabinoxylan extract obtained previously from wheat bran and used as raw material in this work is given in Table 1. Table 1 shows the percentage of

each sugar in monomeric and oligomeric form. Around 50% of total arabinose was in monomeric form, whereas 95% of total xylose was in oligomeric form.

The initial total amount of arabinose and xylose (monomers + oligomers) was 3.1 and 6.2 $g \cdot L^{-1}$, respectively. Therefore, these are the maximum possible values for the concentration of arabinose and xylose after hydrolysis. These maximum concentrations can be achieved only when: i) all the oligomers are converted into monomers and ii) monomers are not further degraded.

Table 1. Chemical composition of the initial extract.

Compound			
Sugars	Monomeric sugars ($mg \cdot L^{-1}$)	Oligomeric sugars ($mg \cdot L^{-1}$)	Olig. (%)[b]
Glucose	195 ± 32	1609 ± 197	89
Xylose	284 ± 9	5944 ± 188	95
Galactose	82 ± 26	255 ± 34	76
Arabinose	1522 ± 112	1605 ± 34	51
Mannose	70 ± 9	2 ± 44	2

[b] % Olig. = percentage of each sugar in oligomeric form = sugar in oligomeric form (g)/total sugar (g) x 100.

3.2 Catalyst characterization

The properties of the different solid acid catalysts used in this work are summarized in Table 2. Specific surface area (S_{BET}), total pore volume (V_{pore}), pore diameter (d_{pore}) and total acidity were determined. MCM-48 and Al-MCM-48 have specific surface areas of 1298 and 1352 $m^2 \cdot g^{-1}$, and pore volumes of 0.87 and 0.81 $cm^3 \cdot g^{-1}$, respectively. According to these results, no significant changes in surface area and pore volume were observed between MCM-48 and Al-MCM-48. The pore diameter was however slightly higher for Al-MCM-48 (2.5 nm) than for MCM-48 (2.2 nm). After the desposition of $RuCl_3$ or $FeCl_3$, a decrease in the specific surface area and pore volume was detected. This fact can be attributed to the partial blocking of the porous network of the supports. The pore size did not change after the deposition of $RuCl_3$ on MCM-48. However, the

pore size increased slightly from 2.5 nm to 2.7 nm and 2.6 nm after the impregnation of $RuCl_3$ and $FeCl_3$, respectively, on Al-MCM-48. This indicates slender modifications of the pore structure, suggesting a higher pore blocking in Al-MCM-48 than in MCM-48. Ruthenium and iron content for $RuCl_3$ and $FeCl_3$-based catalysts was around 4% in both cases, determined by atomic absorption spectroscopy (AAS).

Acidity is a key parameter of solid catalysts in hydrolysis reactions. The acidity of the catalysts used in this work exhibited the following trend: MCM-48 < Al-MCM-48 < $RuCl_3$/MCM-48 < $RuCl_3$/Al-MCM-48 < $FeCl_3$/Al-MCM-48. The incorporation of aluminum atoms (Al^{+3}) in the silica tetrahedral network of MCM-48 derives in Brönsted acid sites, which increases the total acidity of Al-MCM-48 (Collart et al., 2004; Kao et al., 2008). In the case of Ru^{+3} or Fe^{+3}, the ratio between the charge and the ionic radius (e/r) has been used to measure the electron-withdrawing ability, or in other words, to determine the Lewis acidity of metal cations (Shimizu et al., 2009).

Table 2. Structural characterization of solid catalysts.

Catalyst	Ru (%)[c]	S_{BET} ($m^2 \cdot g^{-1}$)[d]	V_{pore} ($cm^3 \cdot g^{-1}$)[e]	d_{pore} (nm)[f]	Acidity (mEq $H^+ \cdot g\ cat^{-1}$)[g]
MCM-48	-	1298	0.87	2.2	0.293
Al-MCM-48	-	1352	0.81	2.5	0.598
$RuCl_3$/MCM-48	4.1	1032	0.63	2.2	0.738
$RuCl_3$/Al-MCM-48	4.3	1017	0.63	2.7	1.130
$FeCl_3$/Al-MCM-48	4.2	1018	0.59	2.6	1.429

[c] Determined by AAS.
[d] Determined by the multipont BET method at $P/P_0 \leq 0.3$.
[e] Determined from N_2 uptake at $P/P_0 \geq 0.99$.
[f] Determined by BJH adsorption average.
[g] Determined by titration with NaOH.

3.3 Arabinoxylan hydrolysis experiments

The effect of different solid acid catalysts (MCM-48, Al-MCM-48, $RuCl_3$/MCM-48 and $RuCl_3$/Al-MCM-48) as well as the influence of catalyst loading, reaction time and several metal cations were examined in the hydrolysis process of an arabinoxylan extract

obtained from destarched wheat bran. The results were discussed in terms of the yields of arabinose and xylose and oligomers conversion. The formation of furfural, as main degradation product derived from the dehydration of arabinose and xylose, was also considered.

3.3.1 Effect of different mesoporous silica materials and $RuCl_3$-based catalysts

A first screening of different mesoporous silica materials and the corresponding $RuCl_3$-supported catalysts was carried out. The activity of MCM-48, Al-MCM-48, $RuCl_3$/MCM-48 and $RuCl_3$/Al-MCM-48 was compared in arabinoxylan hydrolysis (Figure 1). The experimental conditions were 180 ºC, 15 minutes and 50 bar N_2. The ratio of catalyst to carbon content in initial hemicelluloses was 0.6 $g \cdot g^{-1}$, which corresponds to the ratio used in the previous wheat bran fractionation.

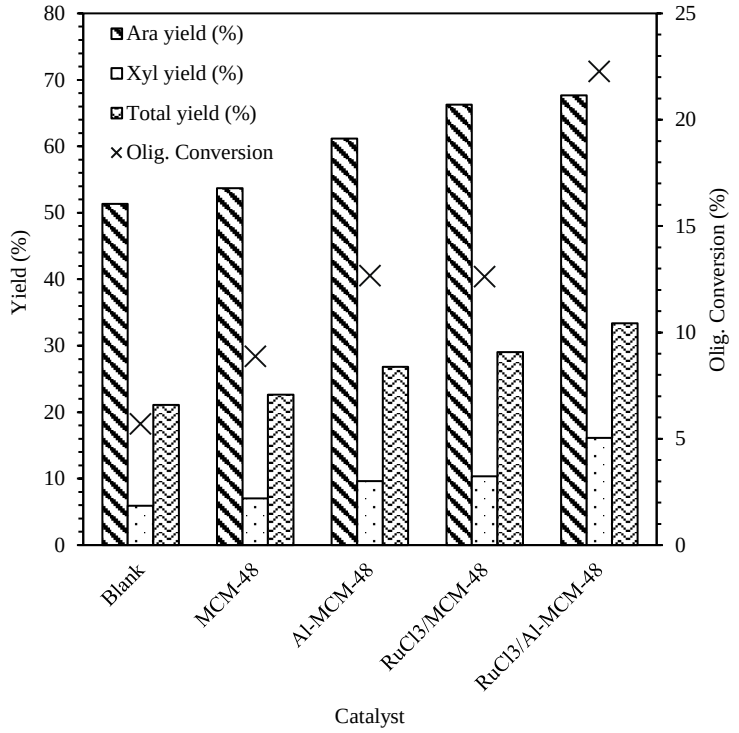

Figure 1. Comparison of different solid acid catalysts in monomeric yield and oligomers conversion. Reaction conditions: 180 ºC, 50 bar N_2, 15 min, 0.6 g catalyst·g C^{-1} in initial hemicelluloses.

The total monomeric yield (arabinose + xylose) showed the following trend: Blank ≈ MCM-48 < Al-MCM-48 < $RuCl_3$/MCM-48 < $RuCl_3$/Al-MCM-48. This is in agreement with the acidity values of the catalysts: a higher acidity resulted in higher yields. In the absence of a catalyst (blank reaction), the amount of monomeric arabinose and xylose turned out to be the same as in the initial AX solution (Table 1). At 180 ºC, the pK_w of water is low, which means that the amount of protons derived from water is relatively high (Bandura and Lvov, 2006). However, the water protonation at 180 ºC was not enough to break the bonds between the arabinoxylan molecules. Importantly, the monomers existing from the previous fractionation were not further degraded.

MCM-48 did not practically enhance the monomeric yield due to the nature of its acid sites. MCM-48 has a low acidity corresponding to silanol groups (Si – OH) which are weak Lewis acid sites (Xue et al., 2004). Al-MCM-48 exhibited a higher catalytic activity. During the synthesis of Al-MCM-48, a silicon atom (Si^{+4}) is replaced by an aluminum atom (Al^{+3}) in a tetrahedral network. Thus, a cation, usually a proton, is required to balance the aluminum tetrahedron. This compensation proton derives in a Brönsted acid site, which increases the total acidity of Al-MCM-48 (Collart et al., 2004; Kao et al., 2008) and, therefore, its catalytic activity. $RuCl_3$-supported catalysts ($RuCl_3$/MCM-48 and $RuCl_3$/Al-MCM-48) demonstrated to be more active than the corresponding mesoporous silica materials (MCM-48 and Al-MCM-48, respectively). The higher activity of $RuCl_3$ catalysts in hydrolysis reactions is related to the additional moderate Lewis acidity attributed to Ru^{+3} cations (Shimizu et al., 2009). As shown in Table 2, the deposition of $RuCl_3$ resulted in a higher total acidity of the catalysts. In all the cases, the formation of furfural was negligible in comparison with the amount of arabinose and xylose.

Although a more acidic catalyst led to a higher conversion of AXs into monosaccharides, the monomeric yield and oligomers conversion were still very low under these operating conditions (180 ºC, 15 minutes, 0.6 g catalyst·g C^{-1}). Therefore, $RuCl_3$/Al-MCM-48, as the most active catalyst, was chosen for a further study to improve the production of monomers.

3.3.2 Effect of catalyst loading and reaction time

$RuCl_3$ supported on Al-MCM-48 was used to study the influence of reaction time and catalyst loading. First, a low catalyst loading (0.6 g·g C^{-1}) was tested at 180 ºC, 50 bar N_2 and different reaction times (15 – 180 min) (Figure 2). The yield of arabinose achieved a maximum (68%) after 15 minutes. For longer times, the concentration of arabinose decreased slightly due to its further degradation (Figure 2B). The maximum yield of xylose (30%) was obtained however after 180 minutes. In addition to this, the concentration of furfural became important at long times because of the degradation of xylose and arabinose (Figure 2B). This implies that part of the oligomers was converted into monosaccharides, which were further degraded to furfural. The large amount of furfural evidenced that, under these operating conditions, the hydrolysis of arabinoxylans into arabinose and xylose was slower than the degradation of sugars to furfural. This gave rise to a relatively low monomeric yield and a high furfural concentration.

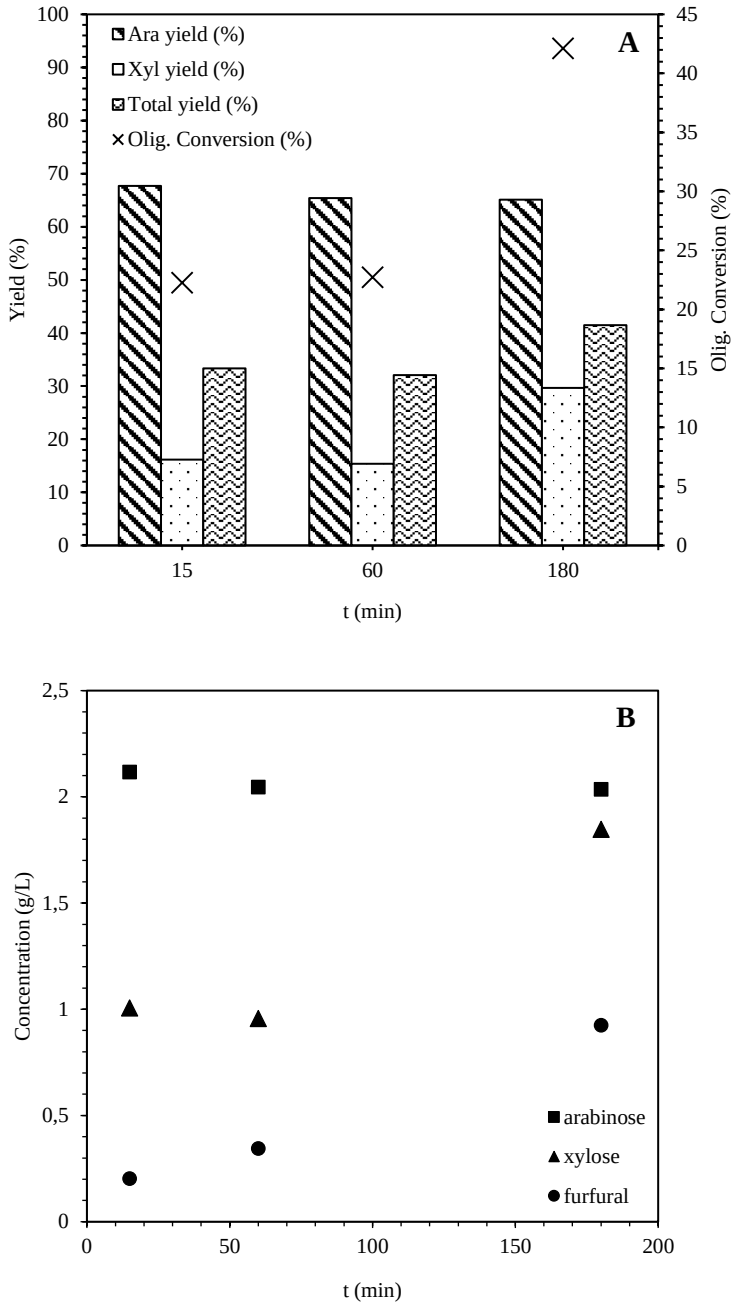

Figure 2. Effect of time in arabinoxylan hydrolysis with a low catalyst loading. Reaction conditions: 180 ºC, 50 bar N_2, catalyst: $RuCl_3$/Al-MCM-48, catalyst loading: 0.6 g catalyst·g C^{-1} in initial hemicelluloses. A) Monomeric yield and oligomers conversion, B) Composition of hydrolysate (g·L^{-1}).

In order to speed up the hydrolysis step and inhibit further degradation, higher catalyst loadings (0.6, 2.4 and 4.8 g·g C^{-1}) were tried at 3 hours (Figure 3). The yield of arabinose and xylose reached 85% and 70%, respectively, with a catalyst loading of 2.4 g·g C^{-1}. By

increasing the catalyst loading from 0.6 to 2.4 g·g C^{-1}, the amount of xylose and arabinose increased in a greater proportion than that of furfural. This means that the formation of arabinose and xylose was faster than the subsequent degradation to furfural. This fact was also observed by Sahu and Dhepe (2012). They studied the effect of substrate/catalyst ratio on hemicelluloses hydrolysis using HUSY zeolite as catalyst. Interactions between the substrate (hemicelluloses) and the available active sites of the catalyst decreased as increasing substrate/catalyst ratio (decreasing catalyst amount). In that work, a xylose + arabinose yield of 35% was achieved at a substrate/catalyst ratio of 130. However, at a ratio of 10, the yield of arabinose + xylose increased up to 56%. It was concluded that the conversion rate of hemicelluloses into monomers was higher than the subsequent degradation to furfural when the amount of catalyst increased.

We tried then a higher catalyst loading of 4.8 g·g C^{-1}. The conversion of oligomers was total. Nevertheless, a drastic decrease in the concentration of sugars was observed and a black sediment appeared. This black solid corresponded probably to humins derived from furfural, *i.e.* arabinose and xylose were degraded to furfural and this later to humins. This explains a drop in the amount of arabinose and xylose but not a sharp increase in the concentration of furfural (Figure 3B).

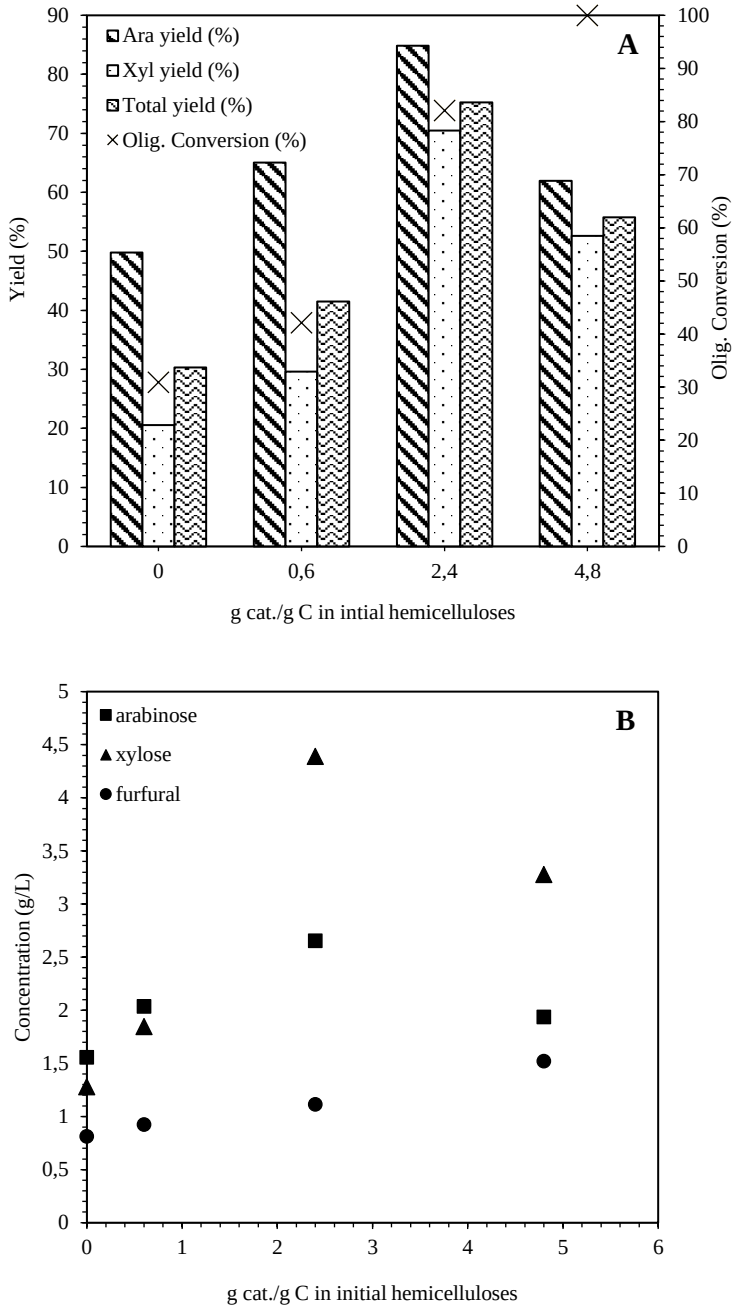

Figure 3. Effect of catalyst loading in arabinoxylan hydrolysis. Reaction conditions: 180 ºC, 3 h, 50 bar N_2, catalyst: $RuCl_3$/Al-MCM-48. A) Monomers yield and oligomers conversion, B) Composition of hydrolysate ($g \cdot L^{-1}$).

As mentioned before, the hydrolysis of arabinoxylans into sugars was faster than the degradation to furfural using a catalyst loading of 2.4 $g \cdot g\ C^{-1}$. Despite the high total monomeric yield (75%) achieved after 3 hours, the amount of furfural obtained was still important (Figure 3B). In order to reduce the reaction time and minimize the degradation

of sugars and consequently the formation of furfural, the highest catalyst loading (4.8 g·g C^{-1}) was tested at shorter times (< 180 min) (Figure 4).

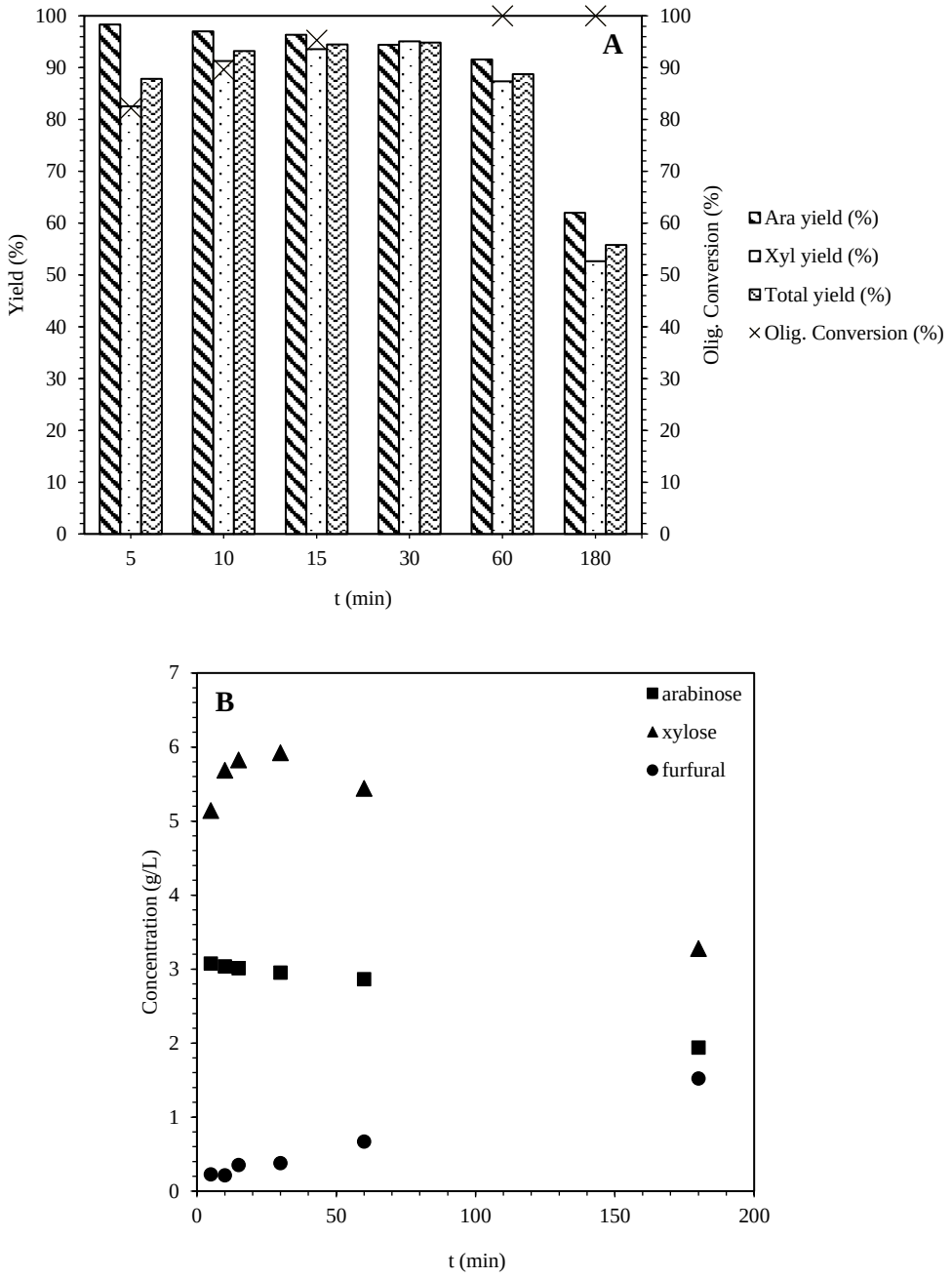

Figure 4. Effect of time in arabinoxylan hydrolysis with a high catalyst loading. Reaction conditions: 180 ºC, 50 bar N_2, catalyst: $RuCl_3$/Al-MCM-48, catalyst loading: 4.8 g catalyst·g C^{-1} in initial hemicelluloses. A) Monomeric yield and oligomers conversion, B) Composition of hydrolysate ($g \cdot L^{-1}$).

The yield of arabinose achieved a maximum after 5 minutes (98%), whereas the maximum yield of xylose was obtained after 15 – 30 minutes (94 – 95%). The yield of arabinose was higher than that of xylose in all the experiments. This is related to the type of bond between the different molecules. The side chains are composed by arabinose molecules linked by α-glycosidic bonds, whereas the backbone consists mainly of xylose units connected by β-glycosidic bonds. α-glycosidic bonds are more easily hydrolysable than β-glycosidic bonds, which explains the faster release of arabinose than xylose. In addition to this, the better access to side chains than to the backbone also explains the higher yield of arabinose than that of xylose in all the experiments (Negahdar et al. 2016). In conclusion, a high total monomeric yield was achieved at 180 ºC after 15 minutes with a catalyst loading of 4.8 g·g C^{-1}. The yields of arabinose and xylose were 96% and 94%, respectively. Under these conditions, the process was optimized. The concentrations of xylose and arabinose reached roughly their maximum, whereas the concentration of furfural was very low.

3.3.3 Effect of different metal cations (Ru^{+3}, Fe^{+3})

The effect of different Lewis acid cations (Ru^{+3}, Fe^{+3}) was studied using $RuCl_3$ and $FeCl_3$ supported on Al-MCM-48 as catalysts (Figure 5). Experiments were performed at 180 ºC, 15 minutes and 50 bar N_2 using a catalyst loading of 4.8 g·g C^{-1}. For comparison purposes, a reaction with bare Al-MCM-48 was also carried out. These results are shown in Figure 5. The incorporation of $RuCl_3$ or $FeCl_3$ enhanced the total monomeric yield compared to Al-MCM-48. The yield of arabinose achieved roughly its maximum over both supported catalysts. However, a higher yield of xylose was obtained over $RuCl_3$/Al-MCM-48, despite the greater acidity of $FeCl_3$/Al-MCM-48 (Table 2). Fe^{+3} and Ru^{+3} cations have demonstrated to be active in hydrolysis of cellobiose and cellulose (Jing et al., 2016; Shimizu et al., 2009). Nevertheless, higher reaction rates were observed for

metals with moderate Lewis acidity, such as Ru^{+3}, than for those with high Lewis acidity, such as Fe^{+3} (Shimizu et al., 2009), which is according to our results.

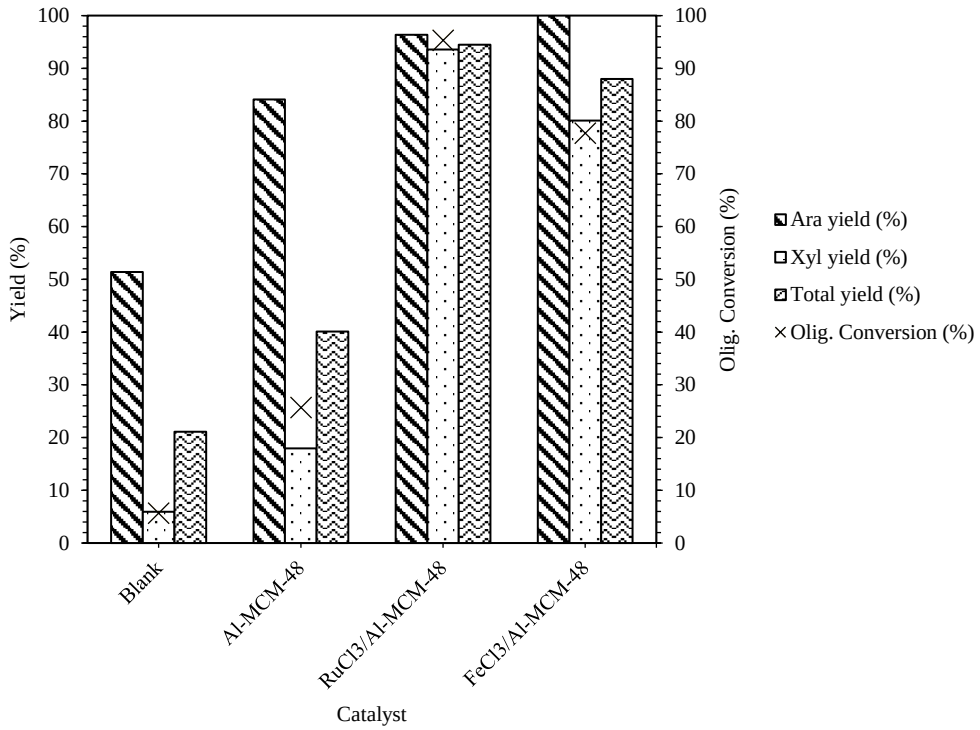

Figure 5. Effect of different Lewis acid cations (Ru^{+3}, Fe^{+3}) in monomeric yield and oligomers conversion. Reaction conditions: 180 ºC, 15 min, 50 bar N_2, catalyst loading: 4.8 g catalyst·g C^{-1} in initial hemicelluloses.

4. Conclusions

The use of $RuCl_3$ catalysts supported on mesoporous silica has demonstrated to be a good option for the hydrolysis of arabinoxylans from wheat bran. The activity of MCM-48, Al-MCM-48, $RuCl_3$/MCM-48 and $RuCl_3$/Al-MCM-48 was compared. Al-MCM-48 led to higher yields than MCM-48 due to its higher acidity and Brönsted acid sites. $RuCl_3$-supported catalysts were more active than the bare corresponding supports. This was attributed to the higher global acidity of $RuCl_3$ catalysts due to the moderate Lewis acid nature of Ru^{+3} cations. Different Lewis cations (Ru^{+3}, Fe^{+3}) were also tested. Higher yields were obtained over $RuCl_3$ catalysts than $FeCl_3$ catalysts. Under optimum conditions (180 ºC, 15 minutes, 4.8 g $RuCl_3$/Al-MCM-48·g C^{-1}) a high monomeric yield

of arabinose (96%) and xylose (94%) was achieved. In addition to this, the amount of furfural was very low, indicating a minor degradation of sugars. Our results demonstrated that the amount of monomeric C_5 sugars can be maximized by using a two-step process consisting of a first hydrothermal fractionation of arabinoxylans and a subsequent hydrolysis using $RuCl_3$/Al-MCM-48 and 180 ºC in both steps, and a total time of 25 minutes.

References

Aden, A., Ruth, M., Ibsen, K., Jechura, J., Neeves, K., Sheehan, J., Wallace, B., Montague, L., Slayton, A., and Lukas, J. Lignocellulosic biomass to ethanol process design and economics utilizing co-current dilute acid prehydrolysis and enzymatic hydrolysis for corn stover. NREL/TP-510-32438, 2002.

Apprich, S., Tirpanalan, Ö., Hell, J., Reisinger, M., Böhmdorfer, S., Siebenhandl-Ehn, S., Novalin, S., and Kneifel, W. Wheat bran-based biorefinery 2: Valorization of products. *LWT - Food Science and Technology,* 56 (2014) 222–231.

Bandura, A.V., and Lvov, S.N. The ionization constant of water over wide ranges of temperature and density. *Journal of Physical and Chemical Reference Data*, 35 (2006) 14–30.

Cará, P.D., Pagliaro, M., Elmekawy, A., Brown, D.R., Verschuren, P., Shiju, N.R., and Rothenberg, G. Hemicellulose hydrolysis catalysed by solid acids. *Catalysis Science & Technology*, 3 (2013) 2057–2061.

Collart, O., Cool, P., Van Der Voort, P., Meynen, V., Vansant, E.F., Houthoofd, K., Grobet, P.J., Lebedev, O.I., and Tendeloo, G.V. Aluminum Incorporation into MCM-48 toward the creation of Brønsted acidity. *The Journal of Physical Chemistry B,* 108 (2004) 13905–13912.

Dhepe, P.L., and Sahu, R. A solid-acid-based process for the conversion of hemicellulose. *Green Chemistry*, 12 (2010) 2153–2156.

Hendriks, A.T.W.M., and Zeeman, G. Pretreatments to enhance the digestibility of lignocellulosic biomass. *Bioresource Technology,* 100 (2009) 10–18.

Hilpmann, G., Becher, N., Pahner, F-A., Kusema, B., Mäki-Arvela, P., Lange, R., Murzin, D.Y., and Salmi, T. Acid hydrolysis of xylan. *Catalysis Today,* 259 (2016) 376–380.

Hu, H., Li, Z., Wu, Z., Lin, L., and Zhou, S. Catalytic hydrolysis of microcrystalline and rice straw-derived cellulose over a chlorine-doped magnetic carbonaceous solid acid. *Industrial Crops and Products,* 84 (2016) 408–417.

Hu, L., Tang, X., Wu, Z., Lin, L., Xu, J., Xu, N., and Dai, B. Magnetic lignin-derived carbonaceous catalyst for the dehydration of fructose into 5-hydroxymethylfurfural in dimethylsulfoxide. *Chemical Engineering Journal,* 263 (2015) 299–308.

Izydorczyk, M.S., and Biliaderis, C.G. Arabinoxylans: Technologically and nutritionally functional plant polysaccharides. In *Functional food carbohydrates*, Izydorczyk, M.S., and Biliaderis, C.G., (Eds.), CRC Press: Boca Raton, 2007.

Jia, L., Budinova, G.A.L.G., Takasugi, Y., Noda, S., Tanaka, T., Ichinose, H., Goto, M., and Kamiya, N. Synergistic degradation of arabinoxylan by free and immobilized xylanases and arabinofuranosidase. *Biochemical Engineering Journal,* 114 (2016) 268–275.

Jing, S., Cao, X., Zhong, L., Peng, X., Zhang, X., Wang, S., and Sun, R. In situ carbonic acid from CO_2: A green acid for highly effective conversion of cellulose in the presence of Lewis acid. *ACS Sustainable Chemistry & Engineering,* 4 (2016) 4146–4155.

Kao, H-M., Chang, P-C., Liao, Y-W., Lee, L-P., and Chien, C-H. Solid-state NMR characterization of the acid sites in cubic mesoporous Al-MCM-48 materials using trimethylphosphine oxide as a P NMR probe. *Microporous and Mesoporous Materials,* 114 (2008) 352–364.

Kim, Y., Kreke, T., and Ladisch, M.R. Reaction mechanisms and kinetics of xylo-oligosaccharide hydrolysis by dicarboxylic acids. *AlChE Journal*, 59 (2013) 188–199.

Koutinas, A.A., Wang, R., Campbell, G.M., and Webb, C. A whole crop biorefinery system: A closed system for the manufacture of non-food products from cereals. In *Biorefineries – Industrial Processes and Products*, Kamm, B., Gruber, P.R., and Kamm, M., (Eds.), Wiley-VCH Verlag GmbH: Weinheim, 2008.

Kusema, B.T., Hilmann, G., Mäki-Arvela, P., Willför, S., Holmbom, B., Salmi, T., and Murzin, D.Y. Selective hydrolysis of arabinogalactan into arabinose and galactose over heterogeneous catalysts. *Catalysis Letters*, 141 (2011) 408–412.

Kusema, B.T., Tönnov, T., Mäki-Arvela, P., Salmi, T., Willför, S., Holmbom, B., and Murzin, D.Y. Acid hydrolysis of O-acetyl-galactoglucomannan. *Catalysis Science & Technology*, 3 (2013) 116–122.

Lee, H.J., Kim, I.J., Kim, J.F., Choi, I-G., and Kim, K.H. An expansin from the marine bacterium Hahella chejuensis acts synergistically with xylanase and enhances xylan hydrolysis. *Bioresource Technology*, 149 (2013) 516–519.

Li, F., Wang, H., Xin, H., Cai, J., Fu, Q., and Jin, Y. Development, validation and application of a hydrophilic interaction liquid chromatography-evaporative light scattering detection based method for process control of hydrolysis of xylans obtained from different agricultural wastes. *Food Chemistry*, 212 (2016) 155–161.

Li, H., Xue, Y., Wu, J., Wu, H., Qin, G.; Li, C., Ding, J., Liu, J., Gan, L., and Long, M. Enzymatic hydrolysis of hemicelluloses from Miscanthus tomonosaccharides or xylo-oligosaccharides by recombinant hemicellulases. *Industrial Crops and Products*, 79 (2016) 170–179.

Liu, W-J., Tian, K., Jiang, H., and Yu, H-Q. Facile synthesis of highly efficient and recyclable magnetic solid acid from biomass waste. *Scientific Reports,* 3 (2013) 2419.

Lou, H., Yuan, L., Qiu, X., Qiu, K., Fu, J., Pang, Y., and Huang, J. Enhancing enzymatic hydrolysis of xylan by adding sodium lignosulfonate and long-chain fatty alcohols. *Bioresource Technology,* 200, (2016) 48–54.

Mäki-Arvela, P., Salmi, T., Holmbom, B., Willför, S., and Murzin, D.Y. Synthesis of sugars by hydrolysis of hemicelluloses-A review. *Chemical Reviews,* 111 (2011) 5638–5666

Moreira, L.R.S., and Filho, E.X.F. Insights into the mechanism of enzymatic hydrolysis of xylan. *Applied Microbiology and Biotechnology,* 100 (2016) 5205–5214.

Nakasu, P.Y.S, Ienczak, L.J., Costa, A.C., and Rabelo, S.C. Acid post-hydrolysis of xyloolisaccharides from hydrothermal pretreatment for pentose ethanol production. *Fuel,* 185 (2016) 73–84.

Negahdar, L., Delidovich, I., and Palkovits, R. Aqueous-phase hydrolysis of cellulose and hemicelluloses over molecular acidic catalysts: Insights into the kinetics and reaction mechanism. *Applied Catalysis B: Environmental,* 184 (2016) 285–298.

Oh, Y.H., Eom, I.Y., Joo, J.C., Yu, J.H., Song, B.K., Lee, S.H., Hong, S.H., and Park, S.J. Recent advances in development of biomass pretreatment technologies used in biorefinery for the production of bio-based fuels, chemicals and polymers. *Korean Journal of Chemical Engineering,* 32 (2015) 1945.

Ormsby, R., Kastner, and J.R., Miller, J. Hemicellulose hydrolysis using solid acid catalysts generated from biochar. *Catalysis Today,* 190 (2012) 89–97.

Peng, F., Peng, P., Xu, F., and Sun, R-C. Fractional purification and bioconversion of hemicelluloses. *Biotechnology Advances,* 30 (2012) 879–903.

Prückler, M., Siebenhandl-Ehn, S., Apprich, S., Höltinger, S., Haas, C., Schmid, E., and Kneifel, W. Wheat bran-based biorefinery 1: Composition of wheat bran and strategies of functionalization. *LWT - Food Science and Technology,* 56 (2014) 211–221.

Putro, J.N., Soetaredjo, F.E., Lin, S-Y., Ju, Y-H., and Ismadji, S. Pretreatment and conversion of lignocellulose biomass into valuable chemicals. *RSC Advances,* 6 (2016) 46834–46852.

Romero, A., Alonso, E., Sastre, Á., and Nieto-Márquez, A. Conversion of biomass into sorbitol: cellulose hydrolysis on MCM-48 and D-glucose hydrogenation on Ru/MCM-48. *Microporous and Mesoporous Materials,* 224 (2016) 1–8.

Sahu, R., and Dhepe, P.L. A one-pot method for the selective conversion of hemicellulose from crop waste into C5 sugars and furfural by using solid acid catalysts. *ChemSusChem,* 5 (2012) 751–761.

Salmi, T., Murzin, D., Wärna, J., Mäki-Arvela, P., Kusema, B., Holmbom, B., and Willför, S. Hemicellulose hydrolysis in the presence of heterogeneous catalysts. *Topics in Catalysis,* 57 (2014) 1470–1475.

Sánchez-Bastardo, N., Romero, A., and Alonso, E. Extraction of arabinoxylans from wheat bran using hydrothermal processes assisted by heterogeneous catalysts. *Carbohydrate Polymers,* 160 (2017) 143–152.

Shimizu, K-I., Furukawa, H., Kobayashi, N., Itaya, Y., and Satsuma, A. Effects of Brønsted and Lewis acidities on activity and selectivity of heteropolyacid-based catalysts for hydrolysis of cellobiose and cellulose. *Green Chemistry,* 11 (2009) 1627–1632.

Singhvi, M.S., Chaudhari, S., and Gokhale, D.V. Lignocellulose processing: a current challenge. *RSC Advances,* 4 (2014) 8271.

Sluiter, A., Hames, B., Ruiz, R., Scarlata, C., Sluiter, J., and Templeton, D. Determination of sugars, byproducts, and degradation products in liquid fraction process samples. Laboratory Analytical Procedure (LAP). Technical Report NREL/TP-510-42623, 2008.

Vilcocq, L., Castilho, P.C., Carvalheiro, F., and Duarte, L.C. Hydrolysis of oligosaccharides over solid acid catalysts: A review. *ChemSusChem*, 7 (2014) 1010–1019.

Wang, J., Xu, W., Ren, J., Liu, X., Lu, G., and Wang, Y. Efficient catalytic conversion of fructose into hydroxymethylfurfural by a novel carbon-based solid acid. *Green Chemistry*, 13 (2011) 2678–2681.

Xue, P., Lu, G., Guo, Y., Wang, Y., and Guo, Y. A novel support of MCM-48 molecular sieve for immobilization of penicillin G acylase. *Journal of Molecular Catalysis B: Enzymatic*, 30 (2004) 75–81.

Zhang, H., Ye, G., Wei, Y., Li, X., Zhang, A., and Xie, J. Enhanced enzymatic hydrolysis of sugarcane bagasse with ferric chloride pretreatment and surfactant. *Bioresource Technology*, 229 (2017) 96–103.

Zhang, Z., Smith, C., and Li, W. Extraction and modification technology of arabinoxylans from cereal by-products: A critical review. *LWT - Food Science and Technology*, 65 (2014) 423–436.

Zheng, F-C., Chen, Q-W., Hu, L., Yan, N., and Kong, X-K. Synthesis of sulfonic acid-functionalized Fe3O4@C nanoparticles as magnetically recyclable solid acid catalysts for acetalization reaction. *Dalton Transactions*, 43 (2014) 1220–1227.

Zhou, L., Shi, M., Cai, Q., Wu, L., Hu, X., Yang, X., Chen, C., and Xu, J. Hydrolysis of hemicellulose catalyzed by hierarchical H-USY zeolites – The role of acidity and pore structure. *Microporous and Mesoporous Matererials*, 169 (2013) 54–59.

Zhong, C., Wang, C., Huang, F., Wang, F., Jia, H., Zhou, H., and Wei, P. Selective hydrolysis of hemicellulose from wheat straw by a nanoscale solid acid catalyst. *Carbohydrate Polymers,* 131 (2015) 384–391.

CHAPTER III

HYDROLYSIS OF ARABINOXYLANS FROM WHEAT BRAN OVER MESOPOROUS AND MICROPOROUS SILICA CATALYSTS

Abstract

The conversion of biomass into high value-added products is of great importance to develop sustainable chemical processes. A wide range of valuable chemicals can be produced from renewable resources. Arabinoxylans are an important example. They belong to the hemicellulosic fraction of biomass and are especially abundant in agricultural waste. Although arabinoxylans have significant applications in pharmaceutical and food industries, their monomeric compounds (arabinose and xylose) are of higher interest. In this work, the hydrolysis of arabinoxylans from wheat bran into arabinose and xylose was studied over different mesoporous (MCM-48 and Al-MCM-48) and microporous (H-ZSM-5 (23), H-ZSM-5 (80) and H-Y (12)) silica materials. H-ZSM-5 zeolite with a SiO_2/Al_2O_3 ratio of 23 demonstrated to be the most active catalyst. Despite the small pore size, H-ZSM-5 (23) has a high total acidity and strong Brönsted acid sites, which make H-ZSM-5 (23) suitable for arabinoxylan hydrolysis. Besides different solid acid catalysts, other parameters such as reaction time and catalyst loading were examined. Under optimal conditions (180 °C, 15 minutes, 9.2 g·g C^{-1} of H-ZSM-5 (SiO_2/Al_2O_3 = 23)), 76% of arabinoxylans were converted into monomers without major degradation. The yields corresponding to arabinose and xylose were 96% and 67%, respectively.

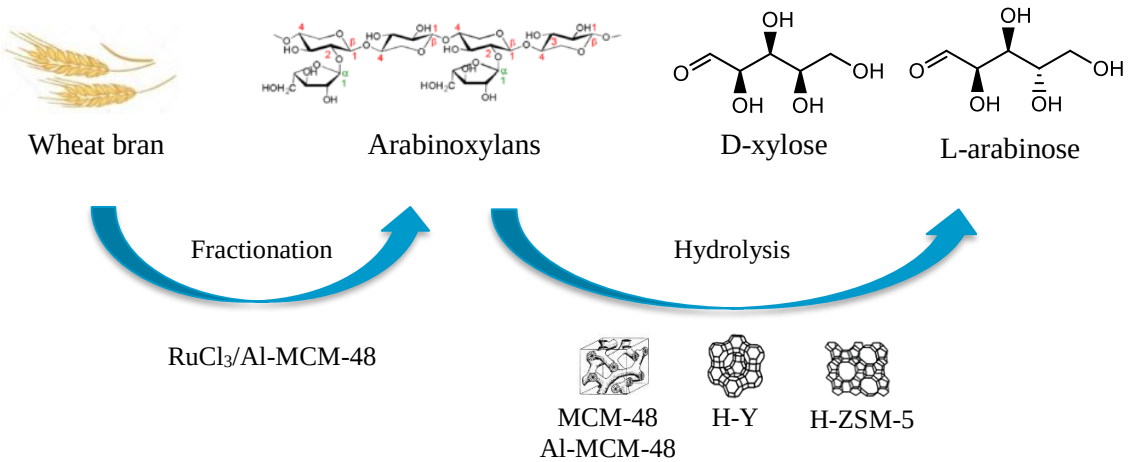

1. Introduction

The use of renewable sources as sustainable feedstocks for the production of chemicals and fuels has become an issue of great interest due to the current depletion of fossil resources (Hara et al., 2015; Putro et al., 2016). Lignocellulosic biomass, the most plentiful bio-based carbon resource, is a promising renewable feedstock alternative to such fossil-based sources (Deng et al., 2015; Oh et al., 2015). Lignocellulosic biomass consists mainly of three components: cellulose (ca. 35 – 50%), hemicelluloses (ca. 25 – 30%) and lignin (ca. 15 – 30%) (Deng et al., 2015). Arabinoxylans (AXs) belong to the hemicellulosic part of biomass and are especially abundant in agricultural waste, such as wheat bran, which has an arabinoxylan content between 10.9 – 26.0% (Apprich et al., 2014; Izydorczyk and Biliaderis, 2006). AXs as polymers have important applications in pharmaceutical and food industries. Nevertheless, monomers derived from them (*i.e.* arabinose and xylose) have a larger market as precursors of many platform chemicals (arabitol, xylitol, furfural) (Vilcocq, et al., 2014).

An overview of wheat bran processing to obtain C_5 sugars (arabinose and xylose) is shown in Figure 1.

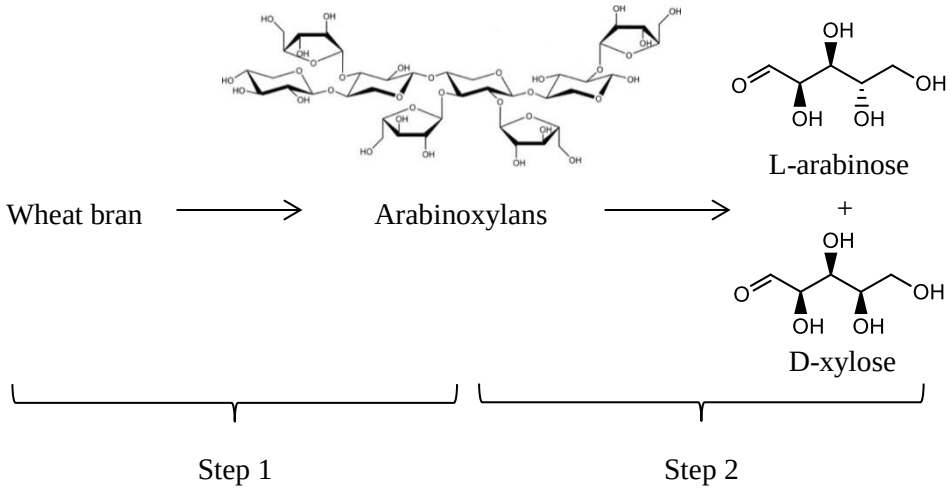

Figure 1. Overview of monomers production from wheat bran arabinoxylans.

During wheat bran fractionation, AXs are partly solubilized and hydrolyzed in water with a relatively high molecular weight (Figure 1. Step 1). Thus, completing the hydrolysis process of arabinoxylan polymers into monomers is a crucial task for the development of a biorefinery (Figure 1. Step 2). The hydrolysis of hemicelluloses is usually catalyzed by mineral acids or enzymes (Carà et al., 2013; Dhepe and Sahu, 2012; Sahu and Dhepe, 2012). Mineral acids are cheap reagents, but the corrosion resistant equipment required for these processes increase dramatically the capital costs. Moreover, calcium ions are needed to remove the acid, which lead to lime deposits (Negahdar et al., 2016). Enzymes are very selective, but they are currently not commercial (Sahu and Dhepe, 2012). The main reason is the difficult separation and recycling of enzymes from liquid mixtures (Carà et al., 2013; Sahu and Dhepe, 2012). The hydrolysis of hemicelluloses (AXs in this case) using solid acid catalysts overcomes these problems. Heterogeneous catalysts can be easily separated and recovered. Moreover, a stable catalyst can be reused, decreasing the operating costs. In general, solid acid catalysts keep the advantages of mineral acids, but also improve the selectivity to sugars. These reasons explain their growing use in biorefineries (Vilcocq et al., 2014). The development of solid acid catalysts for the hydrolysis of hemicelluloses has been widely studied by several authors in the last few years. Table 1 summarizes some of the most important results obtained in this field.

Table 1. Most important results on hemicelluloses hydrolysis using solid acid catalysts.

Raw material	Hydrolysis conditions	Catalyst	Yield (%)	Reference
Beechwood xylan	140 ºC, 3 h, 10 bar Ar	Sulfonic acid functionalized silica gel	50[a]	(Carà et al., 2013)
Beechwood xylan	120 ºC, 20 h, 10 bar Ar	H-Y (Si/Al=5.1)	20[a]	
Beechwood xylan	120 ºC, 20 h, 10 bar Ar	H-ZSM-5 (Si/Al=50)	33[a]	
Beechwood xylan	120 ºC, 20 h, 10 bar Ar	H-ZSM-5 (Si/Al=80)	29[a]	
Beechwood xylan	120 ºC, 20 h, 10 bar Ar	H-Ferrierite	43[a]	
Beechwood xylan	120 ºC, 4 h, 10 bar Ar	Amberlyst 35	80[a]	
Beechwood xylan	120 ºC, 4 h, 10 bar Ar	Amberlyst 70	76[a]	
Beechwood xylan	120 ºC, 4 h, 10 bar Ar	D5081	55[a]	
Beechwood xylan	120 ºC, 4 h, 10 bar Ar	D5082	70[a]	
Oat Spelt	170 ºC, 3 h, 50 bar N_2	-	5[a]	(Dhepe and Sahu, 2012)
Oat Spelt	170 ºC, 3 h, 50 bar N_2	H-USY (Si/Al=15)	41[a]	
Oat Spelt	170 ºC, 3 h, 50 bar N_2	H-Beta (Si/Al=19)	37[a]	
Oat Spelt	170 ºC, 3 h, 50 bar N_2	H-MOR (Si/Al=10)	36[a]	
Oat Spelt	170 ºC, 3 h, 50 bar N_2	Al-MCM-41 (Si/Al=50)	15[a]	
Oat Spelt	170 ºC, 3 h, 50 bar N_2	Al-SBA-15 (Si/Al=100)	5[a]	
Oat Spelt	170 ºC, 3 h, 50 bar N_2	K10 Clay	27[a]	
Oat Spelt	170 ºC, 3 h, 50 bar N_2	Al_2O_3	20[a]	
Oat Spelt	170 ºC, 3 h, 50 bar N_2	Nb_2O_5	20[a]	
Oat Spelt	170 ºC, 3 h, 50 bar N_2	SO_4^{2-}/ZrO_2	19[a]	
Oat Spelt	170 ºC, 3 h, 50 bar N_2	$Cs_{2.5}H_{0.5}PW_{12}O_{40}$	35[a]	
Arabinogalatan	90 ºC, 24 h	Smopex-101	85[b] 15[c]	(Kusema et al., 2011)
Arabinogalatan	90 ºC, 24 h	Amberlyst 15	50[b] 0[c]	
Xylan	90 ºC, 22 h	Smopex-101	34[d]	(Hilpmann et al., 2016)

[a] Xyl. + Ara. monomeric.
[b] Ara. monomeric.
[c] Gal. monomeric.
[d] Xyl. Monomeric.

Different solid acid catalysts have been tested in hemicelluloses hydrolysis reactions: mesoporous silica materials, sulfonated and polystyrene resins, zeolites, metal oxides,

clays, heteropolyacids, etc. Carà et al. (2013) studied the effect of several solid acid catalysts on the hydrolysis reaction of commercial beechwood xylan. They discussed the advantages and drawbacks of acidic ion exchange resins, sulfonated silica gels and zeolites. Sulfonated resins were highly active but they rapidly lost their activity as a consequence of the leaching of sulfonic acid groups. Sulfonated silica gels were less active, but more stable. And zeolites were moderately active but the most stable, since they exhibited the best recyclability. Dhepe and Sahu (2012) also compared the activity and stability of different catalysts (zeolites, mesoporous silica materials, metal oxides, etc.). Among them, zeolites were the most active and stable catalysts. Therefore, zeolites appear to be a good option as heterogeneous catalysts for hemicelluloses hydrolysis. For this reason, zeolites were used in the present work. Not only microporous aluminosilicates (zeolites) but also mesoporous silica catalysts were tested, since they have already shown to be active in a previous research (Dhepe and Sahu, 2012). Most works use commercial substrates as raw materials (beechwood xylan, oat spelt, arabinogalactan). However, in this work an aqueous fraction rich in AXs from wheat bran was used as feedstock. These mixtures have a high arabinoxylan content although their composition is not limited to them. They also contain other biomass compounds, such as extractives, ash or proteins. The activity of solid catalysts might be affected by these species. Therefore, the study of hydrolysis reactions of a real biomass fraction is essential for an integrated biorefinery.

In this work, we have studied the hydrolysis process of wheat bran arabinoxylans using different solid acid catalysts (Figure 1. Step 2). Mesoporous and microporous silica materials were examined. We tested MCM-48 and Al-MCM-48, which consist of a mesoporous channel structure with wide pore openings (> 2.0 nm). H-ZSM-5 with different Si/Al ratios and H-Y zeolites were also used as crystalline materials with small pore diameters (0.6 – 0.8 nm). Besides different textural properties, these materials also

differ in the acidity as well as in the nature and strength of the acid sites. Results were discussed in terms of all these parameters. Likewise, the reaction time and catalyst loading were optimized to maximize the yield of arabinose (Ara) and xylose (Xyl) and minimize further dehydration reactions to furfural.

2. Experimental

2.1 Catalyst preparation

Five different catalysts were tested in this study: three zeolites (microporous aluminosilicates) and two MCM-48-type materials (mesoporous silica). Zeolites were purchased from Zeolyst International (Y, SiO_2/Al_2O_3 = 12; ZSM-5, SiO_2/Al_2O_3 = 23; ZSM-5, SiO_2/Al_2O_3 = 80). All of them were initially in ammonium form. The protonation of zeolites was done by calcination at 550 ºC for 5 hours applying a heating rate of 5 $ºC \cdot min^{-1}$ from 80 to 550 ºC (in general, $Z^-NH_4^+ \rightarrow Z^-H^+ + NH_3\uparrow$) (Schmidt, 2006). Mesoporous silica catalysts (MCM-48 and Al-MCM-48) were synthetized according to the sol-gel method described by Romero et al. (2016) in a previous work. Briefly, 42 mL of distilled water, 18 mL of ethanol (absolute; PanReac AppliChem) and 13 mL of an aqueous ammonia solution (20% w/w; PanReac AppliChem) were added to 2.0 g of n-hexadecyltrimethylammonium bromide (for molecular biology, ≥ 99%; Sigma-Aldrich). 0.077 g of sodium aluminate (technical, anhydrous; Sigma-Aldrich) were incorporated after 15 minutes stirring only for the synthesis of Al-MCM-48. Then, 4 mL of tetraethyl orthosilicate (≥ 99.0% (GC); Sigma-Aldrich) were added dropwise and the solution was further stirred for 18 h. The resulting white precipitate was recovered by filtration and rinsed thoroughly with distilled water. The samples were first dried at 60 ºC overnight and then calcined at 550 ºC for 24 hours to eliminate the surfactant.

2.2 Catalyst characterization

Small Angle X-Ray Scattering (SAXS) and X-Ray Diffraction (XRD) were performed on a Bruker Discover D8 diffractometer using Cu Kα radiation (λ = 0.15406 nm). Diffraction intensities for SAXS and XRD were measured over an angle range of $0.5^o < 2\theta < 8^o$ and $2^o < 2\theta < 90^o$, respectively. A step size of 0.020º and a step time of 0.80 s were applied.

Nitrogen adsorption-desorption isotherms were performed with ASAP 2020 (Micromeritics, USA) to determine the specific surface area, the total pore volume (V_{pore}) and the average pore size (d_{pore}) of the catalysts. Samples were outgassed at 350 ºC overnight prior to analysis. For mesoporous catalysts (MCM-48-type silica), the multipoint BET method at $P/P_0 \leq 0.3$ was used to determine the total specific surface area. The total specific pore volume was evaluated from N_2 uptake at $P/P_0 \geq 0.99$ and the pore diameter was determined by BJH adsorption average ($4 \cdot V \cdot A^{-1}$, nm). For microporous catalysts (zeolites), the Langmuir model was applied to calculate the surface area. The Horvath-Kawazoe method was used to determine the pore volume (from N_2 uptake at $P/P_0 \geq 0.99$) and the average pore size of zeolites.

Acidities of the samples were characterized by temperature-programmed desorption of ammonia (NH_3-TPD) on a Micromeritics 2910 (TPD/TPR) equipment fitted with a thermal conductivity detector. Prior to the analysis, samples were outgassed under helium flow (50 $NmL \cdot min^{-1}$) with a heating rate of 15 $ºC \cdot min^{-1}$ up to 560 ºC and kept at this temperature for 30 min. After cooling, an ammonia flow (10 vol%) of 35 $NmL \cdot min^{-1}$ was passed through the sample at 180 ºC for 30 min. First, the physisorbed ammonia was removed by flowing helium (50 $mL \cdot min^{-1}$) at 180 ºC for 90 min. The chemisorbed ammonia was then eliminated (50 $mL \cdot min^{-1}$ helium) by increasing the temperature up to 550 ºC with a heating rate of 15 $ºC \cdot min^{-1}$ and kept at this temperature for 30 min.

2.3 Arabinoxylan hydrolysis experiments

The hydrolysis of arabinoxylans, which are solubilized in an aqueous phase obtained after a hydrothermal fractionation of destarched wheat bran, was studied in this work. The average molecular weight of the AXs in this fraction was around 9 KDa. More details concerning the fractionation step were described in a previous work (Sánchez-Bastardo et al., 2017).

The aim of this work was to complete the conversion of arabinoxylans into monomers (arabinose and xylose). The hydrolysis experiments were carried out in a commercial stainless steel high pressure reactor (30 mL, Berghoff® BR-25) equipped with a PID controlled. In a typical experiment, the reactor was loaded with the solid catalyst and flushed three times with nitrogen to remove the air. Thereafter, the reactor was pressurized with N_2 and heated up to the operating temperature (180 ºC). An inert atmosphere was required to avoid the oxidation of sugars into undesired products, *e.g.* organic acids (Jin and Enomoto, 2011). When the temperature reached 180 ºC, the AXs aqueous mixture preheated at 50 ºC was pumped (PU-2080 Plus; Jasco). After pumping, the temperature inside the reactor dropped to around 170 ºC. The initial time (0 min) was taken when the temperature reached again 180 ºC (this lasted approximately 3 minutes). At this moment, the nitrogen pressure was adjusted to the operating pressure (50 bar). At the end of the experiments, the reactor was rapidly quenched with chilled water. The product was filtered to separate the solid catalyst from the liquid phase. The liquid was used for further analysis (monomeric and oligomeric sugars, degradation products and by-products).

2.4 Initial and final products analysis

High Performance Liquid Chromatography (HPLC) was performed to identify and quantify the products in the liquid mixture after the experiments. The analysis of

monosaccharides and degradation products was performed directly in the liquid sample after filtration (pore size 0.22 μm, Diameter 25 mm, Nylon; FILTER-LAB). An acid hydrolysis for total sugars determination (total sugars = oligomers + monomers) was carried out according to the Laboratory Analytical Procedure (LAP) described by NREL (Sluiter et al., 2008). All the samples were analyzed using a chromatography system consisting of an isocratic pump (Waters 1515; Waters Corporation) and an automatic injector (Waters 717; Waters Corporation). Different HPLC columns were used for the determination of sugars and degradation products: 1) Supelcogel Pb (Supelco) for sugars (milli-Q water as mobile phase, 0.5 $mL \cdot min^{-1}$ as flow rate and 85 ºC as temperature) and 2) Sugar SH-1011 (Shodex) for degradation products (sulfuric acid 0.01 N as mobile phase, 0.8 $mL \cdot min^{-1}$ as flow rate and 50 ºC as temperature). Sugars and acids were identified using a RI detector (Waters 2414; Waters Corporation). 5-hydroxymethylfurfural (5-HMF) and furfural were determined with an UV-Vis detector (Waters 2487; Waters Corporation) at a wavelength of 254 and 260 nm, respectively. The standards employed for the HPLC analysis were: cellobiose (98%), glucose (99%), xylose (99%), galactose (99%), arabinose (99%), mannose (99%), fructose (99%), glyceraldehyde (95%), glycolaldehyde (99%), lactic acid (85%), formic acid (98%), acetic acid (99%), levulinic acid (98%), acrylic acid (99%), pyruvaldehyde (40%), 5-hydroxymethylfurfural (99%) and furfural (99%). All these chemicals were purchased from Sigma-Aldrich (Spain) and used as received.

The yields of arabinose and xylose, as well as the total monomeric yield and the oligomers conversion, are defined below (Eq. 1 – 4):

$$\%\ \text{Ara yield} = \frac{\text{Ara as monomer (g)}}{\text{Ara as total sugars}^{e}\ \text{in initial liquid extract (g)}} \times 100 \qquad \text{(Eq. 1)}$$

$$\% \text{ Xyl yield} = \frac{\text{Xyl as monomer (g)}}{\text{Xyl as total sugars}^{e} \text{ in initial liquid extract (g)}} \times 100 \quad \text{(Eq. 2)}$$

$$\% \text{ Total yield} = \frac{\text{(Ara+Xyl) as monomers (g)}}{\text{(Ara+Xyl) as total sugars}^{e} \text{ in initial liquid extract (g)}} \times 100 \quad \text{(Eq. 3)}$$

$$\% \text{ Olig. Conversion} = \frac{\text{Oligomers}_{final} - \text{Oligomers}_{initial}}{\text{Oligomers}_{initial}} \times 100 \quad \text{(Eq. 4)}$$

[e] Total sugars refer to the sum of the corresponding sugar (arabinose and/or xylose) as monomer and oligomer

It should be noted that the yield considers total monomers after hydrolysis, *i.e.* the monomers which have been obtained during the previous fractionation step and those which have been formed and not degraded during the hydrolysis process itself. However, the oligomers conversion considers the oligomers obtained after fractionation which have been hydrolyzed during the hydrolysis step.

3. Results and discussion

3.1 Composition of initial AX fraction

The composition of the initial arabinoxylan extract is given in Table 2. The percentage of each sugar in monomeric and oligomeric form is detailed. Almost 50% of total arabinose appeared as monomer after the fractionation step. Nonetheless, about 95% of total xylose remained still in oligomeric form. The average molecular weight of the liquid extract was 9 kDa, determined by HPLC-SEC.

The initial total amounts of arabinose and xylose (monomers + oligomers) were 3.1 and 6.2 $g \cdot L^{-1}$, respectively. Therefore, these are the maximum concentrations expected for each sugar after the hydrolysis process. These concentrations can be only achieved when all the oligomers are converted into monomers and they are not further degraded.

Table 2. Chemical composition of the initial extract.

Compound			
Sugars	Monomeric sugars ($mg \cdot L^{1}$)	Oligomeric sugars ($mg \cdot L^{-1}$)	Olig. (%)[f]
Glucose	195 ± 32	1609 ± 197	89
Xylose	284 ± 9	5944 ± 188	95
Galactose	82 ± 26	255 ± 34	76
Arabinose	1522 ± 112	1605 ± 34	51
Mannose	70 ± 9	2 ± 44	2

[f] % Olig. = percentage of each sugar in oligomeric form = sugar in oligomeric form (g)/total sugar (g) x 100.

3.2 Catalyst characterization

3.2.1 Small Angle X-Ray Scattering (SAXS) and X-Ray Diffraction (XRD)

The structure of the mesoporous and microporous materials was characterized by Small Angle X-Ray Scattering (SAXS) and X-Ray Diffraction (XRD), respectively. Figure 2A shows SAXS patterns of MCM-48 and Al-MCM-48. Both exhibit three main diffraction peaks at 2θ = 2.55º, 2.94º and 4.92º, which are assigned to (211), (220) and (332) planes, respectively, indicating an Ia3d symmetry (Romero et al., 2016). The intensity of the peak at (211) reflection is lower in Al-MCM-48 than in MCM-48, suggesting a negative impact of alumina on the structure of MCM-48. In fact, the incorporation of alumina has already been reported to decrease the structural order of the cubic network (Huang et al., 2008). Figure 2B displays XRD patterns of the commercial zeolites H-Y (12), H-ZSM-5 (23) and H-ZSM-5 (80) after calcination. H-Y (12) possesses typical diffraction peaks of a faujasite (FAU) structure in the range 5 – 35º (Choudhary et al., 2015; Dik et al., 2014; Mu et al., 2014; Saxena et al., 2013; Xia et al., 2010). H-ZSM-5 zeolites exhibit well-resolved diffraction peaks at 2θ = 8 – 9º, 23 – 25º, and 45º (JCPDS Card no. 00-037-0359), which are characteristic of a typical MFI structure (Dong et al., 2017; Guo et al., 2014; Jin et al., 2015; Rachel-Tang et al., 2017).

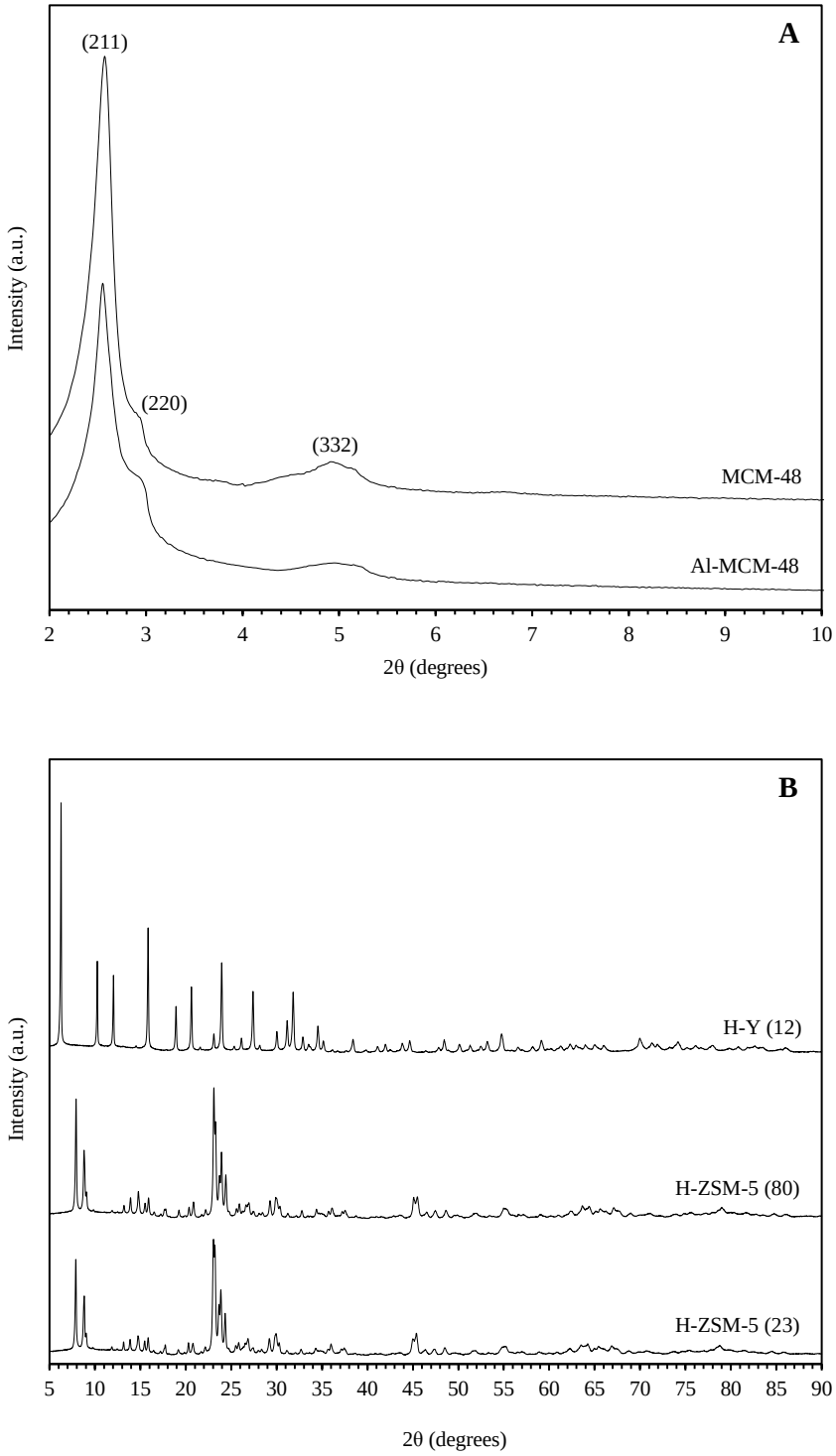

Figure 2. A) SAXS patterns of MCM-48 and Al-MCM-48 and B) XRD patterns of H-Y (12), H-ZSM-5 (23) and H-ZSM-5 (80).

3.2.2 Nitrogen adsorption-desorption isotherms

Figure 3 shows the nitrogen adsorption-desorption isotherms of the catalysts at -196 ºC. The curves for MCM-48 and Al-MCM-48 (Figure 3A) display type IV isotherms according to IUPAC classification, which is characteristic of mesoporous materials (Brunauer et al., 1940). The initial part of type IV isotherms ($P/P_0 < 0.1$) is attributed to monolayer – multilayer adsorption (Kolasinski, 2012). The sharp increase in the relative pressure range $P/P_0 = 0.1 – 0.3$ is associated with capillary condensation in the mesoporous channels of the cubic structure. The sharpness of this step indicates a uniform pore size and a narrow size distribution, as demonstrated in Figure 4A (Giraldo et al., 2016; Huang et al., 2008; Kong et al., 2005; Schumacher et al., 2000). The nitrogen adsorption-desorption isotherm of Al-MCM-48 exhibits a distinct condensation step at a P/P_0 range = 0.5 – 0.9. However, the lack of the hysteresis loop for MCM-48 indicates a decrease in the amount of capillary condensation in the mesopores of this material (Ghosh et al., 2015). Figure 3B shows type I isotherms for H-ZSM-5 (23 and 80) and H-Y (12), typical of microporous materials. They exhibit a sharp increase of nitrogen sorption at very low partial pressures ($P/P_0 \leq 0.01$) due to micropores filling (Xie et al., 2017). The rise observed at $P/P_0 > 0.95$ is related to nitrogen condensation in the void volume between the particles (Fu et al., 2016). In addition to this, the isotherms of all the zeolites display slight type H4 hysteresis loops (ALOthoman, 2012). This kind of hysteresis is often associated with narrow slit-like pores, but in the case of type I isotherms is indicative of a microporous structure with a low contribution of mesopores (Beyer et al., 1995; Cychosz et al., 2017; Fu et al., 2016; Lü et al., 2003; Peng et al., 2015). However, as shown in Figure 4B, C, D, the pore size distribution (PSD) of the zeolites can be considered a unimodal microporous distribution. Therefore, the small hysteresis loop and the narrow pore size distribution imply that zeolites are characterized mainly by a

microporous structure. The PSD of H-Y (12), H-ZSM-5 (23) and H-ZSM-5 (80) presents a maximum at 0.67, 0.68 and 0.67, respectively.

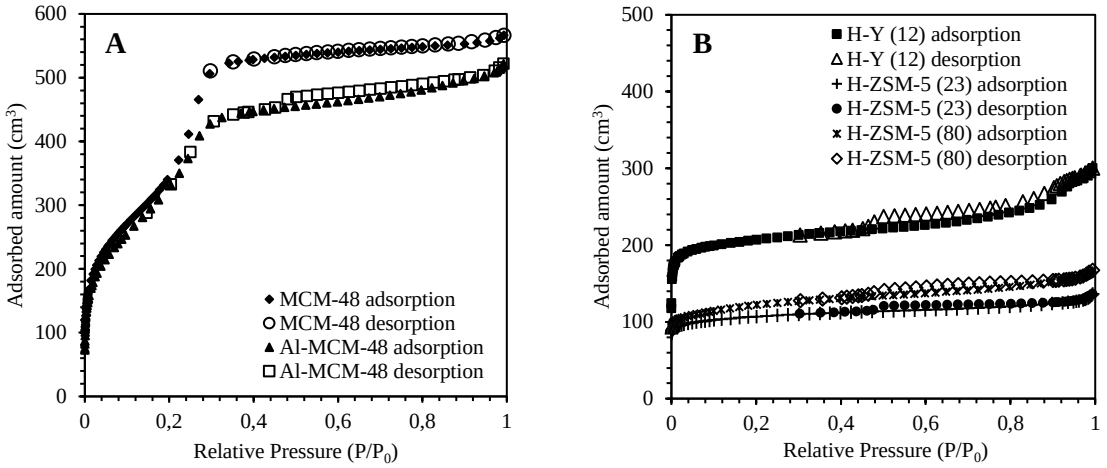

Figure 3. Nitrogen adsorption-desorption isotherms of A) MCM-48 and Al-MCM-48 and B) H-ZSM-5 (23), H-ZSM-5 (80) and H-Y (12).

Table 3 gathers the textural properties of the catalysts. The specific surface area, the total pore volume and the pore diameter were calculated from the adsorption-desorption nitrogen isotherms. MCM-48-type materials showed higher specific surface areas, pore volumes and pore sizes than zeolites. This was in agreement with the mesoporous character of MCM-48 materials and the microporous structure of zeolites (Schmidt, 2006). Comparing the two mesoporous catalysts (MCM-48 and Al-MCM-48), not significant changes were observed in the specific surface area (1298 and 1352 $m^2 \cdot g^{-1}$, respectively) and in the pore volume (0.87 and 0.81 $cm^3 \cdot g^{-1}$, respectively). However, Al-MCM-48 presented a higher pore diameter (2.5 nm) than MCM-48 (2.2 nm), which indicates slender modifications of the pore structure due to aluminum incorporation during the synthesis of Al-MCM-48. A unimodal pore size distribution centered at approximately 2 nm is exhibited by both MCM-48 materials (Figure 4A). The different zeolites also differed in their structural properties. H-Y presented a higher specific surface area than H-ZSM-5 zeolites. This is associated to the bigger average pore size of H-Y

than H-ZSM-5 zeolites (Schmidt, 2006). H-Y displayed also greater pore volume and pore diameter than H-ZSM-5, which is related to the type of pore windows. H-Y zeolites consist of 12MR pore windows, whereas ZSM-5 zeolites possess 10MR channels (Corma et al., 1998; Schmidt, 2006). In the case of H-ZSM-5 (23) and H-ZSM-5 (80) they exhibited very similar textural properties.

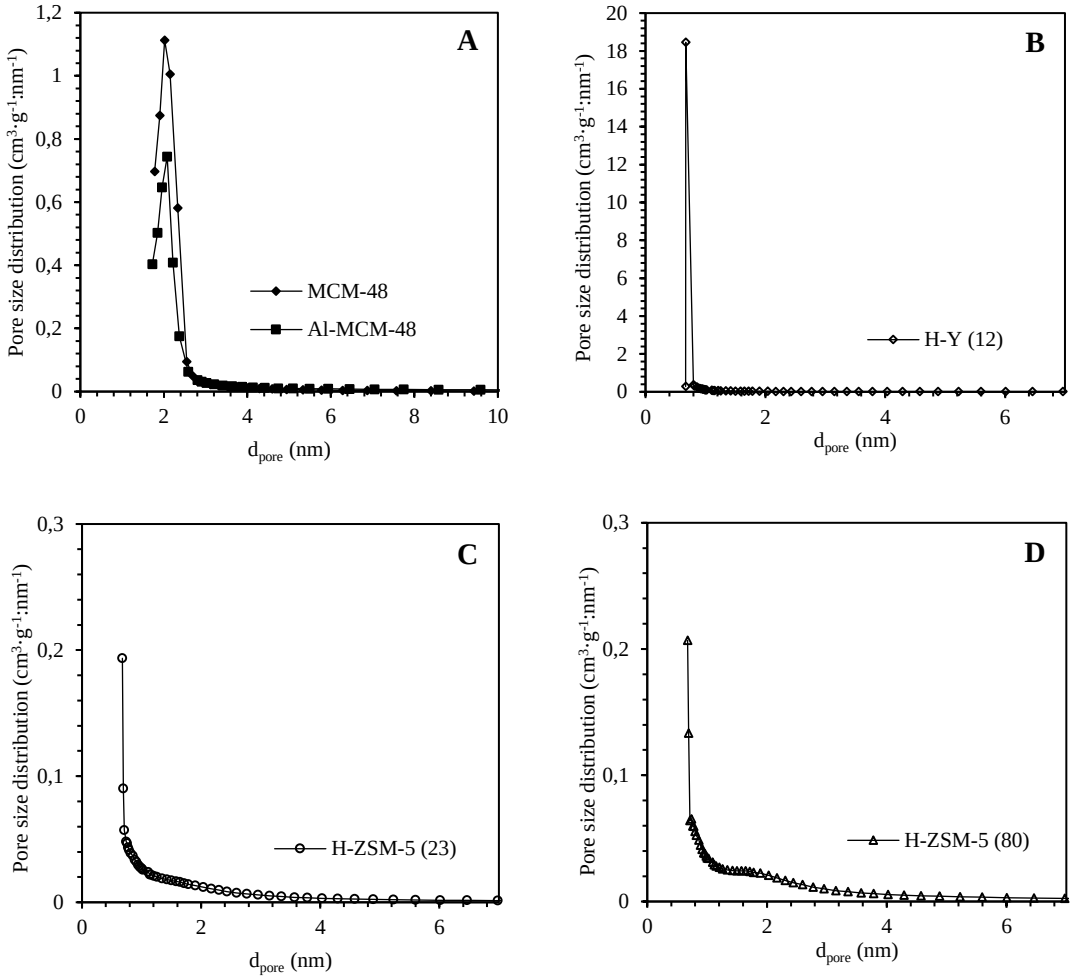

Figure 4. Pore size distributions (PSD) of A) MCM-48 and Al-MCM-48, B) H-Y (12), C) H-ZSM-5 (23) and D) H-ZSM-5 (80).

Table 3. Textural properties of the catalysts.

Catalyst	Specific surface area ($m^2 \cdot g^{-1}$)	V_{pore} ($cm^3 \cdot g^{-1}$)	d_{pore} (nm)
MCM-48	1298[g]	0.87[i]	2.2[k]
Al-MCM-48	1352[g]	0.81[i]	2.5[k]
H-Y (12)	927[h]	0.46[j]	0.78[j]
H-ZSM-5 (23)	483[h]	0.21[j]	0.68[j]
H-ZSM-5 (80)	562[h]	0.26[j]	0.67[j]

[g] Determined by the multipont BET method at $P/P_0 \leq 0.3$.
[h] Determined by Langmuir model.
[i] Determined from N_2 uptake at $P/P_0 \geq 0.99$.
[j] Determined by Horvath-Kawazoe method.
[k] Determined by BJH adsorption average ($4 \cdot V \cdot A^{-1}$, nm).

3.2.3 Temperature-programmed desorption of ammonia (NH_3-TPD)

Acidity plays a key role in the catalytic activity of solid acid catalysts. Temperature-programmed desorption of ammonia (NH_3-TPD) was used to determine the quantity and strength of the acid sites (Table 4). The quantity of acid sites is given by the total amount of NH_3 desorbed per gram of sample ($mEq \cdot g^{-1}$). The strength distribution of the acid sites is estimated from the deconvoluted TPD plots by means of Gaussian curves (Figure 5). Likewise, the average desorption temperature was calculated considering the partial desorption temperatures corresponding to each of the deconvoluted curves.

In the case of mesoporous silica catalysts, Al-MCM-48 showed a higher total acidity than MCM-48 due to the incorporation of aluminum onto the mesoporous network. Although the total number of weak and strong acid sites was greater in Al-MCM-48, MCM-48 presented a higher ratio between strong/weak acid sites. The average desorption temperatures were 298 ºC and 268 ºC for MCM-48 and Al-MCM-48, respectively, indicating that MCM-48 has stronger acid sites. The nature of the acid sites is also different. MCM-48 possesses mainly Lewis acid sites (Xue et al., 2004), while the incorporation of aluminum atoms creates Brönsted acid sites in Al-MCM-48 (Kosslick et al., 1998).

The total acidity in zeolites displayed the following trend: H-ZSM-5 (23) > H-Y (12) > H-ZSM-5 (80). These zeolites also differed in the strength and nature of the acid sites. Most of the acid sites in H-ZSM-5 zeolites were strong, while H-Y zeolite exhibited more weak than strong acid sites. In addition to this, the average desorption temperature for H-ZSM-5 zeolites was higher than that for H-Y, which means that the acid sites were markedly stronger in H-ZSM-5-type zeolites. The same trend was already reported in previous works (Carà et al., 2013; Corma et al., 2000; González-Velasco et al., 2000; Zhou et al., 2016; Steen et al., 2004). The nature of the acid sites in commercial zeolites was previously studied by Corma et al. (2000). They used infrared spectroscopy of pyridine to identify Lewis and Brönsted acid sites. H-ZSM-5 zeolites exhibited predominately Brönsted acidity while H-Y contained Brönsted and Lewis acid sites. This fact was also observed by Zhou et al. (2016). H-ZSM-5 zeolites with different Si/Al ratios also showed different properties of the acid sites. The total acidity of H-ZSM-5 (23) was higher than that of H-ZSM-5 (80), as expected from the higher aluminum content of the former (Al-Dughaither and De Lasa, 2014; Gao et al., 2016; Kim et al., 2013). H-ZSM-5 (23) presented a higher average desorption temperature than H-ZSM-5 (80), which demonstrates that acid sites were stronger in H-ZSM-5 zeolites with higher aluminum content. This is in agreement with previous works (Al-Dughaither and De Lasa, 2014; Gao et al., 2016; Kim et al., 2013; Shafaghat et al., 2015).

Comparing the acidity properties of mesoporous silicas and microporous aluminosilicates (zeolites), it was found that zeolites have a higher total acidity as well as stronger acid sites than MCM-48 or Al-MCM-48.

Table 4. Acidity of the solid acid catalysts.

Catalyst	Total acidity ($mEq \cdot g^{-1}$)	Weak acid sites ($mEq \cdot g^{-1}$)[o]	Strong acid sites ($mEq \cdot g^{-1}$)	Average desorption T (ºC)	Nature of acid sites
MCM-48	0.147	0.069	0.077	298	Mainly Lewis[l]
Al-MCM-48	0.863	0.553	0.310	268	Lewis + Brönsted[m]
H-Y (12)	5.237	3.211	2.025	312	Lewis + Brönsted[n]
H-ZSM-5 (23)	6.269	1.781	4.487	341	Mainly Brönsted[n]
H-ZSM-5 (80)	2.990	1.063	1.927	334	Mainly Brönsted[n]

[l] Xue et al., 2004.
[m] Kosslick et al., 1998.
[n] Corma, et al., 2000.
[o] Weak acid sites were determined for temperatures lower than 280 ºC (Zhou et al., 2016).

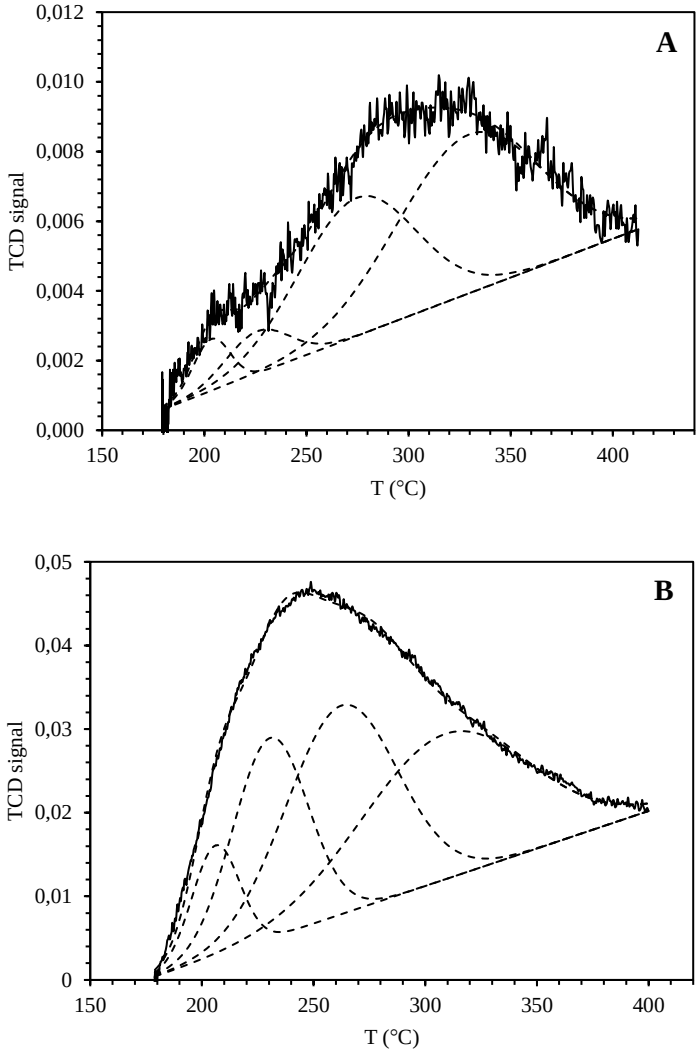

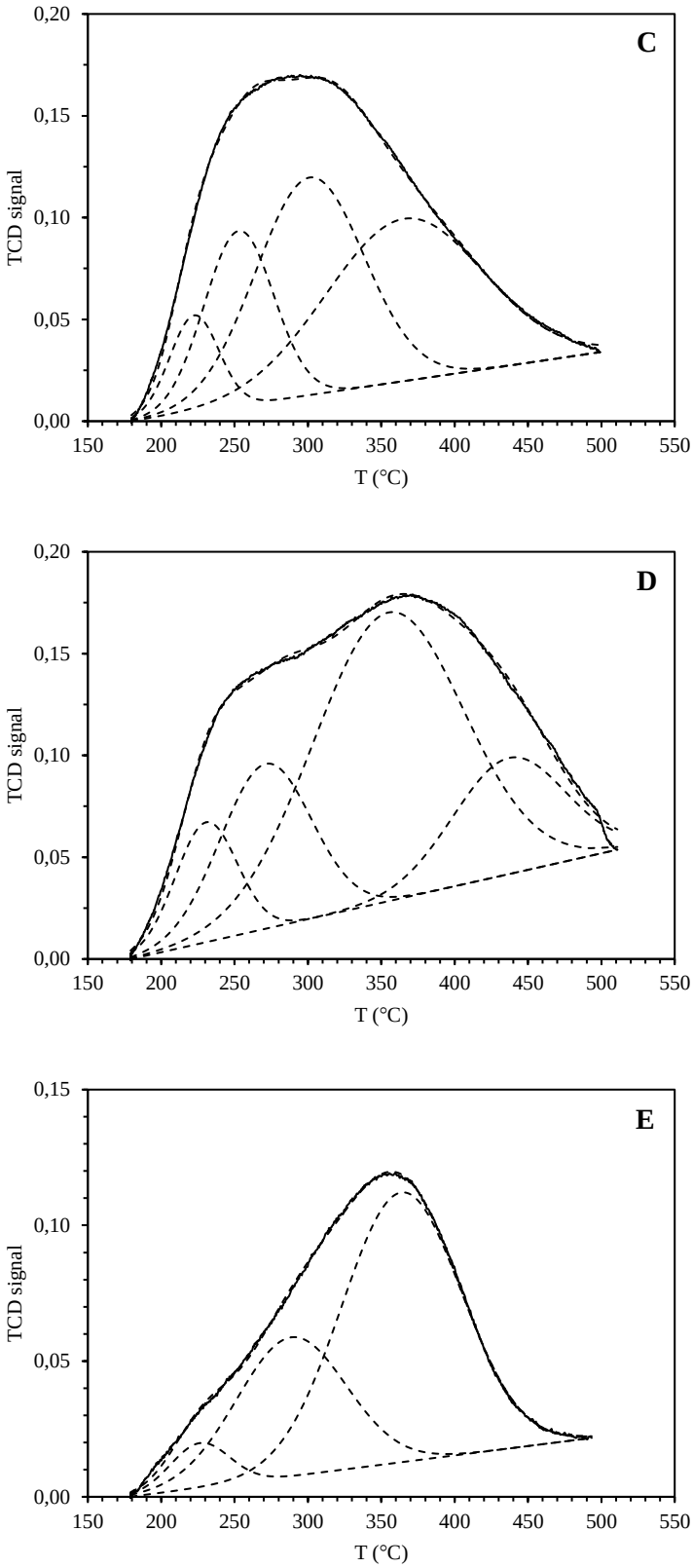

Figure 5. Deconvoluted NH_3-TPD curves of A) MCM-48, B) Al-MCM-48, C) H-Y (12), D) H-ZSM-5 (23) and E) H-ZSM-5 (80).

3.3 Arabinoxylan hydrolysis experiments

3.3.1 Effect of different solid acid catalysts

Figure 6 shows the hydrolysis results over different mesoporous and microporous silica materials. It should be noted that the yield considers the total monomers after hydrolysis, which also includes the monomers previously formed during wheat bran fractionation. Half of the total arabinose was in monomeric form after fractionation, whereas most of the xylose remained in oligomeric form.

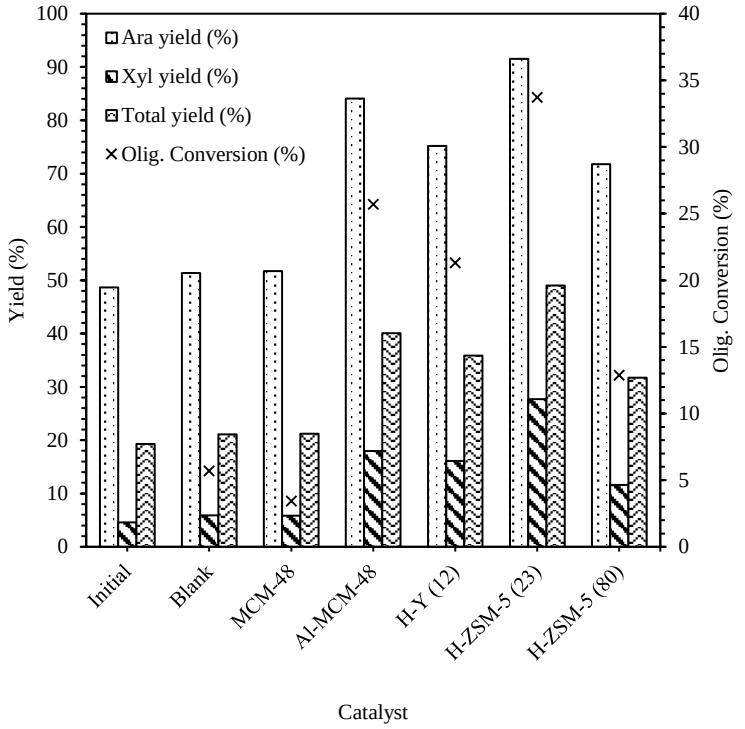

Figure 6. Comparison of different solid acid catalysts in monomeric yield and oligomers conversion. Reaction conditions: 20 mL of liquid extract, 180 ºC, 15 minutes, catalyst loading: 4.6 g catalyst·g C^{-1} in initial hemicelluloses, 50 bar N_2.

The amount of arabinose and xylose as monosaccharides in the blank experiment and over MCM-48 was roughly the same as in the initial extract. In addition to this, the oligomers conversion was very low, and furfural was obtained in minor amounts after these two experiments (Table 5). This means that sugars remained basically intact: oligomers were not hydrolyzed, and the initially existing monomers were not significantly

degraded. MCM-48 has a very low acidity (Table 4), which corresponds mostly to Lewis acid sites (Xue et al., 2004). Such acid sites were unable to cleave the glycosidic bonds between the molecules of the oligomers, or to convert the existing monomers into by-products. Al-MCM-48 improved significantly the total sugar yield from 21% to 40%. This was attributed to the higher acidity and Brönsted acid sites generated after the incorporation of aluminum (Collart et al., 2004; Kao et al., 2008).

Different zeolites were also tested in arabinoxylan hydrolysis. The performance of these zeolites showed the following trend: H-ZSM-5 (23) > H-Y (12) > H-ZSM-5 (80). We compared first the activity of H-ZSM-5 (23) and H-Y (12), which display the highest acidity values (Table 4). The total monomeric yields over H-Y (12) and H-ZSM-5 (23) were 36% and 49%, respectively. The good catalytic activity of H-ZSM-5 (23) is related to its high acidity but also to the nature and strength of the acid sites. H-ZSM-5 (23) has more acid sites than H-Y (12) (Table 4). As mentioned before, the type and strength of the acid sites is also different in H-Y and H-ZSM-5 zeolites (Al-Dughaither and De Lasa, 2014; Boréave et al., 1997; Corma et al., 2000; Gao et al., 2016). H-ZSM-5 (23) possesses mainly strong and Brönsted acid sites. However, H-Y (12) has more weak than strong acid sites, which are at the same time weaker to those of H-ZSM-5 (23), as demonstrated by the lower average desorption temperature (Table 4). In addition to this, H-Y (12) shows a combination of Lewis and Brönsted acid sites (Corma et al., 2000). Therefore, the high activity of H-ZSM-5 (23) in arabinoxylan hydrolysis can be attributed to several reasons summarized as follows. H-ZSM-5 (23) has: i) high acidity, ii) mainly Brönsted acid sites, iii) high strong/weak acid sites ratio and iv) strong acid sites, which determine its good catalytic activity.

The activity of H-ZSM-5 zeolites with different Si/Al ratios was then compared. H-ZSM-5 (23) demonstrated to be more active than H-ZSM-5 (80). Both catalysts have Brönsted

acid sites, but the greater aluminum content of H-ZSM-5 (23) increases their total acidity and the strength of their acid sites, as seen in Table 4. This consequently improved the monomeric yield. Zeolites with a high aluminum content were already reported to be suitable for hemicelluloses hydrolysis in a previous work (Carà et al., 2013).

A comparison between H-ZSM-5 (23) and Al-MCM-48 must also be done since they have a very different number of acid sites (Table 4) but a similar catalytic activity (Figure 6). Al-MCM-48 has a mesoporous structure which decreases the mass transfer limitations of oligosaccharides to enter the pores. In this case, the arabinoxylan hydrolysis takes place not only on the external acid sites, but also on those located inside the pores. Unlike Al-MCM-48, the hydrolysis of arabinoxylans must occur on the external acid sites of H-ZSM-5 during the first hydrolysis stages. H-ZSM-5 (23) shows a microporous structure and thus the initial large oligosaccharides cannot enter the pores until they have been converted into shorter oligomers. Hydrolysis processes in zeolites takes place first on the external acid sites and later on the internal pores (Carà et al., 2013). Therefore, the good performance of Al-MCM-48 despite its lower acidity is explained because all the acid sites of the catalyst (external and internal) are available to oligosaccharides from the beginning of the reaction. In the case of H-ZSM-5 (23), the hydrolysis starts only on the external acid sites and then continues also on the internal ones. However, this implies no limitations because H-ZSM-5 (23) has strong acid sites on its external surface resulting in a rapid arabinoxylan hydrolysis, which makes mass transfer limitations be neglected.

Table 5 shows the final concentration of xylose, arabinose and furfural after hydrolysis over the different solid acid catalysts.

Table 5. Concentration of monomeric sugars and furfural after hydrolysis experiments. Reaction conditions: 20 mL of liquid extract, 180 ºC, 15 minutes, catalyst loading: 4.6 g catalyst·g C^{-1} in initial hemicelluloses, 50 bar N_2.

Main products[p]	Initial (g/L)	Catalyst					
		Blank	MCM-48	Al-MCM-48	H-Y (12)	H-ZSM-5 (23)	H-ZSM-5 (80)
Xylose	0.28	0.37	0.37	1.12	1.00	1.73	0.72
Arabinose	1.52	1.61	1.62	2.63	2.35	2.86	2.25
Furfural	0.07	0.16	0.16	0.17	0.14	0.02	0.00

[p] Traces of glycolaldehyde, formic acid, acetic acid and 5-HMF were detected in all the cases.

The amount of furfural was analyzed since it is the main degradation product which can be obtained from C_5 sugars. Other by-products, such as glycolaldehyde, formic acid or 5-HMF, were also detected in smaller proportion. They can be formed from xylose and arabinose, but also from glucose, which is present in minor amounts after fractionation (Aida et al., 2010; Watanabe et al., 2005). For the sake of simplification, these by-products were omitted, and the results were discussed in terms of xylose, arabinose and furfural. Furfural was already formed during wheat bran fractionation (~0.07 g·L^{-1}) and therefore was present in the initial mixture. The amount of furfural after hydrolysis was between 0.14 – 0.17 g·L^{-1} in the experiments performed over MCM-48, Al-MCM-48 and H-Y (12). This small amount of furfural demonstrated the low degradation of the sugars. A different trend was observed in the experiments over H-ZSM-5 zeolites: furfural was detected after hydrolysis in lower amounts than in the initial extract. Our first hypothesis was to associate this fact with the further degradation of furfural into other compounds (Filiciotto et al., 2018) or humins (Filiciotto et al., 2018; Tsilomelekis et al., 2016). Surprisingly, no other products were detected by HPLC. Humins are insoluble black residues formed via polymerization of furanic compounds (Filiciotto et al., 2018). They

are characterized by a black, shining and coal appearance (Blanksma and Egmond, 1976), which was not observed after hydrolysis. Thus, degradation of furfural into other by-products was discarded. Other hypothesis to explain the disappearance of furfural could be attributed to its occlusion inside the pores of H-ZSM-5 zeolites. H-ZSM-5 zeolites have the smallest pore diameter of all the catalysts tested. Furfural has a molecular diameter of 0.57 nm (Karinen et al., 2011) and therefore it may have more problems to leave the pores of H-ZSM-5 than those of any other catalyst. In this case, furfural would remain inside the pores and would not be detected in the liquid. To prove this hypothesis, thermogravimetric analyses (TGA) were performed (Figure 7).

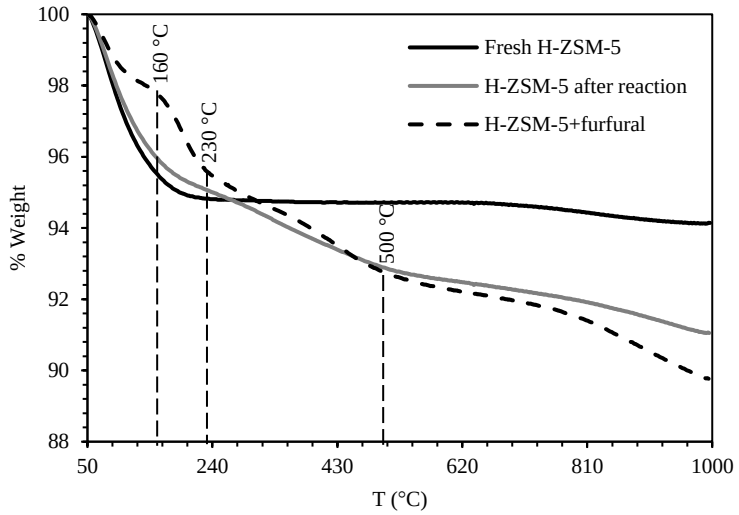

Figure 7. Thermogravimetric analyses of H-ZSM-5 (23): fresh, after reaction and a prepared mixture of fresh zeolite + furfural.

H-ZSM-5 (23) was analyzed before and after the reaction. In addition to this, a mixture of a fresh zeolite and pure furfural was prepared and analyzed by TGA for comparison purposes. The TGA curve of the fresh zeolite showed only a sharp weight loss between 50 and 200 ºC. However, three different remarkable weight losses were observed in the TGA curve of the zeolite after reaction: 50 – 230 ºC, 230 – 500 ºC and 500 – 1000 ºC. The changes in the curve of the spent zeolite between 230 – 500 ºC and 500 – 1000 ºC were very similar to those observed for the prepared mixture of H-ZSM-5 and furfural,

indicating that furfural was adsorbed on the zeolite during the reaction. The prepared mixture of the zeolite and furfural exhibited two additional mass losses from 50 to 160 ºC and from 160 to 230 ºC, which corresponded to furfural weakly adsorbed on the zeolite. From these results, it can be stated that furfural was not weakly but moderately and strongly adsorbed on H-ZSM-5 (23) after hydrolysis. Therefore, it can be concluded that furfural was formed during the hydrolysis reaction with H-ZSM-5 (23) but not detected in the liquid because it was adsorbed inside the zeolite pores.

H-ZSM-5 (23) was chosen as the most active catalyst in arabinoxylan hydrolysis and a further optimization process was carried out. The influence of reaction time and catalyst loading were then discussed.

3.3.2 Effect of reaction time

First, several experiments at different times were carried out with a H-ZSM-5 (23) loading of 4.6 g·g C^{-1} (Figure 8). The amount of monomeric arabinose achieved a maximum at short times: 92% of the initial total arabinose (oligomers + monomers) was in monomeric form after 15 minutes. For longer times, the concentration of arabinose remained roughly constant, which demonstrated the high stability of this sugar under the operating conditions. It is important to remind that the percentage of the initial arabinose in oligomeric and monomeric form was 50%/50%. Therefore, these results suggested that the initial monomers were not degraded. In addition to this, the arabino-oligosaccharides were converted into monomers without major degradation. Xylose exhibited a different behavior. The amount of monomeric xylose increased over time in the study range (15 – 60 minutes). Even after 1 hour only ~68% of the initial xylose was detected as monosaccharide. Thus, arabino-oligosaccharides were more readily hydrolyzed than xylo-oligosaccharides. This fact is related to the position of arabinose and xylose in the arabinoxylan structure and to the different bonds existing between the molecules. The

molecules of arabinose belong to the side chains, whereas the backbone is composed mainly of xylose units. In addition to this, arabinose molecules are linked by α-glycosidic bonds and xylose molecules by β-glycosidic bonds. Hence, the easier access to side chains and the more easily hydrolysable α-glycosidic bonds lead to a faster release of arabinose than xylose (Negahdar et al., 2016).

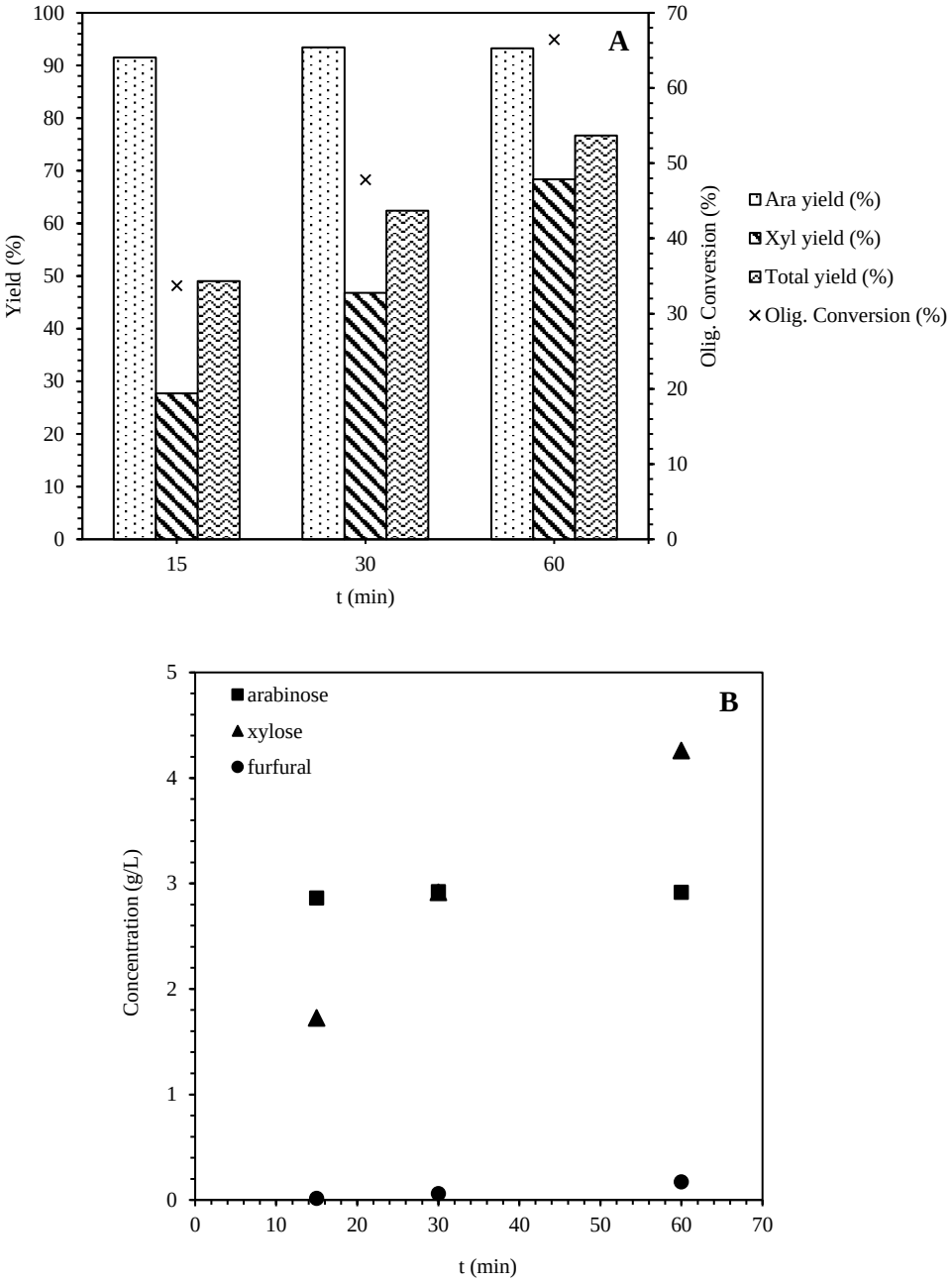

Figure 8. Influence of time in AX hydrolysis. A) Monomeric yield and oligomers conversion and B) Composition of hydrolysate (g/L). Reaction conditions: 20 mL of

liquid extract, 180 ºC, catalyst: H-ZSM-5 (23), catalyst loading: 4.6 g catalyst·g C^{-1} in initial hemicelluloses, 50 bar N_2.

3.3.3 Effect of catalyst loading

The influence of catalyst loading was studied over H-ZSM-5 (23) (Figure 9). The yield of arabinose was higher than that of xylose for the same catalyst amount. For instance, the yield of arabinose was already very high (~92%) with a catalyst loading of 4.6 g·g C^{-1}. However, only ~28% of the initial xylose was present as monosaccharide under the same experimental conditions. The optimal catalyst loading to obtain xylose in monomeric form was 9.2 g·g C^{-1} (67%). Thus, a higher number of acid sites was required to cleave xylo-oligosaccharides than arabino-oligosaccharides. As mentioned before, this is associated with the most difficult access and the stronger bonds existing between xylose molecules than between arabinose units. It should be noted that even if arabinose reached a high yield with 4.6 g catalyst·g C^{-1}, it was not further degraded by increasing the catalyst loading up to 9.2 g·g C^{-1}.

Thereafter, an attempt to improve the yield of xylose was done by increasing the catalyst amount (18.4 g·g C^{-1}), but not an enhancement was obtained. Higher catalyst/substrate ratios demonstrated to be more efficient in hydrolysis of hemicelluloses (Sahu and Dhepe, 2012). Nevertheless, the catalyst loading used in this case was too high and mass transfer limitations played an important role.

From these results, it can be concluded that the optimum conditions to maximize the amount of monomers (arabinose + xylose) were 180 ºC, 15 minutes and using H-ZSM-5 (23) with a loading of 9.2 g·g C^{-1}. Under these conditions, the yields of arabinose and xylose were 96% and 67%, respectively. This corresponded to a global monomeric yield of 76%.

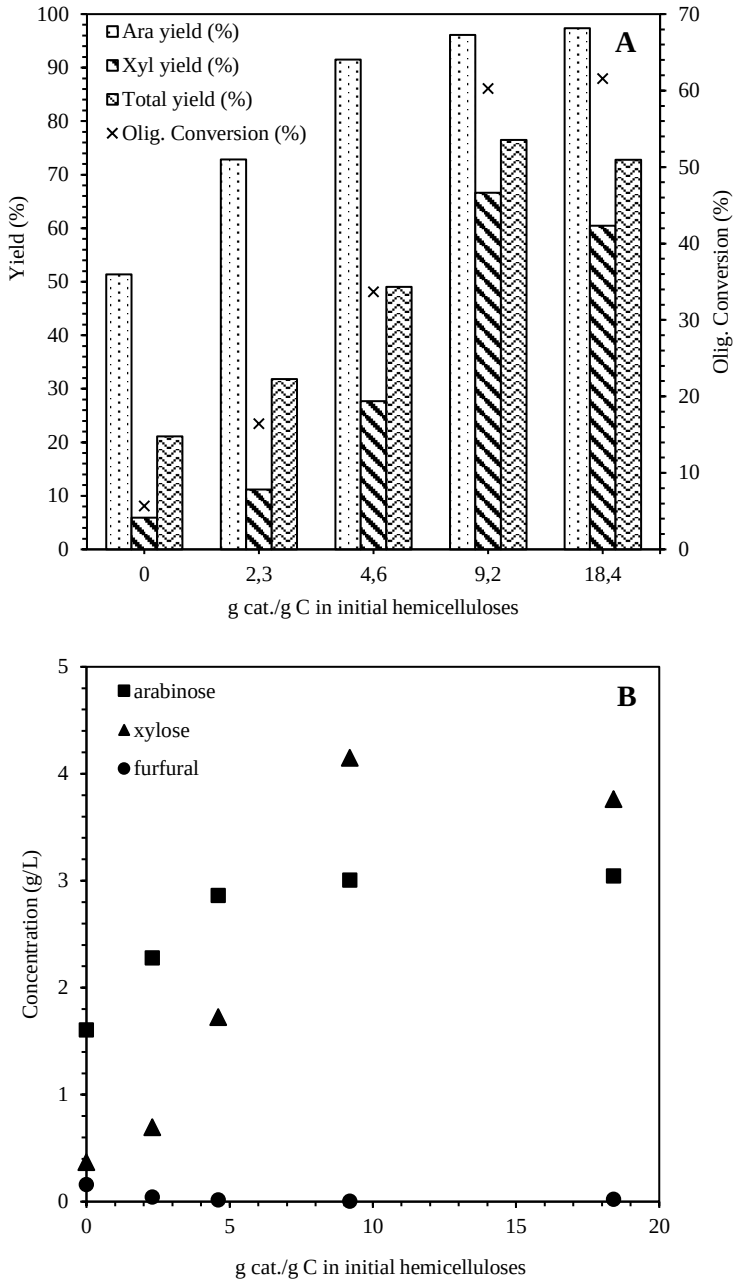

Figure 9. Effect of catalyst loading in AX hydrolysis. A) Monomeric yield and oligomers conversion and B) Composition of hydrolysate (g/L). Reaction conditions: 20 mL of liquid extract, 180 ºC, 15 minutes, H-ZSM-5 (23), 50 bar N_2.

4. Conclusions

The conversion of biomass into valuable chemicals has been widely studied during the last years. Wheat bran is a suitable source of arabinoxylans, which have important applications in pharmaceutical and food industries. However, arabinoxylans can also be

converted into C_5 sugars, *i.e.* arabinose and xylose, which are of a greater interest. After a first fractionation step to isolate the arabinoxylan fraction from wheat bran, we have examined in this work the hydrolysis of arabinoxylans into monosaccharides over solid acid catalysts. Heterogeneous catalysts have attracted considerable attention in biomass conversion, as they have significant advantages over homogeneous catalysts. The catalytic activity of different mesoporous and microporous silica materials was tested in this work. We determined that the activity of the catalysts was related to the total acidity as well as the strength and nature of the acid sites. H-ZSM-5 (SiO_2/Al_2O_3 = 23) was the most active catalyst for the conversion of arabinoxylans into monomers. H-ZSM-5 (23) is the most acidic catalyst of all the tested and has strong acid sites as well as high Brönsted acidity, which explain its good activity. Reaction time and catalyst loading were also optimized. Comparing to xylo-oligosaccharides, arabino-oligosaccharides were faster hydrolyzed. In addition to this, the hydrolysis of arabino-oligosaccharides required a lower number of acid sites than the hydrolysis of xylo-oligosaccharides. The total monomeric yield achieved the optimum at 180 °C, 15 minutes and using a H-ZSM-5 (23) loading of 9.2 $g \cdot g\ C^{-1}$. The yields of arabinose and xylose were 96% and 67%, respectively, which corresponded to a total yield of 76%. In conclusion, the hydrolysis process of arabinoxylans from a real biomass was successfully performed over solid acid catalysts.

References

Aida, T.M., Shiraishi, N., Kubo, M., Watanabe, M., and Smith Jr, R.L. Reaction kinetics of D-xylose in sub- and supercritical water. *The Journal of Supercritical Fluids,* 55 (2010) 208–216.

Al-Dughaither, A.S., and De Lasa, H. HZSM-5 zeolites with different SiO_2/Al_2O_3 ratios. Characterization and NH_3 desorption kinetics. *Industrial & Engineering Chemistry Research,* 53 (2014) 15303–15316.

ALOthoman, Z.A. A Review: Fundamental aspects of silicate mesoporous materials. *Materials,* 5 (2012) 2874–2902.

Apprich, S., Tirpanalan, Ö., Hell, J., Reisinger, M., Böhmdorfer, S., Siebenhandl-Ehn, S., Novalin, S., and Kneifel, W. Wheat bran-based biorefinery 2: Valorization of products. *LWT - Food Science and Technology,* 56 (2014) 222–231.

Beyer, H.K., Nagy, J.B., Karge, H.G., and Kiricsi, I. Volume 94 – Catalysis by microporous materials. In *Studies in Surface Science and Catalysis*, 1st Edition, Elsevier Science, 1995.

Blanksma, J.J., and Egmond, G. Humin from hydroxymethylfurfuraldehyde. *Recueil des Travaux Chimiques des Pays-Bas,* 4 (1946) 309–310.

Boréave, A., Auroux, A., and Guimon, C. Nature and strength of acid sites in HY zeolites: a multitechnical approach. *Microporous Materials,* 11 (1997) 275–291.

Brunauer, S., Deming, L.S., Deming, E., and Teller, E. On a theory of the van der Waals adsorption of gases. *Journal of the American Chemical Society*, 62 (1940) 1723–1732.

Carà, P.D., Pagliaro, M., Elmekawy, A., Brown, D.R., Verschuren, P., Shiju, N.R., and Rothenberg, G. Hemicellulose hydrolysis catalysed by solid acids. *Catalysis Science & Technology*, 3 (2013) 2057–2061.

Choudhary, A., Das, B., and Ray, S. Encapsulation of a Ni salen complex in zeolite Y: an experimental and DFT study. *Dalton Transactions,* 44 (2015) 3753.

Collart, O., Cool, P., Van Der Voort, P., Meynen, V., Vansant, E.F., Houthoofd, K., Grobet, P.J., Lebedev, O.I., and Tendeloo, G.V. Aluminum Incorporation into MCM-48 toward the creation of Brønsted acidity. *The Journal of Physical Chemistry B,* 108 (2004) 13905–13912.

Corma, A., Fornés, V., Forni, L., Márquez, F., Martínez-Triguero, J., and Moscotti, D. 2,6-Di-Tert-Butyl-Pyridine as a probe molecule to measure external acidity of zeolites. *Journal of Catalysis,* 179 (1998) 451–458.

Corma, A., Melo, F.V., Mendioroz, S., and Fierro, J.L.G. 12th International Congress on Catalysis. In *Studies in Surface Science and Catalysis,* 1st Edition, Elsevier Science, 2000.

Cychosz, K.A., Guillet-Nicolas, R., García-Martínez, J., and Thommes, M. Recent advances in the textural characterization of hierarchically structured nanoporous materials. *Chemical Society Reviews,* 46 (2017) 389–414.

Deng, W., Zhang, Q., and Wang, Y. Catalytic transformation of cellulose and its derived carbohydrates into chemicals involving C-C bond cleavage. *Journal of Energy Chemistry,* 24 (2015) 595–607.

Dhepe, P.L., and Sahu, R. A solid-acid-based process for the conversion of hemicellulose. *Green Chemistry,* 12 (2012) 2153–2156.

Dik, P.P., Klimov, O.V., Koryakina, G.I., Leonova, K.A., Pereyma, V.Y., Budukva, S.V., Gerasimov, E.Y., and Noskov, A.S. Composition of stacked bed for VGO hydrocracking with maximum diesel yield. *Catalysis Today,* 220–222 (2014) 124–132.

Dong, H., Zhang, L., Fang, Z., Fu, W., Tang, T., Feng, Y., and Tang, T. Acidic hierarchical zeolite ZSM-5 supported Ru catalyst with high activity and selectivity in the seleno-functionalization of alkenes. *RSC Advances,* 7 (2017) 22008–22016.

Filiciotto, L., Balu, A.M., Van der Waal, J.C., and Luque, R. Catalytic insights into the production of biomass-derived side products methyl levulinate, furfural and humins. *Catalysis Today,* 302 (2018) 2–15.

Fu, X., Sheng, X., Zhou, Y., Fu, Z., Zhao, S., Bu, X., and Zhang, C. Design of micro – mesoporous zeolite catalysts for alkylation. *RSC Advances,* 6 (2016) 50630–50639.

Gao, Y., Zheng, B., Wu, G., Ma, F., and Liu, C. Effect of the Si/Al ratio on the performance of hierarchical ZSM-5 zeolites for methanol aromatization. *RSC Advances,* 6 (2016) 83581–83588.

Ghosh, S., Bose, P., Basak, S., and Naskar, M.K. Solvothermal-assisted evaporation-induced self-assembly process for significant improvement in the textural properties of γ-Al_2O_3, and study dye adsorption efficiency. *Journal of Asian Ceramic Societies,* 3 (2015) 198–205.

Giraldo, L., Bastidas-Barranco, M., and Moreno-Piraján, J.C. Adsorption calorimetry: Energetic characterisation of the surface of mesoporous silicas and their adsorption capacity of non-linear chain alcohols. *Colloids and Surface A: Physicochemical and Engineering Aspects,* 496 (2016) 100–113.

González-Velasco, J.R., López-Fonseca, R., Aranzabal, A., Gutiérrez-Ortiz, J.I., and Steltenpohl, P. Evaluation of H-type zeolites in the destructive oxidation of chlorinated volatile organic compounds. *Applied Catalysis B: Environmental,* 24 (2000) 233–242.

Guo, X., Wang, X., Guan, J., Chen, X., Qin, Z., Mu, X., and Xian, M. Selective hydrogenation of D-glucose to D-sorbitol over Ru/ZSM-5 catalysts. *Chinese Journal of Catalysis,* 35 (2014) 733–740.

Hara, M., Nakajima, K., and Kamata, K. Recent progress in the development of solid catalysts for biomass conversión into high value-added chemicals. *Science and Technology of Advanced Materials,* 16 (2015) 034903.

Hilpmann, G., Becher, N., Pahner, F-A., Kusema, B., Mäki-Arvela, P., Lange, R., Murzin, D.Y., and Salmi, T. Acid hydrolysis of xylan. *Catalysis Today*, 259 (2016) 376–380.

Huang, L., Huang, Q., Xiao, H., and Eic, M. Al-MCM-48 as a potential hydrotreating catalyst support: I – Synthesis and adsorption study. *Microporous and Mesoporous Materials,* 11 (2008) 404–410.

Izydorczyk, M.S., and Biliaderis, C.G. Arabinoxylans: Technologically and nutritionally functional plant polysaccharides. In *Functional food carbohydrates*, Izydorczyk, M.S., and Biliaderis, C.G., (Eds.), CRC Press: Boca Raton, 2007.

Jin, F., and Enomoto, H. Rapid and highly selective conversion of biomass into value-added products in hydrothermal conditions: chemistry of acid/base-catalysed and oxidation reactions. *Energy & Environmental Science,* 4 (2011) 382–397.

Jin, Y., Yang, G., Chen, Q., Niu, W., Lu, P., Yoneyama, Y., and Tsubaki, N. Development of dual-membrane coated Fe/SiO_2 catalyst for efficient synthesis of isoparaffins directly from syngas. *Journal of Membrane Science,* 475 (2015) 22–29.

Kao, H-M., Chang, P-C., Liao, Y-W., Lee, L-P., and Chien, C-H. Solid-state NMR characterization of the acid sites in cubic mesoporous Al-MCM-48 materials using

trimethylphosphine oxide as a P NMR probe. *Microporous and Mesoporous Materials,* 114 (2008) 352–364.

Karinen, R., Vilonen, K., and Niemela, M. Biorefining: Heterogeneously catalyzed reactions of carbohydrates for the production of furfural and hydroxymethylfurfural. *ChemSusChem,* 4 (2011) 1002–1016.

Kim, J.W., Park, S.H., Jung, J., Jeon, J-K., Ko, C.H., Jeong, K-E., and Park, Y-K. Catalytic pyrolysis of mandarin residue from the mandarin juice processing industry. *Bioresource Technology,* 136 (2013) 431–436.

Kolasinski, K.W. Surface Science: Foundations of Catalysis and Nanoscience, 3rd Edition, John Wiley & Sons, Ltd., 2012.

Kong, L., Liu, S., Yan, X., Li, Q., and He, H. Synthesis of hollow-shell MCM-48 using the ternaty surfactant templating method. *Microporous and Mesoporous Materials,* 81 (2005) 251–257.

Kosslick, H., Lischke, G., Landmesser, H., Parlitz, B., Storek, W., and Fricke, R. Acidity and catalytic behavior of substituted MCM-48. *Journal of Catalysis,* 176 (1998) 102–114.

Kusema, B.T., Hilmann, G., Mäki-Arvela, P., Willför, S., Holmbom, B., Salmi, T., and Murzin, D.Y. Selective hydrolysis of arabinogalactan into arabinose and galactose over heterogeneous catalysts. *Catalysis Letters,* 141 (2011) 408–412.

Lü, R., Tangbo, H., Wang, Q., and Xiang, S. Properties and characterization of modified HZSM-5 zeolites. *Journal of Natural Gas Chemistry,* 12 (2003) 56–62.

Mu, M., Chen, L., Liu, Y., Fang, W., and Li, Y. An efficient Fe_2O_3/HY catalyst for Friedel – Crafts acylation of m-xylene with benzoyl chloride. *RSC Advances,* 4 (2014) 36951–36958.

Negahdar, L., Delidovich, I., and Palkovits, R. Aqueous-phase hydrolysis of cellulose and hemicelluloses over molecular acidic catalysts: Insights into the kinetics and reaction mechanism. *Applied Catalysis B: Environmental*, 184 (2016) 285–298.

Oh, Y.H., Eom, I.Y., Joo, J.C., Yu, J.H., Song, B.K., Lee, S.H., Hong, S.H., and Park, S.J. Recent advances in development of biomass pretreatment technologies used in biorefinery for the production of bio-based fuels, chemicals and polymers. *Korean Journal of Chemical Engineering*, 32 (2015) 1945.

Peng, P., Wang, Y., Rood, M.J., Zhang, Z., Subhan, F., Yan, Z., Qin, L., Zhang, Z., Zhang, Z., and Gao, X. Effects of dissolution alkalinity and self-assembly on ZSM-5 based micro-/mesoporous composites: a study of the relationship between porosity, acidity, and catalytic performance. *CrystEngComm*, 17 (2015) 3820–3828.

Putro, J.N., Soetaredjo, F.E., Lin, S-Y., Ju, Y-H., and Ismadji, S. Pretreatment and conversion of lignocellulose biomass into valuable chemicals. *RSC Advances*, 6 (2016) 46834–46852.

Rachel-Tang, D.Y., Islam, A., and Taufiq-Yap, Y.H. Bio-oil production via catalytic solvolysis of biomass. *RSC Advances*, 7 (2017) 7820.

Romero, A., Alonso, E., Sastre, Á., and Nieto-Márquez, A. Conversion of biomass into sorbitol: cellulose hydrolysis on MCM-48 and D-glucose hydrogenation on Ru/MCM-48. *Microporous and Mesoporous Materials*, 224 (2016) 1–8.

Sahu, R., and Dhepe, P.L. A one-pot method for the selective conversion of hemicellulose from crop waste into C5 sugars and furfural by using solid acid catalysts. *ChemSusChem*, 5 (2012) 751–761.

Sánchez-Bastardo, N., Romero, A., and Alonso, E. Extraction of arabinoxylans from wheat bran using hydrothermal processes assisted by heterogeneous catalysts. *Carbohydrate Polymers,* 160 (2017) 143–152.

Saxena, S.K., Viswanadham, N., and Garg, M.O. Cracking and isomerization functionalities of bi-metallic zeolites for naphtha value upgradation. *Fuel,* 107 (2013) 432–438.

Schmidt, W. Chapter 4 – Microporous and Mesoporous Catalysts. In *Surface and Nanomolecular Catalysis*, Richards, R., (Ed.), CRC Press: Boca Raton, 2006.

Schumacher, K., Ravikovitch, P.I., Chesne, A.D., Neimark, A.V., and Unger, K.K. Characterization of MCM-48 Materials. *Langmuir,* 16 (2000) 4648–4654.

Shafaghat, H., Rezaei, P.S., and Daud, W.M.A.W. Catalytic hydrogenation of phenol, cresol and guaiacol over physically mixed catalysts of Pd/C and zeolite solid acids. *RSC Advances*, 5 (2015) 33990–33998.

Sluiter, A., Hames, B., Ruiz, R., Scarlata, C., Sluiter, J., and Templeton, D. Determination of sugars, byproducts, and degradation products in liquid fraction process samples. Laboratory Analytical Procedure (LAP). Technical Report NREL/TP-510-42623, 2008.

Steen, E.V., Callanan, L.H., and Claeys, M. Volume 154C – Recent advances in the science and technology of zeolites and related materials. In *Studies in Surface Science and Catalysis*, 1st Edition, Elsevier Science, 2004.

Tsilomelekis, G., Orella, M.J., Lin, Z., Cheng, Z., Zheng, W., Nikolakis, V., and Vlachos, D.G. Molecular structure, morphology and growth mechanisms and rates of 5-hydroxymethyl furfural (HMF) derived humins. *Green Chemistry*, 18 (2016) 1983–1993.

Vilcocq, L., Castilho, P.C., Carvalheiro, F., and Duarte, L.C. Hydrolysis of oligosaccharides over solid acid catalysts: A review. *ChemSusChem*, 7 (2014) 1010–1019.

Watanabe, M., Aizawa, Y., Iida, T., Levy, C., Aida, T.M., and Inomata, H. Glucose reactions within the heating period and the effect of heating rate on the reactions in hot compressed water. *Carbohydrate Research*, 340 (2005) 1931–1939.

Xia, Y., Yang, Z., and Mokaya, R. Templated nanoscale porous carbons. *Nanoscale*, 2 (2010) 539–659.

Xie, J., Cheng, L., Wang, W-H., Wang, P., Au, C-T., and Ying, S-F. Direct dual-template synthesis of HZSM-5 zeolite for enhanced pxylene selectivity in toluene methylation with CH_3Br. *Catalysis Science and Technology*, 7 (2017) 1211–1216.

Xue, P., Lu, G., Guo, Y., Wang, Y., and Guo, Y. A novel support of MCM-48 molecular sieve for immobilization of penicillin G acylase. *Journal of Molecular Catalysis B: Enzymatic*, 30 (2004) 75–81.

Zhou, L., Liu, Z., Bai, Y., Lu, T., Yang, X., and Xu, J. Hydrolysis of cellobiose catalyzed by zeolites – the role of acidity and micropore structure. *Journal of Energy Chemistry*, 25 (2016) 141–145.

CHAPTER IV

HYDROGENATION KINETICS OF SUGAR MODEL MIXTURES OVER RUTHENIUM CATALYSTS SUPPORTED ON H-ZSM-5

Abstract

The hydrogenation of sugar model mixtures over ruthenium catalysts supported on H-ZSM-5 zeolites was investigated. The reaction is one important step of the transformation of naturally occurring hemicellulose arabinoxylans into valuable sugar alcohols. The effects of SiO_2/Al_2O_3 ratio of the catalyst support, reaction temperature and catalyst loading were examined. The SiO_2/Al_2O_3 ratio of H-ZSM-5 played a crucial role in the hydrogenation of sugars. Ru/H-ZSM-5 (80) exhibited a better catalytic activity than Ru/H-ZSM-5 (23), since a low acidic support promotes hydrogenation over secondary reaction pathways. The experimental results showed that xylose and arabinose were more readily hydrogenated than glucose. Indeed, the optimum yield of sorbitol was achieved at higher reaction temperature and higher catalyst loading than the optimum yield of xylitol and arabitol. Total conversion of xylose and arabinose was reached at 100 ºC with a metal loading of 0.015 g Ru·g C^{-1}. In contrast, glucose required a temperature of 120 ºC for the same metal loading to get a near total conversion. Additionally, a pseudo-first order kinetic model was used to reproduce the experimental data, being the R^2 always higher than 0.950.

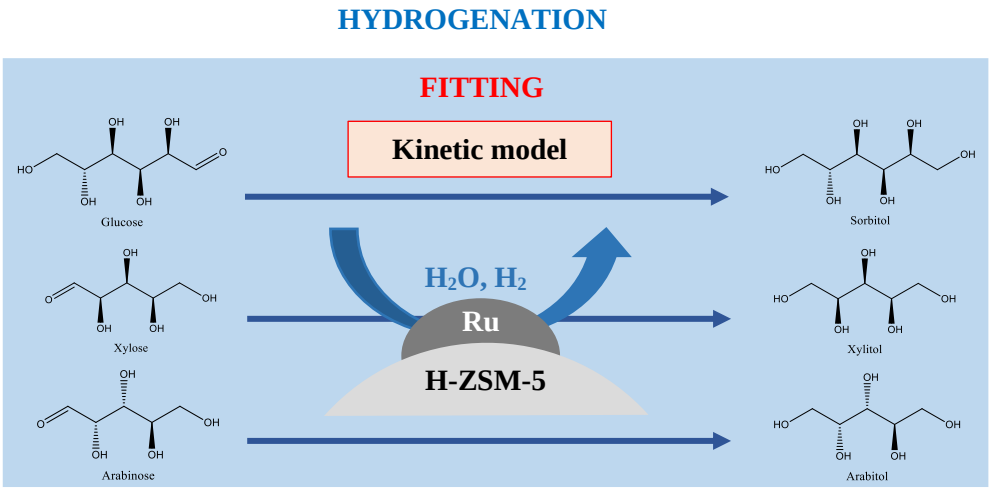

1. Introduction

The need to seek renewable alternatives to fossil resources has become an important issue in the last decades (Baudel et al., 2005; Hara et al., 2015; Putro et al., 2016). Fossil resources are limited, and their current depletion is forcing society to develop processes for chemicals and fuels production from sustainable raw materials (McKendry, 2002). In this context, cellulose and hemicelluloses from biomass can be isolated and transformed into C_6 and C_5 sugars, respectively (Chareonlimkun et al., 2010). These sugars are platform chemicals which can be converted into valuable products (Deng et al., 2015; Müller et al., 2017; Serrano-Ruiz et al., 2011). For instance, sugar alcohols, *i.e.* sorbitol, xylitol and arabitol, are building blocks susceptible to be produced from biomass carbohydrates (Werpy and Petersen, 2004). Sugar alcohols have important applications as sweeteners, food additives or anti-inflammatory agents. They are also precursors of chemicals used in the pharma and cosmetic industry (Besson et al., 2014; De Albuquerque et al., 2014; Koganti and Ju, 2013; Müller et al., 2017).

Sugar alcohols can be produced by chemical (Zada et al., 2017) and biological (Dasgupta et al., 2017; Rao et al., 2016) processes. Biological processes occur under milder conditions, but chemical production, *i.e.* catalytic hydrogenation of sugars, is preferred on an industrial scale. A high yield, a high conversion efficiency and an economic large-scale production make chemical processes more attractive industrially (Dasgupta et al., 2017). In addition to this, the catalytic hydrogenation is an environmentally friendly process. The reaction takes place in an aqueous solution over a solid metal catalyst and under hydrogen pressure. No reducing agents are needed and thus the formation of inorganic salts as waste products is avoided (Yadav et al., 2012).

The hydrogenation of sugars has been traditionally carried out over Raney nickel catalysts or nickel supported catalysts (Gallezot et al., 1994; Jividen et al., 1978; Kusserow et al.,

2003; Ribeiro et al., 2017; Schimpf et al., 2007; Wisniak et al., 1974a). Nickel catalysts have a relatively low price and a good activity and selectivity (Mikkola and Salmi, 2001; Wisniak et al., 1974a, 1974b). In contrast, they are fast deactivated due to the deposition of impurities on the catalyst surface (Kusserow et al., 2003; Yadav et al., 2012) and metal leaching (Gallezot et al., 1998; Kusserow et al., 2003; Schimpf et al., 2007; Yadav et al., 2012). During the last years, catalysts based on different metals, such as platinum (Fukuoka and Dhepe, 2006; Guha et al., 2011; Käldström et al., 2011; Kobayashi et al., 2014; Ribeiro et al., 2017; Tathod and Dhepe, 2015; Tathod et al., 2014), palladium or rhodium (Ribeiro et al., 2017) have been studied in the catalytic conversion of sugars into sugars alcohols. However, ruthenium is the most used metal in hydrogenation of sugars, as demonstrated by the huge amount of publications (Aho et al., 2015; Baudel et al., 2005; Dietrich et al., 2017; Ennaert et al., 2016; Faba et al., 2014; Fukuoka and Dhepe, 2006; Geboers et al., 2011; Guha et al., 2011; Guo et al., 2014; Hernández-Mejia et al., 2016; Herrera et al., 2012; Käldström et al., 2011; Kusema et al., 2012; Kusserow et al., 2003; Mishra et al., 2013, 2014; Murzin et al., 2015a, 2015b; Ribeiro et al., 2016, 2017; Romero et al., 2016; Yadav et al., 2012; Yi and Zhang, 2012). Ruthenium is more efficient than other metal catalysts in terms of activity and selectivity under similar conditions (Baudel et al., 2005). Moreover, ruthenium catalysts are more resistant to deactivation (Yadav et al., 2012). All this converted ruthenium catalysts to the preferred option for hydrogenation reactions. Ribeiro et al. (2017) examined the effect of several metals (Rh, Ru, Pt, Pd, Ni) supported on carbon nanotubes in the hydrogenation of corncob xylan to xylitol. The yield of xylitol over Ru/CNT was ~40%. Under the same experimental conditions, the yield was ~10% over Pt/CNT and only ~5% over Rh, Pd and Ni supported on CNT. Therefore, Ru/CNT was clearly the most effective catalyst for the formation of xylitol. Guha et al. (2011) tested platinum and ruthenium catalysts in the hydrogenation

of sugars from beet fiber. They obtained similar results over Pt/γ-Al_2O_3 and Ru/γ-Al_2O_3 at 130 °C. Nevertheless, the amount of Pt/γ-Al_2O_3 required was twice than that of Ru/γ-Al_2O_3 to achieve the same yield. Thus, ruthenium showed again a higher catalytic activity than platinum. Wisniak et al. (1974b) also studied the influence of different metals on the hydrogenation of xylose and reported that the activity decreased in the order Ru > Ni > Rh > Pd. As evidenced by all these results and despite of its high price, ruthenium seems to be the best choice for the hydrogenation of sugars into sugar alcohols.

The structure and properties of the catalyst support may also play an important role (Romero et al., 2016). Different materials have been used as metal supports: Al_2O_3 (Guha et al., 2011; Tathod and Dhepe, 2015; Tathod et al., 2014), carbon (Aho et al., 2015; Dietrich et al., 2017; Guha et al., 2011; Herrera et al., 2012; Kobayashi et al., 2014; Murzin et al., 2015b; Ribeiro et al., 2016, 2017; Yi and Zhang, 2012), TiO_2 (Hernández-Mejia et al., 2016; Yadav et al., 2012) and MCM-48 (Käldström et al., 2011; Kusema et al., 2012; Romero et al., 2016). Likewise, zeolites, such as beta (Faba et al., 2014), H-Y (Ennaert et al., 2016; Fukuoka and Dhepe, 2006; Geboers et al., 2011; Mishra et al., 2013, 2014; Murzin et al., 2015a) or H-ZSM-5 (Guo et al., 2014), have also demonstrated to be suitable supports for hydrogenation metal catalysts. Table 1 shows some results on hydrogenation of sugars over different ruthenium catalysts obtained in previous works. Mishra et al. (2014) compared the activity of several ruthenium catalysts impregnated on different supports (HY, NiO-TiO_2, TiO_2, C) on glucose hydrogenation. They demonstrated that Ru/HY was the most active catalyst of all the tested, achieving a sorbitol yield of 98% after 20 minutes at 120 ºC and 55 bar H_2 pressure. In another work, same authors studied thoroughly the hydrogenation of xylose over ruthenium supported on HY zeolites with different Si/Al ratio (5.1, 5.2, 30, 60, 80) (Mishra et al., 2013). They observed that the catalyst support played an important role, since an increase in Si/Al

ratio led to a higher conversion of xylose and higher selectivity to xylitol. They also studied the influence of temperature, stirring rate and catalyst amount and carried out kinetics studies of xylose hydrogenation over Ru/HY (80). Guo et al. (2014) investigated the hydrogenation of glucose over Ru/ZSM-5 catalysts prepared by different methods. ZSM-5 zeolites resulted to be a good option as catalyst supports in glucose hydrogenation. A sorbitol yield above 95% was reached over a ruthenium catalyst supported on a commercial zeolite with a Si/Al ratio of 38. However, this study did not consider the influence of other Si/Al ratio or time. Thus, a detailed investigation on sugars hydrogenation should be implemented using Ru/ZSM-5, since it already demonstrated to be a promising catalyst in glucose hydrogenation.

Many works are based on the hydrogenation of a single sugar (Aho et al., 2015; Hernández-Mejia et al., 2016; Kusserow et al., 2003; Mikkola and Salmi, 2001; Mikkola et al., 1999, 2000; Mishra et al., 2013; Schimpf et al., 2007; Wisniak et al., 1974a, 1974b; Yadav et al., 2012). Nevertheless, the hydrolysates obtained from biomass are composed of several sugars, mainly xylose, arabinose and glucose. The proportion of each sugar is determined by the experimental conditions applied during the fractionation and hydrolysis of the biomass. For instance, the main sugars of hemicellulosic hydrolysates are xylose and arabinose, although a smaller amount of glucose is always present (Sánchez-Bastardo and Alonso, 2017). Therefore, it is important to study the hydrogenation of sugar mixtures to approach a more real process and have a more comprehensive understanding.

Table 1. Hydrogenation of sugars over ruthenium catalysts on different supports.

Raw material	Catalyst	Hydrogenation conditions	Sorbitol yield (%)	Xylitol yield (%)	Reference
Glucose	Ru(1)/HY (80)	120 ºC, 20 min, 55 bar H_2	98	-	(Mishra et al., 2014)
Glucose	Ru(1)/NiO-TiO_2	120 ºC, 20 min, 55 bar H_2	96	-	
Glucose	Ru(1)/TiO_2	120 ºC, 20 min, 55 bar H_2	93	-	
Glucose	Ru(5)/C	120 ºC, 20 min, 55 bar H_2	93	-	
Glucose	Ru(4)/MCM-48	120 ºC, 25 min, 25 bar H_2	90	-	(Romero et al., 2016)
Glucose	Ru(4)/TiO_2	120 ºC, 20 min, 25 bar H_2	91	-	
Glucose	Ru(5)/C	120 ºC, 10 min, 25 bar H_2	95	-	
Glucose	Ru/ZSM-5	120 ºC, 2 h, 40 bar H_2	96	-	(Guo et al., 2014)
Xylose	Ru(1)/TiO_2	120 ºC, 3 h, 20 bar H_2	-	93	(Hernández-Mejia et al., 2016)
Xylose	Ru(1)/C	120 ºC, 2 h, 55 bar H_2	-	98	(Yadav et al., 2012)
Xylose	Ru(1)/TiO_2	120 ºC, 2 h, 55 bar H_2	-	99	
Xylose	Ru(1)/NiO(5)-TiO_2	120 ºC, 2 h, 55 bar H_2	-	100	
Xylose	Ru(1)/HY (5.1)	120 ºC, 1 h, 55 bar H_2	-	68	(Mishra et al., 2013)
Xylose	Ru(1)/HY (5.2)	120 ºC, 1 h, 55 bar H_2	-	70	
Xylose	Ru(1)/HY (30)	120 ºC, 1 h, 55 bar H_2	-	86	
Xylose	Ru(1)/HY (60)	120 ºC, 1 h, 55 bar H_2	-	94	
Xylose	Ru(1)/HY (80)	120 ºC, 1 h, 55 bar H_2	-	98	

In this work, the hydrogenation of sugar model mixtures composed of xylose, arabinose and glucose were studied. These mixtures reproduced the sugar composition of hemicellulosic hydrolysates obtained from wheat bran in a previous work (Sánchez-Bastardo and Alonso, 2017). Ruthenium supported catalysts on H-ZSM-5 zeolites with different Si/Al ratios were investigated in this work. These catalysts demonstrated to be a good option for the hydrogenation of glucose into sorbitol as reported previously (Guo et al., 2014). However, no works were found on hydrogenation of C_5 sugars over Ru/H-ZSM-5. To our knowledge, this is the first time in which ruthenium catalysts supported on H-ZSM-5 zeolites are used in the simultaneous hydrogenation of several sugars. The

effects of temperature and catalyst loading were also examined. In addition to this, the modelling of the experimental data was carried out. A deep study of the hydrogenation of sugar model mixtures is crucial to implement the subsequent hydrogenation of a real biomass hydrolysate.

2. Experimental

2.1 Chemicals

D-xylose (≥ 99%), L-arabinose (≥ 99%) and D-glucose (≥ 99.5%) were provided by Sigma Aldrich. Analytical standards used for HPLC purposes (D-fructose (≥ 99%), 5-(hydroxymethyl)furfural (≥ 99%), furfural (≥ 99%), DL-glyceraldehyde (≥ 90%), glycolaldehyde (≥ 99%), formic acid (≥ 98%), xylitol (≥ 99%), L-arabitol (≥ 98%), D-sorbitol (≥ 98%), glycerol (≥ 99%), ethylene glycol (≥ 99.5%), propylene glycol (≥ 99%) and furfuryl alcohol (≥ 98%)) were also purchased from Sigma Aldrich.

The zeolites used as catalyst supports were supplied by Zeolyst International. Two different zeolites were compared: ZSM-5 (23) (CBV 2314, SiO_2/Al_2O_3 = 23) and ZSM-5 (80) (CBV 8014, SiO_2/Al_2O_3 = 80). All of them were in an initial ammonium form and were used after calcination. The ruthenium precursor was ruthenium (III) chloride supplied by Strem Chemicals Inc.

Nitrogen (99.99 %) and hydrogen (99.99 %) from Carburos Metálicos were used for hydrogenation experiments.

2.2 Catalyst preparation

Zeolites were purchased in ammonium form. They were used as catalyst supports in H^+ form. The protonation to obtain H-zeolites was done by calcination at 550 ºC for 5 hours increasing the temperature from 80 to 550 ºC at a heating rate of 5 ºC·min^{-1} (in general, $Z\text{-}NH_4^+ \rightarrow Z\text{-}H^+ + NH_3\uparrow$) (Schmidt, 2006).

Ruthenium catalysts were prepared by wetness impregnation method (Romero et al., 2016). The ruthenium precursor ($RuCl_3$) and the corresponding support were placed separately into two glasses with water and sonicated for 10 minutes. They were then mixed and sonicated for another 10 minutes. The final suspension was heated up from 30 to 80 °C at a rate of 1 °C·min^{-1}. When the water was visibly evaporated, the catalyst was finally dried at 105 °C overnight. Prior to hydrogenation, ruthenium catalyst was reduced at 150 °C for 1 hour under a hydrogen flow at a rate of 2 NL·min^{-1}. This reduction temperature was previously determined by Temperature Programmed Reduction (TPR) for similar catalysts (Romero et al., 2016).

2.3 Catalyst characterization

2.3.1 X-Ray Diffraction (XRD)

X-Ray Diffraction (XRD) analysis of the supports and ruthenium catalysts was performed on a Bruker Discover D8 diffractometer using Cu Kα radiation (λ = 0.15406 nm). The diffraction intensities were measured over an angle range of $2º < 2\theta < 90º$. A step size of 0.020º and a step time of 0.80 s were applied.

2.3.2 Nitrogen adsorption-desorption isotherms

Nitrogen adsorption-desorption isotherms were performed with ASAP 2020 (Micromeritics, USA) to determine the surface area, the total pore volume (V_{pore}) and the average pore size (d_{pore}) of the catalysts. Samples were outgassed at 350 ºC overnight prior to analysis. The Langmuir model was applied to calculate the surface area. The Horvath-Kawazoe method was used to determine the total pore volume (from N_2 uptake at $P/P_0 \geq 0.99$) and the average pore size of the catalysts.

2.3.3 Inductively Coupled Plasma-Atomic Emission Spectrometry (ICP-AES)

The metal loading of ruthenium catalysts was determined by Inductively Coupled Plasma-Atomic Emission Spectrometry (ICP-AES) (Varian Liberty RL sequential ICP-AES) after a digestion of the sample.

2.3.4 Acidity

The acidity of ruthenium catalysts was measured by titration with NaOH. This method is based on procedures already reported by several authors (H. Hu et al., 2016; L. Hu et al., 2015; Liu et al., 2013; Wang et al., 2011; Zheng et al., 2014).

2.4 Catalytic hydrogenation of sugars

A commercial stainless-steel high-pressure reactor (Berghoff® BR-25) was used for the hydrogenation experiments. In a typical experiment, the reactor was loaded with the catalyst and flushed first with nitrogen to remove the oxygen and then filled with hydrogen. The reactor was then pressurized at 40 bar of hydrogen at room temperature. Thereafter, the reactor was heated up to the operating temperature. When the desired temperature was reached, 10 mL of the sugar mixture were pumped (PU-2080 Plus, Jasco) into the reactor and stirred at 1400 rpm during the reaction. After pumping, the pressure was adjusted to 50 bar by opening the outlet valve. This moment was considered as the starting time reaction. At the end of the experiment, the reactor was rapidly quenched and the pressure released. The product was finally filtered to separate the liquid from the solid catalyst. The liquid was further used to determine its composition after the reaction.

2.5 Liquid phase analyses

The reaction products were analyzed by High Performance Liquid Chromatography (HPLC). Prior to analysis, the samples were filtered through a nylon syringe filter (pore size 0.22 μm, FILTER-LAB). The chromatography system consisted of an isocratic pump (Waters 1515), an automatic injector (Waters 717) and two detectors (RI detector, Waters

2414 and UV-Vis detector, Waters 2487), supplied by Waters Corporation. Three HPLC columns were used for the determination of the different compounds: Supelcogel Pb (Supelco), SH1011 (Shodex) and SC1211 (Shodex). Table 2 summarizes the products identified with each column and the operating conditions.

Table 2. Operating conditions of the different HPLC columns used in this work.

Parameter	HPLC Column		
	Supelcogel Pb	SH1011	SC1211
Compounds analyzed	Sugars	Degradation products	Sugar alcohols
Furnace temperature (°C)	85	50	90
Detector temperature (°C)	35	35	35
Mobile phase	Milli-Q water	H_2SO_4 0.01 N in Milli-Q water	H_2O/CH_3CN (65/35 v/v)
Flow rate (mL min^{-1})	0.5	0.8	0.5
Detector	IR	IR and UV-Vis (254 nm for 5-HMF and 260 nm for furfural)	IR

The conversion of sugars, the yield and selectivity into the corresponding sugar alcohols were calculated according to the following equations (Eq. 1 – 7):

$$\% \text{ Sugar conversion} = \frac{n_{sugar,0} - n_{sugar,f}}{n_{sugar,0}} \times 100 \quad \text{(Eq. 1)}$$

$$\% \text{ Xylitol yield} = \frac{n_{xylitol,f}}{n_{xylose,0}} \times 100 \quad \text{(Eq. 2)}$$

$$\% \text{ Xylitol selectivity} = \frac{n_{xylitol,f}}{n_{xylose,0} - n_{xylose,f}} \times 100 \quad \text{(Eq. 3)}$$

$$\% \text{ Arabitol yield} = \frac{n_{arabitol,f}}{n_{arabinose,0}} \times 100 \quad \text{(Eq. 4)}$$

$$\% \text{ Arabitol selectivity} = \frac{n_{arabitol,f}}{n_{arabinose,0} - n_{arabinose,f}} \times 100 \quad \text{(Eq. 5)}$$

$$\% \text{ Sorbitol yield} = \frac{n_{sorbitol,f}}{n_{glucose,0}} \times 100 \quad \text{(Eq. 6)}$$

$$\% \text{ Sorbitol selectivity} = \frac{n_{sorbitol,f}}{n_{glucose,0} - n_{glucose,f}} \times 100 \quad \text{(Eq. 7)}$$

3. Results and discussion

3.1 Catalyst characterization

Figures 1A and 1B show XRD patterns of the calcined zeolites H-ZSM-5 (23) and H-ZSM-5 (80), respectively, and the corresponding ruthenium supported catalysts. H-ZSM-5 zeolites exhibit well-resolved diffraction peaks at 2θ = 8 – 9º, 23 – 25º, and 45º (JCPDS Card no. 00-037-0359), which are characteristic of a typical MFI structure (Dong et al., 2017; Guo et al., 2014; Jin et al., 2015; Rachel-Tang et al., 2017). A distinctive metallic diffraction peak is observed at 2θ = 44.0º in Ru/H-ZSM-5 catalysts, indicating the presence of Hexagonal Close Packing (HCP) Ru^0 particles. Moreover, an additional peak at 2θ = 42.1º can be distinguished in Ru/H-ZSM-5 samples. The rest of the diffraction peaks corresponding to Ru^0 are not observed. This may be attributed to the high crystallinity of zeolites, which was not significantly affected after the metal incorporation, and to the low percent loading of ruthenium (Mishra et al., 2013, 2014).

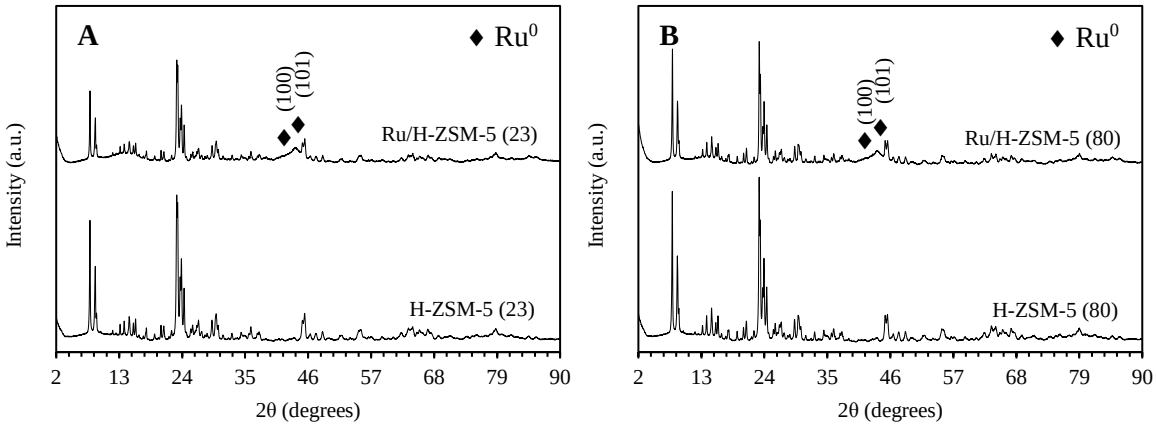

Figure 1. XRD paterns of A) H-ZSM-5 (23) and Ru/H-ZSM-5 (23) and B) H-ZSM-5 (80) and Ru/H-ZSM-5 (80).

Nitrogen adsorption-desorption isotherms of ruthenium catalysts at -196 ºC are represented in Figure 2. Ruthenium catalysts supported on H-ZSM-5 show type I isotherms, characteristic of microporous materials. The steep uptake of nitrogen in the

low relative pressure range ($P/P_0 < 0.01$) is associated to the filling of ultramicropores with a width of two-three molecular diameters, which is governed by the gas – solid interactions (Cychosz et al., 2017). The pore filling process of supermicroporous takes place in the range of relative pressure $P/P_0 = 0.01 – 0.15$ (Cychosz et al., 2017) and the rise observed at $P/P_0 > 0.95$ is related to nitrogen condensation in the void volume between the particles (Fu et al., 2016). Both ruthenium catalysts display slight type H4 hysteresis loops (ALOthoman, 2012). This kind of hysteresis is often associated with narrow slit-like pores, but in the case of type I isotherms is indicative of a microporous structure with a low contribution of mesopores (Beyer et al., 1995; Cychosz et al., 2017; Fu et al., 2016; Lü et al., 2003; Peng et al., 2015). However, the pore size distribution (PSD) (Figures 3A, B) of the ruthenium catalysts supported on zeolites can be considered a unimodal microporous distribution, and only a very low mesoporosity is observed in the enlarged graphs. Therefore, the small hysteresis loop and the narrow pore size distribution imply that zeolites are characterized mainly by a microporous structure. The PSD of Ru/H-ZSM-5 (23) and Ru/H-ZSM-5 (80) presents a maximum at 0.69 and 0.67, respectively.

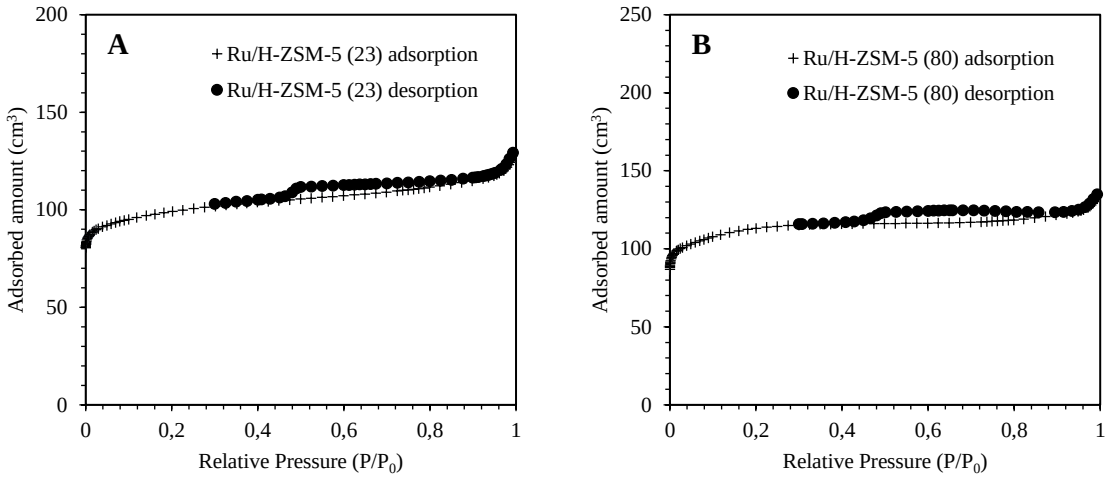

Figure 2. Nitrogen adsorption-desorption isotherms of A) Ru/H-ZSM-5 (23) and B) Ru/H-ZSM-5 (80).

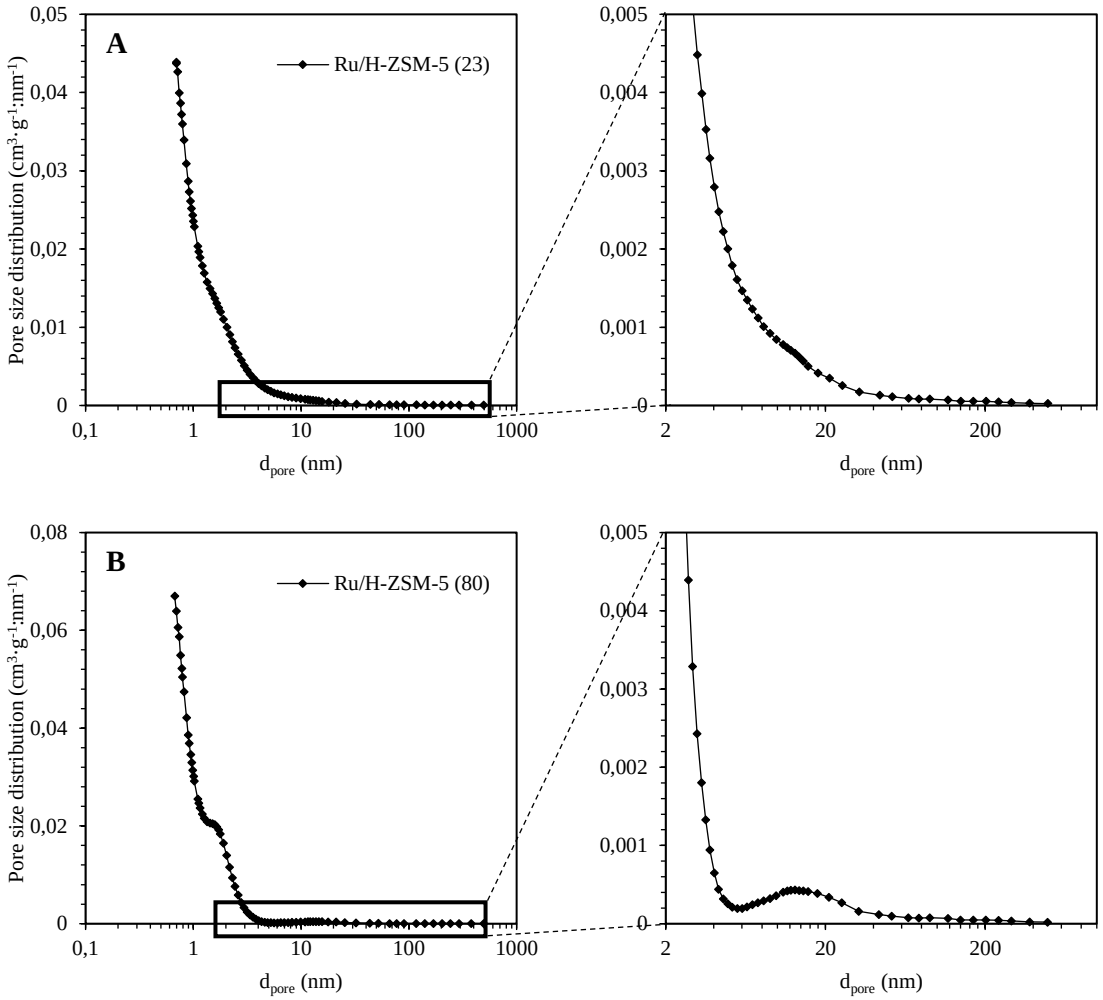

Figure 3. Pore size distributions (PSD) of A) Ru/H-ZSM-5 (23) and B) Ru/H-ZSM-5 (80).

The properties of the reduced ruthenium catalysts and their corresponding supports are summarized in Table 3. The textural properties of the catalysts undergo similar changes after the incorporation of the ruthenium precursor and the subsequent reduction to obtain metallic particles of Ru^0. The specific surface area and total pore volume are slightly lower in the metal catalysts than in their respective supports. This is associated to the shrinkage and blockage of the pore system after the metal deposition (Romero et al., 2016). Unlike the specific surface area and pore volume, the pore diameter is very similar in ruthenium catalysts and their corresponding supports, indicating a good preservation of the pore structure after the metal loading.

The acidity was determined in the reduced ruthenium catalysts. The acidity of Ru/H-ZSM-5 (23) was higher than that of Ru/H-ZSM-5 (80), as expected due to the greater aluminum content of the support H-ZSM-5 (23) (Al-Dughaither and De Lasa, 2014; Gao et al., 2016; Kim et al., 2013).

Table 3. Properties of ruthenium catalysts and their corresponding supports.

Catalyst	Ru (wt.%)[a]	SiO_2/Al_2O_3 (mol·mol^{-1})	Surface area (m^2·g^{-1})[b]	V_{pore} (cm^3·g^{-1})[c]	d_{pore} (nm)[c]	Acidity (mEq H^+·g cat^{-1})[d]
H-ZSM-5 (23)	-	23	483	0.21	0.68	-
Ru/H-ZSM-5 (23)	1.9	23	446	0.20	0.69	0.715
H-ZSM-5 (80)	-	80	562	0.26	0.67	-
Ru/H-ZSM-5 (80)	2.0	80	515	0.21	0.67	0.552

[a] Determined by ICP-AES.
[b] Determined by Langmuir model.
[c] Determined by Horvath-Kawazoe method.
[d] Determined by titration with NaOH.

3.2 Catalytic hydrogenation of sugars mixtures

The influence of different parameters (catalyst support, temperature, catalyst loading) was evaluated on the hydrogenation of sugar model mixtures composed of xylose (6 g·L^{-1}), arabinose (3 g·L^{-1}) and glucose (1.7 g·L^{-1}). These mixtures imitated the sugar composition of wheat bran hydrolysates obtained after fractionation and hydrolysis processes in our previous works (Sánchez-Bastardo and Alonso, 2017; Sánchez-Bastardo et al., 2017).

3.2.1 Influence of catalyst support

The performance of ruthenium catalysts supported on H-ZSM-5 zeolites with different SiO_2/Al_2O_3 ratio was compared in the hydrogenation of sugar model mixtures (Table 4). The experimental results showed that a change in SiO_2/Al_2O_3 ratio of H-ZSM-5 had a significant effect on the catalytic activity of the ruthenium catalyst. Under identical reaction conditions, the conversion of sugars and the selectivity into the corresponding sugar alcohols were remarkably higher over Ru/H-ZSM-5 (80) than over Ru/H-ZSM-5 (23). In order to assess the reasons behind this change in selectivity and conversion, we

examined each individual mass transfer process involved to explain these results: a) mass transfer between the gas phase and the liquid-hydrogen solubility, b) mass transfer between the liquid and the solid and c) adsorption-internal diffusion and reaction. Since the system was well mixed and hydrogen was fed in excess, the mass transfer coefficient between the gas and the liquid phase would be so high that the hydrogen concentration in the liquid can be assumed to be constant and equal to the hydrogen solubility at the operating conditions. This statement was mathematically checked by Mikkola et al. (1999). In addition to this, the mass transfer resistance between the liquid and the solid can be also considered negligible due to the high stirring rate of the reaction mixture, as demonstrated by the preliminary tests at different stirring rates (results not shown). Finally, since the particle size of ZSM-5 zeolites is quite low (< 2 μm) (Groen et al., 2007), the Thiele modulus calculation would lead to an effectiveness factor near 1 and the internal diffusional resistance could be also neglected (Mikkola et al., 2001). For the same reason, the reactants would be only adsorbed on the metal active sites, which means that the support would not affect the equilibrium adsorption. From the previous discussion, it can be concluded that the support does not influence the mass transfer but the reaction mechanism. Indeed, the acidity of the catalyst support has already demonstrated to play a crucial role in the reaction pathway and consequently in the sugar alcohols production (Mishra et al., 2013). In general, a lower SiO_2/Al_2O_3 ratio results in a higher number of acid sites (Table 3) (Al-Dughaither and De Lasa, 2014; Gao et al., 2016; Kim et al., 2013). Over highly acidic zeolites, such as H-ZSM-5 (23), xylose for instance may undergo direct hydrogenation in addition to isomerization into xylulose followed by further hydrogenation (Figure 4) (Mishra et al., 2013). Therefore, the lower selectivity into xylitol over Ru/H-ZSM-5 (23) may be attributed to the formation of xylulose as a reaction intermediate. However, the use of a moderate-low acidic zeolite as

catalyst support, such as H-ZSM-5 (80), promotes hydrogenation over isomerization, so the production of xylulose is inhibited and the selectivity into xylitol is maximum. The conversion of xylose is also lower over Ru/H-ZSM-5 (23), *i.e.* when hydrogenation and isomerization reactions occur in parallel. In this case, the metal active centers of the catalyst are used for the hydrogenation of xylose but also for the hydrogenation of xylulose obtained via isomerization. Nevertheless, all the active sites are exclusively used for xylose hydrogenation over Ru/H-ZSM-5 (80), since only hydrogenation takes place over this catalyst. As a result, a higher conversion of the sugar is obtained in the latter case. Analogous to xylose, arabinose may isomerize into ribulose (Delidovich et al., 2018) and glucose into fructose (Dabbawala et al., 2016) over highly acidic catalysts, which may produce a drop in the conversion and selectivity values of the corresponding sugar and sugar alcohols. Similar results were reported by Mishra et al. (2013). They studied the hydrogenation of xylose over ruthenium catalysts supported on H-Y zeolites with different Si/Al ratio (5.1 – 80) and reported a positive effect on the conversion of xylose and selectivity into xylitol with an increase in Si/Al ratio. They also attributed this fact to the inhibition of secondary reactions over low acidic catalysts. Dabbawala et al. (2016) observed a similar trend in the hydrogenation of glucose into sorbitol. Glucose can give rise to sorbitol via direct hydrogenation or isomerize into fructose. Fructose may be converted at the same time into sorbitol and mannitol. The direct hydrogenation into sorbitol is favored by a low acidic support, whereas the isomerization route competes with the hydrogenation reaction over a highly acidic catalyst support. This fact was evidenced by our results, since a small amount of fructose and mannitol was formed over Ru/H-ZSM-5 (23) but not over Ru/H-ZSM-5 (80). Regarding the hydrogenation of arabinose, the selectivity into arabitol was ~90% over Ru/H-ZSM-5 (23). The rest of the

products was not identified but probably corresponded to the isomeric sugar of arabinose (*i.e.* ribulose) (Delidovich et al., 2018).

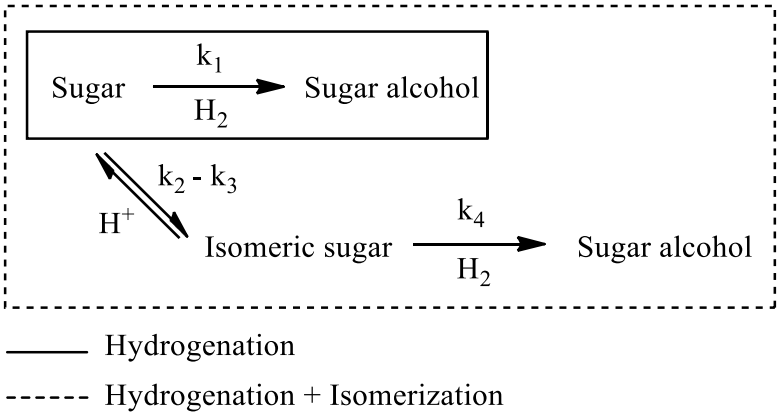

Figure 4. Hydrogenation of sugars with possible side reactions.

The higher conversion of sugars and selectivity into sugar alcohols over low acidic catalysts can be explained mathematically by kinetic equations. Eq. 8 describes the reaction rate of sugars hydrogenation when no side reactions occur, whereas Eq. 9 and 10 are the rate equations corresponding to the behavior of the sugars and their isomers, respectively, when both reactions (hydrogenation and isomerization) happen at the same time:

$$\frac{dC_{sugar}}{dt} = -k_1 \cdot f_{sugar} \cdot C_{sugar} \quad \text{(Eq. 8)}$$

$$\frac{dC_{sugar}}{dt} = -k_1 \cdot f_{sugar} \cdot C_{sugar} - (k_2 - k_3) \cdot C_{sugar} \quad \text{(Eq. 9)}$$

$$\frac{dC_{isomeric\ sugar}}{dt} = (k_2 - k_3) \cdot C_{sugar} - k_4 \cdot (1 - f_{sugar}) \cdot C_{isomeric\ sugar} \quad \text{(Eq. 10)}$$

As mentioned before, a low acidic catalyst favors hydrogenation over isomerization (Eq. 8). However, hydrogenation and isomerization reactions occur in parallel when the acidity of the catalyst is higher (Eq. 9 and 10). We have defined a f_{sugar} factor, which is the fraction of metal active sites available for sugars hydrogenation. Therefore, the term $1 - f_{sugar}$ corresponds to the fraction of metal active sites available for the hydrogenation

of the isomeric sugars. Isomerization is slower than hydrogenation (Delidovich et al., 2018), so the term $(k_2 - k_3)\cdot C_{sugar}$ of Eq. 9 is small compared to the term $k_1 \cdot f_{sugar} \cdot C_{sugar}$. In addition to this, f_{sugar} is a factor between 0 – 1, which is equal to 1 only when the hydrogenation of the sugars (not isomeric sugars) takes place (Eq. 8). In Eq. 9, this factor is lower than 1, since a part of the active sites is used for sugars hydrogenation and the other part for the hydrogenation of isomeric sugars. Therefore, the term $-k_1 \cdot f_{sugar} \cdot C_{sugar}$ of Eq. 9 is smaller than $-k_1 \cdot f_{sugar} \cdot C_{sugar}$ of Eq. 8, resulting in a lower sugar conversion when hydrogenation and isomerization happen at the same time. To our knowledge, this is the first time in which a drop in the conversion of sugars in hydrogenation reactions over highly acidic catalysts is explained mathematically by rate equations.

Table 4. Effect of SiO_2/Al_2O_3 ratio of H-ZSM-5 on sugars hydrogenation catalyzed by Ru/H-ZSM-5.

Catalyst	Conversion (%)			Selectivity (%)		
	Xylose	Arabinose	Glucose	Xylitol	Arabitol	Sorbitol
Ru/H-ZSM-5 (23)	40	41	7	86	90	88
Ru/H-ZSM-5 (80)	73	70	15	> 99	> 99	> 99

Reaction conditions: initial aqueous solution = xylose (6 $g\cdot L^{-1}$) + arabinose (3 $g\cdot L^{-1}$) + glucose (1.7 $g\cdot L^{-1}$); T = 100 ºC; t = 5 min; $V_{sugars\ solution}$ = 10 mL; P (H_2) = 50 bar; g Ru·g C^{-1} = 0.015 ($m_{catalyst}$ = 33.5 mg); Ru content in catalysts = 2 wt.%.

3.2.2 Influence of reaction temperature

Ru/H-ZSM-5 (80) demonstrated a major catalytic performance in terms of conversion and selectivity and thus it was chosen for the rest of the study. The effect of reaction temperature on hydrogenation of sugars mixtures (xylose + arabinose + glucose) was examined with a catalyst loading of 0.015 g Ru·g C^{-1} in the temperature range 80 – 120 ºC between 5 and 30 minutes (Figure 5). This temperature range was chosen based on previous works. For example, Yadav et al. (2012) and Mishra et al. (2013) studied the influence of temperature on xylose hydrogenation. They observed a total conversion of

xylose at 140 ºC but a decrease in the selectivity into xylitol due to the formation of by-products. Similarly, Romero et al. (2016) reported a negative effect on sorbitol selectivity above 120 ºC as a result of thermal degradation of glucose and isomerization of sorbitol into mannitol. The formation of undesired compounds is expected to be inhibited between 80 and 120 ºC and hence, this range was selected for the catalytic experiments. Preliminary tests also confirmed that hydrogenation was not limited by mass transfer at 1400 rpm. This stirring rate was therefore fixed in all the experiments to avoid the gas – liquid mass transfer limitations. This is accordant with the reported in previous works (Mishra et al., 2014; Romero et al., 2016).

The hydrogenation of xylose and arabinose exhibited a similar trend with temperature. At 80 ºC the yield of xylitol and arabitol increased with reaction time. The yield of arabitol achieved a maximum (~80%) after 20 minutes and a plateau was observed for longer times, whereas the yield of xylitol seemed to keep increasing for times over 30 minutes. The yield into C_5 sugar alcohols improved significantly at 100 ºC: 93% and 99% were the respective yields of xylitol and arabitol after 15 minutes. At higher temperatures (120 ºC), a yield of ~91% for both xylitol and arabitol was achieved after just 5 minutes. Both yields kept slowly increasing over time, reaching values higher than 97% after 30 minutes. At 120 ºC, not a significant improvement was noticed respect to the experiments at 100 ºC for times longer than 10 minutes.

The hydrogenation of glucose showed a different behavior. Glucose was more slowly hydrogenated than C_5 sugars, and the yield of sorbitol improved with increasing temperature in all the range 80 – 120 ºC. The yield of sorbitol increased continuously over time (5 – 30 minutes) at 80 and 100 ºC: from 3% to 16% and from 15% to 67%, respectively. However, at 120 ºC the yield of sorbitol achieved a maximum of 96% after 15 minutes which was roughly kept for longer times.

Therefore, the optimum reaction temperatures for hydrogenation of xylose/arabinose and glucose were 100 ºC and 120 ºC, respectively. These results demonstrated that C_5 sugars reacted more readily than glucose. Same conclusions were reported by several authors in previous research (Elliot et al., 2004; Liu et al., 2017). No by-products were observed by HPLC and mass balances closed at > 99% in all the experiments. In addition to this, reactions with each individual component and with binary mixtures (xylose + arabinose; xylose + glucose; arabinose + glucose) were also carried out (results not shown). It was observed that xylose was only hydrogenated into xylitol, arabinose into arabitol and glucose into sorbitol and no other by-products were identified. Thus, secondary reactions pathways were discarded over Ru/H-ZSM-5 (80) under these experimental conditions and the direct hydrogenation of sugars into sugar alcohols was performed without further degradation into by-products.

The reaction conditions of hydrogenation can be tuned to hydrogenate selectively C_5 or C_5 + C_6 sugars. The structural differences between C_6 sugars and C_5 sugar alcohols are more remarkable than between C_5 and C_6 sugar alcohols. This suggests that it will be easier to recover C_5 sugar alcohols from a mixture composed of C_6 sugars/C_5 sugar alcohols than from a mixture of C_5 + C_6 sugar alcohols. Therefore, the selective hydrogenation of C_5 sugars may be interesting for further recovery purposes. In this work, we have found that the maximization of xylitol and arabitol and the minimization of sorbitol is possible at 100 ºC (10 minutes), unlike other studies in which the hydrogenation of C_5 sugars was studied at higher temperatures (Hernández-Mejia et al., 2016; Mishra et al., 2013; Yadav et al., 2012).

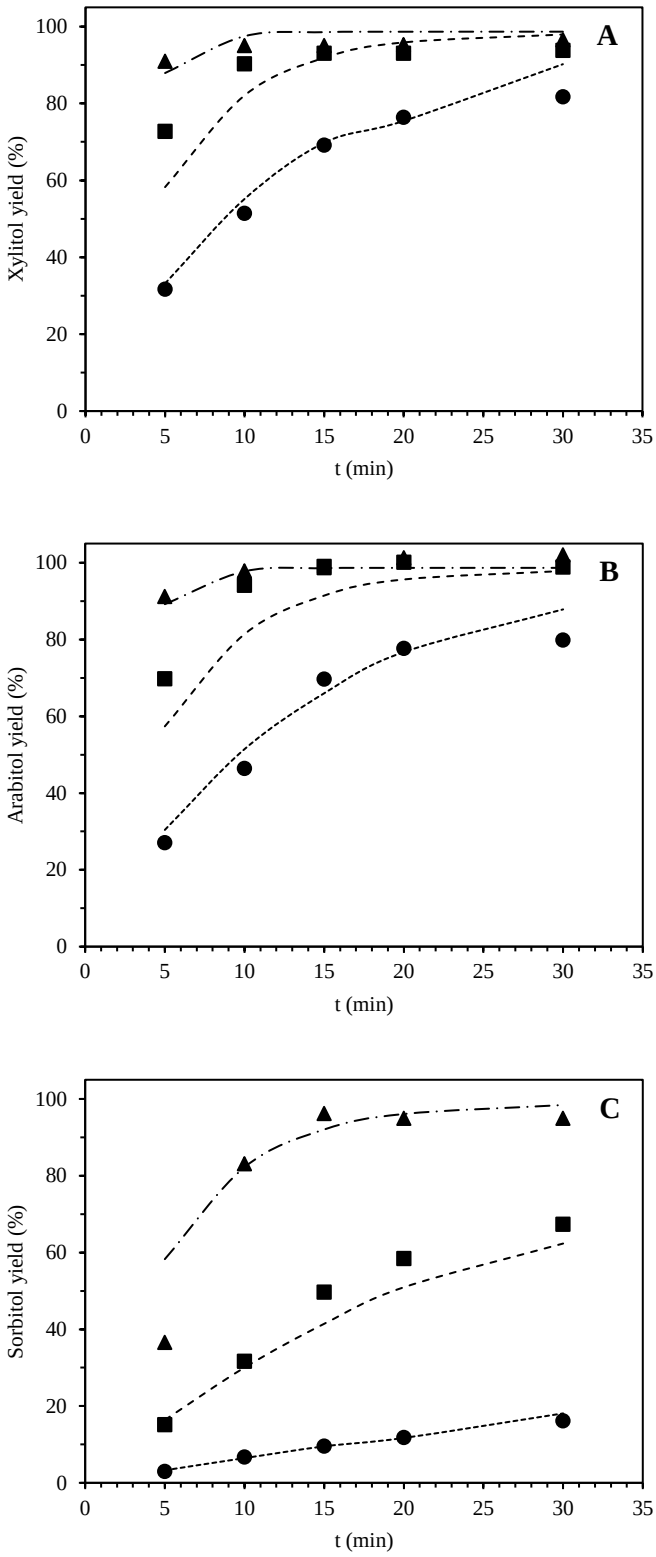

Figure 5. Effect of temperature on the yield of A) xylitol, B) arabitol and C) sorbitol. Reaction conditions: substrate = xylose (6 $g \cdot L^{-1}$) + arabinose (3 $g \cdot L^{-1}$) + glucose (1.7 $g \cdot L^{-1}$); catalyst = Ru/H-ZSM-5 (80); catalyst loading = 0.015 g $Ru \cdot g\ C^{-1}$; P (H_2) = 5 MPa. ● 80 ºC, ■ 100 ºC, ▲ 120 ºC. Simulated values are represented by lines.

3.2.3 Influence of catalyst loading

The effect of catalyst loading on sugars hydrogenation was studied at 100 ºC over time using Ru/H-ZSM-5 (80). The amount of catalyst was varied so that the grams of Ru per gram of carbon in initial sugars (g Ru·g C^{-1}) changed in the range 0 – 0.060 (Figure 6). In the blank experiments, no sugars were converted into sugar alcohols, indicating that hydrogenation is a catalytic reaction. The hydrogenation of sugars only took place when ruthenium catalyst was incorporated into the reaction. In addition to this, selectivity into sugar alcohols was above 97% for all the range of catalyst loading under the experimental conditions tested (100 ºC, 5 MPa H_2, Ru/H-ZSM-5 (80)). Thus, the values of conversion and yield were very close and only the graphs corresponding to the yield were displayed (Figure 6).

The hydrogenation of xylose and arabinose showed a similar behavior with the effect of catalyst loading. At a catalyst loading of 0.008 g Ru·g C^{-1}, a growth in the yield of both C_5 sugar alcohols was observed up to 20 minutes. The yields of xylitol and arabitol increased from 40% and 37% to 74% and 68%, respectively, between 5 and 20 minutes. A roughly plateau was obtained for longer times. A higher catalyst amount corresponding to 0.015 g Ru·g C^{-1} improved the yield of xylitol and arabitol. In this case, the maximum yields were achieved at a shorter time: after 10 minutes for xylitol (~93%) and after 15 minutes (~94%) for arabitol. By increasing the catalyst loading up to 0.030 g Ru·g C^{-1}, the yield of arabitol improved significantly at short times (5 minutes) respect to the experiments at 0.015 g Ru·g C^{-1}, and a slight enhancement was observed for longer times (5 – 20 minutes). From 20 minutes onwards, the yield remained constant and similar to that obtained at 0.015 g Ru·g C^{-1}. The yield of xylitol at 0.030 g Ru·g C^{-1} displayed a different tendency, as the plateau was reached after just 5 minutes. In addition to this, no differences in the yield of xylitol were noticed between catalyst loadings of 0.015 and

0.030 g Ru·g C^{-1} for times ≥ 10 minutes. A catalyst loading of 0.060 g Ru·g C^{-1} was finally tested and a high yield of both C_5 sugars alcohols (> 90%) was obtained over time (5 – 30 minutes).

The hydrogenation of glucose demonstrated again to be slower than the hydrogenation of C_5 sugars, and a higher catalyst loading was required to get a high sorbitol yield. The yield of sorbitol improved continuously by increasing the amount of catalyst from 0.015 to 0.060 g Ru·g C^{-1}. For catalyst loadings between 0.008 and 0.030 g Ru·g C^{-1}, the yield of sorbitol did not reach a plateau even at long times and a growing trend was observed after 30 minutes. Nevertheless, the yield of sorbitol was quite high (~92%) at 0.060 g Ru·g C^{-1} after 15 minutes and did not vary significantly for longer times.

In conclusion, the hydrogenation of glucose required a higher number of active sites than the hydrogenation of xylose/arabinose to get the same yield of sorbitol than that of xylitol or arabitol, respectively.

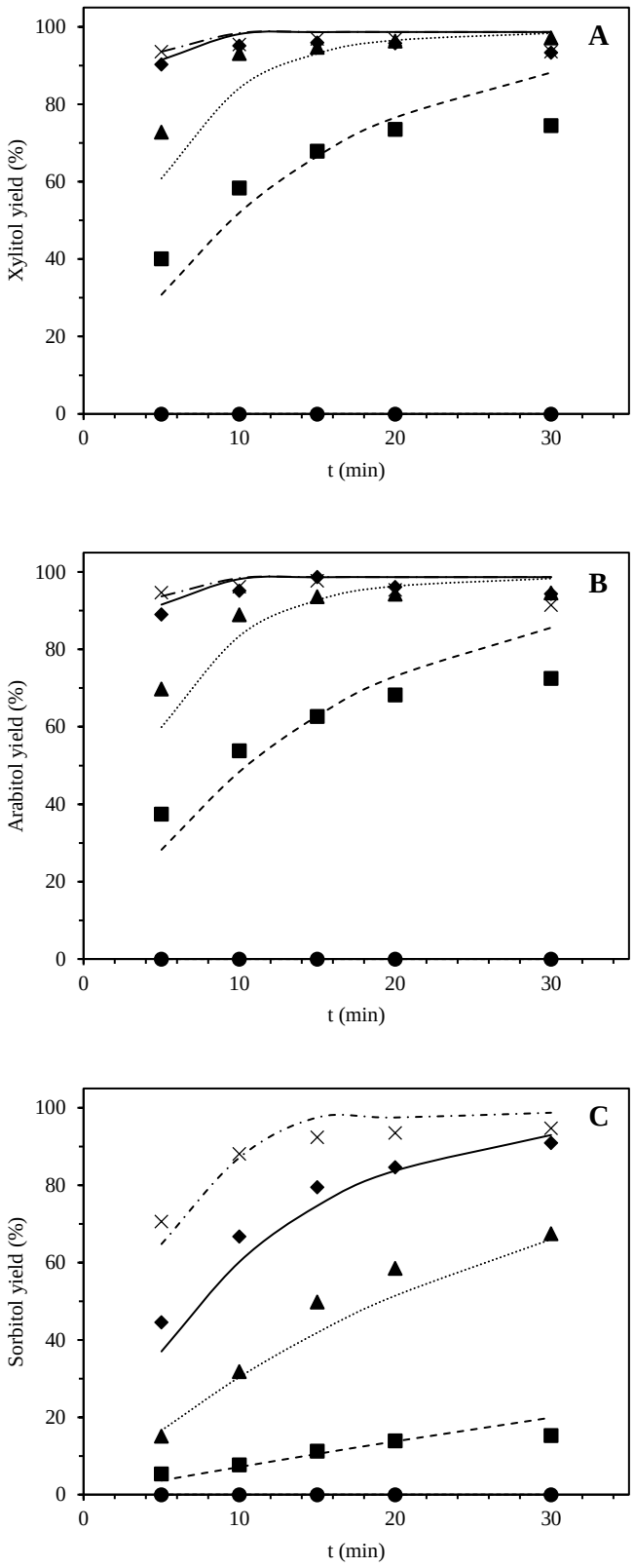

Figure 6. Effect of catalyst loading on the yield of A) xylitol, B) arabitol and C) sorbitol. Reaction conditions: substrate = xylose (6 $g \cdot L^{-1}$) + arabinose (3 $g \cdot L^{-1}$) + glucose (1.7 $g \cdot L^{-1}$); catalyst = Ru/H-ZSM-5 (80); T = 100 ºC; P (H_2) = 5 MPa. ● No catalyst, ■ 0.008 g

Ru·g C^{-1}, ▲ 0.015 g Ru·g C^{-1}, ♦ 0.030 g Ru·g C^{-1}, × 0.060 g Ru·g C^{-1}. Simulated values are represented by lines.

3.3 Modelling

3.3.1 Reaction temperature

The hydrogenation of sugars is commonly assessed as a competitive or semi competitive adsorption model plus reaction (Kilpiö et al., 2013; Mikkola et al., 1999; Verma and Gehlawat, 1989; Wisniak et al., 1974b). This approach proposes a reaction mechanism based on the Langmuir-Hinshelwood's theory. Reactants must find a suitable place in the catalyst to be adsorbed during the hydrogenation. They can further react to produce the final compounds, which will desorb afterwards. For the current process, the whole mechanism is shown in Figure 7. However, this reaction pathway requires a great deal of parameters since each individual mass transfer stage is considered. This would lead to a really overparameterized model. For this reason, a simplified version was selected, defining just overall reaction kinetic for each reactant, like in a homogenous process (Figure 8). Therefore, mass transfer and reaction steps were arrayed in one pseudo kinetic parameter (k) for each compound.

Xylose + * ⇆ Xylose*

Arabinose + * ⇆ Arabinose*

Glucose + * ⇆ Glucose*

H_2 + 2* ⇆ 2H*

Xylose* + 2H* → Xylitol*

Arabinose* + 2H* → Arabitol*

Glucose* + 2H* → Sorbitol*

Xylitol* ⇆ Xylitol + *

Arabitol* ⇆ Arabitol + *

Sorbitol* ⇆ Sorbitol + *

Figure 7. Whole reaction path way. *: available position for adsorption in the catalyst.

Reaction 1: Xylose + H_2 → Xylitol

Reaction 2: Arabinose + H_2 → Arabitol

Reaction 3: Glucose + H_2 → Sorbitol

Figure 8. Simplified version of the reaction pathway to perform the fittings.

The model was obtained applying a non-stationary mass balance for each compound defined in Figure 8 (Eq. 11). Additionally, since the stirring rate was very high during the reaction and the operating pressure was maintained constant, the hydrogen concentration was assumed to be its saturation value (Eq. 12).

$$\frac{dC_i}{dt} = \alpha_i \cdot m_{cat} \cdot k_j \cdot C_i^n \cdot C_{H_2} \quad \text{(Eq. 11)}$$

$$\frac{dC_i}{dt} = \alpha_i \cdot m_{cat} \cdot k_j \cdot C_i^n \cdot C_{H_2}^* = \alpha_i \cdot m_{cat} \cdot k_j' \cdot C_i^n \quad \text{(Eq. 12)}$$

The resolution of the set of the six ordinary differential equations (ODEs) was done by the explicit Euler's method. The fitting of the experimental data was performed by the Solver tool of Excel minimizing the following Absolute Average Deviation (A.A.D.) (Eq. 13):

$$\text{A.A.D.} = \frac{1}{N} \cdot \sum_{i=1}^{N} \left| X_{exp,i} - X_{sim,i} \right| / X_{exp,i} \cdot 100 \quad \text{(Eq. 13)}$$

The quality of the adjustments is displayed in Table 5 and it can be also checked in Figure 9 for the experiments at 80 ºC over Ru/H-ZSM-5 (80). The kinetic parameters are presented in Table 6. From these results, it can be concluded that the model was able to reproduce the experimental behavior quite well since the A.A.D. was low in most of the cases (< 11%). Furthermore, the regression coefficient (R^2) was always higher than 0.95.

Table 5. Goodness of the fittings for sugars hydrogenation at different temperatures in terms of A.A.D. and R^2.

T	A.A.D. (%)					
(ºC)	Xylose[1]	Arabinose[1]	Glucose[1]	Xylitol[2]	Arabitol[2]	Sorbitol[2]
80	5.7	7.6	6.4	6.8	8.4	6.4
100	7.2	7.0	8.0	7.1	7.5	9.8
120	2.6	2.3	13.7	3.9	1.3	14.2
Average	5.2	5.6	9.4	5.9	5.7	10.1
T	R^2					
(ºC)	Xylose	Arabinose	Glucose	Xylitol	Arabitol	Sorbitol
80	0.993	0.988	0.993	0.995	0.982	0.993
100	0.968	0.974	0.992	0.968	0.984	0.991
120	0.997	0.999	0.952	0.996	0.999	0.948
Average	0.986	0.987	0.979	0.987	0.988	0.977

[1] Deviations calculated by comparison between the experimental and calculated conversions.
[2] Deviations calculated by comparison between the experimental and calculated yields.

Table 6. Kinetic parameters obtained.

Kinetic parameters	Reaction		
	1	2	3
k'o ($L^{n-1} \cdot g_{cat.}^{-1} \cdot mol^{1-n} \cdot min^{-1}$)	$6.8 \cdot 10^6$	$2.6 \cdot 10^7$	$8.3 \cdot 10^{12}$
Ea ($kJ \cdot mol^{-1}$)	43.7	47.9	92.0
n	1.00	1.00	1.00

k'o: pre-exponential factor of Arrhenius equation; Ea: activation energy; n: reaction order.

The specific values of the activation energy were similar to those reported in literature for a wide set of catalysts. Our calculated value was 92.0 $kJ \cdot mol^{-1}$ for glucose hydrogenation. In literature this value goes from 12.3 $kJ \cdot mol^{-1}$ for platinum (Ahmed, 2012) to 64.8 $kJ \cdot mol^{-1}$ for Raney-nickel (Verma and Gehlawat, 1989). In the case of ruthenium catalysts, Mishra et al. (2014) reported an activation energy of 32.9 $kJ \cdot mol^{-1}$ for ruthenium supported on HY zeolite, whereas Romero et al. (2016) obtained a value of 44.9 $kJ \cdot mol^{-1}$ when ruthenium over MCM-48 was used as catalyst. Therefore, the hydrogenation of glucose seems to have a wide range of calculated activation energies, which can also explain the difference between our calculated value and the previously reported. The activation energy values for the hydrogenation of xylose and arabinose were similar to those obtained by other authors. For instance, we calculated an activation energy of 43.7 $kJ \cdot mol^{-1}$ for xylose hydrogenation, while the reported values in previous works were 50.1 $kJ \cdot mol^{-1}$ for nickel catalysts (Mikkola et al., 1999) or 46.8 $kJ \cdot mol^{-1}$ for ruthenium over Y zeolites (Mishra et al., 2013). Likewise, we determined a value of 47.9 $kJ \cdot mol^{-1}$ for arabinose hydrogenation, close to the calculated by Herrera et al. (2011) (57.2 $kJ \cdot mol^{-1}$ over ruthenium carbon). The reaction order was one in all the cases, which is accordant to previous works (Ahmed, 2012). Furthermore, it is worth highlighting that the values of the activation energy were quite similar for xylose and arabinose hydrogenation, but almost the double for glucose hydrogenation. This was expected since xylose and arabinose were successfully hydrogenated under the same operational conditions, whereas glucose required a higher temperature or a higher catalyst loading.

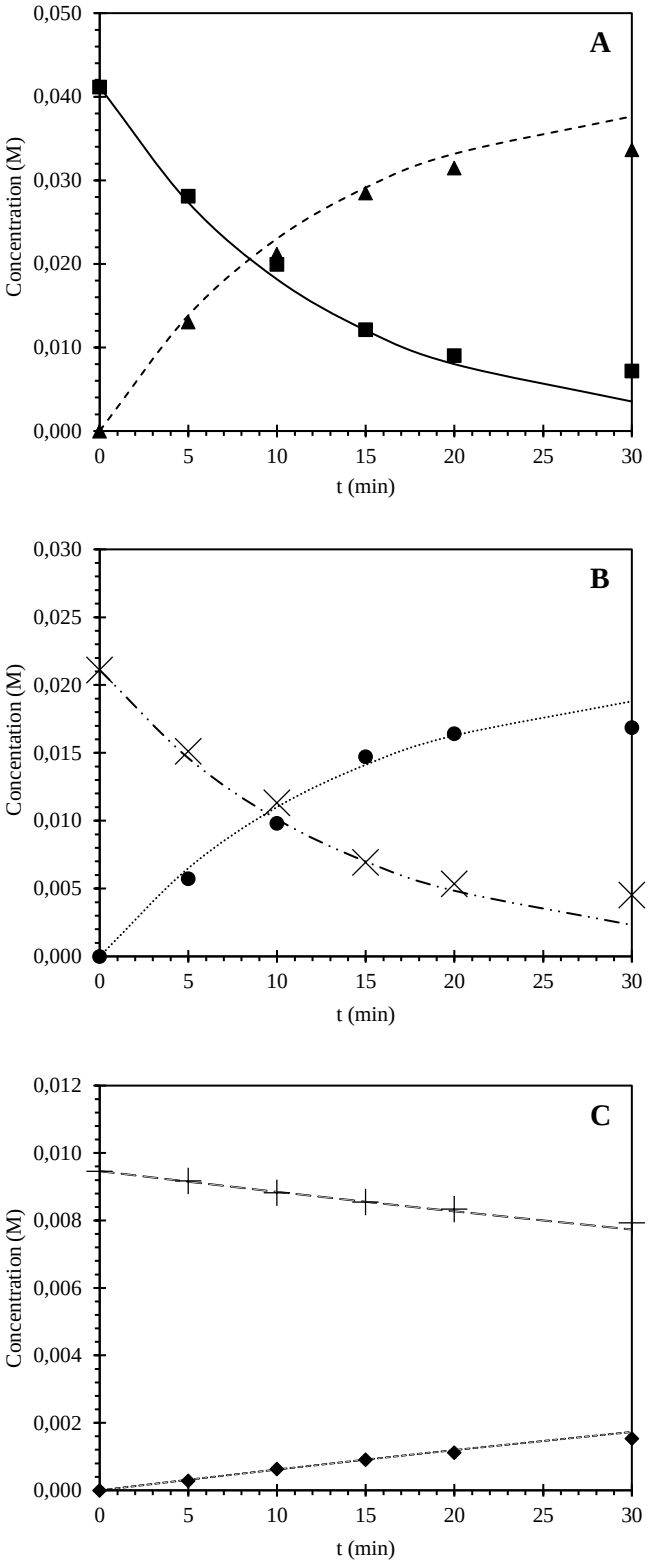

Figure 9. Simulated and experimental concentration profiles of A) ■ xylose, ▲ xylitol, B) × arabinose, ● arabitol and C) + glucose, ♦ sorbitol during hydrogenation at 80 ºC

(0.015 g Ru·g C^{-1}). C: concentration of the corresponding compound in the liquid; t: operating time; Simulated values are represented by lines.

3.3.2 Catalyst loading

Once the kinetic parameters were obtained from the study of the influence of temperature, the effect of the catalyst loading was further considered on the reaction kinetics. To do so, it was assumed that the metal loading affected only the activation energy (Eq. 14). This assumption was made since the catalyst loading was already considered in the model by multiplying the pre-exponential factor.

$$\frac{dC_i}{dt} = \alpha_i \cdot m_{cat} \cdot k_j' \cdot C_i^n = \alpha_i \cdot m_{cat} \cdot k_{oj}' \cdot e^{\frac{-(Ea_o - f(loading))}{RT}} \cdot C_i^n \quad \text{(Eq. 14)}$$

To obtain the parameter *f (loading)* which considers the effect of the catalyst loading, the results derived from these experiments (Figure 6) were fitted using only the activation energy as adjustable parameter (the initial value for the activation energy and the pre-exponential factor were those obtained in the assessing of the temperature role). These results are shown in Table 7 and the goodness of fittings in Table 8 and Figure 10.

Table 7. Activation energies for sugars hydrogenation with different catalysts loadings at 100 ºC.

Catalyst loading	Ea (kJ·mol^{-1})		
(g Ru·g C^{-1})	Xylose	Arabinose	Glucose
0	165.6*	165.6*	165.6*
0.008	44.3	48.8	94.8
0.015	43.7	48.0	92.1
0.030	43.2	47.4	91.0
0.060	43.2	47.4	91.0

*The activation energy values are the same for the hydrogenation of xylose, arabinose and glucose when no catalyst is used. These values are a result of the optimization. The optimum in this case would be an activation energy high enough to avoid the reaction under the most severe operational conditions (120 ºC and 0.06 g Ru·g C^{-1}).

Table 8. Goodness of the fittings for sugars hydrogenation with different catalysts loadings (at 100 ºC) in terms of A.A.D. and R^2.

Catalyst loading	A.A.D. (%)					
(g Ru·g C^{-1})	Xylose[1]	Arabinose[1]	Glucose[1]	Xylitol[2]	Arabitol[2]	Sorbitol[2]
0.008	11.6	12.7	14.8	11.6	12.4	14.8
0.015	5.6	5.4	8.6	5.4	5.3	8.9
0.030	3.7	3.8	3.9	4.6	4.0	3.9
0.060	4.2	4.4	4.3	4.9	5.2	4.3
Average	6.3	6.6	7.9	6.6	6.7	8.0
Catalyst loading	R^2					
(g Ru·g C^{-1})	Xylose	Arabinose	Glucose	Xylitol	Arabitol	Sorbitol
0.008	0.948	0.940	0.932	0.946	0.950	0.932
0.015	0.982	0.984	0.984	0.982	0.983	0.984
0.030	0.998	0.997	0.995	0.999	0.999	0.995
0.060	0.999	0.999	0.994	0.999	0.997	0.994
Average	0.982	0.980	0.976	0.981	0.982	0.976

[1] Deviations calculated by comparison between the experimental and calculated conversions.
[2] Deviations calculated by comparison between the experimental and calculated yields.

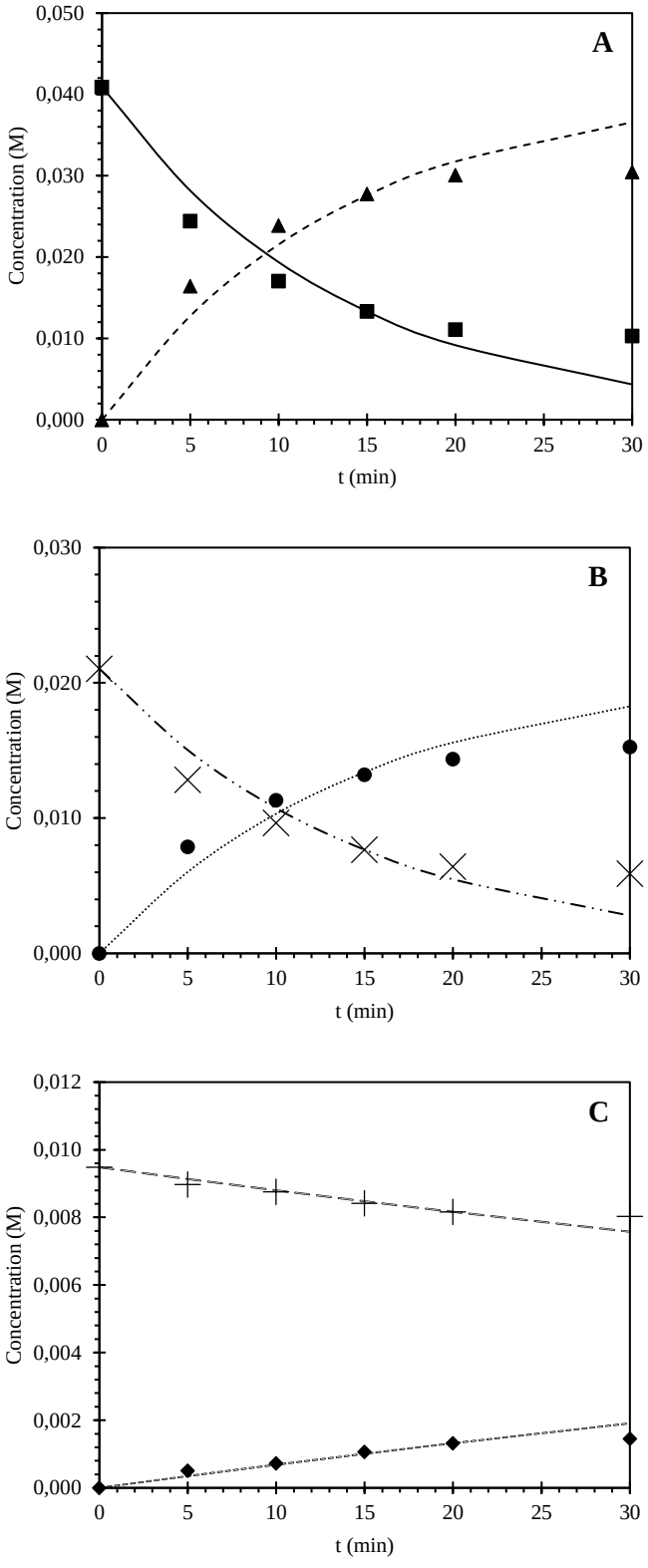

Figure 10. Simulated and experimental concentration profiles of A) ■ xylose, ▲ xylitol, B) × arabinose, ● arabitol and C) + glucose, ♦ sorbitol during hydrogenation at 100 ºC

for a catalyst loading of 0.008 g Ru·g C^{-1}. C: concentration of the corresponding compound in the liquid; t: operating time; Simulated values are represented by lines.

The difference between the activation energy of the blank test (165.7 kJ·mol^{-1}) and that corresponding to the experiments with different catalyst loadings was then calculated. With these differences, a logarithmic trend which relates the activation energy and the catalyst amount was obtained (Eq. 15):

$$\Delta Ea = f(\text{loading}) = a + b \cdot \ln(\text{loading}) \quad \text{(Eq. 15)}$$

where *a* and *b* are the regression parameters for each sugar and whose values are listed in Table 9. A logarithmic trend was expected since the values tend to a maximum, as observed with the results obtained at 0.03 and 0.06 g Ru·g C^{-1}.

Table 9. Regression parameters (*a* and *b*) of equation 15 for xylose, arabinose and glucose.

Regression parameter	Xylose	Arabinose	Glucose
a (kJ·mol^{-1})	124.2	120.5	80.4
b (kJ·mol^{-1})	0.6	0.7	1.8

4. Conclusions

The production of sugar alcohols via hydrogenation of sugar model mixtures was investigated over ruthenium catalysts supported on H-ZSM-5. H-ZSM-5 zeolites with SiO_2/Al_2O_3 ratio of 23 and 80 were tested as ruthenium catalyst supports. Although ruthenium is the active metal in hydrogenation reactions, the acidity of the catalyst support demonstrated to play an important role in the reaction mechanism. A decrease in SiO_2/Al_2O_3 ratio resulted in an increase of the number of acid sites, which had a negative impact on the catalytic hydrogenation of sugars. The conversion and selectivity were remarkably lower over Ru/H-ZSM-5 (23) than over Ru/H-ZSM-5 (80). A highly acidic catalyst support may give rise to secondary reaction pathways, such as the isomerization

of sugars, which results in a lower sugar conversion and a greater amount of undesired products as a consequence of competitive reactions. Our results demonstrated that over Ru/H-ZSM-5 (80) only hydrogenation occurred, but a competition between hydrogenation and isomerization took place over Ru/H-ZSM-5 (23). In the latter case, not only the sugars but also their isomers could be hydrogenated over the metal active sites of the catalyst. Therefore, the number of acid sites available for the hydrogenation of sugars was lower, since part of them was occupied by the isomeric sugars which could also undergo further hydrogenation. This process resulted in an overall decrease of sugars conversion and sugar alcohols selectivity. The influence of reaction temperature was evaluated in the range 80 – 120 ºC over Ru/H-ZSM-5 (80). Xylose and arabinose were more rapidly hydrogenated than glucose. Indeed, the optimum temperature for the hydrogenation of C_5 sugars was 100 ºC, whereas 120 ºC was the most suitable temperature for the hydrogenation of glucose. Therefore, the hydrogenation of C_5 and C_6 sugars can be performed separately just by controlling the temperature. The effect of catalyst loading was examined from 0 to 0.060 g Ru·g C^{-1}. A higher amount of ruthenium and therefore, a higher number of active sites was required to get the maximum yield of sorbitol than that of xylitol/arabitol. A kinetic model was also proposed to study the hydrogenation of the sugars. This model was based on a pseudo-first order kinetics. It reproduced the experimental data with relative low absolute deviations (< 11%) and high regression coefficients, R^2 (higher than 0.950). The activation energies calculated (for a catalyst loading of 0.015 g Ru·g C^{-1}) were 92.0 kJ·mol^{-1}, 43.7 kJ·mol^{-1} and 47.9 kJ·mol^{-1} for glucose, xylose and arabinose, respectively. The activation energies for xylose and arabinose hydrogenation were very close and similar to those reported in literature. The value for glucose hydrogenation was around 30 kJ·mol^{-1} higher than the maximum calculated by other authors. However, this discrepancy was inside the deviation of

previous data (deviations of up to 50 kJ·mol^{-1} were found). Finally, the effect of the catalyst loading on the kinetics was also assessed, proposing an empirical equation to include it into the activation energy.

Nomenclature

Acronyms

A.A.D.: absolute average deviation

HCP: hexagonal close packing

HPLC: high performance liquid chromatography

ICP-AES: inductively coupled plasma-atomic emission spectrometry

ODE: ordinary differential equation

TPR: temperature programmed reduction

XRD: X-ray Diffraction

Symbols

a and *b:* regression coefficients for the effect of the metal loading on the kinetics, kJ·mol^{-1}

α_i*:* stoichiometric coefficient for the compound "i", dimensionless

C_{H_2}*:* hydrogen concentration in the liquid, mol·L^{-1}

C_i*:* sugar concentration in the liquid, mol·L^{-1}

C_{sugar}*:* sugar concentration in the liquid, mol·L^{-1}

$C_{isomeric\ sugar}$*:* isomeric sugar concentration in the liquid, mol·L^{-1}

E_a: activation energy, kJ·mol^{-1}

E_{ao}: activation energy without catalyst, kJ·mol^{-1}

f_{sugar}*:* fraction of active sites available for sugar hydrogenation, dimensionless

$1 - f_{sugar}$*:* fraction of active sites available for isomeric sugar hydrogenation, dimensionless

f (loading): effect of the metal loading on the activation energy, kJ·mol^{-1}

k_j: observable kinetic constant (Arrhenius) for the reaction "j", $L^n \cdot g_{cat}^{-1} \cdot mol^{1-n} \cdot min^{-1} \cdot mol_{H2}^{-1}$

k_j': pseudo observable kinetic constant for the reaction "j", $L^{n-1} \cdot g_{cat}^{-1} \cdot mol^{1-n} \cdot min^{-1}$

k_{oj}': pre-exponential factor of the kinetic constant for the reaction "j", $L^{n-1} \cdot g_{cat}^{-1} \cdot mol^{1-n} \cdot min^{-1}$

k_1: reaction rate of sugar hydrogenation, min^{-1}

k_2: reaction rate of sugar isomerization (direct reaction), min^{-1}

k_3: reaction rate of sugar isomerization (reverse reaction), min^{-1}

k_4: reaction rate of isomeric sugar hydrogenation, min^{-1}

m_{cat}: mass of the catalyst, g

n: reaction order, dimensionless

$n_{sugar,0}$ and $n_{sugar,f}$: amount of each sugar before and after hydrogenation, mol

$n_{xylose,0}$ and $n_{xylose,f}$: initial and final amount of xylose, mol

$n_{xylitol,f}$: final amount of xylitol, mol

$n_{arabinose,0}$ and $n_{arabinose,f}$: initial and final amount of arabinose, mol

$n_{arabitol,f}$: final amount of arabitol, mol

$n_{glucose,0}$ and $n_{glucose,f}$: initial and final amount of glucose, mol

$n_{sorbitol,f}$: final amount of sorbitol, mol

N: number of experiments, dimensionless

$X_{exp,i}$: experimental value of the variable "X" for the experiment "i"

$X_{sim,i}$: simulated value of the variable "X" for the experiment "i"

t: reaction time

References

Ahmed, M.J. Kinetics studies of D-glucose hydrogenation over activated charcoal supported platinum catalyst. *Heat Mass Transfer,* 48 (2012) 343–347.

Aho, A., Roggan, S., Simakova, O.A., Salmi, T., and Murzin, D.Y. Structure sensitivity in catalytic hydrogenation of glucose over ruthenium. *Catalysis Today*, 241 (2015) 195–199.

Al-Dughaither, A.S., and De Lasa, H. HZSM-5 zeolites with different SiO_2/Al_2O_3 ratios. Characterization and NH_3 desorption kinetics. *Industrial & Engineering Chemistry Research,* 53 (2014) 15303–15316.

ALOthoman, Z.A. A Review: Fundamental aspects of silicate mesoporous materials. *Materials,* 5 (2012) 2874–2902.

Baudel, H.M., De Abreu, C.A.M., and Zaror, C.Z. Xylitol production via catalytic hydrogenation of sugarcane bagasse dissolving pulp liquid effluents over Ru/C catalyst. *Journal of Chemical Technology and Biotechnology,* 80 (2005) 230–233.

Besson, M., Gallezot, P., and Pinel, C. Conversion of biomass into chemicals over metal catalysts. *Chemical Reviews,* 114 (2014) 1827–1870.

Beyer, H.K., Nagy, J.B., Karge, H.G., and Kiricsi, I. Volume 94 – Catalysis by microporous materials. In *Studies in Surface Science and Catalysis*, 1st Edition, Elsevier Science, 1995.

Chareonlimkun, A., Champreda, V., Shotipruk, A., and Laosiripojana, N. Reactions of C_5 and C_6-sugars, cellulose, and lignocellulose under hot compressed water (HCW) in the presence of heterogeneous acid catalysts. *Fuel,* 89 (2010) 2873–2880.

Cychosz, K.A., Guillet-Nicolas, R., García-Martínez, J., and Thommes, M. Recent advances in the textural characterization of hierarchically structures nanoporous materials. *Chemical Society Reviews,* 46 (2017) 389–414.

Dabbawala, A.A., Mishra, D.K., and Hwang, J-S. Selective hydrogenation of D-glucose using amine functionalized nanoporous polymer supported Ru nanoparticles based catalyst. *Catalysis Today,* 265 (2016) 163–173.

Dasgupta, D., Bandhu, S., Adhikari, D.K., and Ghosh, S. Challenges and prospects of xylitol production with whole cell bio-catalysis: A review. *Microbiological Research,* 198 (2017) 9–21.

De Albuquerque, T.L., Da Silva, Jr. I.J., De Macedo, G.R., and Rocha, M.V.P. Biotechnological production of xylitol from lignocellulosic wastes: A review. *Process Biochemistry,* 49 (2014) 1779–1789.

Delidovich, I., Gyngazova, M.S., Sánchez-Bastardo, N., Wohland, J.P., Hoppe, C., and Drabo, P. Production of keto-pentoses via isomerization of aldo-pentoses catalyzed by phosphates and recovery of products by anionic extraction. *Green Chemistry,* 20 (2018) 724–734.

Deng, W., Zhang, Q., and Wang, Y. Catalytic transformation of cellulose and its derived carbohydrates into chemicals involving C-C bond cleavage. *Journal of Energy Chemistry*, 24 (2015) 595–607.

Dietrich, K., Hernández-Mejia, C., Verschuren, P., Rothenberg, G., and Shiju, N.R. One-pot selective conversion of hemicellulose to xylitol. *Organic Process Research & Development,* 21 (2017) 165–170.

Dong, H., Zhang, L., Fang, Z., Fu, W., Tang, T., Feng, Y., and Tang, T. Acidic hierarchical zeolite ZSM-5 supported Ru catalyst with high activity and selectivity in the seleno-functionalization of alkenes. *RSC Advances,* 7 (2017) 22008–22016.

Elliot, D.C., Peterson, K.L., Muzatko, D.S., Alderson, E.V., Hart, T.R., and Neuenschwander, G.G. Effects of trace contaminants on catalytic processing of biomass-derived feedstocks. *Applied Biochemistry and Biotechnology,* 113–116 (2004) 807–825.

Ennaert, T., Feys, S., Hemdrikx, D., Jacobs, P.A., and Sels, B.F. Reductive splitting of hemicellulose with stable ruthenium-loaded USY zeolites. *Green Chemistry*, 18 (2016) 5295–5304.

Faba, L., Kusema, B.T., Murzina, E.V., Tokarev, A., Kumar, N., Smeds, A., Díaz, E., Ordóñez, S., Mäki-Arvela, P., Willför, S., Salmi, T., and Murzin, D.Y. Hemicellulose hydrolysis and hydrolytic hydrogenation over proton- and metal modified zeolites. *Microporous and Mesoporous Materials,* 189 (2014) 189–199.

Fu, X., Sheng, X., Zhou, Y., Fu, Z., Zhao, S., Bu, X., and Zhang, C. Design of micro – mesoporous zeolite catalysts for alkylation. *RSC Adances,* 6 (2016) 50630–50639.

Fukuoka, A., and Dhepe, P.L. Catalytic conversion of cellulose into sugar alcohols. *Angewandte Chemie International Edition,* 45 (2006) 5161–5163.

Gallezot, P., Cerino, P.J., Blanc, B., Flèche, G., and Fuertes, P. Glucose hydrogenation on promoted Raney-nickel catalysts. *Journal of Catalysis,* 146 (1994) 93–102.

Gallezot, P., Nicolaus, N., Flèche, G., Fuertes, P., and Perrard, A. Glucose hydrogenation on ruthenium catalysts in a trickle-bed reactor. *Journal of Catalysis,* 180 (1998) 51–55.

Gao, Y., Zheng, B., Wu, G., Ma, F., and Liu, C. Effect of the Si/Al ratio on the performance of hierarchical ZSM-5 zeolites for methanol aromatization. *RSC Advances,* 6 (2016) 83581–83588.

Geboers, J., Van de Vyver, S., Carpentier, K., Jacobs, P., and Sels, B. Efficient hydrolytic hydrogenation of cellulose in the presence of Ru-loaded zeolites and trace amounts of mineral acid. *Chemical Communications,* 47 (2011) 5590–5592.

Groen, J.C., Moulijn, J.A., and Pérez-Ramírez, J. Alkaline posttreatment of MFI zeolites. From accelerated screening to scale-up. *Industrial & Engineering Chemistry Research,* 46 (2007) 4193–4201.

Guha, S.K., Kobayashi, H., Hara, K., Kikuchi, H., Aritsuka, T., and Fukuoka, A. Hydrogenolysis of sugar beet fiber by supported metal catalyst. *Catalysis Communications,* 12 (2011) 980–983.

Guo, X., Wang, X., Guan, J., Chen, X., Qin, Z., Mu, X., and Xian, M. Selective hydrogenation of D-glucose to D-sorbitol over Ru/ZSM-5 catalysts. *Chinese Journal of Catalysis,* 35 (2014) 733–740.

Hara, M., Nakajima, K., and Kamata, K. Recent progress in the development of solid catalysts for biomass conversion into high value-added chemicals. *Science and Technology of Advanced Materials,* 16 (2015) 034903.

Hernández-Mejia, C., Gnanakumar, E.S., Olivos-Suarez, A., Gascon, J., Greer, H., Zhou, W., Rothenberg, G., and Shiju, N.R. Ru/TiO_2-catalysed hydrogenation of xylose: the role of crystal structure of the support. *Catalysis Science & Technology,* 6 (2016) 577–582.

Herrera, V.A.S., Saleem, F., Kusema, B., Eränen, K., and Salmi. T. Hydrogenation of L-arabinose and D-galactose mixtures over a heterogeneous Ru/C catalyst. *Topics in Catalysis,* 55 (2012) 550–555.

Herrera, V.A.S., Oladele, O., Kordás, K., Eränen, K., Mikkola, J-P., Murzin, D.Y., and Salmi, T. Sugar hydrogenation over a Ru/C catalyst. *Journal of Chemical Technology and Biotechnology,* 86 (2011) 658–668.

Hu, H., Li, Z., Wu, Z., Lin, L., and Zhou, S. Catalytic hydrolysis of microcrystalline and rice straw-derived cellulose over a chlorine-doped magnetic carbonaceous solid acid. *Industrial Crops and Products,* 84 (2016) 408–417.

Hu, L., Tang, X., Wu, Z., Lin, L., Xu, J., Xu, N., and Dai, B. Magnetic lignin-derived carbonaceous catalyst for the dehydration of fructose into 5-hydroxymethylfurfural in dimethylsulfoxide. *Chemical Engineering Journal,* 263 (2015) 299–308.

Jin, Y., Yang, G., Chen, Q., Niu, W., Lu, P., Yoneyama, Y., and Tsubaki. N. Development of dual-membrane coated Fe/SiO_2 catalyst for efficient synthesis of isoparaffins directly from syngas. *Journal of Membrane Science,* 475 (2015) 22–29.

Jividen, G.M., Chang, H.M., and Reeves, R.H. U.S. Pat. 4087316, 1978.

Käldström, M., Kumar, N., and Murzin, D.Y. Valorization of cellulose over metal supported on mesoporous materials. *Catalysis Today,* 167 (2011) 91–95.

Kilpiö, T., Aho, A., Murzin, D., and Salmi, T. Experimental and modeling study of catalytic hydrogenation of glucose to sorbitol in a continuously operating packed-bed reactor. *Industrial & Engineering Chemistry Research,* 52 (2013) 7690–7703.

Kim, J.W., Park, S.H., Jung, J., Jeon, J-K., Ko, C.H., Jeong, K-E., and Park, Y-K. Catalytic pyrolysis of mandarin residue from the mandarin juice processing industry. *Bioresource Technology,* 136 (2013) 431–436.

Kobayashi, H., Yamakoshi, Y., Hosaka, Y., Yabushita, M., and Fukuoka, A. Production of sugar alcohols from real biomass by supported platinum catalyst. *Catalysis Today,* 226 (2014) 204–209.

Koganti, S., and Ju, L.K. *Debaryomyces hansenii* fermentation for arabitol production. *Biochemical Engineering Journal,* 79 (2013) 112–119.

Kusema, B.T., Faba, L., Kumar, N., Mäki-Arvela, P., Díaz, E., Ordóñez, S., Salmi, T., and Murzin, D.Y. Hydrolytic hydrogenation of hemicellulose over metal modified mesoporous catalyst. *Catalysis Today*, 196 (2012) 26–33.

Kusserow, B., Schimpf, S., and Claus, P. Hydrogenation of glucose to sorbitol over nickel and ruthenium catalysts. *Advanced Synthesis & Catalysis*, 345 (2003) 289–299.

Liu, Q., Zhang, T., Liao, Y., Cai, C., Tan, J., Wang, T., Qiu, S., He, M., and Ma, L. Production of C_5/C_6 sugar alcohols by hydrolytic hydrogenation of raw lignocellulosic biomass over Zr based solid acids combined with Ru/C. *ACS Sustainable Chemistry & Engineering*, 5 (2017) 5940–5950.

Liu, W-J., Tian, K., Jiang, H., and Yu, H.Q. Facile synthesis of highly efficient and recyclable magnetic solid acid from biomass waste. *Scientific Reports*, 3 (2013) 2419.

Lü, R., Tangbo, H., Wang, Q., and Xiang, S. Properties and characterization of modified HZSM-5 zeolites. *Journal of Natural Gas Chemistry*, 12 (2003) 56–62.

McKendry, P. Energy production from biomass (part 1): Overview of biomass. *Bioresource Technology*, 83 (2002) 37–46.

Mikkola, J.-P., Vainio, H., Salmi, T., Sjöholm, R., Ollonqvist, T., and Väyrynen, J. Deactivation kinetics of Mo-supported Raney Ni catalyst in the hydrogenation of xylose to xylitol. *Applied Catalysis A: General*, 196 (2000) 143–155.

Mikkola, J-P., and Salmi, T. Three-phase catalytic hydrogenation of xylose to xylitol – prolonging the catalyst activity by means of on-line ultrasonic treatment. *Catalysis Today*, 64 (2001) 271–277.

Mikkola, J-P., Salmi, T., and Sjöholm, R. Modelling of kinetics and mass transfer in the hydrogenation of xylose over Raney nickel catalyst. *Journal of Chemical Technology and Biotechnology*, 74 (1999) 655–662.

Mikkola, J-P., Salmi, T., and Sjöholm, R. Effects of solvent polarity on the hydrogenation of xylose. *Journal of Chemical Technology and Biotechnology*, 76 (2001) 90–100.

Mikkola, J-P., Sjöholm, R., Salmi, T., and Mäki-Arvela, P. Xylose hydrogenation: kinetic and NMR studies of the reaction mechanisms. *Catalysis Today*, 48 (1999) 73–81.

Mishra, D.K., Dabbawala, A.A., and Hwang, J-S. Ruthenium nanoparticles supported on zeolite Y as an efficient catalyst for selective hydrogenation of xylose to xylitol. *Journal of Molecular Catalysis A: Chemical*, 376 (2013) 63–70.

Mishra, D.K., Dabbawala, A.A., Park, J.J., Jhung, S.H., and Hwang, J-S. Selective hydrogenation of D-glucose to D-sorbitol over HY zeolite supported ruthenium nanoparticles catalysts. *Catalysis Today*, 232 (2014) 99–107.

Müller, A., Hilpmann, G., Haase, S., and Lange. R. Continuous hydrogenation of L-arabinose and D-galactose in a mini packed bed reactor. *Chemical Engineering & Technology*, 40 (2017) 2113–2122.

Murzin, D.Y., Kusema, B., Murzina, E.V., Aho, A., Tokarev, A., Boymirzaev, A.S., Wärna, J., Dapsens, P.Y., Mondelli, C., Pérez-Ramírez, J., and Salmi, T. Hemicellulose arabinogalactan hydrolytic hydrogenation over Ru-modified H-USY zeolites. *Journal of Catalysis*, 330 (2015a) 93–105.

Murzin, D.Y., Murzina, E.V., Tokarez, A., Shcherban, N.D., Wärna, J., and Salmi, T. Arabinogalactan hydrolysis and hydrolytic hydrogenation using functionalized carbon materials. *Catalysis Today*, 257 (2015b) 169–176.

Peng, P., Wang, Y., Rood, M.J., Zhang, Z., Subhan, F., Yan, Z., Qin, L., Zhang, Z., Zhang, Z., and Gao, X. Effects of disolution alkalinity and self-assembly on ZSM-5 based micro-/mesoporous composites: a study of the relationship between porosity, acidity, and catalytic performance. *CrystEngComm*, 17 (2015) 3820–3828.

Putro, J.N., Soetaredjo, F.E., Lin, S-Y., Ju, Y-H., and Ismadji. S. Pretreatment and conversion of lignocellulose biomass into valuable chemicals. *RSC Advances,* 6 (2016) 46834–46852.

Rachel-Tang, D.Y., Islam, A., and Taufiq-Yap, Y.H. Bio-oil production via catalytic solvolysis of biomass. *RSC Advances,* 7 (2017) 7820–7830.

Rao, L.V., Goli, J.K., Gentela, J., and Koti. S. Bioconversion of lignocellulosic biomass to xylitol: An overview. *Bioresource Technology,* 213 (2016) 299–310.

Ribeiro, L.S., Delgado, J.J., Órfão, J.J.M., and Pereira, M.F.R. A one-pot method for the enhanced production of xylitol directly from hemicellulose (corncob xylan). *RSC Advances,* 6 (2016) 95320–95327.

Ribeiro, L.S., Órfão, J.J.M., and Pereira, M.F.R. Screening of catalysts and reaction conditions for the direct conversion of corncob xylan to xylitol. *Green Processing and Synthesis*, 6 (2017) 265–272.

Romero, A., Alonso, E., Sastre, Á., and Nieto-Márquez, A. Conversion of biomass into sorbitol: Cellulose hydrolysis on MCM-48 and D-glucose hydrogenation on Ru/MCM-48. *Microporous and Mesoporous Materials,* 224 (2016) 1–8.

Sánchez-Bastardo, N., and Alonso, E. Maximization of monomeric C5 sugars from wheat bran by using mesoporous ordered silica catalysts. *Bioresource Technology*, 238 (2017) 379–388.

Sánchez-Bastardo, N., Romero, A., and Alonso, E. Extraction of arabinoxylans from wheat bran using hydrothermal processes assisted by heterogeneous catalysts. *Carbohydrate Polymers,* 160 (2017) 143–152.

Schimpf, S., Louis, C., and Claus, P. Ni/SiO_2 catalysts prepared with ethylenediamine nickel precursors: Influence of the pretreatment on the catalytic properties in glucose hydrogenation. *Applied Catalysis A: General,* 318 (2007) 45–53.

Schmidt, W. Chapter 4 – Microporous and Mesoporous Catalysts. In *Surface and Nanomolecular Catalysis*, Richards, R., (Ed.), CRC Press: Boca Raton, 2006.

Serrano-Ruiz, J.C., Luque, R., and Sepúlveda-Escribano, A. Transformations of biomass-derived platform molecules: from high added-value chemicals to fuels via aqueous-phase processing. *Chemical Society Reviews,* 40 (2011) 5266–5281.

Tathod, A., Kane, T., Sanil, E.S., and Dhepe, P.L. Solid base supported metal catalysts for the oxidation and hydrogenation of sugars. *Journal of Molecular Catalysis A: Chemical*, 388–389 (2014) 90–99.

Tathod, A.P., and Dhepe, P.L. Efficient method for the conversion of agricultural waste into sugar alcohols over supported bimetallic catalysts. *Bioresource Technology,* 178 (2015) 36–44.

Verma, R., and Gehlawat, J.K. Kinetics of hydrogenation of D-glucose to sorbitol. *Journal of Chemical Technology and Biotechnology,* 46 (1989) 295–301.

Wang, J., Xu, W., Ren, J., Liu, X., Lu, G., and Wang, Y. Efficient catalytic conversion of fructose into hydroxymethylfurfural by a novel carbon-based solid acid. *Green Chemistry,* 13 (2011) 2678–2681.

Werpy, T., and Petersen, G. Top Value Added Chemicals from Biomass. In *Volume I – Results of Screening for Potential Candidates from Sugars and Synthesis Gas*. U.S.D. Energy: United States, 2004.

Wisniak, J., Hershkowitz, M., Leibowitz, R., and Stein, S. Hydrogenation of xylose to xylitol. *Industrial & Engineering Chemistry Product Research and Development,* 13 (1974a) 75–79.

Wisniak, J., Hershkowitz, M., and Stein, S. Hydrogenation of xylose over platinum group catalysts. *Industrial & Engineering Chemistry Product Research and Development,* 13 (1974b) 232–236.

Yadav, M., Mishra, D.K., and Hwang, J-S. Catalytic hydrogenation of xylose to xylitol using ruthenium catalyst on NiO modified TiO_2 support. *Applied Catalysis A: General,* 425–426 (2012) 110–116.

Yi, G., and Zhang. Y. One-pot selective conversion of hemicellulose (xylan) to xylitol under mild conditions. *ChemSusChem,* 5 (2012) 1383–1387.

Zada, B., Chen, M., Chen, C., Yan, L., Xu, Q., Li, W., Guo, Q., and Fu, Y. Recent advances in catalytic production of sugars alcohols and their applications. *Science China Chemistry,* 60 (2017) 853–869.

Zheng, F.C., Chen, Q.W., Hu, L., Yan, N., and Kong, X.K. Synthesis of sulfonic acid-functionalized Fe_3O_4@C nanoparticles as magnetically recyclable solid acid catalysts for acetalization reaction. *Dalton Transactions,* 43 (2014) 1220–1227.

CHAPTER V

PURIFICATION OF WHEAT BRAN HYDROLYSATES USING BORONIC ACID CARRIERS FOLLOWED BY HYDROGENATION OF SUGARS OVER RU/H-ZSM-5

Sánchez-Bastardo, N., Delidovich, I., and Alonso, E. From biomass to sugar alcohols: Purification of wheat bran hydrolysates using boronic acid carriers followed by hydrogenation of sugars over Ru/H-ZSM-5. *ACS Sustainable Chemistry & Engineering*, 6 (2018) 11930–11938.

Abstract

Wheat bran is a lignocellulosic waste of milling industry. It contains hemicelluloses which can be valorized into arabitol and xylitol via a few-step approach. It begins with extraction and hydrolysis of hemicelluloses to produce a solution of xylose and arabinose along with proteins and inorganic salts. This work focusses on the purification of sugars of this hydrolysate and the subsequent catalytic production of sugar alcohols. A purification process based on the recovery of sugars by anionic extraction with a boronic acid, followed by back-extraction and a further refining step with ion exchange resins is described. After this process, a high purity sugars solution (~90%) free of inorganic elements and proteins was obtained. The feasibility of the process was also highlighted by a successful recycling of the organic phase containing the boronic acid. The hydrogenation of purified sugars was then performed over Ru/H-ZSM-5. A high yield into pentitols of ~70% with 100% selectivity was achieved. Importantly, the catalytic hydrogenation of sugars in the hydrolysate prior to purification did not occur. We determined that proteins caused the deactivation of the catalyst and consequently the inhibition of the production of sugar alcohols. Therefore, a purification step for proteins removal before hydrogenation of sugars is crucial to avoid the poisoning of the metal catalyst and guarantee its good performance in the catalytic hydrogenation into sugar alcohols.

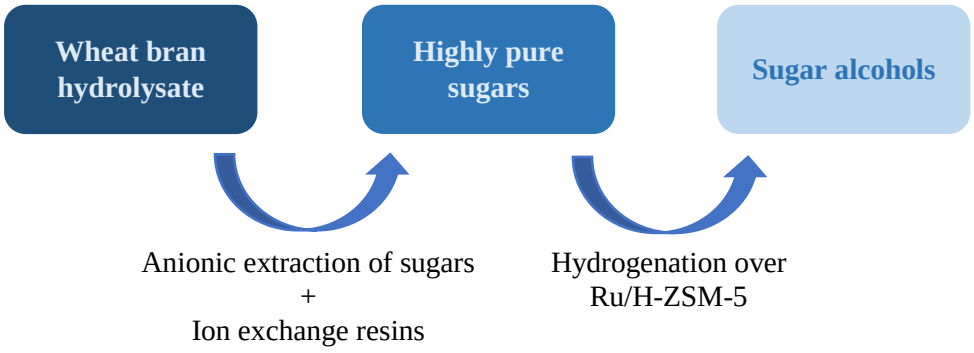

1. Introduction

The conversion of renewable biomass into high value-added products has been extensively investigated during the last decades due to the depletion of fossil resources (Brennan et al., 2010; Hara et al., 2015; Putro et al., 2015). Lignocellulosic biomass is the most abundant bio-based carbon resource suitable for the production of biofuels and valuable chemicals (Deng et al., 2015; Serrano-Ruiz et al., 2011). In this context, xylitol and arabitol are considered by the U.S. Department of Energy (DOE) among the 12 building block chemicals that can be produced from biomass pentoses, *i.e.* hemicelluloses (Werpy and Petersen, 2004). Xylitol and arabitol have important applications in food industry as very low-calorie sweeteners for sugar substitution and in pharmaceutical industry as excipients (Koganti and Ju, 2013; Zada et al., 2017). The conversion of model hemicellulosic compounds, *i.e.* C_5 sugars (Barbaro et al., 2016; Hernández-Mejia et al., 2016; Herrera et al., 2012; Mishra et al., 2013; Morales et al., 2016, 2017; Müller et al., 2017; Pham et al., 2016; Simakova et al., 2016; Yadav et al., 2012) and commercial oligosaccharides (Dietrich et al., 2017; Ennaert et al., 2016; Faba et al., 2014; Kusema et al., 2012; Liu et al., 2016; Murzin et al., 2015a, 2015b; Ribeiro et al., 2016, 2017a, 2017b; Yi and Zhang, 2012) into sugar alcohols has been widely studied for many years. However, works related to the catalytic hydrogenation of real biomass (Guha et al., 2011; Kobayashi et al., 2014; Tathod and Dhepe, 2015) or pentosane-rich hydrolysates are scarce (Baudel et al., 2005; Irmak et al., 2017). Chemical (Zada et al., 2017) and biological (Dasgupta et al., 2017; Rao et al., 2016) processes have been considered to produce sugar alcohols from biomass. Although biotechnological xylitol production occurs under milder process conditions, xylitol is industrially synthesized by chemical processes, *i.e.* by catalytic hydrogenation of xylose. Unlike biological methods, the catalytic route offers high yield and conversion efficiency as well as an economical large

scale production (Dasgupta et al., 2017). The chemical conversion of the hemicellulosic fraction of biomass into sugar alcohols (xylitol and arabitol) consists of several steps: i) isolation of the hemicellulosic fraction composed mainly by poly/oligosaccharides, ii) hydrolysis of these poly/oligosaccharides into monosaccharides, namely xylose and arabinose, iii) catalytic hydrogenation of monosaccharides into sugar alcohols, *i.e.* xylitol and arabitol (Tathod and Dhepe, 2015; Vilcocq et al., 2014). A simplified reaction mechanism for sugar alcohols production from biomass with possible side reactions is shown in Figure 1.

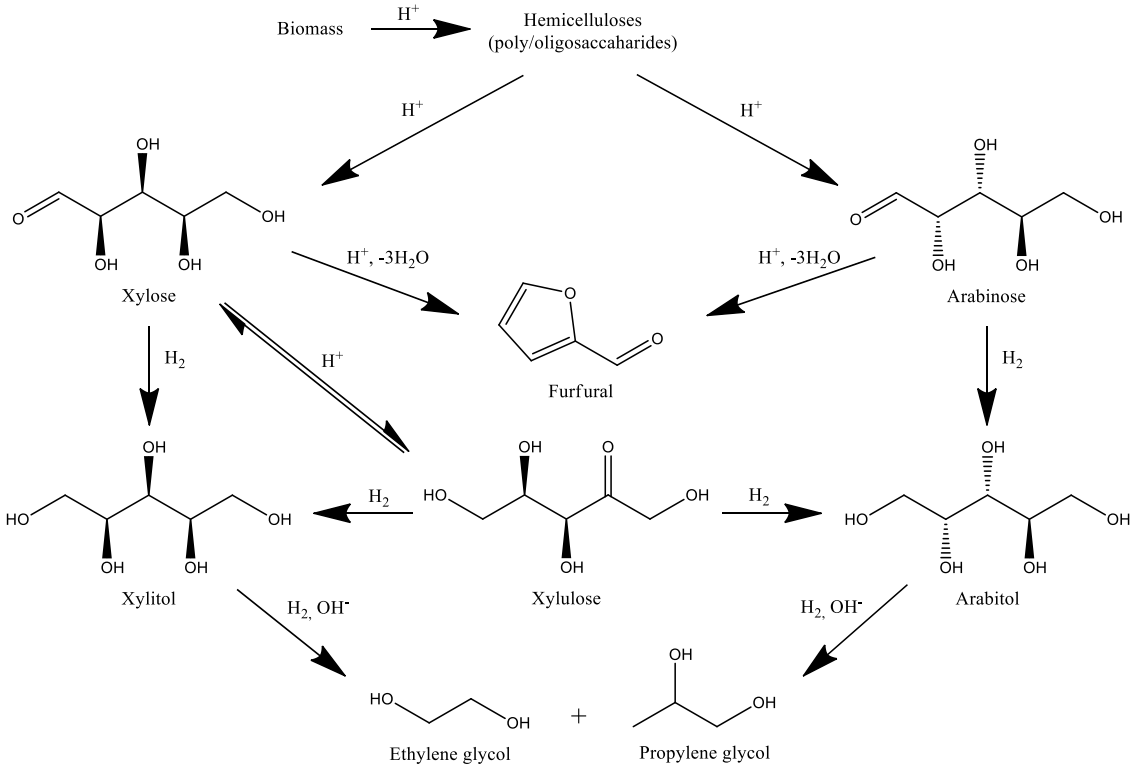

Figure 1. Chemical production of sugar alcohols from biomass with possible side reactions. Adapted from (Huang et al., 2014; Kobayashi et al., 2011; Mishra et al., 2013; Murzin et al., 2015b).

We have recently studied the two first steps, *i.e.* the fractionation of biomass (wheat bran) to isolate the hemicelluloses and their further hydrolysis into monomeric C_5 sugars (Sánchez-Bastardo and Alonso, 2017; Sánchez-Bastardo et al., 2017). Since the content

of monosaccharides in the hydrolysate is quite low (of ca. 0.8 wt.%), additional concentration and purification stages to obtain sugars-rich hydrolysates must be considered before the hydrogenation process (Irmak et al., 2017). The presence of other biomass components in the hydrolysates (*e.g.* inorganic cations, sulfur, organic acids, proteins) may poison and deactivate the metal catalysts required for the hydrogenation (Arena, 1992; Besson and Gallezot, 2003; Borg et al., 2011; Dhepe and Sahu, 2010; Elliot et al., 2004; Ennaert et al., 2016; Rytter and Holmen, 2015; Vilcocq et al., 2014). Arena (1992) studied the hydrogenation of glucose into sorbitol over ruthenium catalysts and proved that even a small amount of sulphur (~15 ppm) present in the initial solution is adsorbed on ruthenium catalysts resulting in a rapid activity loss. The conversion of sugars in hydrolysates containing sulphur compounds is very difficult to achieve over metal catalysts. In this work, Arena also stated that a significant deactivation may also occur due to the presence of organic acids in the hydrolysates formed by the degradation of sugars during the fractionation and hydrolysis steps. Borg et al. (2011) claimed the deactivation of metal catalysts by the presence of alkali (K) and alkaline earth metals (Ca, Mg). They reported a poisoning effect which decreases in the following order: Ca > K > Mg. These cations did not affect the surface area of the catalyst but decreased the activity, probably due to the physical blocking of active metal sites, the reduction of the metal particle size and electronic effects. Elliot et al. (2004) studied the effects of several cations on the catalytic performance of biomass-derived products and concluded that Ca and Mg are potential catalyst poisons as they may plug the pores by insoluble salt precipitation. Likewise, K may also deactivate the catalyst by an alkali attack on the catalyst support. In this work they also demonstrated the inhibitory effect of proteins on catalytic hydrogenation of sugars. They attributed this negative effect to Maillard-type reactions, which enable the formation of condensed structures that can block the active sites of the

catalyst. Vilcocq et al. (2014) reviewed the conversion of oligosaccharides from biomass over heterogeneous catalysts and also reported the deactivation of the catalysts as a result of proteins deposition on the surface.

Different purification processes have been described by Chandel et al. (2011) (Table 1). These methods usually include chemical/physical conditioning steps (Grzenia et al., 2010) followed by evaporative concentration methods (McCabe et al., 2004). The conditioning steps generate large amounts of solid waste whose disposal can be expensive and pose environmental concerns. The evaporation-based concentration methods require high energy consumption and are not economically viable on an industrial scale (Relue and Varanasi, 2012).

Table 1. Purification strategies applied to lignocellulose hydrolysates by removal of different compounds. Adapted from (Chandel et al., 2011).

Process	Removal of
Physical methods	
Evaporation	Acetic acid, furfural, vanillin
Membrane based organic phases	Acetic, formic, levulinic acid, 5-HMF, furfural
Chemical methods	
Neutralization	Furfural, phenolic compounds
Overliming	Furfural, phenolic compounds
Activated carbon	Phenolic compounds
Ion exchange resins	Lignin derivates, acetic, formic, levulinic acid, 5-HMF, furfural
Extraction with ethyl acetate	Acetic acid, furfural, vanillin
Biotechnological methods	Microorganisms can detoxify the inhibitory substances of hydrolysates by transforming their chemical nature

More recently, other authors have focused on isolating sugars from biomass hydrolysates by solvent extraction with boronic acids (Brennan et al., 2010; Griffin and Shu, 2004), as opposed to removing the contaminating compounds. This approach is cost-effective and provide a concentrated sugar solution which can be directly processed without any

posttreatment (Relue and Varanasi, 2012). Solvent extraction methods are based on the ability of boronic acids to form reversibly stable complexes with saccharides (Brennan et al., 2010; Gori et al., 2015; Griffin and Shu, 2004; Griffin, 2005; Matsumoto et al., 2005; Relue and Varanasi, 2012). The mechanism of anionic extraction of sugars can be summarized as follows (Figure 2) (Brennan et al., 2010; Griffin and Shu, 2004). A boronic acid and a quaternary ammonium salt dissolved in an organic solution are stirred with an immiscible aqueous phase containing sugars. At the interface between the aqueous and the organic phases, the boronic acid ionizes with hydroxyl groups. This results in a tetrahedral anion which in turn forms an anion complex with the *cis*-diol groups of a sugar molecule. The anion complex is then dissolved in the organic phase by forming an ion pair with the quaternary ammonium cation (Q^+). The complexation is reversible and the sugars can be recovered from the organic phase in an acidic solution, since the complexes are no longer stable under acidic conditions. Not only purification but also concentration of the final aqueous solution can be achieved with this process. Saturating the organic phase with sugars is also possible by performing several extractions. All these sugars could finally be back-extracted in an acidic solution, resulting in a higher concentration of sugars. This would reduce the operating costs associated to the concentration of aqueous solutions which has historically been carried out by vacuum evaporation.

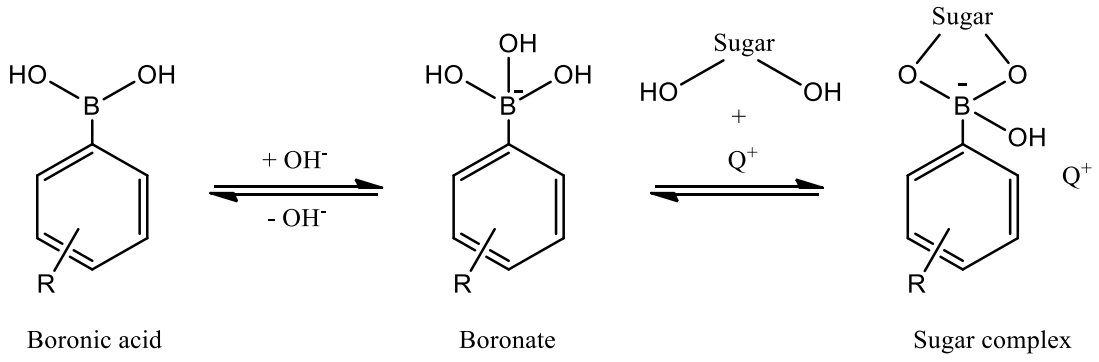

Figure 2. Mechanism of complexation of sugars by anionic extraction.

Several boronic acids with different pK_a have already been studied for the recovery of sugars (*e.g.* phenyboronic acid, 3,5-dimethylphenylboronic acid, 4-*tert*-butylphenylboronic acid, *trans*-*β*-styreneboronic acid, naphthalene-2-boronic acid, *ortho*-hydroxymethyl phenylboronic acid, *ortho*-dimethyl-aminomethyl phenylboronic acid) (Delidovich and Palkovits, 2016; Delidovich et al., 2018; Griffin and Shu, 2004). In order to enable the formation of stable complexes, it is necessary to operate at a pH higher than the pK_a of the boronic acid. Taking into account the moderate stability of sugars under alkaline conditions, working at a pH close to neutral conditions is required. Therefore, boronic acids with relatively low pK_a should be chosen for the extraction of saccharides (Delidovich and Palkovits, 2016). In this work, we chose phenylboronic acid (PBA) as a benchmark, and *ortho*-hydroxymethyl phenylboronic acid (HMPBA). PBA has a relatively high pK_a which is a drawback when operating at neutral conditions to avoid sugars degradation. HMPBA has a quite low pK_a due to intramolecular B-O interactions and it can form more stable complexes with sugars under the desired neutral conditions (Delidovich and Palkovits, 2016). The formulae of the boronic acids studied in this work and their corresponding pK_a values are shown in Figure 3.

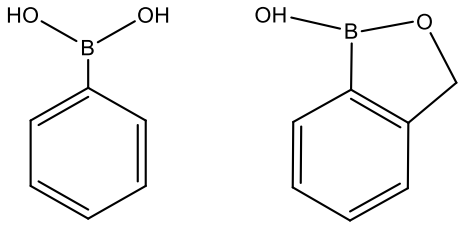

PBA pK_a = 8.8 HMPBA pK_a = 7.2

Figure 3. Formulae of boronic acids selected for the extraction of sugars from wheat bran hydrolysates.

In this work, the purification of hemicellulosic sugars obtained from wheat bran and the subsequent catalytic hydrogenation into sugar alcohols were studied. In the first step, a

combined process for the isolation of sugars using anionic extraction with a boronic acid, followed by back-extraction of sugars with an acidic solution, and further purification by ion exchange resins was investigated. In a second step, these sugars (mainly xylose and arabinose, but also glucose) were hydrogenated over ruthenium catalysts into the corresponding alcohols, mostly xylitol and arabitol, and sorbitol in minor amounts. The deactivation mechanism of the metal catalyst used in hydrogenation of hydrolysates prior to purification was also examined. To our knowledge, this is the first time in which an integration of a purification process of wheat bran hydrolysates followed by a further hydrogenation of sugars was carried out.

2. Experimental

2.1 Raw materials

2.1.1 Wheat bran

Wheat bran was supplied by Emilio Esteban S.A., a cereal milling industry located in Valladolid (Spain), and used in fractionation experiments after a destarching process. The main components of destarched wheat bran were cellulose (15.3%), hemicelluloses (38.0%), acid soluble lignin (21.5%), starch (2.1 %), protein (14.5%) and ash (3.2%). The hemicellulosic fraction, mainly arabinoxylans, was isolated by hydrothermal fractionation. The fractionation was carried out at 180 ºC and 10 minutes using $RuCl_3$/Al-MCM-48 as catalyst. Further details are provided in our previous work (Sánchez-Bastardo et al., 2017).

2.1.2 Wheat bran hydrolysate

After the fractionation of wheat bran, the hydrolysis of hemicelluloses into C_5 sugars was performed under hot compressed water conditions at 180 ºC, 15 minutes and using $RuCl_3$/Al-MCM-48 as catalyst, as reported previously (Sánchez-Bastardo and Alonso, 2017).

The composition of the hydrolysate after fractionation and hydrolysis is shown in Table 2. Other sugars (*i.e.* galactose and mannose) and degradation products (*i.e.* 5-HMF, formic acid and acetic acid) were present in minor amounts hard to quantify and hence omitted. Starch and β-glucans were not detected.

Table 2. Composition of wheat bran hydrolysate.

Component	Concentration (ppm)
Sugars	
Xyl	5594 ± 53
Ara	2829 ± 39
Glc	767 ± 21
Degradation products	
Furfural	275 ± 19
Proteins	945 ± 36
Inorganic elements	
Mg	62 ± 2
Ca	13 ± 1
K	69 ± 3
S	4 ± 1

2.2 Chemicals

D-xylose (≥ 99%), L-arabinose (≥ 99%) and D-glucose (≥ 99.5%) were provided by Sigma Aldrich. Analytical standards used for HPLC purposes (D-cellobiose (≥ 98%), D-galactose (≥ 99%), D-mannose (≥ 99%), D-fructose (≥ 99%), 5-(hydroxymethyl)furfural (≥ 99%), furfural (≥ 99%), DL-glyceraldehyde (≥ 90%), glycolaldehyde (≥ 99%), lactic acid (≥ 85%), formic acid (≥ 98%), acetic acid (glacial, ≥ 99%), levulinic acid (≥ 98%), acrylic acid (anhydrous, ≥ 99%), pyruvaldehyde (40% in water), xylitol (≥ 99%), L-arabitol (≥ 98%), D-sorbitol (≥ 98%), D-mannitol (≥ 98%), galactitol (≥ 99%), glycerol (≥ 99%), ethylene glycol (≥ 99.5%), propylene glycol (≥ 99%) and furfuryl alcohol (≥ 98%)) were also purchased from Sigma Aldrich. Sodium dihydrogen phosphate dihydrate (Reag. Ph. Eur.), 1-octanol (anhydrous, ≥ 99%), Aliquat® 336, Amberlyst® 15 (hydrogen

form) and Amberlite® IRA-96 (free base) were obtained as well from Sigma-Aldrich. Sulfuric acid (96%) and sodium hydroxide were supplied by PanReac AppliChem. Phenylboronic acid (≥ 98%) from Alfa Aesar and *ortho*-hydroxymethyl phenylboronic acid (98%) from abcr were used.

ZSM-5 zeolite (SiO_2/Al_2O_3 = 80) was used as catalyst support and acquired in Zeolyst International. The ruthenium precursor of the Ru/H-ZSM-5 catalyst was ruthenium (III) chloride supplied by Strem Chemicals Inc. Nitrogen (99.99 %) and hydrogen (99.99 %) from Carburos Metálicos were used for hydrogenation experiments.

2.3 Recovery and purification of sugars from wheat bran hydrolysates

In this research, the isolation of C_5 sugars from a wheat bran hydrolysate using anionic extraction of saccharides, followed by back-extraction and a further purification process by means of ion exchange resins was studied. Experiments with model mixtures of sugars were also performed to determine the extractability of the sugars. Figure 4 summarizes the proposed process for the purification of sugars from wheat bran hydrolysates.

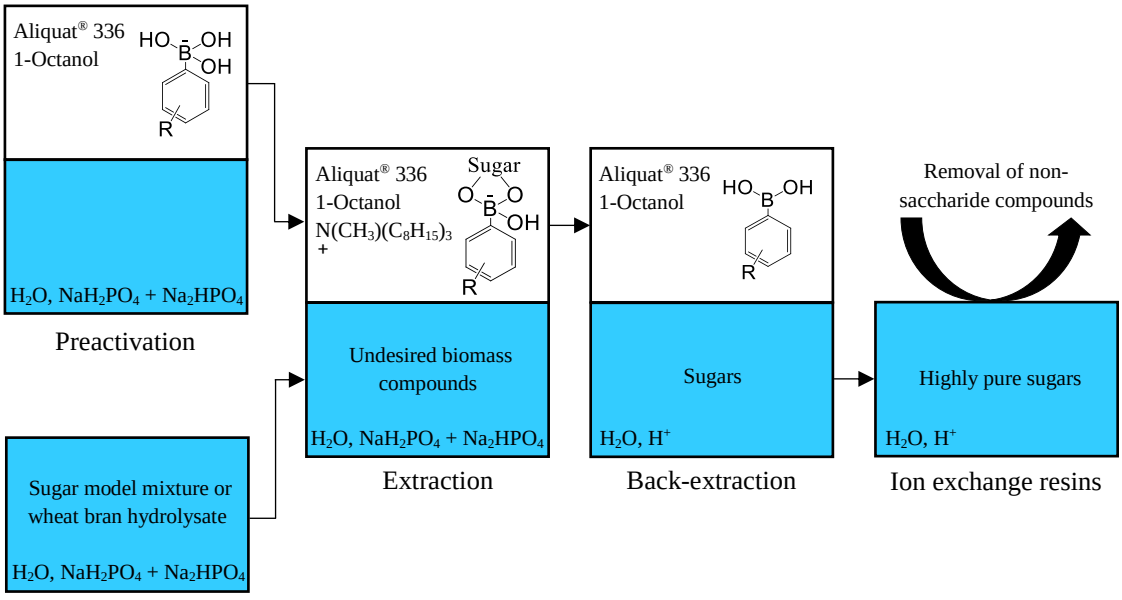

Figure 4. Scheme of the purification process of sugars from wheat bran hydrolysates.

Prior to the recovery of sugars, the hydrolysate or the initial model mixture were prepared in a phosphate buffer to maintain a desired pH value under which the complexes formed between the sugars and the boronic acid are stable. $NaH_2PO_4 \cdot 2H_2O$ was added to the initial aqueous solution and the pH was adjusted at 7.5 by dropwise addition of 4 M NaOH solution. Typically, this process comprises three steps: i) preactivation of the organic phase, ii) extraction of sugars into the organic phase and iii) back-extraction of the sugars in an acidic solution. First, an organic phase containing a mixture of a boronic acid and a quaternary ammonium salt (Aliquat® 336) dissolved in 1-octanol was preactivated by stirring with a buffer phosphate (NaH_2PO_4 + Na_2HPO_4) at an initial pH of 7.5 for 30 minutes. In all the experiments, an equimolar concentration of boronic acid/Aliquat® 336 was used. Aliquat® 336 is required to increase the solubility of the boronic acid in the organic solvent (1-octanol in this case). In addition to this, Aliquat® 336 creates a bulky amine cation needed for an efficient anionic extraction of the sugar-boronic acid complexes (Delidovich and Palkovits, 2016). Thereafter, the extraction of sugars was performed. The pretreated organic phase was stirred with the sugars aqueous solution (a model mixture or wheat bran hydrolysate) at 750 rpm for 1 hour. Centrifugation at 7000 rpm for 1 minute was performed to split the organic and aqueous phases. The organic phase containing the sugars complexes was then treated with a sulfuric acid solution at 750 rpm for 30 minutes to back-extract the sugars. The whole process was carried out at room temperature and using the same volume of organic and aqueous phases in each step. Additionally, a post-treatment after back-extraction with different ion exchange resins (Amberlyst® 15 and Amberlite® IRA-96) was done to increase the purity of the sugars. The aqueous solution was diluted 10-fold and stirred with Amberlyst® 15 (20 mg resin/1 mL solution) for 30 minutes. The solution was then separated by centrifugation and stirred for 1 hour with Amberlite® IRA-96 (50 mg resin/1 mL solution). The liquid was again

recovered by centrifugation. Before the hydrogenation experiments, the pH of the purified sugars solution was adjusted at 7.0 with a NaOH solution. Then the solution was frozen and lyophilized to achieve the sugars concentration prior to the 10-fold dilution.

2.4 Catalytic hydrogenation of purified sugars

After the purification step described in Section 2.3, the catalytic hydrogenation of the sugars over a ruthenium catalyst (Ru/H-ZSM-5) was studied. Likewise, some preliminary hydrogenation tests were performed with sugar model mixtures. A commercial stainless-steel high-pressure reactor (30 mL, Berghoff® BR-25) was used for the hydrogenation experiments. In a typical experiment, the reactor was loaded with the catalyst and flushed with nitrogen and then with hydrogen at room temperature. An initial pressure of hydrogen was fixed, and the reactor was then heated up to 100 ºC, which is the operating temperature in the hydrogenation experiments. Once the desired reaction temperature was reached, 10 mL of the sugar-rich solution were pumped (PU-2080 Plus, Jasco) into the reactor and stirred at 1400 rpm during the reaction period. The H_2 pressure was adjusted to 50 bar after pumping by opening the outlet valve. At the end of the experiment, the reactor was quickly cooled down, the pressure released, and the product filtered to separate the liquid from the solid catalyst.

2.5 Liquid phase analyses

2.5.1 Sugars, degradation products and sugar alcohols

The identification and quantification of sugars, degradation products and sugar alcohols in the aqueous phases were performed by High Performance Liquid Chromatography (HPLC). Prior to these analyses, the samples were filtered through a nylon syringe filter (pore size 0.22 μm, FILTER-LAB). HPLC analyses were carried out using a chromatography system consisting of an isocratic pump (Waters 1515), an automatic injector (Waters 717) and two detectors (RI detector, Waters 2414 and UV-Vis detector,

Waters 2487). These devices were purchased from Waters Corporation. Three HPLC columns were used for the determination of the different compounds: Supelcogel Pb (Supelco), SH1011 (Shodex) and SC1211 (Shodex). The products analyzed with each column and the operating conditions are summarized in Table 3.

Table 3. Operating conditions of the different HPLC columns used in this work.

Parameter	HPLC Column		
	Supelcogel Pb	SH1011	SC1211
Compounds analyzed	Sugars	Degradation products	Sugar alcohols
Furnace temperature (°C)	85	50	90
Detector temperature (°C)	35	35	35
Mobile phase	Milli-Q water	H_2SO_4 0.01 N in Milli-Q water	H_2O/CH_3CN (65/35 v/v)
Flow rate (mL min^{-1})	0.5	0.8	0.5
Detector	IR	IR and UV-Vis (254 nm for 5-HMF and 260 nm for furfural)	IR

The extraction and back-extraction yields in the purification process were calculated using the equations 1 – 2:

$$\% \text{ Extraction yield}_i = \frac{m_{i,0} - m_{i,E}}{m_{i,0}} \times 100 \quad \text{(Eq. 1)}$$

$$\% \text{ Back-extraction yield}_i = \frac{m_{i,BE}}{m_{i,0} - m_{i,E}} \times 100 \quad \text{(Eq. 2)}$$

where $m_{i,0}$, $m_{i,E}$ and $m_{i,BE}$ are the amounts of the component *i* in the initial phase and in the aqueous phases after extraction and back-extraction, respectively.

The conversion of sugars, the yield and selectivity into the corresponding alcohols in the hydrogenation experiments were calculated according to the equations 3 – 7:

$$\% \text{ Sugar conversion} = \frac{n_{sugar,0} - n_{sugar,f}}{n_{sugar,0}} \times 100 \quad \text{(Eq. 3)}$$

$$\% \text{ Pentitols yield} = \frac{n_{pentitols,f}}{n_{C5\ sugars,0}} \times 100 \quad \text{(Eq. 4)}$$

$$\% \text{ Pentitols selectivity} = \frac{n_{pentitols,f}}{n_{C5\ sugars,0} - n_{C5\ sugars,f}} \times 100 \quad \text{(Eq. 5)}$$

$$\% \text{ Sorbitol yield} = \frac{n_{sorbitol,f}}{n_{glucose,0}} \times 100 \quad \text{(Eq. 6)}$$

$$\% \text{ Sorbitol selectivity} = \frac{n_{sorbitol,f}}{n_{glucose,0} - n_{glucose,f}} \times 100 \quad \text{(Eq. 7)}$$

where $n_{sugar,0}$ and $n_{sugar,f}$ are the moles of each sugar before and after the hydrogenation reaction, respectively; $n_{C5\ sugars,0}$ and $n_{C5\ sugars,f}$ are the initial and final moles of xylose + arabinose, respectively; $n_{glucose,0}$ and $n_{glucose,f}$ are the initial and final moles of glucose, respectively; $n_{pentitols,f}$ are the moles of xylitol + arabitol formed from xylose + arabinose; and $n_{sorbitol,f}$ are the moles of sorbitol formed from glucose.

2.5.2 Total Organic Carbon (TOC)

The percentage of each component in the final aqueous phase after back-extraction (before and after the treatment with ion exchange resins) was calculated in terms of Total Organic Carbon (TOC) (Eq. 8). This analysis was performed using a Shimadzu TOC-VCSH equipment.

$$\% \text{ i} = \frac{C_i}{TOC} \times 100 \quad \text{(Eq. 8)}$$

where *i* represents the component *i*, C_i is the carbon content of the component *i* (g) and TOC is the value given by Total Organic Carbon (g).

2.5.3 Inorganic elements

Wheat bran contains different inorganic elements (namely, Ca, Mg, K and S) which may be dissolved in water during the fractionation step. Inductively Coupled Plasma-Atomic Emission Spectrometry (ICP-AES) was performed on a Varian Liberty RL sequential ICP-atomic emission spectrometer to quantify Ca, Mg and K in the initial hydrolysate and in the aqueous phases after extraction and back-extraction. In the same way, boron

(B) was analyzed in the aqueous phases to determine the leaching of boronic acid from the organic phase into the aqueous phase.

The content of S was determined by Ion exchange Chromatography (IC) on a Metrohm device composed by a pump for the mobile phase (709 IC), a pump for the ionic suppressor (752 Pump Unit) and a conductivity detector (732 IC detector). The column used was Metrosep Asupp4 250 and the mobile phase consisted of 1.8 mmol of carbonates and 1.7 mmol of bicarbonates.

2.5.4 Proteins

The nitrogen content in the different aqueous phases was determined by Kjeldahl method according to the standard procedure AOAC 984.13 (Hames et al., 2008). A nitrogen to protein conversion factor of 5.7 for wheat bran was used to determine the amount of protein (Hames et al., 2008; Maes and Delcour, 2002; Seyer and Gélinas, 2009). Likewise, the carbon content in the proteins was calculated using a factor of 0.53 g C per g of protein (Rouwenhorst et al., 1991).

2.5.5 Lignin derivatives

Acid soluble lignin was analyzed qualitatively in the aqueous phases after an acid hydrolysis described previously by Sluiter et al. (2008). It was determined by measuring the maximum absorbance of the sample between 240-320 nm with an UV-Visible spectrophotometer (Shimadzu UV-2550) (Reisinger et al., 2014).

2.6 Catalyst synthesis and characterization

2.6.1 Preparation of Ru/H-ZSM-5 catalyst

The ZSM-5 zeolite (SiO_2/Al_2O_3 = 80) used as the catalyst support was purchased in ammonium form. The protonation of the zeolite to obtain H-ZSM-5 was done by calcination at 550 ºC for 5 hours at a heating rate of 5 ºC min^{-1} from 80 to 550 ºC (in general, $Z\text{-}NH_4^+ \rightarrow Z\text{-}H^+ + NH_3\uparrow$) (Schmidt, 2006). The ruthenium catalyst supported on

H-ZSM-5 (SiO_2/Al_2O_3 = 80) was then prepared by wetness impregnation method (Romero et al., 2016). The ruthenium precursor ($RuCl_3$) and the calcined zeolite were placed separately into two glasses with water and sonicated for 10 minutes. Then they were mixed and sonicated for another 10 minutes. This suspension was heated up from 30 to 80 °C at a rate of 1 °C min^{-1}. After the complete evaporation of water, the catalyst was dried overnight at 105 °C. Prior to hydrogenation, the catalyst was reduced at 150 °C for 1 hour under a hydrogen flow at a rate of 2 ln min^{-1}. This reduction temperature was previously determined by Temperature Programmed Reduction (TPR) for similar catalysts (Romero et al., 2016).

2.6.2 X-Ray Diffraction (XRD)

X-Ray Diffraction (XRD) patterns for H-ZSM-5 and Ru/H-ZSM-5 were recorded on a Bruker Discover D8 diffractometer using Cu Kα radiation (λ = 0.15406 nm). The diffraction intensities were measured over an angle range of $2º < 2\theta < 90º$ with a step size of 0.020º and a step time of 0.80 s.

2.6.3 Nitrogen adsorption-desorption isotherms

Nitrogen adsorption-desorption isotherms were performed on an ASAP 2020 (Micromeritics, USA) to determine the surface area, the total pore volume (V_{pore}) and the average pore size (d_{pore}) of the catalysts. Prior to analysis, the samples were outgassed at 350 ºC overnight. The surface area was calculated by Langmuir model, whereas Horvath-Kawazoe method was used to determine the pore volume (from N_2 uptake at $P/P_0 \geq 0.99$) and the average pore size of the catalysts.

2.6.4 Inductively Coupled Plasma-Atomic Emission Spectrometry (ICP-AES)

The metal loading of Ru/H-ZSM-5 was determined by Inductively Coupled Plasma-Atomic Emission Spectrometry (ICP-AES) (Varian Liberty RL sequential ICP-AES) after a digestion of the sample.

3. Results and discussion

3.1 Catalyst characterization

XRD patterns of H-ZSM-5 and reduced Ru/H-ZSM-5 are shown in Supplementary information (Figure S1). H-ZSM-5 shows different diffraction peaks at 2θ = 8° – 9°, 23° – 25°, and 45°, which are characteristic of the MFI-type structure. The presence of Ru^0 on Ru/H-ZSM-5 is evidenced by the characteristic metallic diffraction peaks in the spectrum at 2θ = 42.1° and 44.0° (Li et al., 2004).

Figure S2 displays the nitrogen adsorption-desorption isotherms and pore size distribution (PSD) of H-ZSM-5 and Ru/H-ZSM-5. Figure S2A exhibits type I isotherms, typical of microporous materials, with a slight H4 hysteresis loop (ALOthoman, 2012). The pore size distribution (PSD) (Figure S2B) shows basically a unimodal microporous distribution centered at approximately 0.67 nm for both solids.

Table 4 gathers the textural properties of H-ZSM-5 and reduced Ru/H-ZSM-5. The specific surface area does not change significantly after the metal loading. The pore diameter is the same for both catalysts, but a decrease in the pore volume is observed in Ru/H-ZSM-5 and might be attributed to a partial blocking of the microporous due to a filling with ruthenium (Hu et al., 2015; Romero et al., 2016).

Table 4. Textural properties of H-ZSM-5 and Ru/H-ZSM-5.

Catalyst	Ru (wt.%)[a]	Surface area ($m^2 \cdot g^{-1}$)[b]	V_{pore} ($cm^3 \cdot g^{-1}$)[c]	d_{pore} (nm)[c]
H-ZSM-5	-	562	0.26	0.67
Ru/H-ZSM-5	2.0 ± 0.3	515	0.21	0.67

[a] Determined by ICP-AES.
[b] Determined by Langmuir model.
[c] Determined by Horvath-Kawazoe method.

The catalyst was tested for hydrogenation of sugars in a hydrolysate obtained via extraction of hemicelluloses and their hydrolysis. However, no reaction was observed

(see Section 3.4 for details). Therefore, we decided to recover xylose and arabinose from the hydrolysate using an anionic extraction with boronic acids.

3.2 Recovery of sugars from model mixtures

Prior to the purification of hydrolysates, the extractability of C_5 sugars from model mixtures in a phosphate buffer at pH 7.5 was studied following the scheme represented in Figure 4. Xylose and arabinose were chosen for the investigation of model mixtures since they are the major saccharides in the hydrolysates obtained from wheat bran (Table 2).

First, two different boronic acids, namely PBA and HMPBA, were tested. The results of the experiments to compare the efficiency of the extraction by PBA and HMPBA are shown in Figure 5. For the same boronic acid concentration, the amount of sugars extracted with HMPBA was higher than with PBA. In a previous work, HMPBA has also demonstrated to be more efficient than PBA for the extraction of saccharides (Delidovich and Palkovits, 2016). The complexation constants of HMPBA with sugars are higher than the corresponding to PBA-sugars. This is related to a lower pK_a of HMPBA and the formation of an intrinsic hydrogen bond between HMPBA and saccharides (Bérubé et al., 2008; Delidovich and Palkovits, 2016; Dowlut and Hall, 2006). As expected, a higher concentration of boronic acid enables a higher amount of sugars extracted into the organic phase. Additionally, xylose and arabinose were extracted basically in the same proportion, which is due to the similar complexation constants of both sugars with boronic acids (Nicholls and Paul, 2004; Van der Berg, 1994). The back-extraction of the sugars was performed by an acidic solution of 0.25 M H_2SO_4. In all the cases, 100% of both sugars was recovered since the complexes are no longer stable under acidic conditions.

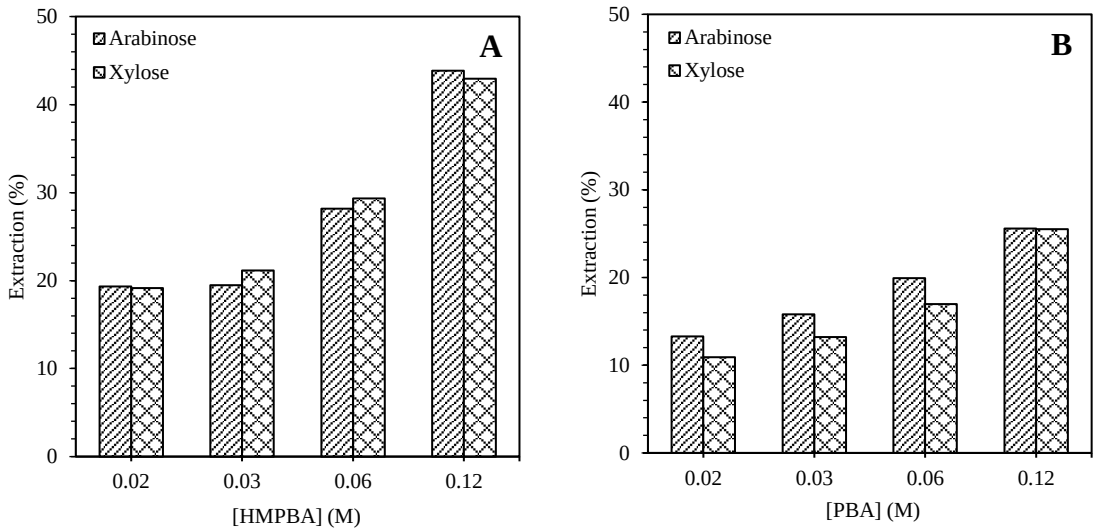

Figure 5. Extraction of arabinose and xylose with different concentrations of boronic acid: A) with HMPBA and B) with PBA.

Prior to the extraction of sugars, the organic phase was pretreated with a phosphate buffer at a pH_0 7.5. The preactivation of the organic phase was demonstrated to be very important in previous studies to improve the extraction of saccharides (Delidovich and Palkovits, 2016; Karpa et al., 1997). During this pretreatment, the pH of the buffer phosphate slightly decreased due to the transfer of hydroxyl groups from the aqueous to the organic phase. These OH^- groups are the responsible for the ionization of boronic acid, which enables the formation of the complexes with sugars.

The feasibility of obtaining more concentrated sugar solutions after the back-extraction was also studied (Figure 6). To do so, the organic phase was saturated with sugars by performing several extractions. Each extraction was carried out by stirring the same organic phase with a new sugar solution every time. The amount of the extracted sugars was very similar for each of these successive runs. However, the initial concentration of xylose was higher than arabinose (imitating a real hydrolysate), resulting therefore in a greater amount of xylose in the organic phase than arabinose after each extraction (Figure 6A). The stripping of the sugars was performed with a solution 0.25 M H_2SO_4.

Nevertheless, this acid concentration was not enough to recover all the sugars, but only around 60%. A higher H_2SO_4 concentration (0.50 M) was tested to improve the amount of the back-extracted sugars. In this case, the sugars were completely recovered into the acidic solution, which gave rise to a sugar solution ~2.4 times more concentrated than the initial (Figure 6B).

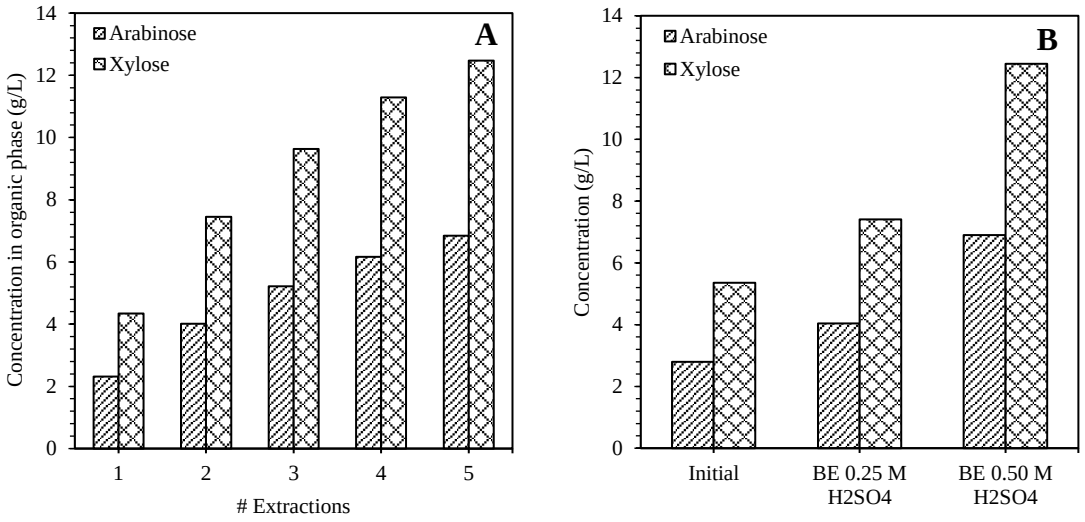

Figure 6. Concentration of sugar solutions by several extractions (Extraction with 0.5 M HMPBA): A) amount of sugars in the organic phase after each extraction and B) amount of sugars in the initial and final aqueous solutions after back-extraction with 0.25 M and 0.50 M H_2SO_4.

3.3 Purification of sugars from wheat bran hydrolysates

3.3.1 Behavior of the different compounds in the purification sequence

3.3.1.1 Sugars

The hydrolysates obtained after fractionation of wheat bran and hydrolysis of hemicelluloses were used for investigating the isolation of sugars by anionic extraction. HMPBA was shown to be more efficient than PBA for the recovery of sugars in model mixtures and therefore tested in real hydrolysates. For a given HMPBA concentration, xylose and arabinose were extracted approximately in the same extension, as it happened in model mixtures. However, the extraction of glucose was quite lower than that of C_5

sugars. This fact is explained because the complexation constant with boronic acids is similar for xylose and arabinose and at the same time, higher than that for glucose (Brennan et al., 2010; Nicholls and Paul, 2004; Soh et al., 2002; Tong et al., 2001; Van der Berg et al., 1994). A higher extraction of xylose and arabinose results in a higher ratio C_5 sugars/glucose, which will probably give rise to a solution rich in pentitols after the final hydrogenation step.

The concentration of HMPBA was varied to optimize the extraction of C_5 sugars (Figure 7). At a concentration of 0.25 M, the amounts of glucose, xylose and arabinose extracted were 29%, 57% and 60%, respectively. An improvement in the sugars extraction (glucose: 53%, xylose: 79%, arabinose: 82%) was obtained with a higher HMPBA concentration of 0.50 M. Nevertheless, a further increase in the boronic acid concentration up to 0.75 M did not practically enhance the recovery of C_5 sugars but a more significant amount of glucose was extracted (glucose: 66%, xylose: 83%, arabinose: 84%). In order to achieve a high recovery of the C_5 saccharides simultaneously keeping a reasonably high ratio of C_5/C_6 sugars, a concentration of 0.50 M HMPBA was chosen as an optimum. 100% of sugars were finally recovered in an acidic solution by performing back-extraction with 0.25 M H_2SO_4.

To investigate the extraction mechanism of sugars, two different blank experiments without boronic acid were carried out using the following organic phases: Aliquat® 336 in 1-octanol and only 1-octanol. No sugars were extracted into the organic phase after these experiments. This implies that sugars are chemically extracted by forming a complex with the boronic acid, and not by physical extraction.

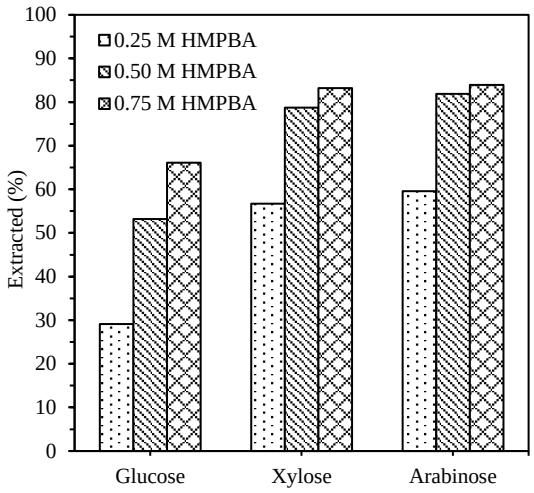

Figure 7. Influence of HMPBA concentration on sugars extraction from wheat bran hydrolysates.

3.3.1.2 Degradation products in initial wheat bran hydrolysate

Furfural was also analyzed in the aqueous phases after extraction and back-extraction in the previous experiments. The same percentage of furfural (around 80%) was extracted no matter the HMPBA concentration. This trend was also observed in the two blank experiments using Aliquat® 336/1-octanol and 1-octanol. Therefore, unlike sugars, furfural was physically extracted. During the stripping, only around 20 – 25% of furfural was recovered. This implies that the final aqueous phase contains around 80 – 85% less furfural than the initial hydrolysate, resulting in a higher purity of the sugars. As mentioned before, other minor compounds such as acetic acid, formic acid and 5-HMF were also present in the initial hydrolysate. The concentrations of all of them were so low that it was impossible to quantify them accurately. However, none of these products were identified even in small amounts in the aqueous phases after extraction and back-extraction. Apparently, they were extracted and remained in the organic phase. The extraction mechanism of these compounds may be explained by their behavior in the blank experiments (with 1-octanol and Aliquat® 336/1-octanol). Acetic and formic acid may have been extracted by a reactive mechanism with Aliquat® 336, as they remained

in the initial hydrolysate in the experiment with 1-octanol, but not when the organic phase consisted of a mixture Aliquat® 336/1-octanol. However, 5-HMF was probably extracted due to its higher distribution in organic solvents (1-octanol), since no 5-HMF was detected in the hydrolysate after extraction in any of the two blank experiments. This is accordant with the results previously reported by Grzenia et al. (2010).

3.3.1.3 Inorganic elements

Inorganic elements, such as Ca, Mg, K and S, may be part of the composition of different agricultural biomass as they are required for their growth and survival (Dhepe and Sahu, 2010). In our case, they are present in the wheat bran hydrolysate (Table 2) and their removal may be critical for a good performance in the subsequent hydrogenation step.

In the experiments performed with and without HMPBA, the inorganic compounds remained in the initial hydrolysate. They were not extracted into the organic phase and consequently they were not present in the aqueous phase after the stripping of sugars (Table 5). Inorganic compounds are more soluble in polar than in nonpolar solvents (Katzin, 1957). Water is one of the most common polar solvents, whereas the relative polarity of 1-octanol is 0.537. For this reason, inorganic elements were not extracted and remained in the initial hydrolysate.

In the event that these elements may cause the deactivation of the catalyst used in the hydrogenation reactions, this purification process is suitable for their removal.

Table 5. Distribution of inorganic elements in the hydrolysate and in the aqueous phases after extraction and back-extraction.

Experiment		Inorganic elements (ppm)			
		Ca	Mg	K	S
Initial hydrolysate		13	62	69	4
0.25 M HMPBA	Extraction	12	63	70	5
	Back-extraction	ND	ND	ND	*
0.50 M HMPBA	Extraction	12	65	76	4
	Back-extraction	ND	ND	ND	*
0.75 M HMPBA	Extraction	12	67	71	4
	Back-extraction	ND	ND	ND	*
1-octanol	Extraction	13	62	69	3
	Back-extraction	ND	ND	ND	*
Aliquat® 336/1-octanol	Extraction	11	64	68	4
	Back-extraction	ND	ND	ND	*

* Sulfur detected after back-extraction corresponds to H_2SO_4 used for the recovery of sugars. This cannot correspond to S from the hydrolysate since the S content after extraction is the same as in the initial solution.

3.3.1.4 Proteins

Proteins are released during the first fractionation step of wheat bran. These proteins may cause the fouling of the catalyst in the final hydrogenation stage due to the coverage of the metal active sites (Bootsma et al., 2008; Elliot et al., 2004; Kim et al., 2005; Vilcocq et al., 2014). For that reason, the removal of proteins from the hydrolysate is an issue to consider before the hydrogenation of sugars. Proteins were analyzed in the aqueous phases after extraction and back-extraction. The trend observed in the experiments with and without HMPBA was virtually the same. Only 30% of the proteins in the initial hydrolysate were extracted into the organic phase. The low amount of proteins extracted is explained by the higher solubility of proteins in polar solvents (*i.e.* water) than in non-aqueous solvents (*i.e.* 1-octanol) (Chin et al., 1994). When proteins are in polar solvents, such as water, the presence of a charge at the protein surface makes them interact with water rather than with other protein molecules, leading to their solubilization. As a

consequence, proteins are solubilized preferably in polar than in low polar solvents (Alberts et al., 1998). After back-extraction, no proteins were detected in the liquid, and a protein-free solution suitable for hydrogenation was obtained.

3.3.1.5 Lignin derivatives

Table 6 shows the percentage of each component in terms of carbon in the final aqueous phase calculated according to Eq. 8.

Table 6. Composition of the final aqueous phase after back-extraction and back-extraction + treatment with Amberlyst® 15 and Amberlite® IRA-96.

Experiment		% g C/TOC			
		Sugars	Furfural	Proteins	NI
0.25 M HMPBA	Back-extraction	70	1	ND	29
	Back-extraction + Resins	90	1	ND	8
0.50 M HMPBA	Extraction	70	1	ND	30
	Back-extraction + Resins	90	1	ND	9
0.75 M HMPBA	Extraction	69	1	ND	30
	Back-extraction + Resins	88	1	ND	12

After the back-extraction, a final aqueous solution with a high recovery of sugars, traces of furfural and free of inorganic elements and proteins was obtained. Nonetheless, the purity in sugars was limited to ~70%, and still ~30% of the carbon compounds were not identified. After a treatment with Amberlyst® 15 and Amberlite® IRA-96, the sugars purity improved up to ~90% and only ~10% of the carbon products remained unknown. The HPLC analysis before and after the post-treatment with resins revealed that no sugars and furfural were adsorbed on these resins. Therefore, the carbon compounds removed from the final solution may correspond to lignin derivatives (*i.e.* aromatic compounds) solubilized during wheat bran fractionation. Several authors have already claimed the efficiency of ion exchange resins to remove lignin compounds from biomass hydrolysates (Vázquez et al., 2006; Víctor-Ortega et al., 2016). To prove this fact, the acid soluble

lignin was analyzed qualitatively in the aqueous samples after extraction, back-extraction and the treatment with resins (Figure 8). These analyses were performed with an UV-spectrophometer after an acid hydrolysis (Sluiter et al., 2008). The maximum absorbance between 240 – 320 nm is attributed to acid soluble lignin (Reisinger et al., 2014).

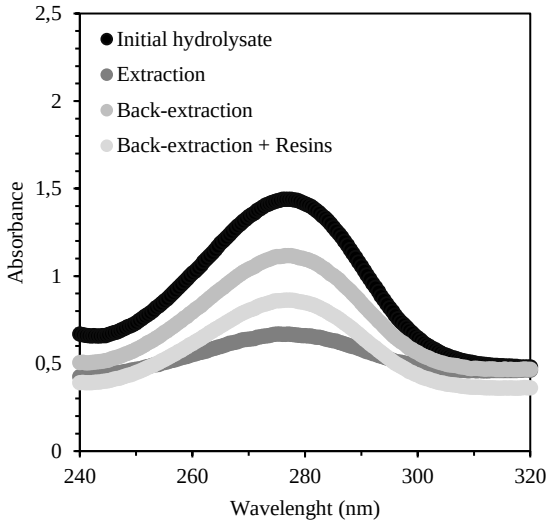

Figure 8. Absorbance spectra of a sample after extraction, back-extraction and before and after the treatment with Amberlyst® 15 and Amberlite® IRA-96.

In all the experiments, the maximum absorbance in the aqueous phase after extraction was remarkably lower than in the initial hydrolysate. However, this absorbance increased again after the back-extraction. These results demonstrate that some ex-lignin compounds were extracted into the organic phase and then part of them were recovered during the stripping. As reported in a previous work (Grzenia et al., 2008), the extraction of a significant amount of lignin into the organic phase is attributed to the presence of 1-octanol. Interestingly, the maximum absorbance decreased about ~20% in the samples after the use of the resins. This can be related to the adsorption of some lignin products on them which results in a high purity sugars solution. After the process with Amberlyst® 15 and Amberlite® IRA-96, the carbon mass balance closes at ~90%. Moreover, this 90% corresponds basically to the percentage of sugars. The unknown products (~9%) will probably correspond to some lignin derivatives not adsorbed on the resins, as the

maximum absorbance between 240 – 320 nm is still representative after the use of these materials.

3.3.2 Summary of purification results

Figure 9 displays the composition in terms of carbon of the initial hydrolysate and after the complete purification process. After back-extraction, the hydrolysate was diluted 10-fold for a suitable performance of the resins. In order to get the same concentration as before the use of the resins, the purified hydrolysate was lyophilized and pH adjusted at 7.0 prior to hydrogenation experiments. Figure 9B shows the composition of the purified hydrolysate after this posttreatment. The purity of sugars increased from 64% in the initial hydrolysate up to 90% after the purification step.

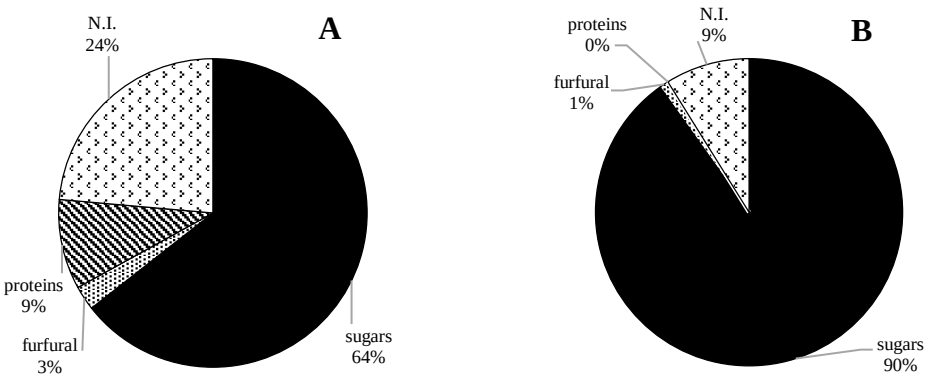

Figure 9. A) Purity of the initial hydrolysate and B) purity after the purification process (experiment with 0.50 M HMPBA) based on carbon balance.

3.3.3 Organic phase recycling

The feasibility of the whole process depends not only on the ability to purify sugars but also on the possibility of recycling the organic phase. Table 7 shows the extraction yield of the different compounds with a fresh and a reused organic phase. Not significant differences were appreciated between the first and the second run. The good performance of the organic phase after recycling is related to the no leaching of the boronic acid along

the process. Boron (B) was quantified in the aqueous phases after preactivation, extraction and back-extraction, and the leaching of B was determined to be less than 2% in all the experiments. Therefore, it can be concluded that boronic acid remains in the organic phase, which enables a successful recycling.

Table 7. Extraction of the different compounds using fresh and recycled organic phase.

Experiment		Extraction (%)				
		Glucose	Xylose	Arabinose	Furfural	Proteins
0.50 M HMPBA	Fresh	53	79	82	80	34
0.50 M HMPBA	Recycling	59	81	82	70	38

To sum up, hydrolysates from wheat bran were successfully purified by anionic extraction of sugars using HMPBA followed by the recovery of sugars in an acidic solution and a post-treatment with Amberlyst® 15 and Amberlite® IRA-96. The purified hydrolysate consists of a sugar mixture (mainly xylose and arabinose) with a minor amount of furfural and free of inorganic elements and proteins. Hydrolysates with a high purity degree in sugars are required for the next hydrogenation step in order to obtain a high selectivity into sugar alcohols and guarantee a good performance of the metal catalyst. We also demonstrated that a reuse of the organic phase is possible without loss in the efficiency of the process.

3.3.4 Sustainability of the proposed purification approach

The proposed recovery approach presents a multistep procedure utilizing auxiliary chemicals. In this regard, assessment of sustainability of the proposed method is of interest and can be performed, for example, by using a simple E factor (sEF) (Sheldon, 2017). The sEF can be calculated a formula: sEF = **(**total mass of raw materials + total mass of reagents - total mass of products) ⁄ total mass of products. Calculation of sEF does not include water and solvents (Sheldon, 2017). The organic phase can also be excluded from the formula since it can be easily recycled. Additionally, we do not take

into account the mass of the resins because they can be potentially regenerated and reused. Thus, the following estimation of the sEF can be performed considering 1 mL of a hydrolysate:

sEF = [0.00956 g (a total mass of the organics and inorganics in hydrolysate according to Table S1) + 0.0655 g (a mass of NaH_2PO_4+Na_2HPO_4 added to the hydrolysate before extraction) + 0.0245 g (a mass of H_2SO_4 used for back-extraction) – 0.007146 g (a mass of obtained sugars)] / [0.007146 g (a mass of obtained sugars)] = 12.9

Though the obtained value of the sEF is rather high, we believe that further developments can improve the sustainability of the proposed method. Thus, in this work we optimized neither the concentration of phosphates nor H_2SO_4 concentration rather focusing on proof-of-concept for applying the proposed method for recovery of sugars from the hydrolysates. Taking into account the low concentration of monosaccharides in hydrolysates, a significantly lower concentrations of phosphates and sulfuric acid would be most probably sufficient for the recovery of sugars thus improving the sEF value.

3.4 Hydrogenation experiments

3.4.1 Hydrogenation of sugar model mixtures

First, we evaluated the activity of the Ru/H-ZSM-5 catalyst in the hydrogenation of sugar model mixtures into sugar alcohols. Ruthenium catalysts were chosen as they have demonstrated to be very active for hydrogenation of sugars in numerous works (Barbaro et al., 2016; Baudel et al., 2005; Dietrich et al., 2017; Ennaert et al., 2016; Faba et al., 2014; Guha et al., 2011; Hernández-Mejia et al., 2016; Herrera et al., 2012; Irmak et al., 2017; Kusema et al., 2012; Mishra et al., 2013; Müller et al., 2017; Murzin et al., 2015a, 2015b; Pham et al., 2016; Ribeiro et al., 2016, 2017a, 2017b; Simakova et al., 2016; Yadav et al., 2012; Yi and Zhang, 2012). The experiments involved xylose and arabinose, as major components of the purified hydrolysate, but also glucose, as it is present after

the purification. The temperature and H_2 pressure were 100 °C and 50 bar, respectively, in all the reactions. Figure 10 shows the results corresponding to the hydrogenation of model mixtures composed of xylose, arabinose and glucose. The yields of pentitols (xylitol + arabitol) and sorbitol were calculated according to the Eq. 4 and 6, respectively. Xylitol and arabitol may be formed from both xylose and arabinose (Figure 1), so the yield was evaluated in terms of total pentitols. Selectivity was in all the experiments ~100%, which means that C_5 sugars were converted only into xylitol and arabitol, and glucose into sorbitol. The formation of by-products (*e.g.* mannitol, levulinic acid, glycerol, ethylene glycol, propylene glycol or furfuryl alcohol) as reported in previous studies (Tathod and Dhepe, 2015) was not observed in any experiment. Furthermore, mass balances were above 98% in all the cases, corroborating the maximum selectivity into the alcohols of interest. Under the same experimental conditions, xylose and arabinose were hydrogenated more readily than glucose. This was previously reported by several authors (Elliot et al., 2004; Kobayashi et al., 2014; Tathod and Dhepe, 2015). Different catalysts loadings were tested (Figure 10). No sugars conversion and hence no alcohols production were observed in the blank experiments without catalyst. The maximum yield of pentitols was achieved at 100 °C after 10 minutes with a ratio of 0.015 grams of ruthenium per gram of total carbon in sugars. In the case of sorbitol, best results were obtained at 100 °C/15 min/0.06 g Ru g C^{-1} or at 100 °C/30 min/0.03 g Ru g C^{-1}. As we are in interested in the maximization of pentitols and minimization of hexitols, our optimum conditions were selected at 100 °C/10 min/0.015 g Ru g C^{-1}.

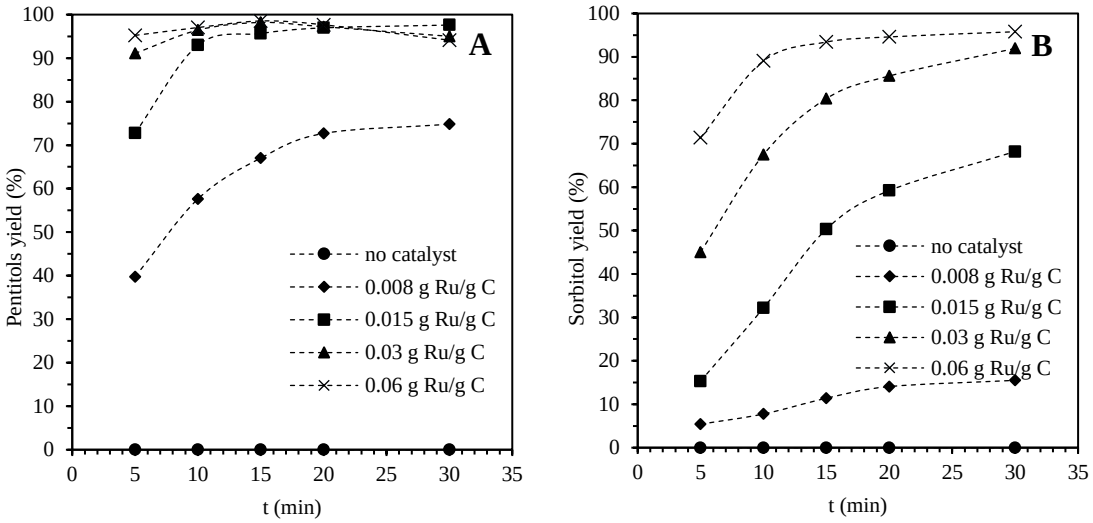

Figure 10. Influence of catalyst loading in hydrogenation of sugar model mixtures. Conditions: xylose + arabinose + glucose, Ru/H-ZSM-5, 100 °C, 50 bar H_2. A) Pentitols yield and B) sorbitol yield.

3.4.2 Hydrogenation of wheat bran hydrolysates before and after purification

After proving the high activity of Ru/H-ZSM-5 catalyst in the hydrogenation reactions of sugar model mixtures, an attempt to hydrogenate a real hydrolysate from wheat bran prior to purification was undertaken at 100 °C and 10 minutes (Figure 11).

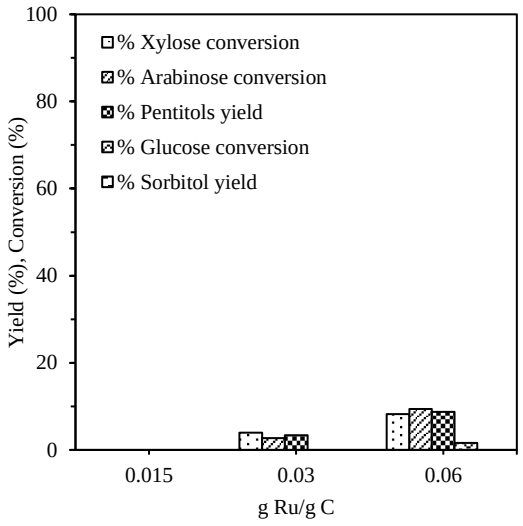

Figure 11. Hydrogenation of hydrolysates before purification. Conditions: Ru/H-ZSM-5, 100 °C, 10 min, 50 bar H_2.

Surprisingly, even with the highest catalyst loading, only a pentitols yield of ~9% was obtained. Sorbitol was not detected even in traces. In addition to this, the conversion of sugars was also negligible, and therefore, alternative reaction routes into other products were discarded.

Then, the hydrogenation of the sugars of a purified hydrolysate (composition given in Figure 12) was tested. The hydrogenation was successfully performed at 100 °C, after 10 minutes and using a catalyst loading corresponding to 0.06 g Ru g C^{-1} (Figure 13). Under these conditions, a high pentitols yield of ~70% was achieved. As expected, the production of sorbitol was quite lower (~13%). The samples were also analyzed to identify possible by-products, but not detectable amounts were observed.

A similar result was obtained for converting bio-2,3-butanediol into methyl ethyl ketone in the presence of H_2SO_4. Direct utilization of fermentation broths led to formation of humins only. After a purification using PBA, bio-2,3-butanediol could be successfully converted into methyl ethyl ketone in high yield (Drabo et al., 2017).

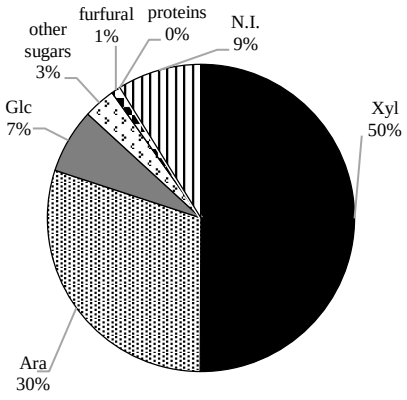

Figure 12. Composition of the purified hydrolysate based on carbon balance (lyophilized and at pH 7.0).

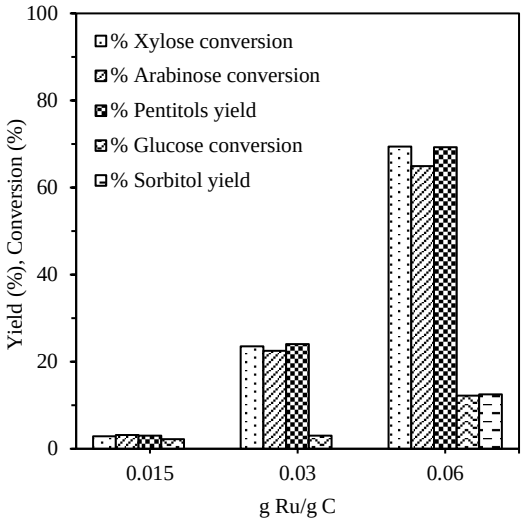

Figure 13. Hydrogenation of hydrolysates after purification. Conditions: Ru/H-ZSM-5, 100 °C, 10 min, 50 bar H_2.

The deactivation of Ru/H-ZSM-5 during the hydrogenation of the impure hydrolysate may be due to different contaminants which are potential catalyst poisons: inorganic elements (Ca, Mg, K or S) and/or proteins. Ca and Mg may deactivate the catalyst by pore plugging derived from salt precipitation. K may attack the catalyst support due to its alkali nature. And proteins may collapse the catalyst pores by precipitation of denatured forms. Not only pore plugging but also coverage of the metal active sites may occur due to these contaminants (Elliot et al., 2004). To investigate the deactivation mechanism of Ru/H-ZSM-5, different pretreatments to the initial hydrolysate followed by further hydrogenation were carried out. These pretreatments are summarized in Table 8:

Table 8. Pretreatments performed in the initial wheat bran hydrolysate.

Pretreatment	Removed compounds	Non-removed compounds
Activated carbon	S	Ca, Mg, K, proteins
Dowex® Monosphere® MR-450 UPW	Ca, Mg, K	S, proteins
Activated carbon + Dowex® Monosphere® MR-450 UPW	S, Ca, Mg, K	Proteins
Anionic extraction + Back-extraction + Amberlyst® 15 + Amberlite® IRA-96	S, Ca, Mg, K, proteins	-

We analyzed the composition of the hydrolysate after each pretreatment. Activated carbon was able to remove sulfur but the rest of the inorganic elements and proteins were still present in a significant amount. Activated carbon is known for its good properties to remove sulfur (Alhamed and Bamufleh, 2009; Ge et al., 2017; Hariz et al., 2014; Kumar and Srivastava, 2012; Lee et al., 2002) but not inorganic cations such as Ca, Mg or K (Roy, 2014). Dowex® Monosphere® MR-450 UPW (Sigma Aldrich) is a mixed bed ion exchange resin capable of deionizing water. After its use, no inorganic cations were detected but the amount of sulfur and proteins remained basically constant. We also performed a pretreatment with activated carbon followed by the use of Dowex® Monosphere®. As expected, no sulfur neither inorganic cations were found in the hydrolysate. However, a high percentage of the initial proteins remained in the solution. Therefore, the only pretreatment able to isolate the sugars from the proteins, besides the inorganic elements, was the anionic extraction of sugars followed by back-extraction and the subsequent purification with ion exchange resins (Amberlyst® 15 + Amberlite® IRA-96). After all these pretreatments, the corresponding hydrogenation experiments were carried out. The hydrogenation of sugars only took place in the latter case, *i.e.* when no proteins were present in the hydrolysate. The yield into pentitols in the hydrogenation experiments after the rest of the pretreatments was very similar to the obtained with the unpurified hydrolysate (~8 – 11%). From these results, we can conclude that proteins were the main responsible for the catalyst deactivation. The inorganic elements were probably in such low amounts which did not poison the metal catalyst. Elliot et al. (2004) made similar conclusions in a previous study. They tested the effect of different inorganic elements and a protein of wheat bran (peptone) in the hydrogenation of sugar model mixtures (xylose + glucose) over a ruthenium catalyst. They concluded that proteins were responsible for the catalyst poisoning. The high inhibitory effect of the proteins was

attributed to Maillard-type reactions which produce condensed structures. These structures act as potential poisons which block the active catalyst sites inhibiting the hydrogenation of sugars.

4. Conclusions

A purification process of C_5 sugars in hydrolysates from wheat bran followed by the catalytic hydrogenation of the sugars is proposed in this study. The method for purification is based on the recovery of sugars by anionic extraction with a boronic acid dissolved in an organic phase composed by a quaternary ammonium salt and 1-octanol. The purification procedure consists of four steps, including organic phase preactivation, sugars extraction from the hydrolysate into the organic phase, sugars recovery using an acidic solution and further refining of the final solution by ion exchange resins. First, the feasibility of the extraction of saccharides (xylose and arabinose) from model sugars solutions was studied with two different boronic acids (PBA and HMPBA). HMPBA appeared to be more efficient compared to PBA. Additionally, the possibility of concentrating sugars was considered by performing several extractions. The organic phase was saturated with sugars which were finally recovered after back-extraction, resulting in a solution ~2.4 times more concentrated than the initial one. The purification process of a real wheat bran hydrolysate was then studied. In the first step, sugars, furfural, part of the proteins and some lignin compounds were extracted into the organic phase. The inorganic elements (Ca, Mg, K, S) remained all in the initial hydrolysate. During the stripping, all the sugars, traces of furfural and part of the lignin derivatives were recovered. However, no proteins were back-extracted. It is also important to notice that xylose and arabinose were more easily extracted than glucose, which finally resulted in a higher C_5/C_6 sugars ratio. The ion exchange resins (Amberlyst® 15 + Amberlite® IRA-96) used after back-extraction removed a high percentage of the lignin products, and

consequently the purity in sugars in terms of carbon increased up to ~90%. This purification process is therefore suitable for obtaining highly pure C_5 sugars hydrolysates. The hydrogenation of sugars in the purified hydrolysate was further studied. First, the activity of the Ru/H-ZSM-5 catalyst was tested in the hydrogenation of sugar model mixtures. Different catalyst loadings over time were studied. A high conversion of the sugars and a 100% selectivity into the corresponding alcohols were obtained. Then, an attempt to hydrogenate a real wheat bran hydrolysate prior to purification was carried out but failed even with the highest catalyst loading. However, after purification, a high yield into pentitols of ~70% with 100% selectivity was achieved. The deactivation mechanism of the catalyst during the hydrogenation of real mixtures was further investigated. To do so, different pretreatments with activated carbon and a Dowex® resin were performed to remove the inorganic cations. Surprisingly, the hydrogenation did not take place after these treatments. With these pretreatments, only the inorganic cations were removed but proteins remained still in the hydrolysate. The results derived from these experiments show the deactivation of Ru/ZSM-5 caused by proteins, which can plug the pore and cover the metal active sites of the catalyst. This can be concluded because hydrogenation of sugars was only possible when no proteins were present in the hydrolysate, *i.e.* after the purification process by anionic extraction of sugars followed by back-extraction and the use of ion exchange resins.

References

Alberts, B., Bray, D., and Johnson, A. Essential Cell Biology: An introduction to the molecular miology of the cell. 1st ed., Garland Science: New York, 1998.

Alhamed, Y.A., and Bamufleh, H.S. Sulfur removal from model diesel fuel using granular activated carbon from dates' stones activated by $ZnCl_2$. *Fuel,* 88 (2009) 87–94.

ALOthoman, Z.A. A Review: Fundamental aspects of silicate mesoporous materials. *Materials,* 5 (2012) 2874–2902.

Arena, B.J. Deactivation of ruthenium catalysts in continuous glucose hydrogenation. *Applied Catalysis A: General,* 87 (1992) 219–229.

Barbaro, P., Liguori, F., and Moreno-Marrodan, C. Selective direct conversion of C_5 and C_6 sugars to high added-value chemicals by a bifunctional, single catalytic body. *Green Chemistry,* 18 (2016) 2935–2940.

Baudel, H.M., De Abreu, C.A.M., and Zaror, C.Z. Xylitol production via catalytic hydrogenation of sugarcane bagasse dissolving pulp liquid effluents over Ru/C catalyst. *Journal of Chemical Technology and Biotechnology,* 80 (2005) 230–233.

Bérubé, M., Dowlut, M., and Hall, D.G. Benzoboroxoles as efficient glycopyranoside-binding agents in physiological conditions: structure and selectivity of complex formation. *Journal of Organic Chemistry,* 73 (2008) 6471–6479.

Besson, M., and Gallezot, P. Deactivation of metal catalysts in liquid phase organic reactions. *Catalysis Today,* 81 (2003) 547–559.

Bootsma, J.A., Entfort, M., Eder, J., and Shanks, B.H. Hydrolysis of oligosaccharides from distillers grains using organic-inorganic hybrid mesoporous silica catalysts. *Bioresource Technology,* 99 (2008) 5226–5231.

Borg, Ø., Hammer, N., Enger, B.C., Myrstad, R., Lindvåg, O.A., Eri, S., Skagseth, T.H., and Rytter, E. Effect of biomass-derived synthesis gas impurity elements on cobalt Fischer-Tropsch catalyst performance including *in situ* sulphur and nitrogen addition. *Journal of Catalysis*, 279 (2011) 163–173.

Brennan, T.C.R., Datta, S., Blanch, H.W., Simmons, B.A., and Holmes, B.M. Recovery of sugars from ionic liquid biomass liquor by solvent extraction. *Bioenergy Research*, 3 (2010) 123–133.

Chandel, A.K., Da Silva, S.S., and Singh, O.V. Detoxification of lignocellulosic hydrolysates for improved bioethanol production. In *Biofuel Production - Recent Developments and Prospects*, Dr. Bernardes, M.A.D.S., (Ed.), InTech, 2011.

Chin, J.T., Wheeler, S.L., and Klibanov, A.M. On protein solubility in organic solvents. *Biotechnology and Bioengineering*, 44 (1994) 140–145.

Dasgupta, D., Bandhu, S., Adhikari, D.K., and Ghosh, S. Challenges and prospects of xylitol production with whole cell bio-catalysis: A review. *Microbiological Research*, 198 (2017) 9–21.

Delidovich, I., and Palkovits, R. Fructose production *via* extraction-assisted isomerization of glucose catalyzed by phosphates. *Green Chemistry*, 18 (2016) 5822–5830.

Delidovich, I., Gyngazova, M.S., Sánchez-Bastardo, N., Wohland, J.P., Hoppe, C., and Drabo, P. Production of keto-pentoses *via* isomerization of aldo-pentoses catalyzed by phosphates and recovery of products by anionic extraction. *Green Chemistry*, 20 (2018) 724–734.

Deng, W., Zhang, Q., and Wang, Y. Catalytic transformation of cellulose and its derived carbohydrates into chemicals involving C-C bond cleavage. *Journal of Energy Chemistry*, 24 (2015) 595–607.

Dhepe, P.L., and Sahu, R. A solid-acid-based process for the conversion of hemicellulose. *Green Chemistry*, 12 (2010) 2153–2156.

Dietrich, K., Hernández-Mejia, C., Verschuren, P., Rothenberg, G., and Shiju, N.R. One-pot selective conversion of hemicellulose to xylitol. *Organic Process Research and Development*, 21 (2017) 165–170.

Dowlut, M., Hall, and D.G. An improved class of sugar binding boronic acids, soluble and capable of complexing glycosides in neutral water. *Journal of the American Chemical Society*, 128 (2006) 4226–4227.

Drabo, P., Tiso, T., Heyman, B., Sarikaya, E., Gaspar, P., Förster, J., Büchs, J., Blank, L.M., and Delidovich, I. Anionic extraction for efficient recovery of bio-based 2,3-butanediol - a platform for bulk and fine chemicals. *ChemSusChem*, 10 (2017) 3252–3259.

Elliot, D.C., Peterson, K.L., Muzatko, D.S., Alderson, E.V., Hart, T.R., and Neuenschwander, G.G. Effects of trace contaminants on catalytic processing of biomass-derived feedstocks. *Applied Biochemistry and Biotechnology*, 113–116 (2004) 807–825.

Ennaert, T., Aelst, J.V., Dijkmans, J., De Clercq, R., Schutyser, W., Dusselier, M., Verboekend, D., and Sels, B.F. Potential and challenges of zeolite chemistry in the catalytic conversion of biomass. *Chemical Society Reviews*, 45 (2016) 584–611.

Ennaert, T., Feys, S., Hemdrikx, D., Jacobs, P.A., and Sels, B.F. Reductive splitting of hemicellulose with stable ruthenium-loaded USY zeolites. *Green Chemistry*, 18 (2016) 5295–5304.

Faba, L., Kusema, B.T., Murzina, E.V., Tokarev, A., Kumar, N., Smeds, A., Díaz, E., Ordóñez, S., Mäki-Arvela, P., Willför, S., Salmi, T., and Murzin, D.Y. Hemicellulose

hydrolysis and hydrolytic hydrogenation over proton- and metal modified beta zeolites. *Microporous and Mesoporous Materials,* 189 (2014) 189–199.

Ge, S., Liu, Z., Furuta, Y., and Peng, W. Characteristics of activated carbon remove sulfur particles against smog. *Saudi Journal of Biological Sciences,* 24 (2017) 1370–1374.

Gori, S.S., Raju, M.R., Fonseca, D.A., Satyavolu, J., Burns, C.T., and Nantz, M.H. Isolation of C-5 sugars from the hemicellulose-rich hydrolysate of distillers dried grains. *ACS Sustainable Chemistry and Engineering,* 3 (2015) 2452–2457.

Griffin, G.J. Purification and concentration of xylose and glucose from neutralized bagasse hydrolysates using 3,5-Dimethylphenylboronic acid and modified Aliquat 336 as coextractants. *Separation Science and Technology,* 40 (2005) 2337–2351.

Griffin, G.J., and Shu, L. Solvent extraction and purification of sugars from hemicellulose hydrolysates using boronic acid carriers. *Journal of Chemical Technology and Biotechnology,* 79 (2004) 505–511.

Grzenia, D.L., Schell, D.J., and Wickramasinghe, S.R. Membrane extraction for extraction of acetic acid from biomass hydrolysates. *Journal of Membrane Science,* 322 (2008) 189–195.

Grzenia, D.L., Schell, D.J., and Wickramsinghe, S.R. Detoxification of biomass hydrolysates by reactive membrane extraction. *Journal of Membrane Science,* 348 (2010) 6–12.

Guha, S.K., Kobayashi, H., Hara, K., Kikuchi, H., Aritsuka, T., and Fukuoka, A. Hydrogenolysis of sugar beet fiber by supported metal catalyst. *Catalysis Communications,* 12 (2011) 980–983.

Hames, B., Scarlata, C., and Sluiter, A. Determination of protein content in biomass. Laboratory Analytical Procedure (LAP). Technical Report NREL/TP-510-42625, 2008.

Hara, M., Nakajima, K., and Kamata, K. Recent progress in the development of solid catalysts for biomass conversion into high value-added chemicals. *Science and Technology of Advanced Materials,* 16 (2015) 034903.

Hariz, I.B., Ayni, F.A., and Monser, L. Removal of sulfur compounds from petroleum refinery wastewater through adsorption on modified activated carbon. *Water Science & Technology,* 70 (2014) 1376–1382.

Hernández-Mejia, C., Gnanakumar, E.S., Olivos-Suarez, A., Gascon, J., Greer, H., Zhou, W., Rothenberg, G., and Shiju, N.R. Ru/TiO_2-catalysed hydrogenation of xylose: the role of crystal structure of the support. *Catalysis Science and Technology,* 6 (2016) 577–582.

Herrera, V.A.S., Saleem, F., Kusema, B., Eränen, K., and Salmi, T. Hydrogenation of L-arabinose and D-galactose mixtures over a heterogeneous Ru/C catalyst. *Topics in Catalysis,* 55 (2012) 550–555.

Hu, H., Lyu, J., Cen, J., Zhang, Q., Wang, Q., Han, W., Rui, J., and Li, X. Promoting effects of MgO and Pd modification on the catalytic performance of hierarchical porous ZSM-5 for catalyzing benzene alkylation with methanol. *RSC Advances,* 5 (2015) 63044–63049.

Huang, Z., Chen, J., Jia, Y., Liu, H., Xia, C., and Liu, H. Selective hydrogenolysis of xylitol to ethylene glycol and propylene glycol over copper catalysts. *Applied Catalysis B: Environmental,* 147 (2014) 377–386.

Irmak, S., Canisag, H., Vokoun, C., and Meryemoglu, B. Xylitol production from lignocellulosics: Are corn biomass residues good candidates? *Biocatalysis and Agricultural Biotechnology,* 11 (2017) 220–223.

Karpa, M.J., Duggan, P.J., Griffin, G.J., and Freudigmann, S.J. Competitive transport of reducing sugars through a lipophilic membrane facilitated by aryl boron acids. *Tetrahedron*, 53 (1997) 3669–3678.

Katzin, L.I. Factors affecting the solution of inorganic salts in organic solvents. *Journal of Inorganic and Nuclear Chemistry*, 4 (1957) 187–204.

Kim, Y., Hendrickson, R., Mosier, N., and Ladisch, M.R. Plug-flow reactor for continuous hydrolysis of glucans and xylans from pretreated corn fiber. *Energy & Fuels*, 19 (2005) 2189–2200.

Kobayashi, H., Komanoya, T., Guha, S.K., Hara, K., and Fukuoka, A. Conversion of cellulose into renewable chemicals by supported metal catalysts. *Applied Catalysis A: General*, 409-410 (2011) 13–20.

Kobayashi, H., Yamakoshi, Y., Hosaka, Y., Yabushita, M., and Fukuoka, A. Production of sugar alcohols from real biomass by supported platinum catalyst. *Catalysis Today*, 226 (2014) 204–209.

Koganti, S., and Ju, L-K. *Debaryomyces hansenii* fermentation for arabitol production. *Biochemical Engineering Journal*, 79 (2013) 112–119.

Kumar, D.R., and Srivastava, V.C. Studies on adsorptive desulfurization by activated carbon. *Soil Air Water*, 40 (2012) 545–550.

Kusema, B.T., Faba, L., Kumar, N., Mäki-Arvela, P., Díaz, E., Ordóñez, S., Salmi, T., and Murzin, D.Y. Hydrolytic hydrogenation of hemicellulose over metal modified mesoporous catalyst. *Catalysis Today*, 196 (2012) 26–33.

Lee, S.H.D., Kumar, R., and Krumpelt, M. Sulfur removal from diesel fuel-contaminated methanol. *Separation and Purification Technology*, 26 (2002) 247–258.

Li, W., Ye, L., Long, P., Chen, J., Ariga, HAsakura, K., and Yuan, Y. Efficient Ru – Fe catalyzed selective hydrogenolysis of carboxylic acids to alcoholic chemicals. *RSC Advances,* 4 (2004) 29072–29082.

Liu, S., Okuyama, Y., Tamura, M., Nakagawa, Y., Imai, A., and Tomishige, K. Selective transformation of hemicellulose (xylan) into n-pentane, pentanols or xylitol over rhenium-modified iridium catalyst combined with acids. *Green Chemistry,* 18 (2016) 165–175.

Maes, C., and Delcour, J.A. Structural characterisation of water-extractable and water-unextractable arabinoxylans in wheat bran. *Journal of Cereal Science,* 35 (2002) 315–326.

Matsumoto, M., Ueba, K., and Kondo, K. Separation of sugar by solvent extraction with phenylboronic acid and trioctylmethylammonium chloride. *Separation and Purification Technology*, 43 (2005) 269–274.

McCabe, W.L., Smith, J.C., and Harriott, P. Units Operation of Chemical Engineering. 7th ed., McGraw Hills Chemical Engineering Series, 2004.

Mishra, D.K., Dabbawala, A.A., and Hwang, J-S. Ruthenium nanoparticles supported on zeolite Y as an efficient catalyst for selective hydrogenation of xylose to xylitol. *Journal of Molecular Catalysis A: Chemical,* 376 (2013) 63–70.

Morales, R., Campos, C.H., Fierro, J.L.G., Fraga, M.A., and Pecchi, G. Perovskite as nickel catalyst precursor – Impact on catalyst stability on xylose aqueous-phase hydrogenation. *RSC Advances,* 6 (2016) 67817–67826.

Morales, R., Campos, C.H., Fierro, J.L.G., Fraga, M.A., and Pecchi, G. Stable reduced Ni catalysts for xylose hydrogenation in aqueous medium. Catalysis Today, 310 (2018) 59–67.

Müller, A., Hilpmann, G., Haase, S., and Lange, R. Continuous hydrogenation of L-arabinose and D-galactose in a mini packed bed reactor. *Chemical Engineering and Technology*, 40 (2017) 2113–2122.

Murzin, D.Y., Kusema, B., Murzina, E.V., Aho, A., Tokarev, A., Boymirzaev, A.S., Wärna, J., Dapsens, P.Y., Mondelli, C., Pérez-Ramírez, J., and Salmi, T. Hemicellulose arabinogalactan hydrolytic hydrogenation over Ru-modified H-USY zeolites. *Journal of Catalysis*, 330 (2015a) 93–105.

Murzin, D.Y., Murzina, E.V., Tokarez, A., Shcherban, N.D., Wärna, J., and Salmi, T. Arabinogalactan hydrolysis and hydrolytic hydrogenation using functionalized carbon materials. *Catalysis Today*, 257 (2015b) 169–176.

Nicholls, M.P., and Paul, P.K.C. Structures of carbohydrate-boronic acid complexes determined by NMR and molecular modelling in aqueous alkaline media. *Organic & Biomolecular Chemistry*, 2 (2004) 1434–1441.

Pham, T.N., Samikannu, A., Rautio, A-R., Juhasz, K.L., Konya, Z., Wärna, J., Kordas, K., and Mikkola, J-P. Catalytic hydrogenation of D-xylose over Ru decorated carbon foam catalyst in a SpinChem® rotating bed reactor. *Topics in Catalysis*, 59 (2016) 1165–1177.

Putro, J.N., Soetaredjo, F.E., Lin, S-Y., Ju, Y-H., and Ismadji, S. Pretreatment and conversion of lignocellulose biomass into valuable chemicals. *RSC Advances*, 6 (2016) 46834–46852.

Rao, L.V., Goli, J. K., Gentela, J., and Koti, S. Bioconversion of lignocellulosic biomass to xylitol: An overview. *Bioresource Technology*, 213 (2016) 299–310.

Reisinger, M., Tirpanalan, Ö., Huber, F., Kneifel, W., and Novalin, S. Investigations on a wheat bran biorefinery involving organosolv fractionation and enzymatic treatment. *Bioresource Technology*, 170 (2014) 43–61.

Relue, B.L.P., and Varanasi, S. Simultaneous isomerization and reactive extraction of biomass sugars for high yield production of ketose sugars. *Green Chemistry*, 14 (2012) 2436–2444.

Ribeiro, L.S, Órfão, J.J.M., and Pereira, M.F.R. Screening of catalysts and reaction conditions for the direct conversion of corncob xylan to xylitol. *Green Processing and Synthesis*, 6 (2017a) 265–272.

Ribeiro, L.S., Delgado, J.J., Órfão, J.J.M., and Pereira, M.F.R. A one-pot method for the enhanced production of xylitol directly from hemicellulose (corncob xylan). *RSC Advances*, 6 (2016) 95320–95327.

Ribeiro, L.S., Órfão, J.J.M., and Pereira, M.F.R. Simultaneous catalytic conversion of cellulose and corncob xylan under temperature programming for enhanced sorbitol and xylitol production. *Bioresource Technology*, 244 (2017b) 1173–177.

Romero, A., Alonso, E., Sastre, Á., and Nieto-Márquez, A. Conversion of biomass into sorbitol: Cellulose hydrolysis on MCM-48 and D-glucose hydrogenation on Ru/MCM-48. *Microporous and Mesoporous Materials*, 224 (2016) 1–8.

Rouwenhorst, R.J., Jzn, J.F., Scheffers, W.A., and Dijken, J.P.V. Determination of protein concentration by total organic carbon analysis. *Journal of Biochemical and Biophysical Methods*, 22 (1991) 119–128.

Roy, G.M. Activated carbon applications in the food and pharmaceutical industries. 1st ed., CRC Press: Pennsylvania, 2014.

Rytter, E., and Holmen, A. Deactivation and regeneration of commercial type Fischer-Tropsch Co-catalysts – A mini-review. *Catalysts*, 5 (2015) 478–499.

Sánchez-Bastardo, N., and Alonso, E. Maximization of monomeric C5 sugars from wheat bran by using mesoporous ordered silica catalysts. *Bioresource Technology*, 238 (2017) 379–388.

Sánchez-Bastardo, N., Romero, A., and Alonso, E. Extraction of arabinoxylans from wheat bran using hydrothermal processes assisted by heterogeneous catalysts. *Carbohydrate Polymers*, 160 (2017) 143–152.

Schmidt, W. Chapter 4 – Microporous and Mesoporous Catalysts. In *Surface and Nanomolecular Catalysis*, Richards, R., (Ed.), CRC Press: Boca Raton, 2006.

Serrano-Ruiz, J.C., Luque, R., and Sepúlveda-Escribano, A. Transformations of biomass-derived platform molecules: from high added-value chemicals to fuels *via* aqueous-phase processing. *Chemical Society Reviews*, 40 (2011) 5266–5281.

Seyer, M-É., and Gélinas, P. Bran characteristics and wheat performance in whole wheat bread. *International Journal of Food Science & Technology*, 44 (2009) 688–693.

Sheldon, R.A. The E factor 25 years on: the rise of green chemistry and sustainability. *Green Chemistry*, 19 (2017) 18–43.

Simakova, I.L., Demidova, Y.S., Murzina, E.V., Aho, A., and Murzin, D.Y. Structure sensitivity in catalytic hydrogenation of galactose and arabinose over Ru/C catalysts. *Catalysis Letters*, 146 (2016) 1291–1299.

Sluiter, A., Hames, B., Ruiz, R., Scarlata, C., Sluiter, J., and Templeton, D. Determination of sugars, byproducts, and degradation products in liquid fraction process samples. Laboratory Analytical Procedure (LAP). Technical Report NREL/TP-510-42623, 2008.

Soh, N., Kitano, K., and Imato, T. Evaluation of interactions between monosaccharides and a stationary phase modified with alkylboronic acid by means of a liquid-chromatographic method. *Analytical Sciences,* 18 (2002) 1159–1161.

Tathod, A.P., and Dhepe, P.L. Efficient method for the conversion of agricultural waste into sugar alcohols over supported bimetallic catalysts. *Bioresource Technology,* 178 (2015) 36–44.

Tong, A-J., Yamauchi, A., Hayashita, T., Zhang, Z-Y., Smith, B.D., and Teramae, N. Boronic acid fluorophore/*β*-cyclodextrin complex sensors for selective sugar recognition in water. *Analytical Chemistry,* 73 (2001) 1530–1536.

Van der Berg, R., Peters, J.A., and Van Bekkum, H. The structure and (local) stability constants of borate esters of mono- and di-saccharides as studied by ^{11}B and ^{13}C NMR spectroscopy. *Carbohydrate Research,* 253 (1994) 1–12.

Vázquez, M.J., Alonso, J.L., Domínguez, H., and Parajó, J.C. Enhancing the potential of oligosaccharides from corncob autohydrolysis as prebiotic food ingredients. *Industrial Crops and Products,* 24 (2006) 152–159.

Víctor-Ortega, M.D., Ochando-Pulido, J.M., and Martínez-Ferez, A. Performance and modeling of continuous ion exchange processes for phenols recovery from olive mill wastewater. *Process Safety and Environmental,* 100 (2016) 242–251.

Vilcocq, L., Castilho, P.C., Carvalheiro, F., and Duarte, L.C. Hydrolysis of oligosaccharides over solid acid catalysts: A review. *ChemSusChem,* 7 (2014) 1010–1019.

Werpy, T., and Petersen, G. Top Value Added Chemicals from Biomass. In *Volume I – Results of Screening for Potential Candidates from Sugars and Synthesis Gas*. U.S.D. Energy: United States, 2004.

Yadav, M., Mishra, D.K., and Hwang, J-S. Catalytic hydrogenation of xylose into xylitol using ruthenium catalyst on NiO modified TiO_2 support. *Applied Catalysis A: General,* 425–426 (2012) 110–116.

Yi, G., and Zhang, Y. One-pot selective conversion of hemicellulose (xylan) to xylitol under mild conditions. *ChemSusChem,* 5 (2012) 1383–1387.

Zada, B., Chen, M., Chen, C., Yan, L., Xu, Q., Li, W., Guo, Q., and Fu, Y. Recent advances in catalytic production of sugars alcohols and their applications. *Science China Chemistry,* 60 (2017) 853–869.

Supplementary Information

X-Ray Diffraction (XRD)

The diffraction peaks in the spectrum at 2θ = 42.1° and 44.0° demonstrate the presence of Ru^0 on Ru/H-ZSM-5 (Figure S1).

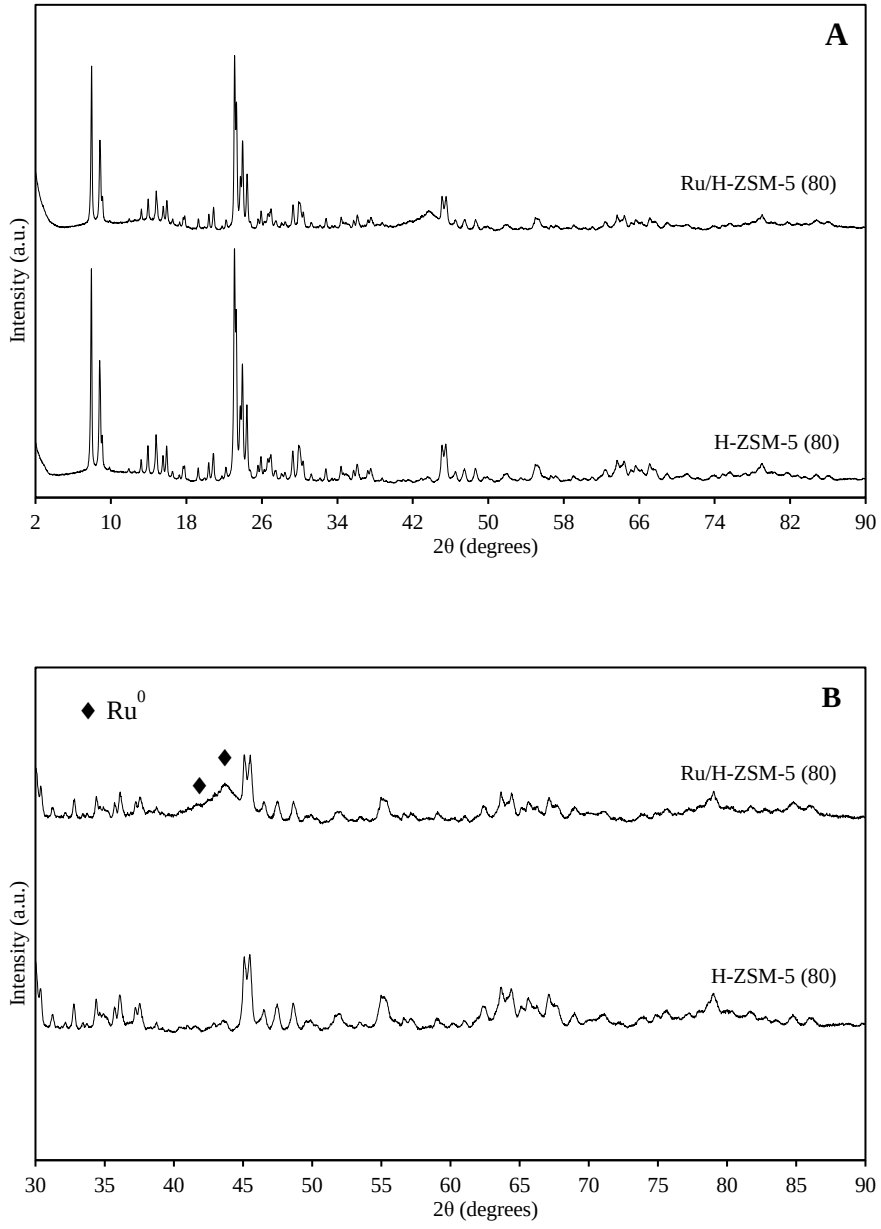

Figure S1. XRD patterns of H-ZSM-5 and reduced Ru/H-ZSM-5. A) 2° – 90° and B) expanded region from 30° – 90 °.

These reflections are assigned to the (100) and (002) diffraction planes of bulk hexagonal Ru^0 particles (JCPDS-ICDD card No. 06-0663) (Li et al., 2004). The low intensity of the diffraction peaks is probably due to the low metal loading and high dispersion of Ru^0 particles onto the support (Yao et al., 2015).

Nitrogen adsorption-desorption isotherms

Figure S2A displays type I isotherms, typical of microporous materials which exhibit a sharp increase of nitrogen sorption at very low partial pressures ($P/P_0 \leq 0.01$) due to the filling of ultramicropores with a width of two-three molecular diameters, which is governed by the gas – solid interactions (Cychosz et al., 2017). The pore filling process of supermicroporous occurs in the range of relative pressure $P/P_0 = 0.01 – 0.15$ (Cychosz et al., 2017) and the rise observed at $P/P_0 > 0.95$ is related to nitrogen condensation in the void volume between the particles (Fu et al., 2016). H-ZSM-5 and Ru/H-ZSM-5 display a slight H4 hysteresis loop (ALOthoman, 2012). This kind of hysteresis is often associated with narrow slit-like pores, but in the case of type I isotherms is indicative of a microporous structure with some contribution of mesopores (Beyer et al., 1995; Cychosz et al., 2017; Fu et al., 2016; Peng et al., 2015). However, the pore size distribution (PSD) (Figure S2B) shows basically a unimodal microporous distribution centered at approximately 0.67 nm for both solids. A slight shoulder but also in the micropore region was observed. Therefore, the small hysteresis loop and the narrow pore size distribution suggests that mesoporosity in H-ZSM-5 and Ru/H-ZSM-5 is very low. Besides mesoporosity, several authors have attributed the hysteresis at relatively high pressures ($P/P_0 \geq 0.45$) to zeolites with low aluminum content, as in the case of H-ZSM-5 with a SiO_2/Al_2O_3 ratio of 80 (Al-Thawabeia and Hodali, 2015; Cejka et al., 2007; Hudec et al., 1998; Müller and Unger, 1988; Sing, 1982).

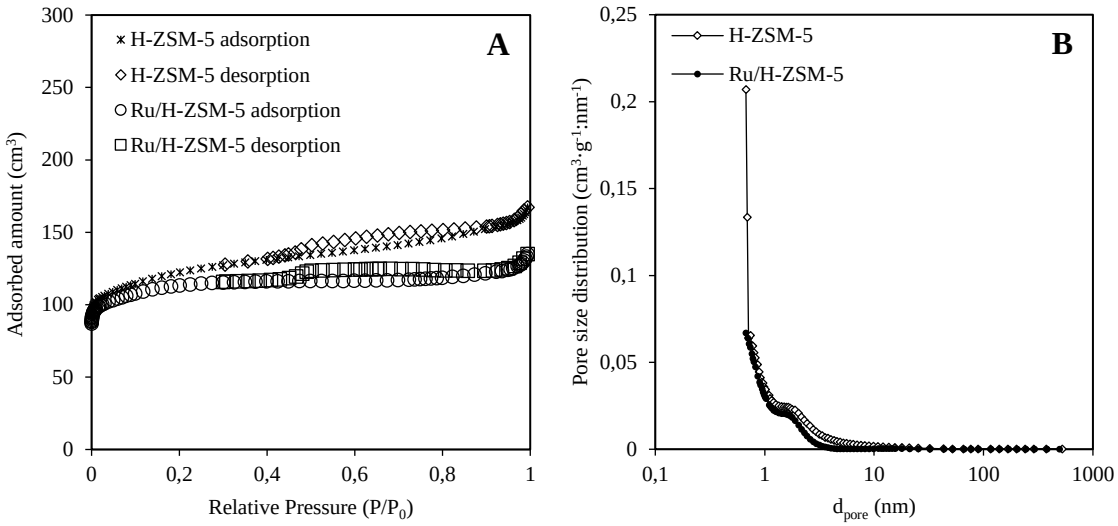

Figure S2. A) Nitrogen adsorption-desorption isotherms and B) pore size distributions (PSD) of H-ZSM-5 and Ru/H-ZSM-5.

References

ALOthoman, Z.A. A Review: Fundamental aspects of silicate mesoporous materials. *Materials,* 5 (2012) 2874–2902.

Al-Thawabeia, R.A., and Hodali, H.A. Use of zeolite ZSM-5 for loading and release of 5-fluorouracil. *Journal of Chemistry,* 2015 (2015) Article ID 403597.

Beyer, H.K., Nagy, J.B., Karge, H.G., and Kiricsi, I. Volume 94 – Catalysis by microporous materials. In *Studies in Surface Science and Catalysis*, 1st ed., Elsevier Science, 1995.

Cejka, J., Van Bekkum, H., and Schueth, C. Introduction to zeolite molecular sieves. 3rd ed., Elsevier Science: New York, 2007.

Cychosz, K.A., Guillet-Nicolas, R., García-Martínez, J., and Thommes, M. Recent advances in the textural characterization of hierarchically structures nanoporous materials. *Chemical Society Reviews,* 46 (2017) 389–414.

Fu, X., Sheng, X., Zhou, Y., Fu, Z., Zhao, S., Bu, X., and Zhang, C. Design of micro – mesoporous zeolite catalysts for alkylation. *RSC Adances,* 6 (2016) 50630–50639.

Hudec, P., Smieskova, A., Zidek, Z., Zubek, M., Schneider, P., Kocirik, M., and Kozankova, J. Adsorption properties of ZSM-5 zeolites. *Collection of Czechoslovak Chemical Communications,* 63 (1998) 141–154.

Li, W., Ye, L., Long, P., Chen, J., Ariga, HAsakura, K., and Yuan, Y. Efficient Ru – Fe catalyzed selective hydrogenolysis of carboxylic acids to alcoholic chemicals. *RSC Advances*, 4 (2004) 29072–29082.

Müller, U., and Unger, K.K. Sorption studies on large ZSM-5 crystals: the influence of aluminium content, they type of exchangeable cations and the temperature of nitrogen hysteresis effects. *Studies in Surface Science and Catalysis,* 39 (1988) 101–108.

Peng, P., Wang, Y., Rood, M.J., Zhang, Z., Subhan, F., Yan, Z., Qin, L., Zhang, Z., Zhang, Z., and Gao, X. Effects of disolution alkalinity and self-assembly on ZSM-5 based micro-/mesoporous composites: a study of the relationship between porosity, acidity, and catalytic performance. *CrystEngComm*, 17 (2015) 3820–3828.

Sing, K. Reporting physisorption data for gas/solid systems. *Pure and Applied Chemistry*, 54 (1982) 2201–2218.

Yao, G., Wu, G., Dai, W., Guan, N., and Li, L. Hydrodeoxygenation of lignin-derived phenolic compounds over bi-functional Ru/H-Beta under mild conditions. *Fuel,* 150 (2015) 175–183.

CONCLUSIONS

WHEAT BRAN BIOREFINERY: VALORIZATION OF HEMICELLULOSES TO SUGAR ALCOHOLS

FRACTIONATION – HYDROLYSIS – PURIFICATION – HYDROGENATION

A multi-stage process for the production of sugar alcohols from wheat bran has been successfully developed in this PhD Thesis. The global process has been divided and studied in several sequential steps, summarized as follows:

v) Extraction of arabinoxylans from wheat bran

vi) Hydrolysis of arabinoxylans into monosaccharides

vii) Purification of wheat bran hydrolysates

viii) Hydrogenation of purified hydrolysates to obtain sugar alcohols

The main conclusions of the overall work are presented below:

- The arabinoxylan fraction of wheat bran, an agricultural residue from our region *Castilla y León*, has been revalorized into high added-value products: i) a purified hydrolysate with a high content in sugars (50% xylose, 30% arabinose and 7% glucose, based on carbon balance) which can be used in subsequent processes, and ii) the derived sugar alcohols with a yield of 70% in pentitols and a selectivity of 100%.
- Water-based extraction of arabinoxylans from destarched wheat bran can be successfully performed with MCM-48 type materials and the corresponding $RuCl_3$ catalysts supported on them.
    - The tendency in the arabinoxylan extraction yield is directly related to the acidity of the catalyst, *i.e.* the higher the acidity the higher the extraction yield: MCM-48 < Al-MCM-48 < $RuCl_3$/MCM-48 < $RuCl_3$/Al-MCM-48.
    - Al-MCM-48 results in higher arabinoxylan extraction yields than MCM-48, ascribed to the higher Brönsted acidity of Al-MCM-48 after aluminum incorporation. $RuCl_3$-based catalysts are more efficient than the corresponding silica supports due to the additional moderate Lewis acidity attributed to Ru^{+3} cations.

- Arabinoxylans are solubilized mainly as poly/oligosaccharides, whereas a minor amount is obtained as monosaccharides.
- A combination of relatively high temperatures, short times and solid acid catalysts favors the extraction yield of arabinoxylans with low molecular weight.
- The extraction of arabinoxylans as oligosaccharides and its subsequent hydrolysis to monomers must be carried out in two different steps in order to avoid the co-extraction of cellulose and increase the purity of the extracted arabinoxylans.
- Heterogeneous catalysts have demonstrated to be good substitutes for the traditional homogeneous acids used in biomass fractionation and hydrolysis processes. Comparing results reported on literature based on homogenous extraction with the obtained in this PhD Thesis by using solid acid catalysts, it can be stated that:
    - Solid acid catalysts are more selective and minimize the co-extraction of undesired biomass compounds.
    - The degradation of arabinoxylans is lower by using solid acid catalysts than homogenous acids.
    - Heterogeneous catalysts can be easily recovered from the liquid extract by a filtration process, whereas the separation process of the homogeneous acids raises sharply the operating costs.
    - Acid treatments are not environmentally-friendly and cause corrosion problems, so that the equipment costs increase. This can be avoided by means of solid acid catalysts.

- Optimum experimental conditions are 180 ºC, 10 minutes and using $RuCl_3$/Al-MCM-48 as catalyst. Under such conditions, the total arabinoxylan yield is 78% and the average molecular weight equal to 9 kDa.

- MCM-48, Al-MCM-48 and $RuCl_3$ catalysts supported on them have been used to complete the hydrolysis of arabinoxylans into arabinose and xylose.
  - The catalyst acidity and the monomeric yield exhibit the same tendency as in the previous hydrothermal extraction yield: MCM-48 < Al-MCM-48 < $RuCl_3$/MCM-48 < $RuCl_3$/Al-MCM-48.
  - A high total acidity and the combination of Brönsted acidity (due to aluminum incorporation) and moderate Lewis acidity (due to Ru^{+3} cations) lead to higher monomeric yields.
  - Metal cations with moderate Lewis acidity (Ru^{+3}) are more active than those with high Lewis acidity (Fe^{+3}).
  - Arabinose molecules are faster released than xylose units.
  - Optimum operating conditions are 180 ºC, 15 minutes and using $RuCl_3$/Al-MCM-48 as catalyst with a loading of 4.8 g·g C^{-1}. The formation of furfural is almost completely inhibited under such conditions and the total monomeric yield (arabinose + xylose) is 95%.

- The catalytic activity of mesporous silica materials (MCM-48 and Al-MCM-48) and zeolites (H-Y (12), H-ZSM-5 (23) and H-ZSM-5 (80)) has been tested and compared in the hydrolysis of arabinoxylans from wheat bran into monosaccharides.
  - The strength and nature of acid sites play a crucial role in the arabinoxylan hydrolysis.

- H-ZSM-5 (23) is the most suitable catalyst for the conversion of arabinoxylans into arabinose and xylose. This is attributed to the high acidity and strong Brönsted acid sites of H-ZSM-5 (23).
- Optimum conditions are 180 ºC, 15 minutes and using H-ZSM-5 (23) as catalyst with a loading of 9.2 $g \cdot g\ C^{-1}$. The arabinose and xylose yields are 96% and 67%, respectively, which correspond to a global yield of 76%.

- Sugars were selectively recovered from wheat bran hydrolysates by solvent extraction with boronic acids and further purified with ion exchange resins.
  - An organic phase composed of a quaternary ammonium salt (Aliquat® 336) and a boronic acid dissolved in 1-octanol is used to extract the sugars from wheat bran hydrolysates.
  - *Ortho*-hydroxymethyl phenylboronic acid (HMPBA) is more efficient for the extraction of sugars than phenylboronic acid (PBA).
  - Arabinose and xylose are more easily extracted than glucose.
  - With a 0.5 M concentration of HMPBA, 66%, 83% and 84% of initial glucose, xylose and arabinose, respectively, are extracted into the organic phase. After back-extraction, all the sugars are recovered in an aqueous solution of 0.25 M H_2SO_4.
  - The final hydrolysate is free of inorganic elements, proteins and has a lower content of sugar degradation products and lignin derivatives than the hydrolysate before purification.
  - Lignin derivatives are removed by ion exchange resins (Amberlyst® 15 and Amberlite® IRA-96).
  - Sugar concentration in the purified hydrolysate is 90% (based on carbon balance), compared to 64% of the initial hydrolysate.

- Sugar model mixtures composed of glucose, xylose and arabinose were hydrogenated over ruthenium catalysts supported on different H-ZSM-5 zeolites.
    - Low acidic supports (H-ZSM-5 (80)) promote sugar hydrogenation over isomerization reactions. The conversion of sugars and the yield to sugar alcohols are higher over Ru/H-ZSM-5 (80) than over Ru/H-ZSM-5 (23).
    - Xylose and arabinose are more readily hydrogenated than glucose.
    - Optimum temperature for xylose and arabinose hydrogenation is 100 ºC, whereas 120 ºC is the optimum for glucose hydrogenation.
    - Glucose requires a higher catalyst loading than xylose or arabinose to be successfully hydrogenated.
    - Experimental data is reproduced by a pseudo-first order kinetic model, obtaining low absolute deviations and high regression coefficients.
    - The energy activation values for glucose, xylose and arabinose hydrogenation are 92.0 $kJ \cdot mol^{-1}$, 43.7 $kJ \cdot mol^{-1}$ and 47.9 $kJ \cdot mol^{-1}$, respectively.
- Sugars concentrate from wheat bran hydrolysates were hydrogenated over Ru/H-ZSM-5 (80).
    - Hydrogenation of sugars does not take place before the purification step.
    - Proteins deactivate ruthenium catalysts.
    - Sugars from wheat bran hydrolysates are successfully hydrogenated over Ru/H-ZSM-5 (80) after the purification process. A pentitols yield of 70% is achieved at 100 ºC, 10 minutes and using a catalyst loading corresponding to 0.06 g $Ru \cdot g\ C^{-1}$.

FUTURE WORK

In this PhD Thesis, the arabinoxylan fraction from wheat bran has been valorized into valuable products. The residual solid after the isolation of arabinoxylans, which is rich in cellulose and lignin, can also be further converted to high value-added products by subsequent processes. For example, cellulose can be transformed into glucose, which is the platform molecule of a wide range of chemicals (gluconic acid, lactic acid, sorbitol). Bioethanol can be also obtained from cellulose by fermentation processes. Lignin, for instance, is the base for the obtaining of bioplastics, nanocomposites and nanoparticles. It can also be depolymerized into valuable chemicals such as vanillin, vanillic acid, *p*-coumaric acid, *p*-hydroxybenzoic acid or sinapyl alcohol.

Sugars with high purity can be not only used for sugar alcohols production but also for other purposes. For instance, sugars can be converted into biofuels by fermentation processes, in which high purity hydrolysates are required. Xylose and arabinose can also be used for obtaining furfural or succinic acid, which are listed among the high added-value products to be produced from biomass, according to the U.S. Department of Energy. Likewise, sugar alcohols (xylitol and arabitol) can be transformed into short-chain alkanes, such as pentanes, by means of hydrogenation processes under acidic conditions. Pentane can further be used for the production of polystyrene foams or gasolines, as solvent or in liquid chromatography. Under basic conditions, sugar alcohols can react to produce ethylene glycol and propylene glycol, which have applications in medicine (as excipients), cosmetics (skin creams) or in chemical industry (herbicides or pesticides, lubricants).

Regarding the process, a further investigation is required to study the following issues:

- Catalyst recycling after fractionation, hydrolysis and hydrogenation processes.
- Evaluation of the catalyst regeneration and recycling costs.
- Scaling-up of the process from laboratory scale to pilot plant.

- Substitution of discontinuous processes by continuous processes.
- Intensification of the process by reducing the number of stages.
- Life cycle assessment to evaluate the environmental impacts of the process throughout the different steps.

RESUMEN

BIORREFINERÍA DE SALVADO DE TRIGO: VALORIZACIÓN DE HEMICELLULOSAS EN ALCOHOLES DE AZÚCAR

FRACCIONAMIENTO – HIDRÓLISIS – PURIFICACIÓN – HIDROGENACIÓN

Durante los últimos años, la transformación de biomasa en compuestos químicos y combustibles se ha convertido en un asunto de gran relevancia que ocupa el tema central de muchas de las investigaciones actuales. El agotamiento de combustibles fósiles, así como la mayor preocupación por el cambio climático y la promulgación de leyes ambientales más estrictas ha hecho que la sociedad actual se centre en la búsqueda de materias primas renovables que permitan sustituir al petróleo en un futuro no tan lejano. En este contexto, la biomasa lignocelulósica ha recibido especial atención debido a su carácter renovable y sostenible y a su gran abundancia. Una biorrefinería se define como "una industria que integra procesos y equipos que permiten la obtención de combustibles, energía, calor y productos de alto valor añadido utilizando biomasa como materia prima". Los procesos de una biorrefinería están diseñados con el objetivo de maximizar la producción de compuestos de alto valor y minimizar la obtención de residuos. Son muchos los procesos que se han utilizado para la transformación de biomasa en combustibles y compuestos químicos. Así, el uso de catalizadores heterogéneos es una de las alternativas que permite el desarrollo de procesos respetuosos con el medio ambiente que requieren condiciones de operación relativamente suaves.

La biomasa lignocelulósica está compuesta principalmente por celulosa, hemicelulosa y lignina, cuyos contenidos varían de una biomasa a otra. En esta Tesis Doctoral, se ha elegido salvado de trigo como materia prima para la producción de alcoholes a partir de su fracción hemicelulósica, en concreto, de arabinoxilanos. El salvado de trigo es un subproducto de la industria de la molienda del cereal. Alrededor de 150 millones de toneladas de salvado de trigo se producen cada año en todo el mundo. El salvado de trigo se utiliza básicamente como ingrediente de bajo valor añadido en la alimentación del ganado y solo una pequeña parte se destina a la alimentación humana. Por este motivo, la industria del cereal está actualmente buscando alternativas que permitan dotar al salvado

de trigo de un mayor valor. El salvado de trigo, una vez desalmidonado, tiene un alto contenido en hemicelulosas, alrededor del 38 – 47%, del cual la mayor parte corresponde a arabinoxilanos. Los arabinoxilanos son un componente estructural de las paredes celulares de los cereales. Están formados por un esqueleto principal constituidos por moléculas de xilosa conectadas entre sí por enlaces β-(1→4). De dicho esqueleto principal, derivan ramificaciones más cortas formadas por arabino-oligosacáridos, galactosa, D-4-*O*-ácido metilglucorónico, ácido ferúlico o ácido cumárico. Los arabinoxilanos tienen importantes aplicaciones en muchos sectores industriales, como el cosmético o farmacéutico, o en la obtención de distintos materiales. También se utilizan en el campo de la nutrición debido a su carácter prebiótico. Sin embargo, el volumen de mercado de los arabinoxilanos es mayor cuando se encuentran como monosacáridos, es decir, arabinosa y xilosa. Estos azúcares se pueden convertir en arabitol y xilitol, respectivamente, los cuales se encuentran entre los 12 compuestos de alto valor añadido que se pueden obtener a partir de biomasa, de acuerdo con el Departamento de Energía de los Estados Unidos.

Objetivos

El objetivo principal de esta Tesis Doctoral es estudiar la obtención de alcoholes de azúcar (arabitol y xilitol) a partir de salvado de trigo. Para ello, se han considerado cada una de las etapas que constituyen el proceso global (Figura 1) y que se pueden resumir en:

1. Extracción de la fracción de arabinoxilanos de salvado de trigo
2. Hidrólisis de los arabinoxilanos en azúcares simples (arabinosa y xilosa)
3. Purificación de los hidrolizados
4. Hidrogenación de los azúcares purificados para obtener los correspondientes alcoholes (arabitol y xilitol)

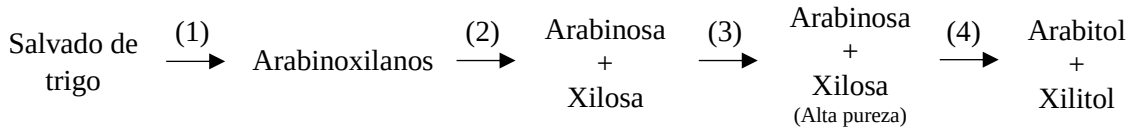

Figura 1. Obtención de alcoholes a partir de salvado de trigo.

Los objetivos específicos de esta Tesis Doctoral son:

- Desarrollo de procesos de biorrefinería aplicados a biomasa real:
    - Revalorización de biomasa agrícola procedente de nuestra región Castilla y León, como salvado de trigo.
- Fraccionamiento de salvado de trigo utilizando materiales de sílice mesoporosos y acidificados para aislar la fracción correspondiente a arabinoxilanos:
    - Estudio de la influencia de MCM-48 y Al-MCM-48 así como de los correspondientes catalizadores de $RuCl_3$.
    - Optimización de la temperatura y tiempo para obtener altos rendimientos de extracción de arabinoxilanos con bajo peso molecular.
- Hidrólisis de los arabinoxilanos obtenidos previamente en arabinosa y xilosa mediante el uso de catalizadores heterogéneos:
    - Estudio del efecto de sílices mesoporosas (MCM-48, Al-MCM-48) y catalizadores de $RuCl_3$ ($RuCl_3$/MCM-48, $RuCl_3$/Al-MCM-48). Influencia de diferentes cationes metálicos (Ru^{+3}, Fe^{+3}). Optimización de la carga de catalizador y tiempo de reacción para maximizar la conversión selectiva de arabinoxilanos en arabinosa y xilosa evitando su posterior degradación.
    - Comparación de sílices mesoporosas (MCM-48, Al-MCM-48) y zeolitas (H-Y (12), H-ZSM-5 (23), H-ZSM-5 (80)). Maximización de azúcares y minimización de productos de degradación mediante el ajuste del tiempo de reacción y la carga de catalizador.

- Recuperación de azúcares de hidrolizados de salvado de trigo mediante la extracción de los mismos con ácidos borónicos y posterior purificación usando resinas de intercambio iónico:
    - Análisis del comportamiento de los azúcares, productos de degradación, sales inorgánicas, proteínas y derivados de lignina en las diferentes etapas de las que se compone el proceso global de purificación.
- Hidrogenación de mezclas modelo de azúcares (xilosa, arabinosa, glucosa) sobre catalizadores de rutenio soportados en zeolitas:
    - Estudio de zeolitas tipo H-ZSM-5 con diferentes ratios SiO_2/Al_2O_3 empleadas como soportes del catalizador.
    - Estudio del efecto de la temperatura de reacción, tiempo y carga de catalizador.
    - Ajuste de los datos experimentales a un modelo cinético de pseudo primer orden.
    - Determinación de los parámetros cinéticos (factor pre-exponencial de Arrhenius y energías de activación).
- Hidrogenación de hidrolizados de salvado de trigo con catalizadores de rutenio depositados sobre H-ZSM-5 (80):
    - Hidrogenación de hidrolizados de salvado de trigo antes y después del proceso de purificación.
    - Estudio de la influencia de la carga de catalizador en la obtención de alcoholes.
    - Análisis del mecanismo de desactivación de los catalizadores de rutenio.

Contenidos

Esta Tesis Doctoral está estructurada en cinco capítulos a lo largo de los cuales se estudian cada una de las etapas necesarias para la producción de alcoholes a partir de salvado de trigo. Los principales contenidos de cada capítulo se resumen a continuación.

En el **Capítulo 1** titulado "*Hydrothermal extraction of arabinoxylans from wheat bran assisted by heterogeneous catalysts*" se ha estudiado la extracción de la fracción de arabinoxilanos de salvado de trigo usando procesos hidrotermales en combinación con catalizadores heterogéneos. El objetivo de este capítulo era obtener altos rendimientos de arabinoxilanos con bajo peso molecular para facilitar su posterior hidrólisis en monosacáridos. Se estudiaron distintos materiales de sílice mesoporosos, como MCM-48 y Al-MCM-48, así como los correspondientes catalizadores de $RuCl_3$, que aportan una mayor acidez. Además, se variaron la temperatura (140 – 180 ºC) y tiempo (10 – 30 minutos) para estudiar su influencia en el rendimiento de extracción y el peso molecular de los arabinoxilanos obtenidos.

En primer lugar, se examinó el efecto del catalizador de $RuCl_3$ soportado sobre MCM-48, comparando su actividad con la MCM-48. Tanto MCM-48 como $RuCl_3$/MCM-48 mejoraron el rendimiento de extracción de arabinoxilanos respecto a la prueba sin catalizador. MCM-48 tiene una acidez relativamente baja correspondiente a grupos silanol (sitios ácidos de Lewis) en su superficie, mientras que $RuCl_3$ aporta una mayor acidez debido al carácter moderado ácido de Lewis de los cationes Ru^{+3}. De ahí que el rendimiento obtenido con $RuCl_3$/MCM-48 fuera mayor que con MCM-48. Asimismo, con el uso de estos catalizadores, el peso molecular de los arabinoxilanos obtenidos aumentó respecto a los solubilizados en el experimento sin catalizador.

Después se estudió el efecto de la temperatura entre 140 y 180 ºC. En este caso se observó que un aumento de la temperatura favorecía la extracción de arabinoxilanos. Su efecto en

el peso molecular de los arabinoxilanos mostró la siguiente tendencia. A 140 ºC, el peso molecular era bajo, lo que, junto al bajo rendimiento de extracción obtenido, significa que únicamente las cadenas secundarias de los arabinoxilanos (formadas mayormente por arabinosa) se solubilizaron en agua. A 160 ºC, tanto el rendimiento como el peso molecular aumentaron significativamente. En este caso, se extrajo el esqueleto principal de los arabinoxilanos, pero las condiciones de operación no eran lo suficientemente severas como para causar su hidrólisis en oligómeros de cadena corta. Sin embargo, a 180 ºC, el rendimiento aumentó mientras que el peso molecular disminuyó drásticamente, lo que indica que se consiguió extraer la cadena principal de los arabinoxilanos, así como su posterior hidrólisis en oligómeros más pequeños.

La influencia del tiempo se estudió a continuación a 180 ºC. El rendimiento de extracción y la pureza del extracto disminuyeron tras 20 minutos respecto a los experimentos a tiempos más cortos (10 minutos). En este caso, los arabinoxilanos comenzaban a degradarse a partir de los 20 minutos y otros compuestos se empezaban a extraer, lo que daba lugar a un extracto con más impurezas.

Finalmente, se estudió la influencia del soporte (Figura 2) a 180 ºC tras 10 minutos de operación. Se determinó que el rendimiento de extracción de arabinoxilanos estaba directamente relacionado con la acidez del catalizador: MCM-48 < Al-MCM-48 < $RuCl_3$/MCM-48 < $RuCl_3$/Al-MCM-48. Además, el peso molecular de los arabinoxilanos disminuía cuando el $RuCl_3$ estaba presente en el catalizador. Las mejores condiciones de extracción se obtuvieron a 180 ºC, 10 minutos y utilizando $RuCl_3$/Al-MCM-48 como catalizador. Bajo estas condiciones, se extrajo aproximadamente el 78% de los arabinoxilanos totales presentes en el salvado de trigo con un bajo peso molecular de 9 kDa.

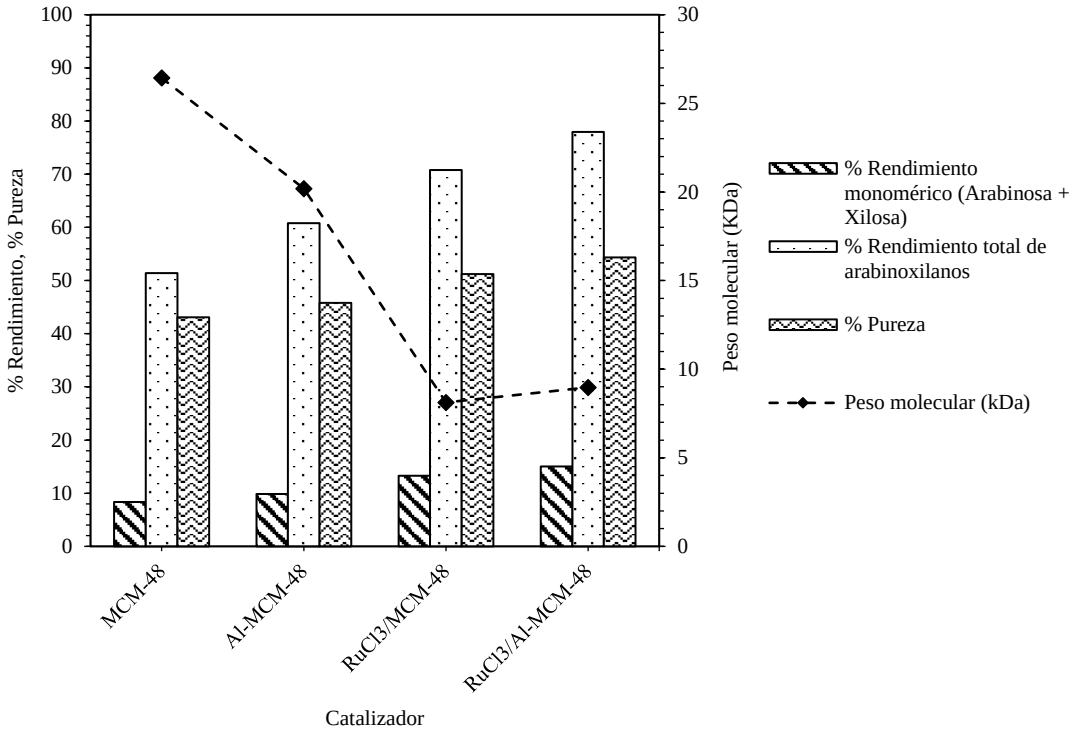

Figura 2. Influencia de distintas sílices mesoporosas y los correspondientes catalizadores de $RuCl_3$ en la extracción de arabinoxilanos de salvado de trigo. Condiciones de operación: 180 ºC, 10 minutos.

En el **Capítulo 2** titulado "*Maximization of monomeric C_5 sugars from wheat bran by using mesoporous ordered silica catalysts*" se ha estudiado el proceso de hidrólisis de los arabinoxilanos previamente extraídos de salvado de trigo, en condiciones subcríticas mediante el uso de materiales de sílice mesoporosa y los correspondientes catalizadores de $RuCl_3$. Tras la primera etapa de extracción, la arabinosa y xilosa se encontraban tanto en forma monomérica como oligomérica. El objetivo de este capítulo ha sido maximizar la conversión de arabinoxilanos en arabinosa y xilosa y, al mismo tiempo, evitar la degradación de los monosacáridos (los ya existentes tras la primera etapa de extracción y los formados durante la propia etapa de hidrólisis) en subproductos. Para ello, se ha estudiado la influencia de diferentes parámetros, como el tipo y carga de catalizador y el tiempo de reacción.

Un primer cribado de diferentes catalizadores sólidos ácidos (MCM-48, Al-MCM-48, $RuCl_3$/MCM-48, $RuCl_3$/Al-MCM-48) se llevó a cabo a 180 ºC para determinar cuál de ellos era más activo en el proceso de hidrólisis (Figura 3). Al igual que ocurría en el fraccionamiento de arabinoxilanos (Capítulo 1), una mayor acidez condujo a un mayor rendimiento en monosacáridos. La sílice MCM-48 apenas mejoró el rendimiento respecto al experimento sin catalizador. Como ya se ha mencionado anteriormente, esto se debe a que la MCM-48 tiene sólo unos pocos sitios ácidos de Lewis. Sin embargo, al incorporar aluminio a la estructura de la MCM-48, se crean sitios ácidos de Brönsted que, en combinación con los sitios ácidos de Lewis, mejoraron la hidrólisis de arabinoxilanos. Por su parte, los catalizadores de $RuCl_3$ preparados sobre los soportes anteriores también hacían que el rendimiento monomérico aumentara respecto a sus correspondientes soportes. En este caso, los cationes Ru^{+3} son ácidos moderados de Lewis que aumentan la acidez de las sílices mesoporosas y consiguientemente la obtención de arabinosa y xilosa. Por tanto, $RuCl_3$/Al-MCM-48 resultó ser el catalizador más activo para la obtención de azúcares C_5. En todos los experimentos se observó que el rendimiento en arabinosa era mayor que el correspondiente al de xilosa, lo cual se atribuye a la distinta posición de la arabinosa y xilosa en el esqueleto de los arabinoxilanos y a los diferentes enlaces químicos existentes entre dichas moléculas. Las unidades de xilosa forman parte del esqueleto principal y están unidas por enlaces glicosídicos tipo β, mientras que las moléculas de arabinosa forman parte de las cadenas secundarias ramificadas y están conectadas por enlaces glicosídicos tipo α. El mejor acceso a las cadenas laterales, así como el carácter débil de los enlaces glicosídicos tipo α explican una liberación más rápida de arabinosa que de xilosa.

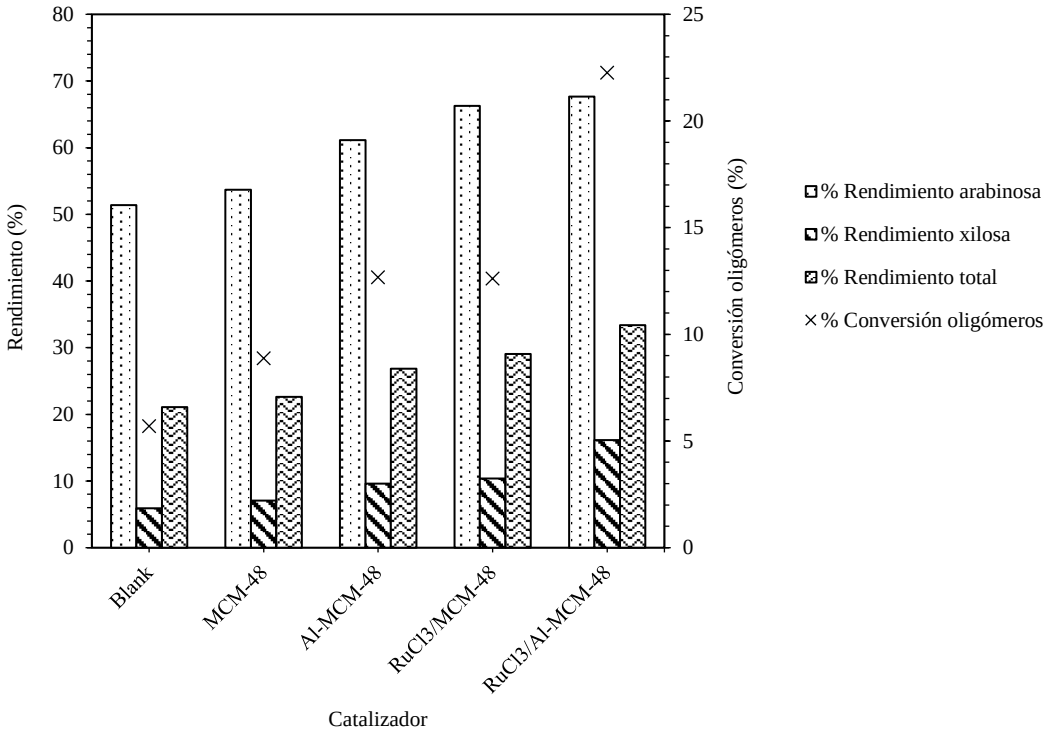

Figura 3. Influencia de distintas sílices mesoporosas y los correspondientes catalizadores de $RuCl_3$ en el rendimiento en arabinosa y xilosa. Condiciones de reacción: 180 ºC, 15 minutos, 50 bar N_2, 0.6 g catalizador·g C^{-1}.

A continuación, se estudió la influencia del tiempo y de la carga de catalizador ($RuCl_3$/Al-MCM-48). Con una carga de catalizador baja (0.6 g·g C^{-1}), se obtuvo un rendimiento total en monómeros relativamente bajo (~42%) incluso a tiempos largos (3 horas). Bajo estas condiciones de operación (180 ºC, 0.6 g catalizador·g C^{-1}), la velocidad de reacción de la etapa de hidrólisis era más lenta que la degradación de los monómeros a productos secundarios, de forma que los azúcares ya existentes y los que se iban formando se degradaban rápidamente a furfural. Con el fin de aumentar el rendimiento en arabinosa y xilosa y disminuir su degradación a furfural, se probaron cargas de catalizador más altas a tiempos largos de reacción (3 horas). Para una carga de 2.4 g catalizador·g C^{-1}, el rendimiento monómerico aumentó de forma significativa, alcanzando alrededor del 75%. Para cargas más altas (4.8 g catalizador·g C^{-1}), se consiguió una conversión de arabinoxilanos total. Sin embargo, el rendimiento en arabinosa y xilosa era del 55%, ya

que los monosacáridos no sólo se habían formado, sino también degradado tras 3 horas de reacción (Figura 4).

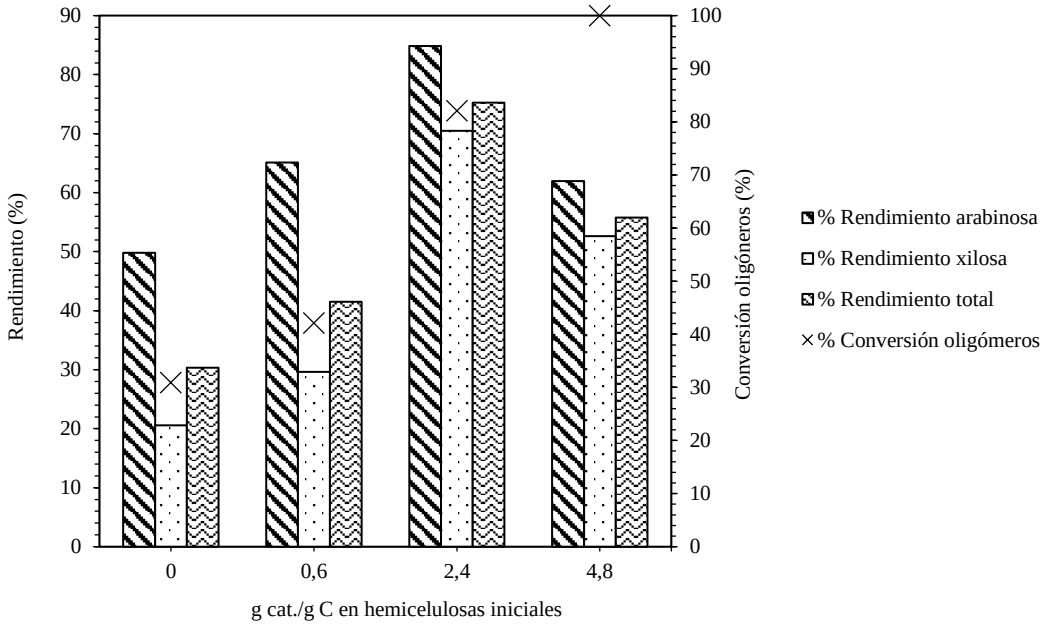

Figura 4. Influencia de distintas cargas de catalizador en el rendimiento en arabinosa y xilosa. Condiciones de reacción: 180 ºC, 3 horas, 50 bar N_2, catalizador: $RuCl_3$/Al-MCM-48.

Con el fin de reducir el tiempo de reacción, la carga de catalizador más alta (4.8 g catalizador·g C^{-1}) se probó a tiempos más cortos. Con esta cantidad de catalizador y tan sólo tras 15 minutos de reacción, se alcanzó el óptimo de reacción. En estas condiciones, el rendimiento en arabinosa y xilosa era del 95% y la formación de furfural fue inhibida casi por completo. Esto quiere decir, por una parte, que los arabinoxilanos se hidrolizaron completamente en monómeros y, por otra, que tanto los monómeros existentes tras la primera etapa de extracción como los formados tras esta segunda etapa de hidrólisis no se degradaron.

Finalmente, se comparó la actividad de cationes con diferente acidez de Lewis (Ru^{+3}, Fe^{+3}). Aunque la acidez del catalizador $FeCl_3$/Al-MCM-48 era mayor que la del $RuCl_3$/Al-MCM-48, el rendimiento en monómeros se vio favorecido utilizando este

último catalizador. Cationes con acidez de Lewis moderada, como el Ru^{+3}, ya han demostrado ser más activos que aquellos con acidez de Lewis más fuerte, como el Fe^{+3}, en procesos de hidrólisis de celulosa y celobiosa en varios trabajos encontrados en la literatura.

En el **Capítulo 3** titulado "*Hydrolysis of arabinoxylans from wheat bran over mesoporous and microporous silica catalysts*" se ha comparado el comportamiento de materiales de sílice mesoporosa (MCM-48 y Al-MCM-48) y distintas zeolitas (H-Y (12), H-ZSM-(23) y H-ZSM-5 (80)) en el proceso de hidrólisis de arabinoxilanos de salvado de trigo. Al igual que en el Capítulo 2, el objetivo principal de este trabajo ha sido maximizar la hidrólisis de arabinoxilanos en arabinosa y xilosa, así como minimizar la degradación de los azúcares a productos secundarios. Asimismo, se ha analizado la influencia de distintos parámetros, como el tiempo de reacción y la carga de catalizador.

En primer lugar, se analizó la influencia de los distintos catalizadores en el rendimiento en monosacáridos (arabinosa y xilosa) (Figura 5). De las dos sílices mesoporosas, se obtuvo un rendimiento considerablemente más alto utilizando Al-MCM-48. A diferencia de la MCM-48 y tal y como se ha indicado anteriormente, este material posee sitios ácidos de Brönsted creados tras la incorporación del aluminio, lo cual hace que la hidrólisis de oligosacáridos, arabinoxilanos en este caso, mejore respecto a los resultados obtenidos con MCM-48.

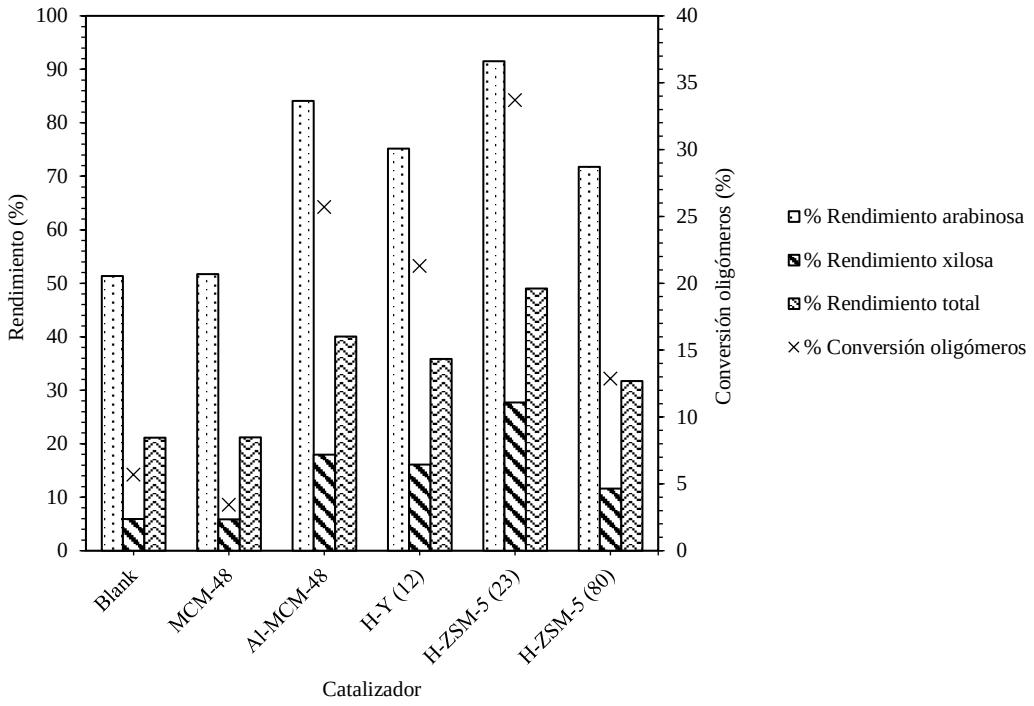

Figura 5. Comparación de los distintos catalizadores en el rendimiento en arabinosa y xilosa. Condiciones de reacción: 180 ºC, 15 minutos, 50 bar N_2, 4.6 g catalizador·g C^{-1}.

En el caso de las zeolitas (aluminosilicatos microporosos), su actividad en hidrólisis siguió la siguiente tendencia: H-ZSM-5 (23) > H-Y (12) > H-ZSM-5 (80), lo cual está relacionado no sólo con el número de sitios ácidos sino también con su naturaleza y fuerza. Primero se comparó la actividad de las dos zeolitas más ácidas, es decir, H-ZSM-5 (23) y H-Y (12). H-ZSM-5 (23) dio lugar a mejores rendimientos de hidrólisis que H-Y (12). Ambas zeolitas son comerciales, y según lo encontrado en bibliografía, las del tipo H-ZSM-5 poseen mayoritariamente sitios ácidos de Brönsted. Por su parte, las zeolitas H-Y tienen sitios ácidos de Lewis y Brönsted que, además, son más débiles que en las zeolitas H-ZSM-5, tal y como demostraron los análisis de acidez por TPD-NH_3. Por tanto, un número alto de sitios ácidos de Brönsted fuertes favorecen el proceso de hidrólisis de arabinoxilanos. Al comparar las zeolitas H-ZSM-5 con diferente contenido en aluminio, el rendimiento en monómeros fue mayor empleando H-ZSM-5 (23) que H-ZSM-5 (80). Esto está directamente relacionado con la ratio SiO_2/Al_2O_3. H-ZSM-5 (23)

tiene una menor ratio SiO_2/Al_2O_3, que se traduce en un mayor número de sitios ácidos (Brönsted y Lewis) los cuales, además, son más fuertes que los que posee la H-ZSM-5 (80). De todos estos materiales (mesoporosos y microporosos), la zeolita H-ZSM-5 (23) condujo al mayor rendimiento en monosácaridos. Este catalizador se utilizó posteriormente para el estudio del tiempo y la carga.

La influencia del tiempo se estudió entre 15 y 60 minutos con una carga de H-ZSM-5 (23) correspondiente a 4.8 $g \cdot g\ C^{-1}$. En este rango de tiempo, la arabinosa alcanzó su máximo prácticamente a los 15 minutos de reacción, con un rendimiento del 92%. Por su parte, la cantidad de xilosa monomérica aumentó en todo el rango de tiempo, obteniendo un rendimiento en xilosa del 68% tras 1 hora. Con el objetivo de aumentar el rendimiento global en monómeros a tiempos cortos, se probaron distintas cargas de catalizador a tiempos de reacción de 15 minutos. Empleando una carga de 9.2 $g \cdot g\ C^{-1}$ se obtuvo el óptimo de reacción, alcanzando un rendimiento monomérico total (arabinosa + xilosa) del 76%. Un aumento de la cantidad de catalizador por encima de 9.2 $g \cdot g\ C^{-1}$ no condujo a rendimientos superiores, probablemente debido a limitaciones en la transferencia de materia.

En el **Capítulo 4** titulado "*Hydrogenation kinetics of sugar model mixtures over ruthenium catalysts supported on H-ZSM-5*" se estudió la hidrogenación de mezclas modelo de azúcares sobre catalizadores de rutenio soportados en zeolitas H-ZSM-5. Estas mezclas modelo estaban compuestas por arabinosa, xilosa y glucosa en la misma concentración obtenida tras la hidrólisis de arabinoxilanos utilizando $RuCl_3$/Al-MCM-48 (Capítulo 2). Este estudio constituye un paso previo a la hidrogenación de las mezclas reales derivadas de los procesos de fraccionamiento e hidrólisis de arabinoxilanos de salvado de trigo. En este Capítulo 3 se ha estudiado la influencia de la acidez del soporte (H-ZSM-5) de los catalizadores de rutenio, así como distintas temperaturas, tiempos y

cargas de catalizador. Además, los datos experimentales se han ajustado a un modelo cinético de pseudo primer orden, obteniendo los valores de las energías de activación y de los factores pre-exponenciales de la ecuación de Arrhenius para las reacciones de hidrogenación de cada uno de los azúcares.

En el estudio de la influencia de la acidez del soporte del catalizador, se consideraron las zeolitas H-ZSM-5 (23) y H-ZSM-5 (80), las cuales se diferencian en la ratio SiO_2/Al_2O_3 y, por tanto, en el número de sitios ácidos. Este estudio se llevó a cabo a 100 ºC, 5 minutos, 50 bar de H_2 y empleando una carga de catalizador correspondiente a 0.015 g de Ru por g de carbono en azúcares totales. El catalizador de rutenio preparado sobre H-ZSM-5 (80) demostró una mayor actividad catalítica para la obtención de alcoholes a partir de azúcares. Esto se debe a que soportes con baja acidez promueven las reacciones de hidrogenación frente a caminos de reacción secundarios, como la isomerización de los azúcares, que ocurre cuando se emplean soportes más ácidos. Así, tanto la conversión de los azúcares (arabinosa, xilosa y glucosa) como la selectividad hacia alcoholes (arabitol, xilitol y sorbitol) se vieron favorecidas por el catalizador de rutenio depositado en H-ZSM-5 (80).

A continuación, se estudió el efecto de distintas temperaturas (80 – 100 – 120 ºC) empleando Ru/H-ZSM-5 (80) (Figura 6). En todos los experimentos, la selectividad hacia alcoholes fue superior al 99%, por lo que los valores de rendimiento y conversión prácticamente coincidían. En cualquier caso, la arabinosa y la xilosa se hidrogenaban más fácilmente que la glucosa. De hecho, la temperatura óptima para la hidrogenación de azúcares C_5 era de 100 ºC, mientras que la glucosa necesitaba una temperatura de 120 ºC para conseguir conversiones completas. De esta manera, la temperatura es un parámetro variable que se puede cambiar en función de si se quiere maximizar la producción de pentitoles o hexitoles.

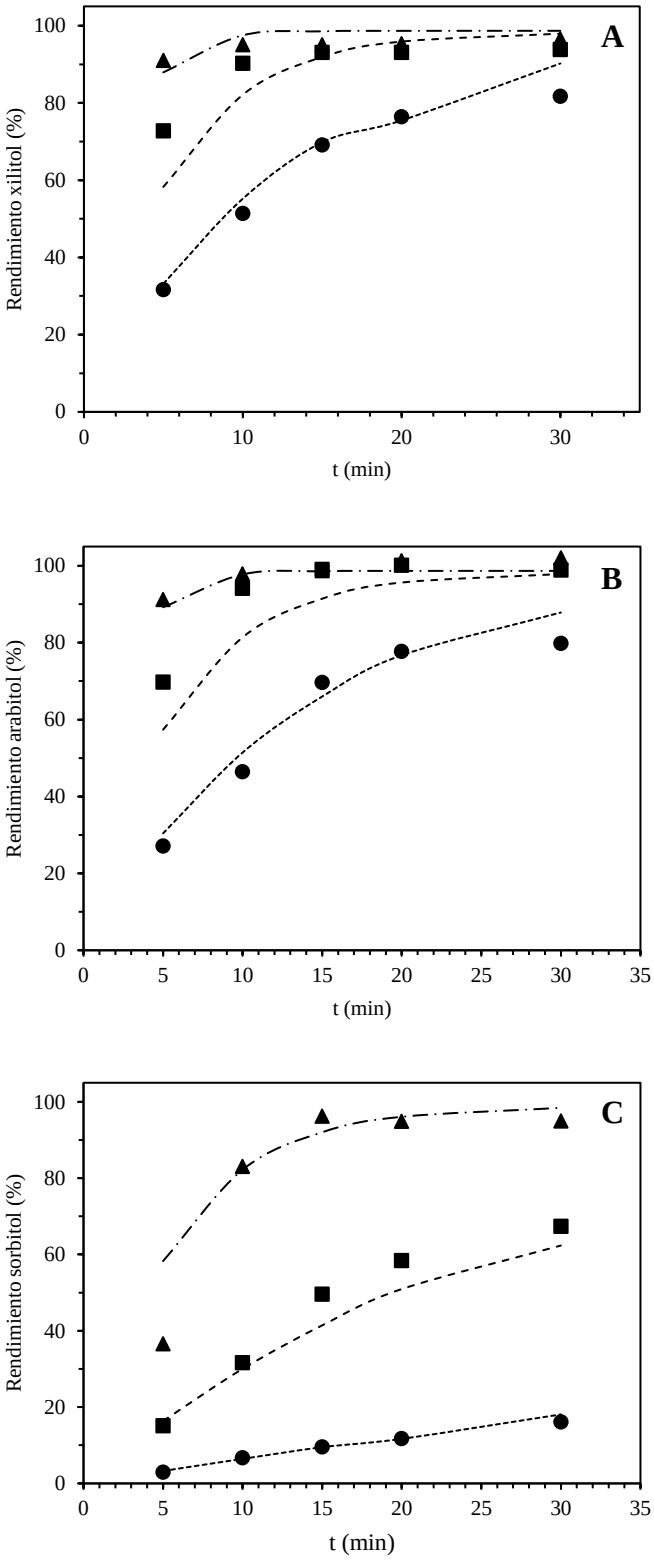

Figura 6. Efecto de la temperatura de reacción en el rendimiento de A) xilitol, B) arabitol y C) sorbitol. Condiciones de reacción: sustrato = xilosa (6 g·L^{-1}) + arabinosa (3 g·L^{-1}) + glucosa (1.7 g·L^{-1}); catalizador = Ru/H-ZSM-5 (80); carga de catalizador = 0.015 g Ru·g

C^{-1}; P (H_2) = 5 MPa. ● 80 ºC, ■ 100 ºC, ▲ 120 ºC. Los valores simulados están representados por líneas.

El estudio de la carga de catalizador se llevó a cabo a 100 ºC en un rango de tiempos de 5 – 30 minutos y de carga de catalizador de 0 – 0.06 g Ru·g C^{-1} (Figura 7). En este caso, también se observó que para la hidrogenación de glucosa se necesitaba una mayor cantidad de catalizador y, por tanto, de rutenio que para la hidrogenación de arabinosa y xilosa. Conversiones prácticamente completas de arabinosa y xilosa se obtuvieron a 10 minutos con una carga de 0.03 g Ru·g C^{-1}, mientras que, en el caso de la glucosa, resultados similares se alcanzaron con una carga de 0.06 g Ru·g C^{-1} tras 15 minutos de reacción.

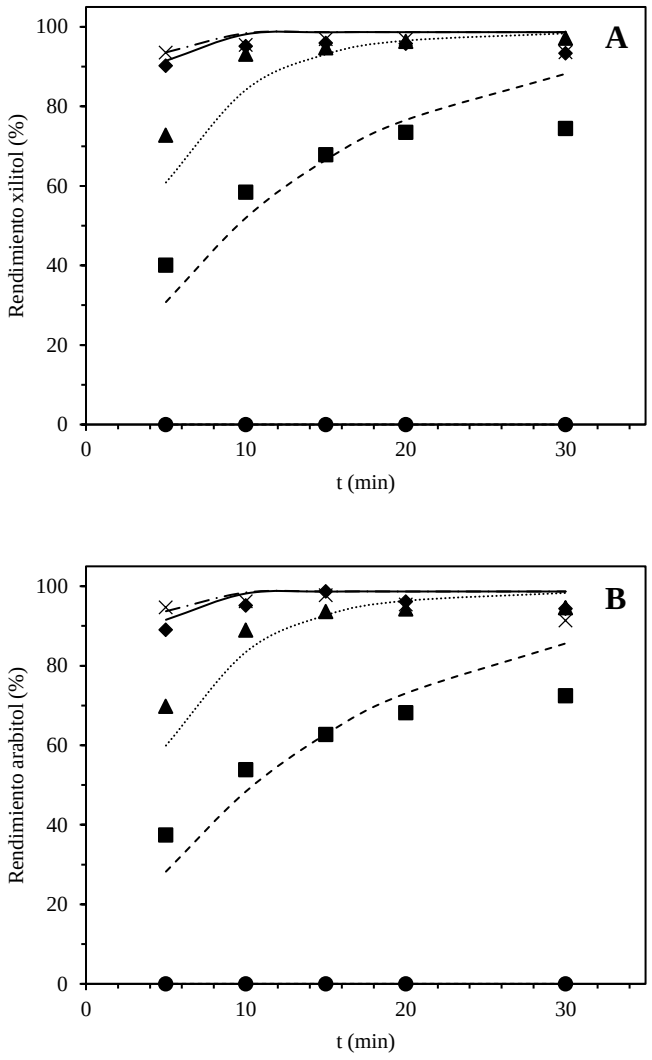

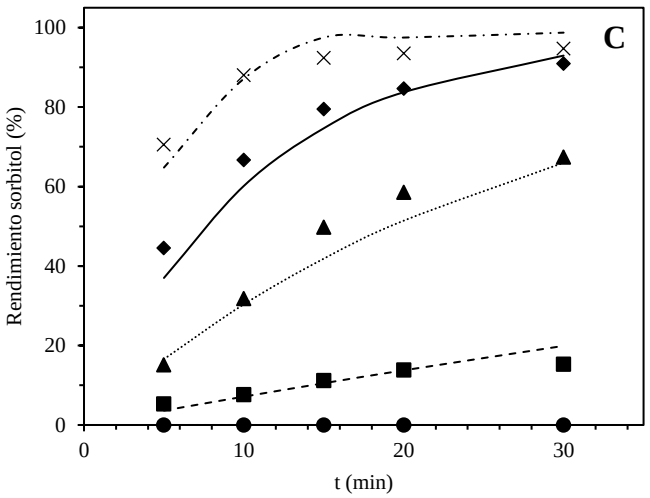

Figura 7. Efecto de la carga de catalizador en el rendimiento de A) xilitol, B) arabitol y C) sorbitol. Condiciones de reacción: sustrato = xilosa (6 $g \cdot L^{-1}$) + arabinosa (3 $g \cdot L^{-1}$) + glucosa (1.7 $g \cdot L^{-1}$); catalizador = Ru/H-ZSM-5 (80); T = 100 ºC; P (H_2) = 5 MPa. ● Sin catalizador, ■ 0.008 g Ru·g C^{-1}, ▲ 0.015 g Ru·g C^{-1}, ♦ 0.030 g Ru·g C^{-1}, × 0.060 g Ru·g C^{-1}. Los valores simulados están representados por líneas.

Los datos experimentales obtenidos se ajustaron finalmente a un modelo cinético de pseudo primer orden, obteniendo unos valores de energía de activación de 92.0 $kJ \cdot mol^{-1}$, 43.7 $kJ \cdot mol^{-1}$ y 47.9 $kJ \cdot mol^{-1}$ para las reacciones de hidrogenación de glucosa, xilosa y arabinosa, respectivamente. El modelo de pseudo primer orden reproducía los resultados experimentales con desviaciones absolutas relativamente bajas (< 11%) y coeficientes de regresión superiores a 0.950. El efecto de la carga de catalizador también se evaluó en las cinéticas de hidrogenación. Para ello, se propuso una ecuación empírica que incluía dicho efecto en el valor de la energía de activación.

En el **Capítulo 5** titulado "*Purification of wheat bran hydrolysates using boronic acid carriers followed by hydrogenation of sugars over Ru/H-ZSM-5*" se estudió el proceso de purificación de los hidrolizados de salvado de trigo (obtenidos en el Capítulo 2) y su posterior hidrogenación para obtener los alcoholes a partir de los azúcares correspondientes.

Tras las etapas de fraccionamiento e hidrólisis (Capítulos 1 y 2), no solo se obtuvieron arabinosa y xilosa, sino que otros compuestos del salvado de trigo, tales como sales inorgánicas, proteínas y derivados de lignina, y productos de degradación derivados de los azúcares (furfural), también formaban parte del hidrolizado disminuyendo la pureza de los azúcares. Con el fin de aumentar su pureza, se utilizó un proceso de tres etapas: i) extracción selectiva de azúcares mediante ácidos borónicos disueltos en una fase orgánica, ii) recuperación de los azúcares extraídos en una disolución acuosa ácida y iii) purificación adicional mediante el uso de distintas resinas de intercambio iónico (Figura 8). Adicionalmente, era necesario una etapa de preactivación de la fase orgánica con un buffer fosfato. Durante esta etapa hay una transferencia de grupos OH^- del buffer fosfato a la fase orgánica, los cuales hacen que el ácido borónico se ionice y permita la formación de complejos con los azúcares.

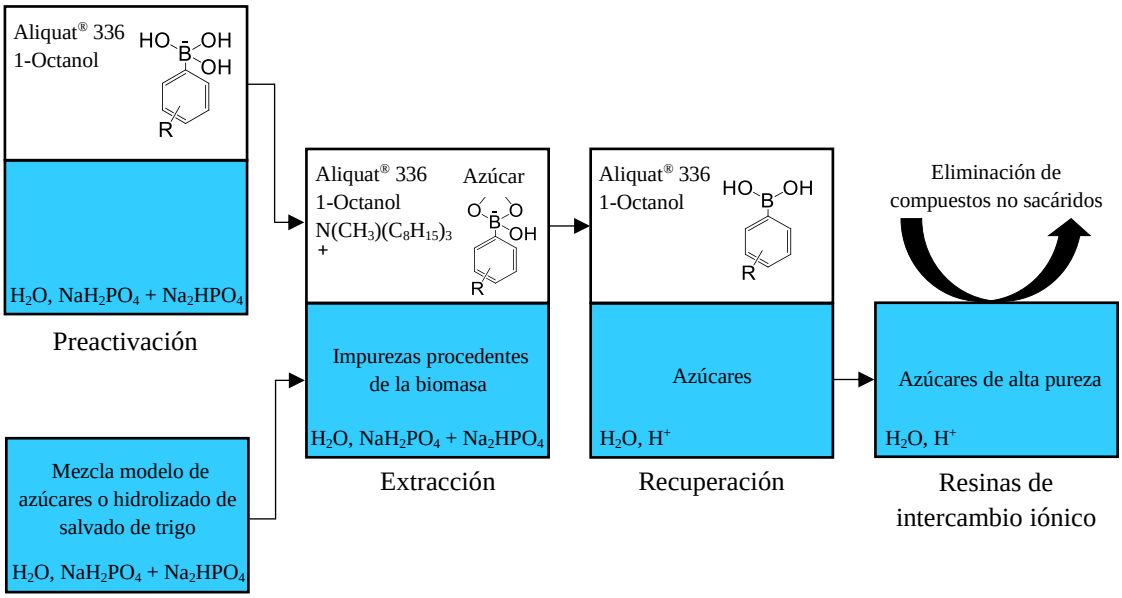

Figura 8. Esquema del proceso de purificación de azúcares procedentes de hidrolizados de salvado de trigo.

La primera etapa (extracción selectiva de azúcares del hidrolizado inicial) se basa en la afinidad que tienen los ácidos borónicos para formar complejos reversiblemente estables con monosacáridos. Estos ácidos borónicos se utilizaron disueltos en una fase orgánica

compuesta por una sal cuaternaria de amonio (Aliquat® 336) y 1-octanol. Primero se probaron dos ácidos borónicos (ácido fenilborónico, PBA; ácido *orto*-hidroximetil fenilborónico, HMPBA) en la extracción de azúcares de mezclas modelo. Para una misma concentración de ácido borónico, HMPBA era capaz de extraer una mayor cantidad de azúcares que PBA, debido a sus mayores constantes de formación de complejos, su menor pK_a y a la formación de puentes de hidrógenos intrínsecos formados entre el HMPBA y los azúcares. HMPBA, se utilizó, por tanto, para la extracción de azúcares de hidrolizados de salvado de trigo. La arabinosa y xilosa se extraían en proporciones similares y a la vez mayores que la glucosa. Con una concentración de HMPBA igual a 0.5 M, las cantidades extraídas de glucosa, xilosa y arabinosa fueron de 66%, 83% y 84%, respectivamente (Figura 9). El 100% de los azúcares se recuperó en una disolución acuosa con una concentración de H_2SO_4 de 0.25 M.

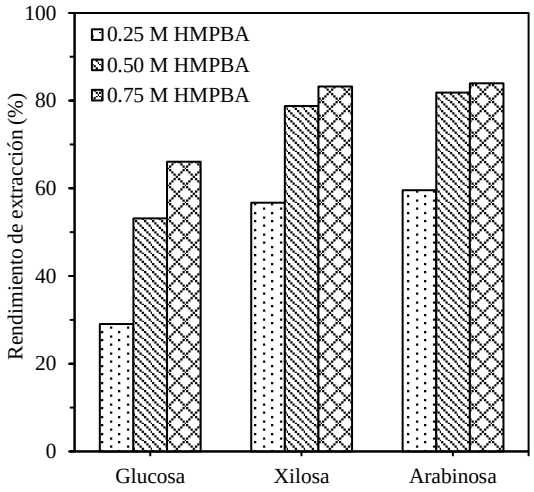

Figura 9. Influencia de la concentración de HMPBA en la extracción de azúcares de hidrolizados de salvado de trigo.

En cuanto a los productos de degradación, furfural era el que se encontraba en mayor proporción respecto al resto (5-HMF, ácido fórmico, ácido acético). El 80% del furfural se extrajo en la fase orgánica, mientras que sólo el 20 – 25% se recuperó en la disolución de H_2SO_4. Esto significa que la concentración final de furfural disminuyó en torno al 80

– 85% respecto a su concentración en el hidrolizado inicial. Los elementos inorgánicos (Ca, Mg, K, S) no se extrajeron en la fase orgánica y permanecieron en el hidrolizado inicial, por lo que al final se obtuvo un hidrolizado libre de estos elementos. En el caso de las proteínas, alrededor del 30% pasaron a la fase orgánica. Sin embargo, no se detectaron proteínas en el hidrolizado final una vez purificado. La última etapa de tratamiento con distintas resinas de intercambio iónico (Amberlyst® 15 y Amberlite® IRA-96) se utilizó para eliminar parte de la lignina solubilizada tras la etapa de fraccionamiento del salvado del trigo. Tras el proceso completo, se obtuvo un hidrolizado con una concentración de azúcares del 90% (en términos de carbono) respecto al 64% del hidrolizado antes de la purificación. Además, se consiguieron eliminar las sales inorgánicas y proteínas y una cantidad importante de productos de degradación derivados de los azúcares en las etapas previas de fraccionamiento e hidrólisis. Del 90% de los azúcares, el 50% correspondía a xilosa, el 30% a arabinosa, el 7% a glucosa y el restante 3% a azúcares minoritarios (manosa, galactosa) (Figura 10).

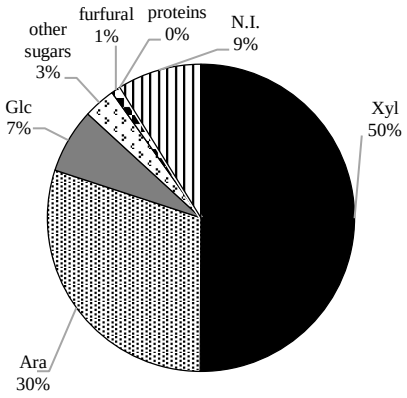

Figura 10. Composición del hidrolizado de salvado de trigo tras purificación (en términos de carbono).

Tras la etapa de purificación, se estudió la hidrogenación de los azúcares utilizando Ru/H-ZSM-5 (80) como catalizador. Previamente se llevó a cabo un intento de hidrogenación de los azúcares del hidrolizado antes de su purificación. Incluso para la carga más alta de

catalizador (0.06 g Ru·g C^{-1}) el rendimiento en pentitoles no superó el 10%. Sin embargo, la hidrogenación de los azúcares tras la purificación tuvo lugar con éxito. Se obtuvo un rendimiento del 70% en pentitoles a 100 ºC tras solo 10 minutos de reacción y con una carga de catalizador de 0.06 g Ru·g C^{-1} (Figura 11).

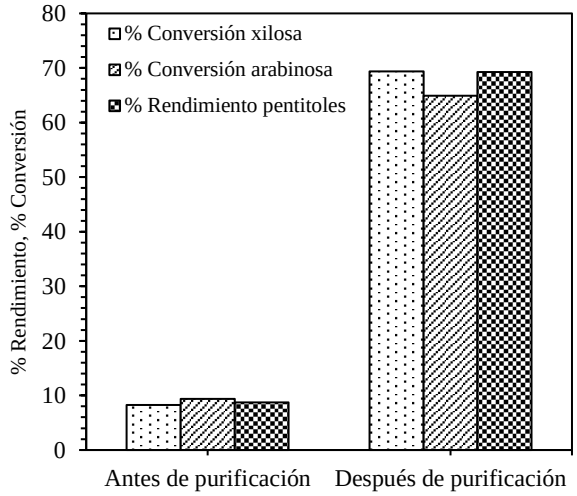

Figura 11. Hidrogenación de los azúcares C_5 antes y después de la purificación del hidrolizado.

La inhibición de la hidrogenación de los azúcares del hidrolizado antes de la etapa de purificación se debe a la desactivación del catalizador de rutenio. Se investigó dicho mecanismo de desactivación, concluyendo que las proteínas actuaban como potenciales venenos para el catalizador que impedían la hidrogenación de los azúcares en los correspondientes alcoholes. Por tanto, un proceso de purificación en el que se eliminen las proteínas es crucial para llevar a cabo la hidrogenación de azúcares procedentes de hidrolizados de salvado de trigo.

Conclusiones

En esta Tesis Doctoral se ha desarrollado un proceso multietapa para la producción de alcoholes a partir de salvado de trigo. El objetivo principal se ha dividido y estudiado en varias etapas secuenciales, que se resumen en:

i) Extracción de la fracción de arabinoxilanos de salvado de trigo

ii) Hidrólisis de arabinoxilanos en monosacáridos

iii) Purificación de hidrolizados de salvado de trigo

iv) Hidrogenación de los hidrolizados tras la purificación para la producción de alcoholes

Las principales conclusiones de este trabajo se presentan a continuación:

- La fracción de arabinoxilanos de salvado de trigo, un residuo agrícola de nuestra región Castilla y León, se ha revalorizado en productos de alto valor añadido: i) se ha obtenido un hidrolizado con una alta pureza en azúcares (50% xilosa, 30% arabinosa y 7% glucosa, expresado en términos de carbono) que puede utilizarse en distintos procesos posteriores, y ii) los correspondientes alcoholes se han obtenido con un rendimiento en pentitoles del 70% y una selectividad del 100%.
- La extracción hidrotermal de arabinoxilanos procedentes de salvado de trigo desalmidonado se puede llevar a cabo de forma eficiente utilizando materiales tipo MCM-48, así como los correspondientes catalizadores de $RuCl_3$.
    - La tendencia en el rendimiento de extracción de arabinoxilanos está directamente relacionada con la acidez del catalizador, es decir, cuanto mayor es la acidez mayor es el rendimiento: MCM-48 < Al-MCM-48 < $RuCl_3$/MCM-48 < $RuCl_3$/Al-MCM-48.
    - Al-MCM-48 conduce a mayores rendimientos de extracción que MCM-48, lo que se atribuye a la mayor acidez de Brönsted del Al-MCM-48 después de la incorporación del aluminio. Los catalizadores de $RuCl_3$ son más eficientes que los correspondientes soportes de sílice, debido a la adicional acidez moderada de Lewis achacada a los cationes Ru^{+3}.

- Los arabinoxilanos se obtienen mayoritariamente como poli/oligosacáridos, mientras que solo una pequeña cantidad se encuentra en forma monomérica.
- Altos rendimientos de extracción de arabinoxilanos con bajo peso molecular se obtienen a temperaturas relativamente altas, tiempos cortos y utilizando catalizadores sólidos ácidos.
- La extracción de arabinoxilanos y su posterior hidrólisis en monómeros se deben llevar a cabo en dos etapas diferentes con el fin de evitar la co-extracción de celulosa y aumentar la pureza de los arabinoxilanos extraídos.
- Los catalizadores heterogéneos han demostrado ser buenos sustitutos de los tradicionales ácidos homogéneos empleados en procesos de fraccionamiento e hidrólisis de biomasa. Comparando los resultados de la literatura basados en extracciones con ácidos homogéneos con los obtenidos en esta Tesis Doctoral, se puede afirmar que:
    - Los catalizadores sólidos ácidos son más selectivos y minimizan la co-extracción de compuestos indeseados de la biomasa.
    - La degradación de los arabinoxilanos es menor con catalizadores sólidos ácidos que con ácidos homogéneos.
    - Los catalizadores heterogéneos se pueden separar fácilmente del extracto líquido mediante filtración, mientras que el proceso de recuperación de ácidos homógeneos aumenta los costes de operación.
    - Los tratamientos con ácidos no son amigables con el medio ambiente y causan problemas de corrosión que consiguientemente

aumentan los costes de equipo. Esto se puede evitar mediante el uso de catalizadores sólidos ácidos.

- Las condiciones experimentales óptimas se alcanzan a 180 ºC, 10 minutos y usando $RuCl_3$/Al-MCM-48 como catalizador. Bajo estas condiciones el rendimiento total de extracción de arabinoxilanos es del 78% y el peso molecular medio de alrededor de 9 kDa.

- MCM-48, Al-MCM-48 y los correspondientes catalizadores soportados de $RuCl_3$ se han utilizado para completar la hidrólisis de arabinoxilanos en arabinosa y xilosa.
  - La acidez de los catalizadores y el rendimiento monomérico muestran la misma tendencia observada en el proceso previo de extracción: MCM-48 < Al-MCM-48 < $RuCl_3$/MCM-48 < $RuCl_3$/Al-MCM-48.
  - Una alta acidez total y la combinación de acidez de Brönsted (debido a la incorporación de aluminio) y acidez de Lewis moderada (debido a los cationes Ru^{+3}) dan lugar a mayores rendimientos de hidrólisis.
  - Cationes metálicos con acidez de Lewis moderada (Ru^{+3}) son más activos que aquellos con alta acidez de Lewis (Fe^{+3}).
  - Las moléculas de arabinosa se liberan más rápidamente que las de xilosa.
  - Las condiciones óptimas de operación son 180 ºC, 15 minutos y usando $RuCl_3$/Al-MCM-48 como catalizador con una carga de 4.8 g·g C^{-1}. La formación de furfural se inhibe de forma casi completa bajo estas condiciones, obteniendo un rendimiento total en monosacáridos (arabinosa + xilosa) del 95%.

- La actividad catalítica de materiales mesoporosos de sílice (MCM-48 y Al-MCM-48) y de zeolitas (H-Y (12), H-ZSM-5 (23) y H-ZSM-5 (80)) se ha probado y

comparado en la hidrólisis de arabinoxilanos de salvado de trigo en monosacáridos.

  - La fuerza y la naturaleza de los sitios ácidos desempeñan un papel fundamental en la hidrólisis de arabinoxilanos.
  - H-ZSM-5 (23) es el catalizador más activo de todos los probados para la conversión de arabinoxilanos en arabinosa y xilosa, lo que se atribuye a su gran acidez, así como a sus sitios ácidos fuertes de Brönsted.
  - Las condiciones óptimas son 180 ºC, 15 minutos y usando H-ZSM-5 (23) como catalizador con una carga de 9.2 $g \cdot g\ C^{-1}$. Los rendimientos de hidrólisis en arabinosa y xilosa son 96% y 67%, respectivamente, que corresponden a un rendimiento total del 76%.

- Los azúcares de los hidrolizados de salvado de trigo se han recuperado selectivamente mediante extracción con ácidos borónicos y se purificaron en una etapa posterior con el uso de distintas resinas de intercambio iónico.
  - Se utiliza una fase orgánica compuesta por una sal cuaternaria de amonio (Aliquat® 336) y un ácido borónico disueltos en 1-octanol para extraer los azúcares de los hidrolizados de salvado de trigo.
  - El ácido ortohidroximetil fenilborónico (HMPBA) es más eficiente que el ácido fenilborónico (PBA) en la extracción de azúcares.
  - La arabinosa y xilosa se extraen más fácilmente que la glucosa.
  - Con una concentración de HMPBA de 0.5 M en la fase orgánica, se extraen el 66%, 83% y 84% de la glucosa, xilosa y arabinosa iniciales, respectivamente. Después el total de los azúcares se recupera en una disolución acuosa de H_2SO_4 0.25 M.

- El hidrolizado tras la purificación no contiene elementos inorgánicos ni proteínas y tiene una menor cantidad de productos de degradación de azúcares y de derivados de lignina que el hidrolizado inicial.
- Una gran parte de los compuestos derivados de la lignina se elimina por medio de resinas de intercambio iónico (Amberlyst® 15 y Amberlite® IRA-96).
- La concentración de azúcares en el hidrolizado purificado es del 90% en términos de carbono, comparado con el 64% del hidrolizado inicial.

- Mezclas modelo de azúcares compuestas por glucosa, xilosa y arabinosa se hidrogenaron sobre catalizadores de rutenio soportados en diferentes zeolitas tipo H-ZSM-5.
  - Soportes con baja acidez (H-ZSM-5(80)) promueven la hidrogenación frente a la isomerización de los azúcares. La conversión de azúcares y el rendimiento a alcoholes son más altos utilizando Ru/H-ZSM-5 (80) que Ru/H-ZSM-5 (23).
  - La xilosa y arabinosa se hidrogenan más rápidamente que la glucosa.
  - La temperatura óptima para la hidrogenación de xilosa y arabinosa es 100 ºC, mientras que 120 ºC es la óptima para hidrogenar glucosa.
  - Para conseguir altos rendimientos en la hidrogenación de glucosa se requiere una mayor cantidad de catalizador que en el caso de la hidrogenación de xilosa y arabinosa.
  - Los datos experimentales obedecen a un modelo cinético de pseudo primer orden que reproduce los datos con bajas desviaciones absolutas obteniendo altos coeficientes de regresión.

  - Los valores de energía de activación para la hidrogenación de glucosa, xilosa y arabinosa son 92.0 $kJ \cdot mol^{-1}$, 43.7 $kJ \cdot mol^{-1}$ y 47.9 $kJ \cdot mol^{-1}$, respectivamente.

- Los azúcares de hidrolizados reales de salvado de trigo se hidrogenaron utilizando Ru/H-ZSM-5 (80).
  - La hidrogenación de los azúcares no tiene lugar en el hidrolizado antes de la etapa de purificación.
  - Las proteínas desactivan los catalizadores de rutenio.
  - Los azúcares de los hidrolizados de salvado de trigo se hidrogenan con éxito después de la etapa de purificación. Se obtiene un rendimiento en pentitoles del 70% a 100 ºC, tras 10 minutos de reacción y utilizando una carga de catalizador de 0.06 g $Ru \cdot g\ C^{-1}$.

Trabajo futuro

En esta Tesis Doctoral, se ha revalorizado la fracción de arabinoxilanos de salvado de trigo en compuestos de alto valor. El residuo sólido obtenido tras la extracción de arabinoxilanos es rico en celulosa y lignina, fracciones que también se pueden convertir en productos de alto valor añadido en procesos posteriores. Por ejemplo, la celulosa se puede hidrolizar en glucosa, que es una molécula base para la obtención de una gran cantidad de químicos (ácido glucónico, ácido láctico, sorbitol). Asimismo, la glucosa se puede transformar en biocombustibles por procesos de fermentación. La lignina, por ejemplo, se puede emplear como base para la obtención de bioplásticos, nanocompuestos y nanopartículas. También se puede depolimerizar en compuestos de alto valor, como vanilina, ácido vanilínico, ácido *p*-cumárico, ácido *p*-hidroxibenzoico o alcohol sinapílico.

La alta pureza de los azúcares obtenidos hace que estos se puedan utilizar no solo para la producción de alcoholes sino también para otros fines. Por ejemplo, los azúcares se pueden convertir en biocombustibles mediante procesos de fermentación para los cuales es crucial que los azúcares sean altamente puros. La xilosa y la arabinosa se pueden utilizar también para la obtención de furfural o ácido succínico, que se encuentran dentro de los compuestos de alto valor añadido que se pueden obtener a partir de biomasa, de acuerdo con el Departamento de Energía de los Estados Unidos.

Los alcoholes obtenidos en la última etapa del proceso (xilitol y arabitol) se pueden convertir en alcanos de cadena corta, como pentanos, mediante procesos de hidrogenación en medio ácido. El pentano se puede utilizar para la producción de espumas de poliestireno o de gasolinas, como disolvente y en cromatografía líquida. En medio básico, estos alcoholes también se pueden transformar en etilenglicol y propilenglicol, que tienen aplicaciones en medicina (como excipientes), cosmética (cremas para la piel) o en la industria química (herbicidas y pesticidas, lubricantes).

En cuanto al proceso, es necesario una investigación posterior que considere los siguientes puntos:

- Reciclaje del catalizador después de los procesos de fraccionamiento, hidrólisis e hidrogenación.
- Evaluación de los costes de regeneración y reciclaje del catalizador.
- Escalado del proceso para pasar de escala de laboratorio a planta piloto.
- Sustitución de procesos discontinuos por procesos continuos.
- Intensificación del proceso mediante la reducción del número de etapas.
- Análisis del ciclo de vida para evaluar los impactos ambientales del proceso durante todas sus etapas.

ACKNOWLEDGEMENTS

Nunca nadie dijo que hacer una tesis doctoral fuera un camino fácil. Y así ha sido. Estos últimos cuatro años han estado llenos de obstáculos, preocupaciones, frustraciones, noches sin dormir, pero también de alegrías y recompensas. La gratificación que uno siente al tener su tesis entre manos no se puede explicar con palabras. A lo largo de estos años no he estado sola y han sido muchas las personas que me han ayudado tanto en lo personal como en lo profesional y a las que quiero agradecer su apoyo.

En primer lugar, me gustaría dar las gracias a mi directora, Esther. A Esther la conocí en el último año de carrera, donde decidí hacer el Proyecto Fin de Carrera con ella. A partir de ahí, también dirigió mi Trabajo Fin de Grado y Trabajo de Máster. Gracias, Esther, por haberme dado la oportunidad de realizar la tesis doctoral y por tu dedicación a lo largo de todos estos años.

I also want to thank Irina, my supervisor during my research stay in Aachen. You helped me a lot in the final stretch of the Thesis. Your advices and suggestions have always been useful. Sincerely, thank you so much for your endless dedication.

Gracias a todos los miembros del Grupo de Alta Presión, profesores y compañeros. Gracias a ellas, Celia, María, Nerea, Rut y Yoana, porque habéis hecho que este camino no fuera meramente profesional. Gracias por los buenos ratos que hemos pasado juntos y por los que seguro están por venir.

Gracias a todos los técnicos. A Isabel, Alvar, Dani, Miguel, Mónica, Enrique, Araceli, Beatriz y especialmente a José María, que siempre ha estado ahí para echarme una mano en lo que necesitara.

Gracias a mi familia, especialmente a mis abuelos, mis padres y mi hermano, por todo el apoyo y el cariño brindado en todo momento. Gracias por haberme escuchado. Que sepáis que nunca he perdido la ilusión y esto, en gran parte, os lo debo a vosotros.

Danke Fabian, weil du das beste Geschenk dieses Lebensabschnitts bist. Wir sind viel gereist, um uns zu sehen. Du warst weit weg, aber immer in meinem Herzen. Danke für alles, du warst meine größte Unterstützung. Bist du bereit? Ich komme!

ABOUT THE AUTHOR

Nuria Sánchez-Bastardo was born in Valladolid in 1991. She grew up in a small village near Valladolid, called Medina de Rioseco. She moved to Valladolid to study the Degree in Industrial Technical Engineering (specialized in Industrial Chemistry) from 2009 to 2013 and received the Special Award of Degree to the best academic marks. She continued studying one more year at the University of Valladolid to obtain the Bachelor in Chemical Engineering, which was finished in 2014. She also studied a Master on Fluid Thermodynamic Engineering at the University of Valladolid from 2013 to 2014 and was awarded with the Special Award of Master.

In the year 2014, she started her PhD Thesis at the High Pressure Processes Group of the University of Valladolid. Her PhD Thesis is based on the catalytic conversion of lignocellulosic biomass into value chemicals and has been carried out under the supervision of Dr. Esther Alonso Sánchez. She developed a three-month predoctoral stay in the "*Lehrstuhl für Heterogene Katalyse und Technische Chemie*" at the *Institut für Technische Chemie und Makromolekulare Chemie* (RWTH Aachen, Germany) under the supervision of Prof. Dr. Regina Palkovits and Dr. Irina Delidovich, where she started to investigate purification processes of biomass hydrolysates.

Publications

- Sánchez-Bastardo, N., Delidovich, I., and Alonso, E. From biomass to sugar alcohols: Purification of wheat bran hydrolysates using boronic acid carriers followed by hydrogenation of sugars over Ru/H-ZSM-5. *ACS Sustainable Chemistry & Engineering*, 6 (2018) 11930–11938.
- Delidovich, I., Gyngazova, M.S., Sánchez-Bastardo, N., Wohland, J.P., Hoppe, C., and Drabo, P. Production of keto-pentoses via isomerization of aldo-pentoses catalyzed by phosphates and recovery of products by anionic extraction. *Green Chemistry*, 20 (2018) 724–734.

- Sánchez-Bastardo, N., and Alonso, E. Maximization of monomeric C5 sugars from wheat bran by using mesoporous ordered silica catalysts. *Bioresource Technology*, 238 (2017) 379–388.
- Sánchez-Bastardo, N., Romero, A., and Alonso, E. Extraction of arabinoxylans from wheat bran using hydrothermal processes assisted by heterogeneous catalysts. *Carbohydrate Polymers*, 160 (2017) 143–152.

Submitted/in preparation publications

- Sánchez-Bastardo, N., Cabeza, Á., Sobrón, F., García-Serna, J., and Alonso, E. Hydrogenation kinetics of sugar model mixtures over ruthenium catalysts supported on H-ZSM-5. *Journal of Industrial and Engineering Chemistry*.
- Sánchez-Bastardo, N., and Alonso, E. Hydrolysis of arabinoxylans from wheat bran over mesoporous and microporous silica catalysts. *Journal of Energy Chemistry*.

Conference contributions

Oral Presentations:

- N. Sánchez-Bastardo and E. Alonso. Fraccionamiento catalítico de hemicelulosas de salvado de trigo en agua caliente presurizada. *IX Reunión de Expertos en Tecnologías de fluidos comprimidos (Flucomp 2018).* Madrid (Spain). June 2018.
- N. Sánchez-Bastardo and E. Alonso. Maximization of C5 sugars from wheat bran over heterogeneous catalysts. *4th International Congress on Catalysis for Biorefineries (CatBior 2017)*. Lyon (France). December 2017.
- N. Sánchez-Bastardo and E. Alonso. Maximization of monomeric C5 sugars from wheat bran by using ruthenium-supported catalysts. *13th International Conference on Renewable Resources and Biorefineries (RRB-13)*. Wroclaw (Poland). June 2017.

- N. Sánchez-Bastardo and E. Alonso. Heterogeneous catalysis for the extraction of arabinoxylans from wheat bran. *5th International Congress on Green Process Engineering (GPE 2016)*. Quebec (Canada). June 2016.
- N. Sánchez-Bastardo, Ó. Benito-Román and E. Alonso. Hydrothermal conversion of sucrose into lactic acid. *5th International Seminar on Engineering Thermodynamics of Fluids*. Tarragona (Spain). July 2014.

Poster Presentations:

- N. Sánchez-Bastardo and E. Alonso. Ru-supported on mesoporous silica as active catalyst for the hydrolysis of the hemicellulosic fraction of wheat bran. *10th World Congress of Chemical Engineering*. Barcelona (Spain). October 2017.
- N. Sánchez-Bastardo and E. Alonso. Heterogeneous catalysis for the extraction of arabinoxylans from wheat bran. *8th Green Solvents Conference*. Kiel (Germany). October 2016.
- N. Sánchez-Bastardo, Ó. Benito-Román and E. Alonso. Hydrothermal conversion of sucrose, glucose and fructose into lactic acid. *3rd International Symposium on Green Chemistry (ISGC 2015)*. La Rochelle (France). May 2015.
- N. Sánchez-Bastardo, Ó. Benito-Román and E. Alonso. Hydrothermal conversion of sucrose into lactic acid. *10th International Conference on Renewable Resources and Biorefineries (RRB-10)*. Valladolid (Spain). June 2014.

Predoctoral training

- "BASF 135th International Summer Course". Ludwigshafen (Germany). August 2018.
- "Green Chemistry" Horizon Kármán Conference. RWTH Aachen University (Germany). February 2017.
- "1th Green Solvents Workshop". Kiel (Germany). October 2016.

- "How to get published in international journals" by Wiley. University of Valladolid (Spain). September 2016.
- "Bioproducts Engineering and Biorefineries". Rafael Luque (from University of Cordoba). University of Valladolid (Spain). June 2016.
- "WINESENSE Spring School". Process Intensification and product development: a focus on grape polyphenols. University of Valladolid (Spain). April 2016.
- "Summer School on Green Chemistry". La Rochelle (France). May 2015.
- "Introducción a la caracterización de adsorbentes y catalizadores". Consejo Superior de Investigaciones Científicas (CSIC) y Grupo Especializado de Adsorción (RRSSEE de Física y Química). Jarandilla de la Vera (Cáceres). June 2014.
- "Shyman Summer School". 7th Framework Program of the European Union SHYMAN Project. University of Valladolid (Spain). May 2014.
- "Catálisis ambiental. Preparación y caracterización de catalizadores y adsorbentes para la purificación de corrientes gaseosas". PhD Program in Chemical and Environmental Engineering, RD 99/2011. Prof. Dr. Alicia Viviana Boix (from Universidad Nacional de Litoral, INCAPE CONICET, Argentina). University of Valladolid (Spain). November 2013.
- "Life Long Learning Intensive Course 2013". Process Intensification by High Pressure Technologies – Actual Strategies for Energy and Resources Conservation. Technical University Darmstadt (Germany). June 2013.

Predoctoral stay

- Short-term stay (3 months) in the "*Lehrstuhl für Heterogene Katalyse und Technische Chemie*" at the *Institut für Technische Chemie und Makromolekulare*

Chemie (RWTH Aachen, Germany) under the supervision of Prof. Dr. Regina Palkovits and Dr. Irina Delidovich. January – April 2017.

PhD Grants

- Grant to attend to International Congresses awarded by the University of Valladolid. June 2016.
- ACTION COST FP1306 grant to attend to the 1st Summer School on Green Chemistry in La Rochelle (France). May 2015.
- Predoctoral contract "Ayuda para la formación de profesorado universitario (FPU 2014)" awarded by the Ministerio de Educación, Cultura y Deporte (Spanish Government). September 2015 – September 2019.
- Predoctoral contract awarded by the University of Valladolid (FPI-Uva 2014). July – September 2015.
- Competitive grant awarded by "Consejo Social" of the University of Valladolid for initiation in research at the Department of Chemical Engineering and Environmental Technology. September 2013 – June 2014.
- Grant to attend the course "Life Long Learning Intensive Course 2013". Process Intensification by High Pressure Technologies - Actual Strategies for Energy and Resources Conservation. Technical University Darmstadt (Germany). July 2013.

Participation in research projects

- BIOFRAHYNERY project from the Spanish Government of Science and Innovation (MINECO, CTQ2015-64892-R) entitled "Biorrefinería lignocelulósica de subproductos de industria agroalimentaria para obtención de bioproductos mediante fraccionamientos hidrotermales e hidrogenación catalítica".

Teaching experience

- Participation in the subject "Experimentación en Ingeniería Química" of the Bachelor in Chemical Engineering. Academic year 2016/2017 and 2017/2018.
- Co-supervisor of the Master Thesis "Hidrólisis de derivados de celulosa y hemicelulosa mediante el empleo de catalizadores ácidos heterogéneos", developed by Manuel Lanza (2016).

Awards

- Special Award of Master (Fluid Thermodynamic Engineering).
- Special Award of Degree (Industrial Technical Engineering, specialized in Industrial Chemistry)